

©Copyright 2021

Megan L Feddern

Applied ecosystem chemistry: linking biogeochemical and
physiological processes to ecological interactions

Megan L Feddern

A dissertation
submitted in partial fulfillment of the
requirements for the degree of

Doctor of Philosophy

University of Washington

2021

Reading Committee:

Gordon W. Holtgrieve, Chair

Eric J. Ward

Tim Essington

Sarah Converse

Program Authorized to Offer Degree:
School of Aquatic and Fishery Sciences

University of Washington

Abstract

Applied ecosystem chemistry: linking biogeochemical and physiological processes to ecological interactions

Megan L Feddern

Chair of the Supervisory Committee:

Assistant Professor Gordon W. Holtgrieve

School of Aquatic and Fishery Sciences

Physical environments are changing globally due to anthropogenic impacts which have the potential to alter ecological interactions. To understand how ecological interactions are changing, long-term datasets are necessary to document ecological baselines from the past that are comparable to current ecological conditions. Stable isotope values can be useful chemical tracers for retrospective analyses which can elucidate changes in biogeochemistry and trophic interactions that influence food webs. My dissertation applies compound-specific stable isotope analysis (CSIA) of amino acids and inorganic nitrogen to understand long-term, regional, ecological responses to physical conditions in the northeast Pacific. I tested the long-term importance of salmon subsidies to Alaskan riparian ecosystems by measuring inorganic nitrogen concentrations, transformation rates, and nitrogen stable isotope values in soil following a 20-year carcass manipulation experiment. Carcass subsidies did not increase soil nitrogen concentrations or transformation rates but the nitrogen stable isotope value of ammonium was significantly enriched in ^{15}N compared to salmon carcasses, indicating the importance of salmon derived nutrients is likely overestimated for some systems. Using museum skull specimens from two species of pinnipeds in the northeast Pacific, harbor seals

(*Phoca vitulina*) and Steller sea lions (*Eumetopias jubatus*), I derived a century of predator stable isotope data. I compared the carbon and nitrogen stable isotope values of source amino acids to regional climate datasets and determined coastal food webs responded to climate regimes, coastal upwelling, and freshwater discharge, yet the strength of responses to individual drivers varied across the northeast Pacific. These findings demonstrate stable isotope data can serve as a tracer of nitrogen resources and phytoplankton dynamics that is specific to resources that are assimilated by food webs. To calculate pinniped trophic position from the historic dataset, I was the first to apply taxa-specific trophic enrichment factors, a system specific beta-value, a temporal lag to account for tissue turnover time, and a multi-trophic amino acid analysis framework within a single study. This approach constrained assumptions regarding physiological processes and vascular plant contributions to the food web, which can confound stable isotope data interpretation. I analyzed long-term predictors of harbor seal trophic position in Washington and identified delayed responses of harbor seals to both physical ocean conditions (upwelling, sea surface, discharge) and prey availability (Pacific hake, Pacific herring and Chinook salmon). Consideration for dynamic responses of harbor seals to their environment is an important factor for understanding predator-prey interactions as harbor seals respond to multiple ecological factors that are often changing simultaneously and their response occurs at multiple temporal scales. I then analyzed regional and decadal trends in pinniped trophic position in Alaska and identified the largest change in trophic position occurred in recent decades (2000 and 2010) but the direction of the trends diverged based on region and species. Gulf of Alaska pinnipeds are experiencing unique food web conditions in recent decades compared to the past likely in response to climate-induced ecological change in the region. Finally, I constructed a compartment model to explore the effect of stable isotope heterogeneity and consumer isotope incorporation rates on consumer trophic position estimates using both bulk stable isotope analysis and CSIA. Bulk stable isotope analysis produced consistent errors in trophic position

estimates by as much as one trophic level that were more pronounced in higher trophic level consumers and CSIA was more accurate than bulk stable isotope analysis. Altogether, these results show CSIA is a useful tracer for elucidating long-term physical forcing mechanisms on food webs and incorporating physiological processes that govern stable isotope fractionation into sampling and analysis design can uncover forcing mechanisms that would otherwise be overlooked.

TABLE OF CONTENTS

	Page
List of Figures	ii
List of Tables	iii
Introduction	1
Chapter 1: Riparian soil nitrogen cycling and isotopic enrichment in response to a long-term salmon carcass manipulation experiment	5
1.1 Abstract	5
1.2 Introduction	6
1.3 Methods	11
1.4 Results	17
1.5 Discussion	19
1.6 Tables	25
1.7 Figures	30
Chapter 2: Stable isotope signatures in historic harbor seal bone link food web-assimilated carbon and nitrogen resources to a century of environmental change	35
2.1 Abstract	35
2.2 Introduction	36
2.3 Methods	40

2.4	Results	47
2.5	Discussion	50
2.6	Tables	59
2.7	Figures	65
Chapter 3:	Delayed trophic response of a marine predator to ocean condition and prey availability during the past century	82
3.1	Abstract	82
3.2	Introduction	83
3.3	Methods	86
3.4	Results	90
3.5	Discussion	93
3.6	Tables	99
3.7	Figures	112
Chapter 4:	Recent divergent changes in Alaskan pinniped trophic position detected using compound-specific stable isotope analysis	123
4.1	Abstract	123
4.2	Introduction	124
4.3	Methods	128
4.4	Results	132
4.5	Discussion	135
4.6	Tables	141
4.7	Figures	143
Chapter 5:	The influence of temporal isotope heterogeneity and isotope incorporation rates on consumer trophic position estimation	150

5.1 Abstract	150
5.2 Introduction	152
5.3 Methods	155
5.4 Results	163
5.5 Discussion	167
5.6 Tables	175
5.7 Figures	179
Conclusion	192
Appendix A: Appendix 1	197
A.1 Text 1: Full analytical details for stable isotopes	197
A.2 Text 2: Identifying size and sex-based trends in harbor seal trophic position	199
A.3 Text 3: Identifying temporal trends in harbor seal trophic position	200
A.4 Text 4: Accounting for variability in trophic enrichment factors	201
Colophon	205
References	209

LIST OF FIGURES

Figure Number	Page
1.1 Nitrogen pathways in soil	30
1.2 Data and predicted values for the model with the most support: Stable Isotopes	31
1.3 Data and predicted values for the model with the most support: Concentrations and Transformations	32
1.4 Residual Plots for Best Models	34
2.1 Mechanisms of stable isotope change	66
2.2 Distribution of harbor seal specimens	67
2.3 Sex and Region based differences	68
2.4 Hierarchical $\delta^{15}N_{Phe}$ and $\delta^{13}C$ Models	69
2.5 Coefficients of Environmental Covariates	70
2.6 Alaska GDFA Results	72
2.7 Washington GDFA Results	73
2.8 Bone collagen stable isotope seasonality analysis	74
2.9 Bone collagen stable isotope length analysis	75
2.10 Time series of $\delta^{15}N_{Phe}$ data	76
2.11 Time series of $\delta^{13}C$ data	77
2.12 Time series of $\delta^{13}C$ data corrected for Suess effect	78
2.13 Time series of bulk $\delta^{15}N$ data	79
2.14 Residuals trends for linear models with the most support	80
2.15 Residuals for linear models with the most support	81

3.1	Spatial and temporal distribution of specimens	112
3.2	Temporal trends of harbor seal trophic position	113
3.3	Sex differences of harbor seal trophic position	114
3.4	Size trends of harbor seal trophic position	115
3.5	Seasonality of harbor seal trophic position	116
3.6	Temporal trends in ocean condition model residuals	117
3.7	Temporal trends in prey availability model residuals	118
3.8	Coefficients of harbor seal trophic position models	119
3.9	Conceptual representation of trophic position response to prey	120
3.10	Trophic position estimates applying $\beta_{(i-o),N}$	121
3.11	Trophic position estimates applying $\beta_{(i-o),NV}$	122
4.1	Spatial and temporal distribution of specimens	143
4.2	General trends in pinniped population abundance	144
4.3	Distribution of harbor seal trophic position data for male (M) and female (F) pinnipeds	146
4.4	Region-species classification included as a random effect (k)	147
4.5	Decade included as a random effect (k)	148
4.6	Combined decade, classification, and the decade-classification interaction effect	149
5.1	BSIA theoretical food web scenarios	180
5.2	CSIA theoretical food web scenarios	181
5.3	Trophic position estimation error effect sizes	182
5.4	BSIA simulated $\delta^{15}N$	183
5.5	BSIA simulated trophic position	184
5.6	CSIA simulated $\delta^{15}N$	185
5.7	CSIA simulated trophic position	186

5.8	BSIA tissue turnover sensitivity analysis	187
5.9	CSIA tissue turnover sensitivity analysis: lysine	188
5.10	CSIA tissue turnover sensitivity analysis: phenylalanine	189
5.11	Observed tissue half-life values	190
5.12	BSIA simulated trophic position: primary consumer baseline	191

LIST OF TABLES

Table Number	Page
1.1 The candidate model set tested for each response variable using AIC analysis	25
1.2 Competing models with relative support ($\Delta\text{AIC} < 2$) using AIC analysis for each response variable	27
1.3 Summary Statistics of Best Models	29
2.1 Ranges of stable isotope data	59
2.2 Environmental Datasets	60
2.3 Reduced Time Series	62
2.4 Nitrogen Phenylalanine T-Test	63
2.5 Bulk Carbon T-Test	64
3.1 Trophic position parameter values	99
3.2 Environmental Datasets	100
3.3 Prey Datasets	101
3.4 Ocean Condition Candidate Models	103
3.5 Prey Availability Candidate Models	105
3.6 Physiological delay top 10 models (ocean condition)	106
3.7 1-year ecological delay top 10 models (ocean condition)	107
3.8 2-year ecological delay top 10 models (ocean condition)	108
3.9 Physiological Delay Top 10 Models (Prey Availability)	109
3.10 1-Year Ecological Top 10 Models (Prey Availability)	110

3.11	2-Year Ecological Top 10 Models (Prey Availability)	111
4.1	Trophic position parameter values for Equation 2	141
4.2	Candidate Models	142
5.1	Baseline environments	175
5.2	Trophic Position Duration of Deviation	176
5.3	Duration of Trophic Position Deviation (days)	177
5.4	Range of Trophic position estimates with different baselines	178

ACKNOWLEDGMENTS

My dissertation research was funded by several grants, Washington Sea Grant, University of Washington, pursuant to National Oceanic and Atmospheric Administration (award nos. NA18OAR4170095 and NA19OAR4170360), and the Joint Institute for the Study of the Atmosphere and Ocean (JISAO) under NOAA Cooperative Agreement NA15OAR4320063 (contribution no. 2020-1116). I personally was funded by the National Marine Fisheries Service -Sea Grant Joint Fellowship Program in Population and Ecosystem Dynamics, the School of Aquatic and Fishery Sciences Departmental Fellowships, incuding the H. Mason Keeler Endowment for Excellence and the Clairmont L. and Evelyn S. Egvedt Fellowship, the American Fisheries Society WA/BC Chapter Jeff Cederholm Scholarship, and Teaching Assistantship positions.

I extend my deepest gratitude to my museum collaborators for permitting sampling and coordinating logistics. Specifically, I would like to thank Jeff Bradley and Sharlene Santana of the UW Burke Museum, Peter Wimberger and Gary Shugart of the Slater Museum, Link Olson and Aren Gunderson of the Museum of the North, Robert Delong of the National Marine Mammal Laboratory, Lesley Kennes and Gavin Hanke of the Royal BC Museum, and Darrin Lunde and John Ososky of the Smithsonian Institute. I thank Megan Stachura and Tom Royer for assistance with environmental datasets, and Chris Harvey and Jens Nielsen for helpful discussions and support. Hyejoo Ro and Karrin Leazer assisted in laboratory work. Mark Haught and Terry Rolfe assisted with GC/C/IRMS method development, maintenance, and troubleshooting.

I thank the Alaska Salmon Program at the University of Washington for facilitating access

to the field siteon Hansen Creek, specifically Jackie Carter, Katie McElroy, and Max Ramos for help with field sampling and logistics. The daily surveys and carcass manipulation (by 3– 5 people) have involved far more individuals than I can name, but I specifically thank Gregory Buck, Harry Rich, Jr., Curry Cunningham, Chris Boatright, Jackie Carter, and the undergraduate students in the Aquatic Ecological Research in Alaska classes.

I am eternally grateful for the community that has supported me over the past five years. Thank you to my advisor, Gordon Holtgrieve, who encouraged my eclectic research interests and always supported me in finding work-life balance. My other committee members — Drs. Eric Ward, Sarah Converse, Tim Essington, and Cecilia Bitz — challenged me to think about my work broadly, communicate clearly, and think critically about my analyses. Although they were not officially part of my committee, Drs. Jens Nielsen at the Alaska Fisheries Science Center, NOAA and Steve Perakis at the Forest and Rangeland Science Center, USGS, taught me so much about chemistry, collaboration, and mentoring. Thank you to to all past and present members of the Holtgrieve Lab for bringing joy and commiseration to the trials and tribulations of lab work. My fellow SAFS graduate students have been an important part of my community, thank you for your support and friendship.

And most importantly, thank you to my parents, brother, and partner. Your support has meant so much to me!

DEDICATION

To my grandmother, Gail Feddern, who has read every publication I have ever written

INTRODUCTION

Anthropogenic climate change will impact nutrient cycles, primary productivity, and thus ecosystem structure in the world's oceans, although considerable uncertainty still exists regarding the variability of these changes and how ecosystems will respond. Changes in primary production has implications for dependent marine ecosystems, as it influences abundance and interactions in both adjacent and non-adjacent trophic levels (Frank, Fisher, & Leggett, 2015; Ware & Thomson, 2005; Winder & Sommer, 2012). This bottom-up control of marine food webs is expected to reduce fishery yields by as much as 20% globally by 2100 due to productivity constraints at lower trophic levels (J. K. Moore et al., 2018). Given both resource availability and community composition of resources impact the function and stability of food webs (Narwani & Mazumder, 2012) it is likely ecosystem interactions will change in response to environmentally induced shifts in resources in the future.

Ecological interactions are a fundamental component to studying the function and dynamics of ecosystems. Currently, anthropogenic and climatic changes are altering ecological interactions at a global scale, thus, understanding how interactions function and how environmental perturbations will alter interactions is imperative. Studies of environmental control of food webs are often limited to only examining low trophic level species (Pershing, Head, Greene, & Jossi, 2010), or only include indices of either primary production or environmental change (E. Chassot, Mélin, Le Pape, & Gascuel, 2007; Ware & Thomson, 2005). Oceanic conditions such as sea surface temperature, freshwater discharge, wind, and ice cover, have been linked to abundance and recruitment of many fish species in the Northeast Pacific (C. J. Cunningham, Westley, & Adkison, 2018; Puerta, Ciannelli, Rykaczewski, Opiekun, & Litzow, 2019; Stachura et al., 2014), but studies rarely include proxies or indicators of either nutrient availability or primary productivity that enable mechanistic understanding of ecosystem response

to the environment.

Lower trophic levels are sensitive to environmental variation in bottom-up drivers of productivity (Frank, Petrie, Shackell, & Choi, 2006; Jennings & Brander, 2010; Ware & Thomson, 2005), but few studies have demonstrated how the impact of these changes span entire food webs on long time scales. Additionally, somatic growth of large bodied marine predators is not continuous and typically occurs on a longer temporal scale than phytoplankton dynamics making it challenging to link higher trophic level species to forcing lower in the food web. Similarly, marine predators can utilize resources at multiple spatiotemporal scales, creating a challenge for linking species abundance to independent observations of phytoplankton or nutrient dynamics. How environmentally induced changes in primary productivity ultimately influences nutrients available to and assimilated by the food web is thus poorly understood.

An empirical understanding of food web responses to environmental drivers requires long time series data that span multiple changes in climate regimes to decouple natural oscillations with long-term changes (Hastings et al., 2018; Litzow & Ciannelli, 2007; Tallis et al., 2010). In recent decades extreme changes in marine environments have become more common and these events have had substantial impacts on ecosystems. Marine ecosystems in Alaska are experiencing unprecedented environmental change that has altered abundance and size distributions of many fish species (Barbeaux, Holsman, & Zador, 2020; K. K. Holsman, Aydin, Sullivan, Hurst, & Kruse, 2019; Oke et al., 2020; Suryan et al., 2021). More recently, atmospheric circulation anomalies in the northeast Pacific Ocean have resulted in abnormally warm sea surface temperatures during the past decade (Walsh et al., 2018) and this environmental shift has altered fish abundances (N. A. Bond, Cronin, Freeland, & Mantua, 2015; Litzow et al., 2020). For example, the unprecedented marine heatwave that occurred in 2014 - 2016 triggered dramatic ecosystem change, including a 71% decline in Pacific cod in the Gulf of Alaska (Barbeaux et al., 2020) and declines in phytoplankton biomass, forage fish abundance, and changes in community structure (Suryan et al., 2021).

Reconstructing time series of indicators of ecosystem interactions is important to understand

how ecosystems have responded to environmental variability in the past and ultimately interpret potential food web responses to environmental conditions in the future; such datasets are distinctly lacking. Modern chemical analyses, such as compound-specific stable isotope analysis (CSIA) of inorganic nitrogen sources or amino acids, have potential to improve our understanding of food web interactions by 1) extending time series through retrospective analyses 2) identifying environmental forcing of the entire food web when measured in predators and 3) informing biologically relevant mechanisms of interactions, a former limitation of many ecosystem studies.

Analyses of nitrogen stable isotopes usually applies bulk stable isotope techniques which measures the $^{15}N/^{14}N$ ratio of nitrogen as a weighted average of all nitrogen present in a given sample. For tissue samples, $^{15}N/^{14}N$ measurements are a weighted average of the concentrations of all amino acids present in the protein of an individual tissue. For soil analyses, typically $^{15}N/^{14}N$ includes both organic and inorganic form. However, the $^{15}N/^{14}N$ of an individual compound, known as compound-specific stable isotope analysis, represents the kinetic and diffusive fractionation factors exerted on that compound through chemical conversions, typically from biogeochemical or physiological processes. Thus, nitrogen isotope values can provide a useful link between biogeochemical reactions that regulate nutrient availability and primary production, and ecological responses, without being confounded by nitrogen containing compounds that are not utilized by an ecosystem.

Here I aim to reconstruct historical food web interactions using stable isotopes as chemical tracers to:

1. Identify how long-term (20-years) changes in salmon abundance impact nitrogen dynamics in riparian soils.
2. Understand the how ocean conditions alter food web-assimilated nitrogen resources and primary production in the northeast Pacific.

3. Identify dominant historical drivers of predator trophic position in the northeast Pacific, using trophic position as an indicator of major changes in food web dynamics and ecological interactions.
4. Establish a framework to improve trophic position estimation of bulk and compound-specific stable isotope analysis for historical and contemporary studies.

Chapter 1

RIPARIAN SOIL NITROGEN CYCLING AND ISOTOPIC ENRICHMENT IN RESPONSE TO A LONG-TERM SALMON CARCASS MANIPULATION EXPERIMENT

A version of this chapter was published as: Feddern, M. L., Holtgrieve, G.W., Perakis, S. S., Hart, J., Ro, H., & Quinn, T. P. (2019). Riparian soil nitrogen cycling and isotopic enrichment in response to a long-term salmon carcass manipulation experiment. *Ecosphere*, 610(11): e02958. <https://doi.org/10.1002/ecs2.2958>

1.1 *Abstract*

Pacific salmon acquire most of their biomass in the ocean before returning to spawn and die in coastal streams and lakes, thus providing subsidies of marine-derived nitrogen (MDN) to freshwater and terrestrial ecosystems. Recent declines in salmon abundance have raised questions of whether managers should mitigate for losses of salmon MDN subsidies. To test the long-term importance of salmon subsidies to riparian ecosystems we measured soil N cycling in response to a 20-year manipulation where salmon carcasses were systematically removed from one bank and deposited on the opposite bank along a 2 km stream in south-western Alaska. Soil samples were taken at different distances from the stream bank along nine paired transects and measured for organic and inorganic nitrogen concentrations, and nitrogen transformation rates. MDN was measured using $^{15}\text{N}/^{14}\text{N}$ for bulk soils, and NH_4^+ and NO_3^- soil pools. Stable isotope analyses confirmed $^{15}\text{N}/^{14}\text{N}$ was elevated on the salmon enhanced bank compared to the salmon depleted bank. However, $^{15}\text{N}/^{14}\text{N}$ values of plant-available inorganic nitrogen exceeded the $^{15}\text{N}/^{14}\text{N}$ of salmon inputs, highlighting N isotope

fractionation in soils that raises significant methodological issues with standard MDN assessments in riparian systems. Surprisingly, despite 20 years of salmon supplementation, the presence of MDN did not cause a long-term increase in soil N availability. This finding indicates the importance of MDN to ecosystem N biogeochemistry and riparian vegetation may be overestimated for some systems. Given that essential nutrients can also be pollutants, we urge more critical analyses of the role of MDN to inform compensatory mitigation programs targeting salmon nutrient enhancement.

1.2 Introduction

Pacific salmon (*Oncorhynchus spp.*) migration from marine environments to freshwater spawning grounds is a textbook case of cross-ecosystem nutrient subsidies, and dozens of studies have identified the presence of marine-derived nitrogen (MDN) from salmon as crossing ecosystem boundaries from oceans to freshwaters and into the terrestrial environment (sensu, (Polis, Power, & Huxel, 2004; Schindler et al., 2003; Scott M, Richard T, Mary F, & Mark S, 2002). Declines in Pacific salmon populations in many areas, caused by human activities (overharvest, habitat degradation, dams) (Richard et al., 2007), and the concern over loss of MDN to coastal watersheds has made restoration of salmon nutrients a focal point for many management and mitigation strategies. For example, in the Columbia River Basin where Pacific salmon populations have declined, legislation requiring compensatory mitigation has led to nutrient enhancement programs, on the foundation that habitats have lost critical nutrients from salmon and therefore augmentation is necessary to maintain ecosystem function (Collins, Marcarelli, Baxter, & Wipfli, 2015).

Salmon bring nutrients, including phosphorus (P) and other compounds in addition to nitrogen (N), into freshwater and terrestrial food webs through two pathways: 1) direct consumption of tissues by predators and scavengers, and 2) autotrophic or heterotrophic assimilation of nutrients released as salmon spawn, die, and eventually decay (Scott M et al., 2002). Salmon are enriched in the heavy isotope of nitrogen (^{15}N) relative to the light isotope

(^{14}N) when compared to terrestrial and watershed-derived N. This isotopic enrichment has been used to quantitatively trace the presence of salmon derived nutrients into watersheds (Schindler et al., 2003). For example, the proportion of N derived from salmon ranges from approximately 30% – 75% in fish and aquatic invertebrates (Naiman, Bilby, Schindler, & Helfield, 2002), 10 – 90% in piscivorous mammals such as bears, and 20 – 40% in piscivorous fishes near salmon spawning grounds (Bilby, Fransen, & Bisson, 1996; Chaloner, Martin, Wipfli, Ostrom, & Lamberti, 2002; Claeson, Li, Compton, & Bisson, 2006; Hilderbrand et al., 1999).

The annual return of this predictable and abundant, yet temporally limited, high quality resource drives the foraging ecology of both terrestrial and aquatic consumers (Quinn, Helfield, Austin, Hovel, & Bunn, 2018; Schindler et al., 2013). Carcasses and roe are documented food sources for over 22 species of mammals, birds (C. J. Cederholm, Houston, Cole, & Scarlett, 1989), fishes (Scheuerell, Moore, Schindler, & Harvey, 2007), and invertebrates (Meehan, Seminet-Reneau, & Quinn, 2005; Winder, Schindler, Moore, Johnson, & Palen, 2005). Bear population density, body size, and reproductive output has been correlated with meat (primarily salmon) consumption, with piscivorous populations having 55 times higher density than their meat-limited counterparts (Hilderbrand et al., 1999). In aquatic ecosystems, salmon carcass abundance has been correlated with elevated growth rates of invertebrates, and with size, density, and condition factor of juvenile salmonids (R. E. Bilby, Fransen, Bisson, & Walter, 1998; Wipfli, Hudson, Caouette, & Chaloner, 2003).

The presence of MDN has been documented in aquatic primary producers, though its overall ecological importance remains ambiguous. Via this bottom-up pathway, salmon supply critical limiting nutrients that can increase primary and/or bacterial productivity, which are subsequently transferred to consumers and up through the food web (Chaloner et al., 2002; Holtgrieve & Schindler, 2011; M. S. Wipfli, Hudson, & Caouette, 1998). Higher salmon returns are correlated with MDN signatures in lower trophic levels including zooplankton and periphyton (B. P. Finney, 2000; Holtgrieve, Schindler, Gowell, Ruff, & Lisi, 2010; Kline

Jr et al., 1993). Both direct ecological and paleolimnological evidence suggest MDN and P positively influence primary production in lakes (Moore et al., 2007). For example, commercial fisheries remove upwards of two-thirds of MDN which would otherwise enter some freshwater lakes in Alaska, resulting in a 3-fold decline in algal production (Schindler, Leavitt, Brock, Johnson, & Quay, 2005). In stream ecosystems, the decomposition of salmon increases dissolved organic and inorganic nutrients, including highly available forms such as orthophosphate (PO_4^{3-}) and ammonia/ammonium ($\text{NH}_3/\text{NH}_4^+$). These nutrients can stimulate epilithon growth (bacteria and algae), though the magnitude of this response is highly variable, and dependent on other growth limiting factors such as sunlight and disturbance (Janetski, Chaloner, Tiegs, & Lamberti, 2009; Johnston, MacIsaac, Tschaplinski, & Hall, 2004; Mitchell & Lamberti, 2005).

In the terrestrial realm, bottom-up effects of MDN from salmon are also thought to be ecologically important, though this has been difficult to demonstrate rigorously. Studies across the range of salmon in North America have inferred that up to 26% of foliar N in riparian plants is marine derived, with foliar N levels often correlating with salmon abundance and distance from the salmon spawning location (e.g., Hocking & Reynolds, 2012; Reimchen & Fox, 2013). While MDN is clearly present in terrestrial producers, direct evidence of the importance of MDN for ecosystem function and productivity is much less evident. Helfield & Naiman (2001) measured tree growth increments in areas with and without salmon and found higher growth in one species (Sitka spruce) in areas where salmon nutrients were present, although these findings were later contested on statistical grounds (Kirchhoff, 2003). Hocking & Reynolds (2012) observed decreased understory plant diversity with increasing salmon abundance, though this pattern was largely attributed to increased dominance of a single N tolerant species (salmonberry). Reimchen & Fox (2013) suggested that salmon abundance increased tree growth, but tree ring $^{15}\text{N}/^{14}\text{N}$ values were not related to salmon abundance; other growth limiting factors such as temperature and location were important covariates. Most recently, Quinn et al. (2018) examined tree growth increments in the

riparian zone of a small Alaskan stream before and after a 20-year, > 200,000 kg, salmon carcass manipulation. In the two decades prior to manipulation, white spruce (*Picea glauca*) on average grew faster on one bank compared to the other. The subsequent decades of carcass manipulation enriched the naturally slower growing side, and were associated with increased growth. However, the growth effect of the carcasses was smaller than the natural side-to-side variation, and other important site and landscape factors such as forest demography, climate, aspect, and water availability were not fully considered, a common trend in MDN studies of riparian vegetation.

Interpreting the contributions of MDN to terrestrial producers using stable isotopes is often highly simplified, and does not consider how variability of N sources and overall N availability may confound results. MDN analyses apply simple two-source mixing models to infer the proportion of total N derived from salmon using equation (1.1):

$$MDN = \frac{SAM - TEM}{MEM - TEM} * 100 \quad (1.1)$$

MDN is the percentage of marine derived nitrogen in a given sample, *TEM* is the terrestrial end member ($\delta^{15}\text{N}$ value representing 0% MDN), *MEM* is the marine end member ($\delta^{15}\text{N}$ value representing 100% MDN) which is typically 12.65‰ for sockeye salmon. *SAM* values are the values in a salmon area and *TEM* is derived from a non-salmon control. When applied to terrestrial vegetation, the terrestrial end-member for the mixing models is typically determined by sampling the $^{15}\text{N}/^{14}\text{N}$ of the same species of plant either laterally away from the stream (where MDN contribution is expected to be small), upstream of barriers to salmon migration, or in watersheds without salmon. For the salmon end-member, a single value equal to the average $^{15}\text{N}/^{14}\text{N}$ of salmon (12.62 ± 0.31 per mille for sockeye salmon) is typically used.

Inherent assumptions with these models therefore include: 1) reference sites are biogeochemically similar to salmon sites and 2) the isotopic signature of salmon is unchanged in the soils prior to plant uptake. N cycling in soils is strongly controlled by position in the landscape and contains a number of chemical reactions which fractionate N isotopically (Högberg,

1998; T. A. Wheeler, Kavanagh, & Daanen, 2014) (Figure 1.1), therefore these assumptions may not be valid.

Experiments examining the contributions of MDN are often limited by short timescales, and relatively few experiments investigate changes in plant-available soil N pools important to plant nutrient uptake and growth (Collins et al., 2015). Studies examining spatial and temporal impacts of salmon on soil inorganic N have identified highly localized responses (effects only observed < 30 cm from carcasses) where soil ammonium (NH_4^+) and nitrate (NO_3^-) increase for weeks to months (Drake, Naiman, & Bechtold, 2006; Gende, Miller, & Hood, 2007; Holtgrieve, Schindler, & Jewett, 2009) and rarely consider long-term N retention in the system. Experiments typically examine the contributions of MDN by nutrient addition not nutrient removal; however, nutrient removal is important for understanding the effects of lower numbers of salmon returning to coastal watersheds due to fishing, habitat reduction, and climate change. In addition, previous research observed a strong effect of watershed slope on $^{15}\text{N}/^{14}\text{N}$ in riparian plants and attributed this to topography concentrating carcasses near streams (Hocking & Reynolds, 2012). However, watershed topography also influences soil water content and N cycling, which affect N isotopes (Högberg, 1998) and therefore complicates MDN assessments.

To resolve the extent to which salmon carcasses contributed MDN to plant-available N pools and the long-term ecological response to this subsidy, we present a second study of the 20-year carcass manipulation experiment described in Quinn et al. (2018). While Quinn et al. (2018) focused on tree growth before and after the manipulation, the objective of this work was to determine whether prolonged enhancement and reduction of salmon subsidies altered long-term soil N cycling, similar to that documented in forests receiving N fertilizer additions (Lu et al., 2011; Prescott, Corbin, & Parkinson, 1992; Prescott, Kishchuk, & Weetman, 1995). If long-term changes in N availability due to salmon enhancement or reduction were observed, compensatory nutrient subsidies may be valuable for maintaining critical ecosystem functions in riparian areas with reduced salmon returns. If not, then the

addition of nutrients as a management response to low salmon returns may have unintended negative consequences (*sensu* Compton et al., 2006). Specifically, the importance of MDN to riparian ecosystems was assessed by 1) evaluating the presence of MDN in soils enhanced and depleted in salmon carcasses through bulk stable isotope analysis of N, 2) quantifying the response of plant-available N pools ($[NH_4^+]$ and $[NO_3^-]$) and their rate of supply via mineralization and nitrification, 3) considering how fractionation in soils may impact mixing model results by measuring $^{15}N/^{14}N$ of NH_4^+ and 4) comparing these results to the vegetation responses measured by Quinn et al. (2018) at the same site. This research fills key knowledge gaps by examining the long-term legacy of inorganic N pools, both salmon addition and removal, and considering site variability that may impact the assumption of biogeochemical similarity between test and control sites, following a 20-year manipulation.

1.3 Methods

1.3.1 Site Description and Sample Collection

This study was conducted on Hansen Creek, a ~2 km long, 2nd order tributary to Lake Aleknagik in the Wood River system of Bristol Bay, AK and uses the same carcass manipulation described in Quinn et al. (2018). Briefly, from 1997-2016 an average of 10,853 sockeye salmon returned to the stream annually. Overstory vegetation is dominated by white spruce and paper birch (*Betula papyrifera*), and unlike many other watersheds in the region, it has a low density of symbiotic N2-fixing alder (*Alnus spp.*) (Helfield & Naiman, 2002). From 1997-2016 the stream was surveyed daily during the annual sockeye salmon (*Oncorhynchus nerka*) run and all dead salmon were removed from the creek and the river right bank to a distance of about 5 m and tossed onto the river left bank. To avoid double counting carcasses on the river left bank, carcasses naturally occurring on the river left bank were also relocated to a distance of about 5 m, thus all carcasses (with the exception of those moved by wildlife, see Quinn et al. (2018)) were located between 3 – 6 m on the river left bank. Therefore, the right side of the stream experienced a reduction in carcass density (depletion) while the

left bank received an increase in carcasses (enhancement). Quinn et al. (2018) calculated that prior to manipulation the both banks averaged 4545.6 kg of salmon annually and after manipulation the river left bank averaged 13,381 kg of salmon and the river right bank averaged 2,260 kg of salmon annually, a 9.6-fold difference. Approximately 108,530 individual fish (in many cases partially consumed by bears) were translocated over the 20-year period representing a total of 267,620 kg of salmon, 8,028 kg of N and 1,356 kg of phosphorus (P) (Quinn et al., 2018). To estimate the mass of nitrogen added per m² we assumed all salmon were tossed within 6 m of the creek's edge along the entire 2 km creek, thus within a 12,000 m² area.

Soil samples were collected from the riparian zone on 13 July, 2017 (prior to arrival of salmon and any carcass manipulation that season) along nine sets of paired transect sites. Paired transects were used to control for naturally occurring salmon density. Transects covered the full 2 km length of the stream and were selected to represent typical riparian vegetation and high annual carcass abundance. Each transect included sampling sites at 1, 3, 6, 10, and 20 m from the bank-full point. Sampling occurred during peak growing season approximately one week prior to the arrival of the first salmon in the creek. Thus, our sampling was intended to capture the long-term legacy of MDN manipulations and specifically avoid short-term pulses following salmon return that may not represent a system-level change in N availability, retention, and recycling in soils, and has already been documented in multiple short-term studies. A 5 cm x 5 cm x 10 cm soil column was taken for each sample site and the litter layer was removed before storing at 4°C in airtight plastic bags for 48 hours prior to processing. Nitrogen cycling decreases dramatically with depth, sampling at this depth includes the O and A horizons where a majority of nitrogen cycling occurs (Sparks, Soil Science Society of, & American Society of, 1996).

1.3.2 Soil nitrogen concentrations and transformations

Soil $[\text{NH}_4^+]$, $[\text{NO}_3^-]$, and N transformations were measured according to Holtgrieve et al. (2009). Briefly, we extracted 10 to 12 g of field-moist sieved ($< 2 \text{ mm}$) soil with 100 mL of 2 M potassium chloride (KCl) by shaking for 60 s, followed by settling for 24 hours prior to filtration through pre-leached Whatman #1 filter papers. Approximately 8 mL of filtered extracts were frozen and later analyzed colorimetrically for $[\text{NH}_4^+]$ and $[\text{NO}_3^-]$ with an Auto-Analyzer 500 Model (Perstorp Analytical Co, Analytical Service Station, Seattle, WA, USA). The remaining extract was frozen prior to stable isotope analyses (see below). To estimate inorganic N transformation rates, a second 10 to 12 g soil subsample was incubated aerobically in the dark for 15 d at 20°C prior to extraction, filtration, and analysis as above. Net mineralization was calculated as the sum of the change in $[\text{NH}_4^+]$ and $[\text{NO}_3^-]$ divided by the incubation duration, and net nitrification was calculated as the change in $[\text{NO}_3^-]$ over the incubation duration and represents the conversion of NH_4^+ to NO_3^- . $[\text{N}_{\text{org}}]$ was calculated by taking total soil N concentration, $[\text{N}_{\text{tot}}]$ determined by elemental analysis (see below) and subtracting $[\text{NH}_4^+]$ and $[\text{NO}_3^-]$. All soil N values were corrected for gravimetric soil water content (g H₂O/g dry soil) determined by drying 50 to 100 g of field-moist soil at 105°C for 48 h (Klute, 1986).

1.3.3 Stable isotope analysis

Fresh soil was freeze dried for 48 h and ground into a uniform powder ($< 212 \mu\text{m}$) using a ball mill prior to analysis for nitrogen ($^{15}\text{N}/^{14}\text{N}$) and carbon ($^{13}\text{C}/^{12}\text{C}$) stable isotope ratios at the University of Washington's IsoLab using a Costech Elemental Analyzer, Conflo III MAT253 for continuous flow-based measurements. This procedure also provided total carbon and nitrogen concentrations, $[\text{C}_{\text{tot}}]$ and $[\text{N}_{\text{tot}}]$, and percent C and N, of the soil samples. Data are reported using standard delta notation, which describes the per mil deviation in the ratio of heavy to light isotope relative to accepted international standards, in this case air and Vienna Pee Dee Belemnite (VPDB) for N and C respectively.

For $^{15}\text{N}/^{14}\text{N}$ stable isotope analysis of NH_4^+ and NO_3^- , KCl extracts were placed in Erlenmeyer flasks for diffusion using modified methods from D. M. Sigman et al. (1997) and Holmes, McClelland, Sigman, Fry, & Peterson (1998). To retrieve NH_4^+ as gaseous NH_3 , 300 mg of MgO and an acid trap (1 cm glass fiber filter treated with KHSO_4 and sealed in Teflon) were added to each flask, immediately stoppered, sealed with parafilm, and shaken for six days prior to removal of acid traps to a desiccator for 3 to 4 days. The same extracts were then shaken uncovered for one day to remove any remaining NH_4^+ . To retrieve NO_3^- as NH_3 , another 300 mg of MgO were added to each extract and immediately followed with 75 mg of Devarda's alloy and an acid trap, then processed as above. Samples were run in four separate batches, for each batch three blanks (KCl with no soil extract) and three reference standards, NH_4Cl and KNO_3 with known $^{15}\text{N}/^{14}\text{N}$, were also run. Batch blanks showed quantifiable N from the KCl; therefore, a two-source mixing model correction was applied to both samples and reference standards using (1.2):

$$\delta^{15}N_{\text{blankcorrected}} = \frac{\delta^{15}N_{\text{measured}} * (N_{\text{blank},x} + N_{\text{extracted}}) - (\delta^{15}N_{\text{blank},x} * N_{\text{blank},x})}{N_{\text{extracted}}} \quad (1.2)$$

Where x represents an individual batch, $N_{\text{blank},x}$ is the average measured mass (μg) of nitrogen in a blank for a given batch, and $\delta^{15}N_{\text{blank},x}$ is the average measured $\delta^{15}\text{N}$ of blanks for a given batch. $\delta^{15}N_{\text{measured}}$ is the $\delta^{15}\text{N}$ value for a given sample, and $N_{\text{extracted}}$ is the mass of nitrogen (μg) measured in the sample. A standard correction was then applied to the blank corrected measurements with (1.3):

$$\delta^{15}N_{\text{corrected}} = \delta^{15}N_{\text{blank,corrected}} - (Standard_{\text{measured},x} - Standard_{\text{true}}) \quad (1.3)$$

Where $Standard_{\text{measured},x}$ is the average measured value of the standard for a given batch. All reported $\delta^{15}\text{N} - \text{NH}_4^+$ and NO_3^- values are expressed as the $\delta^{15}N_{\text{corrected}}$, where a blank and standard correction has been applied. The internal standard of the $\delta^{15}\text{N}$ of NO_3^- had a -23.6 to 9.6‰ deviation from its true value, indicating a significant methodological issue. Given there was not enough sample to refine these methods and the potential for standard corrections of this magnitude to be misleading, $\delta^{15}\text{N}$ of NO_3^- data are not reported here.

C:N ratio, percent nitrification, and %C were also calculated to evaluate N availability and retention across the sites. C:N ratios were calculated on a mass basis Percent nitrification was calculated as (1.4):

$$\text{PercentNitrification} = 100 * \text{NetNitrification}/\text{NetMineralization} \quad (1.4)$$

1.3.4 Statistical analyses

We used multi-model selection procedures via Akaike's information criterion (AIC) to identify how salmon carcass treatment governed a suite of response variables using the stats v3 and lme4 packages in R. These response variables were: $\delta^{15}\text{N}$ and $\delta^{13}\text{C}$ of bulk soil, $\delta^{15}\text{N}$ of NH_4^+ , $[\text{NH}_4^+]$ and $[\text{NO}_3^-]$, net mineralization and net nitrification, $[\text{N}_{\text{org}}]$, gravimetric water content (GW), and C:N. For all response variables, candidate models Table 1.1 included bank (left vs. right) and distance from river's edge. A linear and quadratic interaction structure for bank and distance were fit for each response variable and these interaction terms allowed the effect of distance to vary by bank and the effect of bank to vary by distance. A log_e transformation was used for the distance. GW was considered as a covariate for all response variables, soil $[\text{NH}_4^+]$ was considered as a covariate for net nitrification, and soil $[\text{N}_{\text{org}}]$ was considered as a covariate for net mineralization, given $[\text{N}_{\text{org}}]$ and $[\text{NH}_4^+]$ function as the substrate for mineralization and nitrification respectively. $[\text{N}_{\text{tot}}]$ was considered as a covariate for $\delta^{15}\text{N}$ and $\delta^{13}\text{C}$ of bulk soil, and for $\delta^{15}\text{N}$ of NH_4^+ . The best model was selected from the candidate model set using AIC for each response variable.

Two model parameters – bank (left vs. right) and distance from the stream – were used to test salmon carcass and site variability impacts to soil N cycling. Changing the number of salmon carcasses on each bank was the primary goal of the manipulation; however, the two banks potentially differ in aspect, soil type, and drainage, which can affect nutrient cycling and generate a bank effect unrelated to salmon manipulation (I. Chapin F. Stuart, Matson, Vitousek, & Chapin, 2011). Notably, the salmon enhanced bank has a northwest facing slope within 20 m of the creek edge. Distance from the stream reflects the magnitude of salmon

manipulation because carcasses were placed primarily 3 – 6 m from the stream’s edge. Other factors such as vegetation, soil type, and water availability can also change with distance laterally from the stream edge, though such changes are expected to be more continuous, rather than focused on the same 3 – 6 m band where salmon were placed. These differences in expected lateral patterns in soil properties due to salmon (focused at 3 – 6 m) verse other factors (more continuous) provide a means to test whether salmon significantly altered soil patterns in our experiment.

We inferred that salmon significantly influenced a soil property when that soil property met the following conditions: (a) the property differed between the study banks, (b) varied with distance from the stream edge, and (c) displayed a peak response at 3 - 6 m on the salmon addition bank. All conditions (a, b, c) are required to infer that salmon significantly altered the soils on the treatment bank. In contrast, we inferred that support for only one of these parameters demonstrates underlying site variability in the system. Effects of natural site variability on soil properties is also an important component to test. Control sites are typically assumed to be biogeochemically similar to carcass sites without validating this assumption, despite control sites often being located at different stream reaches or on different streams altogether. For each of the nine response variables, three competing hypotheses were compared, that the differences in response variables were due to H1) a bank and/or distance effect that does not demonstrate a peak response between 3 – 6 m indicating site variability not caused by salmon manipulation, H2) a bank and distance effect as a quadratic interaction with a peak between 3 – 6 m indicating a response to salmon manipulation or H3) no difference caused by distance and bank indicating support for the other covariates tested. These hypotheses were tested by categorizing each candidate model into one of the three hypotheses (Table 1.1) and considering the hypothesis categorization for the model with the most support, and any additional competing models with relative support (ΔAIC value of < 2) [Burnham & Anderson (2003)] for each response variable under consideration (e.g., $[NH_4^+]$, $[NO_3^-]$, $\delta^{15}N$, etc.). If models showed support for H2, the effect

of salmon was confirmed by examining whether the response variable peaked at the salmon enhanced bank between 3 – 6 m. If this did not occur, the response is due to site variability and not salmon.

1.4 Results

Bulk soil stable isotope analysis indicated that salmon carcasses enriched the N isotope pools (Table 1). $\delta^{15}N$ values peaked between 3 and 6 m from the stream edge, which was the distance salmon were typically relocated to during the experiment and declined at distances greater than 6 m. Maximum $\delta^{15}N$ of bulk soils was 11.8‰ for the salmon enhanced bank and 11.6‰ for the salmon depleted bank and no observations exceeded the sockeye salmon end-member value of 12.6‰ (Figure 1.2a). $\delta^{13}C$ was more enriched at greater distances from the bank and on average was highest at 20 m (Figure 1.2b). $\delta^{13}C$ was primarily governed by distance, with some evidence [N_{tot}] and bank also had an effect (1.2).

Salmon carcass manipulation also enriched $\delta^{15}N$ of soil NH₄⁺. Stable isotope values were enriched at 3 m from the stream edge on the salmon enhanced bank, and declined at distances > 3 m. On the salmon depleted bank, $\delta^{15}N$ of soil NH₄⁺ was most enriched at 1 m and declined with distance (Figure @ref(fig:modsupp1.2)C). The only model with support contained a quadratic interaction of distance and bank, which provides strong evidence that $\delta^{15}N$ of NH₄⁺ was affected by salmon (Table 1.2). In contrast to bulk soil N, $\delta^{15}N$ values of NH₄⁺ exceeded the salmon endmember of 12.6‰ for 23% of all observations (n=21).

Inorganic nitrogen concentrations were primarily governed by bank and GW (Table 1.2). The salmon enhanced bank had a higher mean [NH₄⁺] and [NO₃⁻] compared to the salmon depleted bank (Figure 1.3d, e). The most supported models for both [NH₄⁺] and [NO₃⁻] showed evidence for H1, that observed differences were not caused by salmon. For [NH₄⁺] there was substantial model uncertainty, with six competing models receiving relative support ($\Delta AIC < 2$) (Table 1.2) but none of the competing models supported a salmon effect. Two competing models for [NO₃⁻] supported a site variability effect and one competing model

supported a salmon effect (Table 1.2) and all three contained gravimetric water content as a covariate. This indicates $[NH_4^+]$ was driven by site factors unrelated to salmon while $[NO_3^-]$ was driven by gravimetric water content and with some support for salmon enhancement.

Nitrogen transformation rates were unaffected by salmon carcass manipulation. Both net nitrification and net mineralization models with relative support contained N substrate ($[NH_4^+]$ and $[N_{org}]$ respectively), and the models with the most support did not include distance or bank. Net mineralization had some model uncertainty, with four models receiving relative support; however, all of the competing models supported either H1 or H3 with no support for a salmon effect. $[N_{org}]$ was the only covariate included in all of the competing models, indicating $[N_{org}]$ was the most important covariate tested for determining net mineralization. Net nitrification had greater model certainty and both models that received relative support contained $[NH_4^+]$ and gravimetric water content. Similar to net mineralization, these models supported H1 and H3 with no support for H2, the salmon effect, though net nitrification was slightly higher on average between 3 – 6 m on the salmon enhanced bank (Table 1.2). Overall, these results demonstrated the manipulation of salmon carcasses did not have clearly detectable effects on N transformation rates.

Both $[N_{org}]$ and GW indicated there are site differences caused by distance and bank unrelated to salmon carcass manipulation. On average $[N_{org}]$ was higher on the salmon depleted bank than the salmon enhanced bank. There was model support of H1 for both GW and $[N_{org}]$, indicating these variables decrease with distance (Table 1.2, Figure 1.3 h, i). While there was some evidence that there was both a distance and bank effect on GW, it was not caused by salmon as the salmon enhanced bank does not show a peak GW at 3 - 6 m from the stream, which was where there was the highest observed isotopic enrichment and expected MDN. However, one competing model for $[N_{org}]$ did support H2, indicating site factors and salmon may both affect $[N_{org}]$. However, the mean $[N_{org}]$ for the salmon enhanced bank was 18.42 mg/g and 18.97 mg/g for the salmon depleted bank indicating salmon decrease $[N_{org}]$, if they affect it at all.

C:N, percent nitrification, and percent carbon indicate relatively high nitrogen availability across sampling sites in the Hansen Creek system. Mean percent carbon was 24.2 and 24.9 on the enhanced and depleted banks respectively (S3). Soil C:N of bulk isotopes was less than 20 for all sites, with a mean of 15.8 (enhanced) and 14.2 (depleted). These values are well below the critical microbial C:N threshold of 29, demonstrating N is more available to meet microbial metabolic demands relative to C (Figure 1.3j). In contrast, percent nitrification was relatively high with a mean of 64% and 62% on the enhanced and depleted banks (S3).

1.5 Discussion

This study confirmed that MDN was both present in soils and increased on the bank enhanced with salmon carcasses for 20 years. However, plant-available inorganic N pools and N transformation rates measured in soil during the peak growing season immediately prior to the annual return of salmon were largely unaffected by salmon enhancement. Even though the salmon enhanced bank had increased net nitrification compared to the salmon depleted bank, our analysis found no pattern with distance from the stream, suggesting that elevated nitrification was caused by bank characteristics unrelated to salmon carcass density. Given numerous conventional long-term fertilization experiments worldwide have shown a consistent pattern of elevated soil inorganic N pools and N transformations, (Högberg, Fan, Quist, Binkley, & Tamm, 2006; Lu et al., 2011), it was surprising that 20 years of MDN inputs did not clearly accelerate soil N cycling in our study. Soils are the dominant (> 70%) sink for added N in forests worldwide (P. H. Templer et al., 2012) and tree growth in high latitude conifer forests is often strongly N-limited (Nordin, Högberg, & Näsholm, 2001), both of which should have fostered retention of salmon N inputs to our site. Indeed, the 20 years of cumulative salmon N additions in the zone near the stream in our study (~ 6,690 kg N/ha) greatly exceeded typical riparian surface soil N pools (500 to 2500 kg N/ha) (Morris & Stanford, 2011; Perry, Shafroth, & Perakis, 2017; Walker, 1989), suggesting that even

partial retention of salmon N inputs in soils should have increased soil [N_{org}]. The lack of increase in soil [N_{org}] due to salmon that we observed is consistent with the lack of increase in N availability, because soil [N_{org}] fuels long-term changes in N availability and recycling via plant uptake, litterfall, and decomposition (Chappell, Prescott, & Vesterdal, 1999; Perakis & Sinkhorn, 2011; Steven, Joselin, & David, 2012). Combined with observations of low C:N and high percent nitrification, this indicates N from salmon subsidies is not being retained in this system. Overall, the lack of increase in soil organic and inorganic N concentrations and N transformations that we observed following 20-year salmon manipulation raises questions of whether plant growth responses should be expected at our site.

Prior work at Hansen Creek inferred that MDN stimulated white spruce growth based on tree ring analyses (Quinn et al., 2018). However, substantial salmon enhancement corresponding to approximately 669 g/m² (6,690 kg/ ha) of N and 113 g/m² (1,130 kg/ha) of P over the past 20 years was unable to overcome pre-treatment differences in forest growth between banks. For reference, it is estimated white spruce in floodplain stands require approximately 1.35 g/m²/y of N (F. S. Chapin, 2006), which was far exceeded by the mean change of 33.45 g/m²/y of N added from this manipulation. Additionally, fertilization experiments apply N on the order of 100 - 1,000 kg/ha with clear results (Chappell et al., 1999), a much lower application rate than in this study. Factors such as climate, stand demography, and site and landscape variability also affect tree growth in this system. Indeed, white spruce growth response to recent warming across southwest Alaska depends strongly on tree density (M. Wright, Sherriff, Miller, & Wilson, 2018). Basal area density is highly variable across our site, differing on average 40% between salmon-enhanced and salmon-depleted banks, although the difference was not statistically significant (Quinn et al., 2018). Ultimately, the hierarchy of drivers of tree growth in this ecosystem appears to be landscape position (and associated forest demography) followed by climate and thirdly, nutrients. All told, a lack of long-term changes in soil nutrient dynamics and only marginal response in tree growth indicates that salmon nutrients are not a strong bottom-up force in northern riparian forest dynamics.

Our $^{15}\text{N}/^{14}\text{N}$ stable isotope data raise further questions of assessing MDN subsidies to tree growth. Vegetation typically takes up only 17% of added N to forests, with soils instead being the dominant N sink (P. H. Templer et al., 2012). Thus, elevated bulk soil $^{15}\text{N}/^{14}\text{N}$ in our study suggests a potentially significant MDN sink in soil. On the other hand, elevated bulk soil $^{15}\text{N}/^{14}\text{N}$ may also reflect increases in soil N fractionation during N cycling and loss under salmon. Highly localized N pulses (as occur with MDN and other N subsidies) temporarily exceed plant and soil N sinks, leading to accelerated N loss via ammonia volatilization, nitrification and nitrate leaching, and/or denitrification (Perakis, 2002). All of these N loss pathways favor ^{14}N and discriminate against ^{15}N (in some cases with a fractionation up to 30‰), and effects are strongest at high N availability, leading to high values of residual soil ^{15}N (Högberg, 1998). Prior work has shown that MDN inputs accelerate N losses from soil, particularly gaseous N losses (Holtgrieve et al., 2009) that are associated with large isotope fractionation (Högberg, 1998). Our finding that $\delta^{15}\text{N}$ of soil NH_4^+ was greater than bulk soil $\delta^{15}\text{N}$ for 95% of observations on the salmon enhanced bank and 84% of observations on the salmon depleted bank, further confirms that isotopic fractionation is important at Hansen Creek and likely elsewhere.

There is a global trend for higher foliar $\delta^{15}\text{N}$ with increased soil N supply (Craine et al., 2009) indicating accelerated soil N cycling and $\delta^{15}\text{N}$ fractionation due to exogenous N (from salmon or elsewhere) will alter plant foliar $\delta^{15}\text{N}$. This has important implications for using two-source mixing models to assess salmon N subsidies to riparian forests. Typical MDN mixing models assume 1) the isotopic signature of salmon is unchanged in the soils prior to plant uptake, and 2) reference sites are biogeochemically similar to salmon sites. However, our data suggest that both of these assumptions are violated at Hansen Creek, and are likely violated at all salmon-influenced riparian ecosystems. First, we observed that $\delta^{15}\text{N}$ of NH_4^+ , the dominant form of inorganic N in our soils, exceeded the 12.6‰ salmon end-member for 26% of our observations from the salmon enriched bank and 9% of observations from the salmon depleted bank, thus violating assumption (1) above. Our soil N data indicate

Hansen Creek is a site of intermediate fertility relative to other boreal forests, so that soil NH_4^+ (rather than organic N or NO_3^-) is most likely the dominant N source taken up by plants (I. Chapin F. Stuart et al., 2011). Second, $[\text{N}_{\text{Org}}]$, C:N, $\delta^{13}\text{C}$, and GW varied with distance from the stream independent of salmon enhancement indicating site variability is a dominant driver of N cycling in this system. This presents a challenge for selecting control sites to calculate terrestrial end members, as key N cycling factors vary longitudinally away from streams and simply selecting reference sites that are beyond the reach of salmon would likely violate the mixing model assumption of biogeochemical similarity. Additionally, observations of $\delta^{13}\text{C}$ increasing and GW decreasing from the creek edge are consistent with higher water use efficiency and less 13C discrimination by vegetation, resulting in higher $\delta^{13}\text{C}$ in soil due to litterfall (Oltean, Comeau, & White, 2016). These data identify systematic differences between salmon-enhanced vs. salmon-depleted banks that cannot be attributed to salmon, and which likely reflect landscape or soil differences. Previous studies examining contributions of MDN to riparian vegetation have not tested biogeochemical similarity across sites, an assumption that is likely violated beyond Hansen Creek specifically.

Violation of mixing model assumptions can lead to significant bias in calculations of MDN sources. To illustrate this point, we applied a typical mixing model framework to our maximum observed $\delta^{15}\text{N}$ of NH_4^+ values to calculate the percent MDN contribution of salmon to NH_4^+ for the most extreme observation, representing the greatest possible bias in calculations. Assuming soil processes have no effect on the isotopic signature yielded impossible result of 298% MDN contribution. To account for isotopic fractionation in soils, we applied our mean observed $\delta^{15}\text{N}$ of soil NH_4^+ at the 3 m distance (19.25‰) as the marine endmember to mean foliar 15N data at the same site from Quinn et al. (2018) and estimate 59.24% MDN on the salmon bank, which is 27.6% lower than the original estimate of 86.8% using salmon $\delta^{15}\text{N}$ as the marine endmember. Repeating this with our maximum observed value for $\delta^{15}\text{N}$ of NH_4^+ (41.2‰), we estimate only 28.9% of foliar N on salmon enhanced bank was MDN (a 57.9% reduction from Quinn et al. (2018) estimates). Thus, failure to account

for isotopic enrichment associated with soil N transformations can lead to overestimates of MDN contributions to plants, and observed variability in $\delta^{15}\text{N}$ of NH_4^+ can produce a wide range of MDN estimates not previously considered. Given that our elevated $\delta^{15}\text{N}$ of NH_4^+ values are consistent with expected changes during soil N transformation (Högberg, 1998), there is a distinct possibility that previous MDN studies have overestimated the amount of MDN by not considering the effects of $^{15}\text{N}/^{14}\text{N}$ fractionation in mixing model calculations. T. A. Wheeler & Kavanagh (2017) found similar results in a semi-arid ecosystem of central Idaho, where accounting for fractionation from decomposition resulted in a 16% reduction in estimated N deposition rates from salmon carcasses. The effects of fractionation on soil N pools is occurring in both of these systems, and likely elsewhere, and needs to be considered when applying mixing models to MDN data to avoid overestimations of salmon N contributions to riparian systems.

Our study is comprehensive in terms of the number of ecosystems factors considered but limited in that it includes only one seasonal timeframe. As much as 40% of the annual inorganic N flux is released during the eight-month dormant season (September-May) and it has been posited spring and fall may be important for many biogeochemical processes in boreal forests (F. S. Chapin, 2006; Drake et al., 2006; Hobbie & Chapin, 1996). While MDN inputs do not affect the N pools and transformation rates during the summer growth period based on our results, N concentrations and transformations may be elevated in this system on shorter timescales (weeks to months after salmon return). The objective of this study was to identify the long-term legacy of salmon subsidies; short-term effects were both beyond the scope of this study and have been previously investigated in this system (Holtgrieve et al., 2009). Considering long-term effect of N subsidies as opposed to short-term provides new information on sustained N use and retention in the ecosystem and whether these salmon nutrients have lasting impacts on ecosystem function meaningful in a restoration context.

While this study is limited to one system, the results that N transformations cause a fractionation that can bias MDN mixing model estimates and that landscape factors are the primary

driver of long-term N retention and use, are relevant to other systems where anadromous, semelparous salmon are abundant (Pacific, Atlantic, Great Lakes) (Quinn et al., 2018). This result also agrees with related research examining fractionation of mineralization and nitrification (Högberg, 1998), and fertilization studies (Lu et al., 2011). Additionally, it demonstrates salmon N subsidies may have a short-term and likely small spatial scale (Drake et al., 2006) legacy in soils. While the importance of site variability relative to salmon subsidies may vary by system, this work demonstrates the importance of considering site variability and demonstrating biogeochemical similarity when selecting control sites for riparian MDN studies.

Salmon provide critical food resources to many of terrestrial and aquatic consumers (C. Jeff Cederholm, Kunze, Murota, & Sibatani, 1999; Schindler et al., 2003; Scott M et al., 2002), but the evidence that MDN stimulate terrestrial primary production is less certain. The salmon carcass manipulation experiment described here and in Quinn et al. (2018) represents an extreme case of carcass addition and depletion to riparian areas, as measured by bulk $\delta^{15}\text{N}$ and estimated percent contribution was approximately twice previous studies for both trees and soils (Bartz & Naiman, 2005; Helfield & Naiman, 2002). Generally, results of this manipulation were equivocal for soils and a statistically significant but ecologically small effect on trees (Quinn et al., 2018). Simultaneously, other recent changes to boreal forest systems, such as moisture and temperature, appear to have a greater potential than MDN to alter biogeochemical pathways and primary production in these systems (F. S. Chapin, 2006; Lloyd, Duffy, & Mann, 2013; M. Wright et al., 2018; Yarie, 2008). This study also demonstrates the importance of testing biogeochemical and site similarity between experimental and control sites in nutrient subsidy studies, as even banks on the same creek can have landscape and soil variability that alter N concentration, transformations, and vegetative growth. Altogether, while salmon have clear benefits for consumers, management of salmon populations or application of compensatory restoration strategies based on terrestrial productivity response to salmon inputs may be unfounded for some systems, and at least,

hard to predict.

1.6 Tables

Table 1.1: The candidate model set tested for each response variable using AIC analysis where $\{*\}$ denotes models used for all response variables, additional models were used for net mineralization and net nitrification where substrate represents organic nitrogen concentration and NH_4^+ concentration, respectively. For $\delta^{15}\text{N}$ data, GW was not tested as a covariate and total mass of N was tested instead. The four tested hypotheses are 1) bank effect, 2) distance effect, 3) bank and distance effect (salmon effect), and 4) no effect of bank and distance. Response variables include: $\delta^{15}\text{N}$ and $\delta^{13}\text{C}$ of bulk soil, $\delta^{15}\text{N}$ of NH_4^+ , $[\text{NH}_4^+]$ and $[\text{NO}_3^-]$, net mineralization and net nitrification, $[\text{N}_{\text{org}}]$, gravimetric water content (GW), and C:N.

Table 1.1: The candidate model set tested for each response variable using AIC analysis

Candidate Model Set	Hypothesis
$*y = \text{bank}$	1
$*y = \text{bank} + \text{GW}$	1
$*y = \ln(\text{distance}) + \text{GW}$	1
$*y = \ln(\text{distance})$	1
$*y = \text{bank} + \ln(\text{distance}) + \text{bank:ln}(\text{distance}) + \ln(\text{distance})2:\text{bank} + \text{GW}$	2
$*y = \text{bank} + \ln(\text{distance}) + \text{bank:ln}(\text{distance})$	1
$*y = \text{bank} + \ln(\text{distance}) + \text{bank:ln}(\text{distance}) + \text{GW}$	1
$*y = \text{bank} + \ln(\text{distance}) + \text{bank:ln}(\text{distance}) + \ln(\text{distance})2:\text{bank}$	2
$*y = \text{bank} + \ln(\text{distance}) + \text{bank}$	1
$*y = \text{bank} + \ln(\text{distance}) + \text{bank} + \text{GW}$	1
$*y = \text{GW}$	3
$y = \text{bank} + \text{substrate}$	1
$y = \ln(\text{distance}) + \text{substrate}$	1
$y = \text{bank} + \text{GW} + \text{substrate}$	1

y = bank + ln(distance) + bank:ln(distance) + GW + substrate	2
y = bank + ln(distacne) + bank:ln(distance) + substrate	1
y = bank + ln(distance) + bank:ln(distance) + GW + substrate	2
y = bank + ln(distance) + bank:ln(distance) + ln(distance)2:bank + GW+ substrate	2
y = bank + ln(distance) + bank:ln(distance) + ln(distance)2:bank + substrate	2
y = bank + ln(distance) + GW+ substrate	1
y = bank + ln(distance) + substrate	1
y = substrate	3
y = GW + substrate	3

Table 1.2: Competing models with relative support ($\Delta\text{AIC} < 2$) using AIC analysis for each response variable, where the most parsimonious models with the most support are shown in bold. Reported are ΔAIC and the hypothesis supported by each model: H1 is a bank effect not caused by salmon manipulation, H2 is a distance effect not caused by salmon manipulation, H3 is both a bank and distance effect indicating a response to salmon manipulation, and H4 indicates support for the other covariates tested.

Table 1.2: Competing models with relative support ($\Delta\text{AIC} < 2$) using AIC analysis for each response variable

Response Variable	Model Hypothesis	ΔAIC	Covariates Included in Models with Relative Support
Bulk 15N			
	2	0.00	Bank, ln(Distance), Bank:ln(Distance), Bank:ln(Distance)2
	2	0.41	Bank, ln(Distance), Bank:ln(Distance), Bank:ln(Distance)2, [Ntot]
Bulk 13C			
	1	0.00	ln(Distance)
	1	0.22	Bank, ln(Distance)
	1	0.62	ln(Distance), [Ntot]
	1	1.23	Bank, ln(Distance), [Ntot]
15N of NH4+			
[NH4+]	2	0.00	Bank, ln(Distance), Bank:ln(Distance), Bank:ln(Distance)2
	1	0.00	Bank, ln(Distance)
	1	0.69	Bank, ln(Distance), Bank:ln(Distance)
	1	0.69	Bank
	1	0.95	Bank, GW
	1	1.10	Bank, ln(Distance), GW
	1	1.87	Bank, ln(Distance), Bank:ln(Distance), GW
[NO3-]			
	1	0.00	Bank, GW
	1	1.72	Bank, ln(Distance), GW
	2	1.87	Bank, ln(Distance), Bank:ln(Distance), Bank:ln(Distance)2, GW
Net Mineralization			
	3	0.00	[NOrg]
	3	0.61	GW, [NOrg]
	1	0.74	Bank, [NOrg]
	1	1.61	Bank, GW, [NOrg]
Net Nitrification			
	3	0.00	[NH4+], GW
	1	1.02	Bank, [NH4+], GW
[NOrg]			
	1	0.00	ln(Distance), GW
	1	0.22	Bank, ln(Distance), Bank:ln(Distance), GW
	2	0.33	Bank, ln(Distance), Bank:ln(Distance), Bank:ln(Distance)2, GW

Gravimetric Water Content (GW)	1	1.94	Bank, ln(Distance), GW
	1	0.00	ln(Distance), Bank
	1	1.00	ln(Distance)
	1	1.80	Bank, ln(Distance), Bank:ln(Distance)

Table 1.3: Competing models with relative support ($\Delta\text{AIC} < 2$) using AIC analysis for each response variable, where the most parsimonious models with the most support are shown in bold. Reported are ΔAIC and the hypothesis supported by each model: H1 is a bank effect not caused by salmon manipulation, H2 is a distance effect not caused by salmon manipulation, H3 is both a bank and distance effect indicating a response to salmon manipulation, and H4 indicates support for the other covariates tested.

Table 1.3: Summary Statistics of Best Models

Bank		Enhanced	Depleted	Enhanced 1	Depleted 1	Enhanced 2	Depleted 2	Enhanced 3	Depleted 3	Enhanced 4	Depleted 4
Distanew	1m	1m	3m	3m	6m	6m	10m	10m	20m	20m	20m
Bulk 15N (%)	7.4(2.3)	7.2(1.9)	9.2(1.0)	7.8(2.2)	8.5(1.9)	6.9(1.2)	8.2(1.5)	7.3(1.6)	6.5(1.0)	6.6(1.2)	
Bulk 13C (%)	-27.1(0.6)	-27.2(0.4)	-26.9(0.5)	-27.1(0.6)	-26.6(0.5)	-26.7(0.3)	-26.5(0.5)	-26.6(0.3)	-26.4(0.5)	-26.4(0.4)	
15N of NH4+ (%)	10.1(1.8)	8.7(2.8)	16.2(10.7)	8.5(2.5)	13.3(10.5)	6.3(2.8)	8.4(2.5)	5.8(2.9)	6.1(2.3)	6.5(3.3)	
[NH4+] (g N g-1)	47.5 (91.6)	22.3(16.4)	62.9(101.5)	10.6(9.4)	52.5(82.8)	11.0(12.7)	12.3(13.1)	11.5(8.2)	8.6(4.4)	13.2(11.6)	
[NO3-] (g N g-1)	6.0(5.4)	3.4(4.4)	10.8(13.5)	4.3(4.7)	7.6(8.0)	3.3(2.8)	2.4(2.3)	4.0(4.2)	2.8(2.8)	1.7(1.2)	
Net Mineralization (g N g-1 d-1)	2.8(2.0)	1.8(1.2)	4.4(5.2)	1.1(1.0)	2.1(3.6)	3.0(3.6)	1.2(1.1)	1.4(1.0)	1.1(1.5)	2.3(1.9)	
Net Nitrification (g N g-1 d-1)	1.7(1.6)	1.2(1.4)	3.4(4.5)	0.8(1.2)	2.8(2.9)	1.7(1.9)	1.0(0.9)	1.4(0.8)	0.6(0.7)	1.6(1.9)	
[NOrg] (mg N g-1)	22.0(4.7)	19.11(5.8)	18.0(8.2)	19.7(7.6)	17.7(6.6)	19.5(8.5)	13.0(6.3)	18.4(8.9)	9.5(3.3)	13.9(5.5)	
GW	2.6(1.1)	3.2(1.6)	2.4(1.5)	2.2(1.1)	2.2(1.5)	2.8(2.2)	1.5(0.9)	2.6(1.8)	1.4(0.6)	1.9(0.8)	
C:N	11.9(1.4)	11.2(1.1)	11.7(1.6)	10.9(1.5)	12.8(2.2)	12.1(2.7)	14.2(1.7)	12.1(1.7)	17.0(2.0)	14.1(3.0)	
% Nitrification	54.8(44.7)	67.9(43.8)	75.4(35.5)	49.3(39.7)	75.7(36.2)	53.1(39.0)	65.9(36.4)	87.9(15.8)	50.6(33.5)	56.2(39.2)	
% C	30.0(5.5)	25.5(8.8)	26.4(10.1)	24.7(9.7)	25.7(8.2)	27.5(13.3)	21.3(8.8)	25.2(11.7)	19.0(6.7)	21.2(6.7)	

1.7 Figures

Figure 1.1: Nitrogen pathways in soil where MDN enters terrestrial systems via decay of salmon organic tissues or excretion from direct salmon consumers such as bears. Arrows represent conversion pathways with the potential to impart isotopic fractionations on plant available nitrogen (NH_4^+ or NO_3^-).

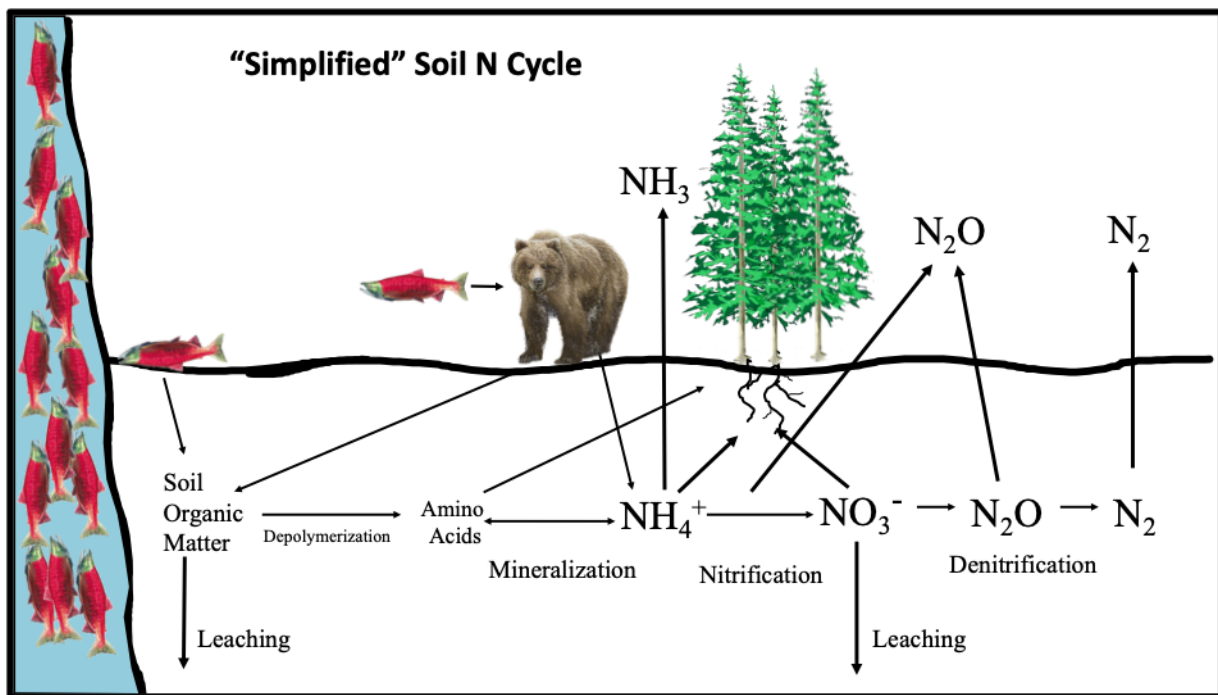


Figure 1.1: Nitrogen pathways in soil

Figure 1.2: Data (closed circles) and predicted values (open circles) for the model with the most support (Table 1.2) for soil organic $\delta^{15}\text{N}$ and $\delta^{13}\text{C}$, $\delta^{15}\text{N}$ of NH_4^+ , and C:N for both the salmon-enhanced and the salmon-depleted banks of Hansen Creek at 1, 3, 6, 10, and 20 m from the edge of the creek bed with 95% confidence intervals (dashed line) for predicted values. Blue (a and c) denotes measures of marine-derived nitrogen, and green (b and d) denotes site variable factors.

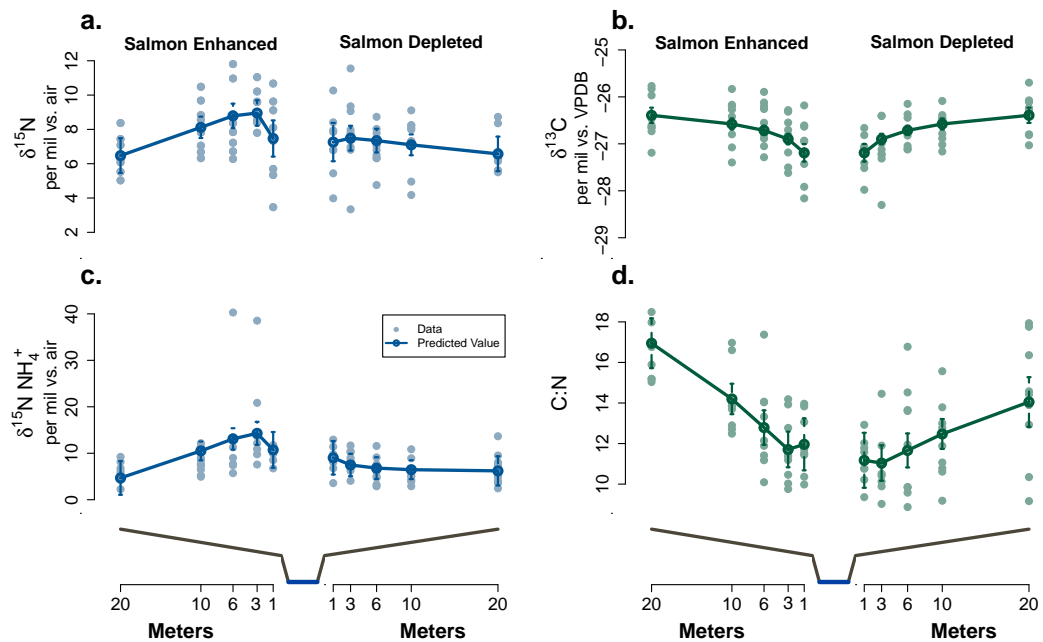


Figure 1.2: Data and predicted values for the model with the most support: Stable Isotopes

Figure 1.3: Data (closed circles) and predicted values (open circles) for the model with the most support (Table 1.2) for NH_4^+ and NO_3^- , net mineralization and nitrification, $[\text{N}_{\text{org}}]$, and gravimetric water content for both the salmon-enhanced and the salmon-depleted banks of Hansen Creek at 1, 3, 6, 10, and 20 m from the edge of the creek bed with 95% confidence intervals (dashed line) for predicted values. Red (a, b, c, d) denotes measures of soil productivity, and green (e and f) denotes site variable factors.

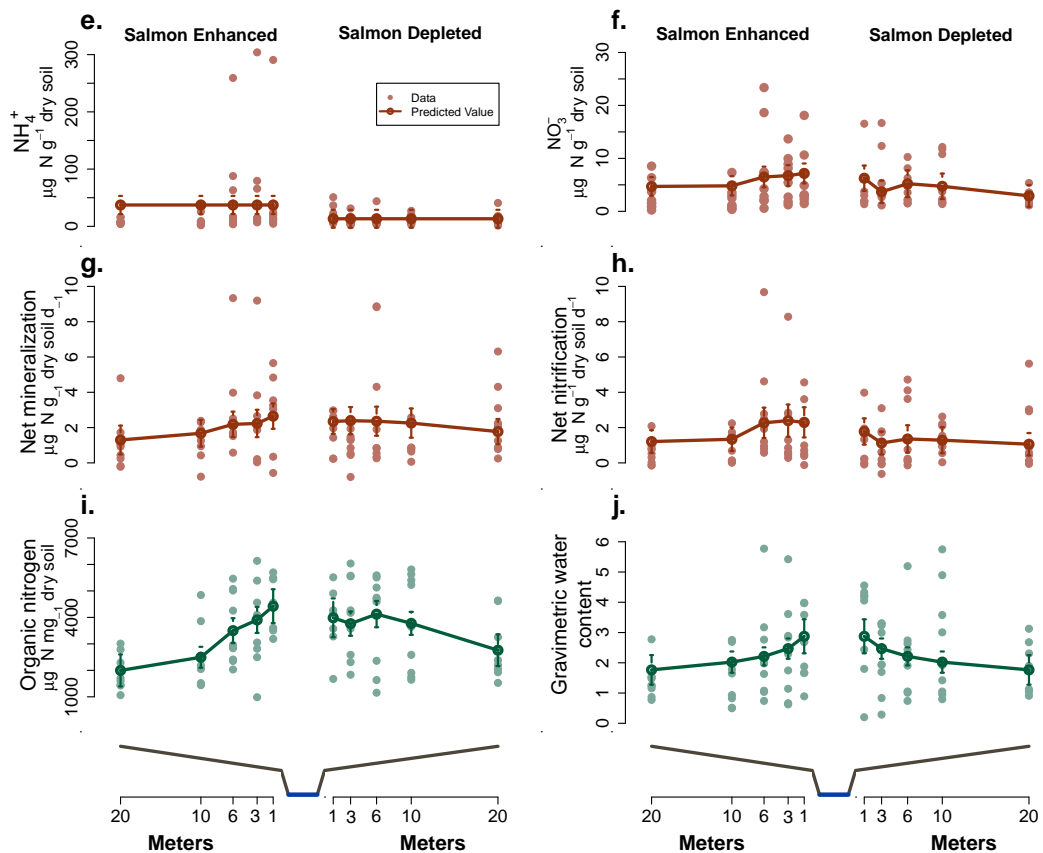


Figure 1.3: Data and predicted values for the model with the most support: Concentrations and Transformations

Figure 1.4: Predicted verse observed values and predicted verse residuals for the model with the most support (Table 1.2, Figure 1.2, 1.3) for each the response variables.

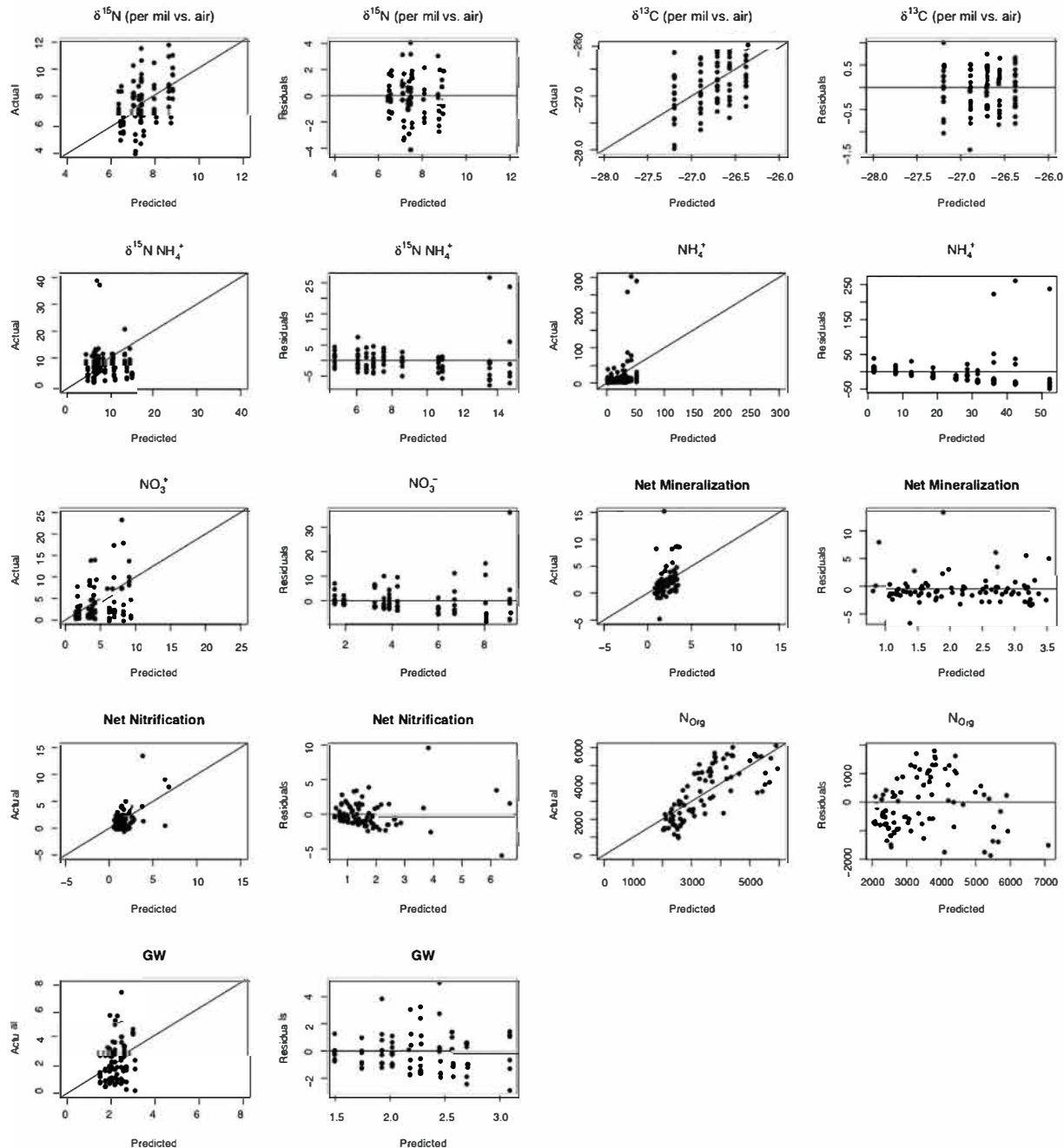


Figure 1.4: Residual Plots for Best Models

Chapter 2

STABLE ISOTOPE SIGNATURES IN HISTORIC HARBOR SEAL BONE LINK FOOD WEB-ASSIMILATED CARBON AND NITROGEN RESOURCES TO A CENTURY OF ENVIRONMENTAL CHANGE

A version of this chapter was published as: Feddern, M. L., Holtgrieve, G.W., & Ward, E. J. (2021). Stable isotope signatures in historic harbor seal bone link food web-assimilated carbon and nitrogen resources to a century of environmental change. *Global Change Biology*, 11: 2328-2342. <https://doi.org/10.1111/gcb.15551>

2.1 Abstract

Anthropogenic climate change will impact nutrient cycles, primary production, and ecosystem structure in the world's oceans, although considerable uncertainty exists regarding the magnitude and spatial variability of these changes. Understanding how regional-scale ocean conditions control nutrient availability and ultimately nutrient assimilation into food webs will inform how marine resources will change in response to climate. To evaluate how ocean conditions influence the assimilation of nitrogen and carbon into coastal marine food webs, we applied a novel dimension reduction analysis to a century of newly acquired molecular isotope data derived from historic harbor seal bone specimens. By measuring bulk $\delta^{13}C$ and $\delta^{15}N$ values of source amino acids of these top predators from 1928-2014, we derive indices of primary production and nitrogen resources that are assimilated into food webs. We determined coastal food webs responded to climate regimes, coastal upwelling, and freshwater discharge, yet the strength of responses to individual drivers varied across the northeast

Pacific. Indices of primary production and nitrogen availability in the Gulf of Alaska were dependent on regional climate indices (i.e., North Pacific Gyre Oscillation) and upwelling. In contrast, the coastal Washington and Salish Sea food webs were associated with local indices of freshwater discharge. For some regions (eastern Bering Sea, northern Gulf of Alaska) food web assimilated production was coupled with nitrogen sources, however other regions demonstrated no production-nitrogen coupling (Salish Sea). Temporal patterns of environmental indices and isotopic data from Washington state varied about the long-term mean with no directional trend. Data from the Gulf of Alaska, however, showed below average harbor seal $\delta^{13}C$ values and above average ocean conditions since 1975, indicating a change in primary production in recent decades. Altogether, these findings demonstrate stable isotope data can provide useful indices of nitrogen resources and phytoplankton dynamics specific to what is assimilated by food webs.

2.2 Introduction

Changing ocean conditions are reshaping the structure and function of marine food webs on regional scales. Ocean temperature (Hoegh-Guldberg & Bruno, 2010), oxygen availability (Breitburg et al., 2018), and climatic regimes such as El Niño Southern Oscillation (ENSO) (Vecchi & Wittenberg, 2010) alter nutrient availability and cycling, and thus, the ecological structure of marine systems. Projected global redistribution of nutrients suggests net primary production in the ocean is likely to change both spatially and temporally. Yet, substantial uncertainty remains, with predictions suggesting both increases and decreases in global net primary productivity of up to 20% by 2100 (L. Bopp et al., 2013; Gregg, Conkright, Gi noux, O'Reilly, & Casey, 2003; Kwiatkowski et al., 2017). An important contributor to this uncertainty is regional variability in phytoplankton response to ocean conditions and how that variability will impact other trophic levels and dependent fisheries (Brander, 2010; J. K. Moore et al., 2018). Ocean conditions (i.e., sea surface temperature, freshwater discharge, wind, and ice cover) have been associated with abundance and recruitment of many fish

species in the Northeast Pacific (C. J. Cunningham et al., 2018; Puerta et al., 2019; Stachura et al., 2014). Nonetheless, these studies rarely include indicators of nutrient availability or primary production linking the ecosystem response to its environment. Understanding how regional and local scale physical drivers control nutrient availability and ultimately nutrient assimilation into food webs will be important for predicting the future availability of marine resources.

A strong empirical understanding of food web response to changing ocean conditions and nutrient constraints requires time series data that span multiple climate regimes to decouple natural variability with long-term anthropogenic changes. Currently, quantitative methods are also limited in their ability to scale primary production trends to ecosystem-level responses. Stable isotope measures of $\delta^{15}N$ ($^{15}N/^{14}N$) of individual amino acids is an emerging tool for reconstructing trends in nitrogen sources from historic specimens (McMahon et al., 2019; Owen A. Sherwood, Guilderson, Batista, Schiff, & McCarthy, 2014; Owen A. Sherwood, Lehmann, Schubert, Scott, & McCarthy, 2011; Whitney, Johnson, Dostie, Luzier, & Wanamaker, 2019). The $\delta^{15}N$ signature at the base of the food web is primarily controlled by utilization and the isotopic signatures of different nitrogen sources, particularly urea, nitrate, and ammonium, by primary producers (N. Ohkouchi et al., 2017; 2009). Measurements of bulk $\delta^{15}N$ values from consumers can be difficult to attribute to changes at the base of the food web because trophic level shifts also effect the isotopic composition of bulk nitrogen (Fry, 2006). Amino acid specific $\delta^{15}N$ data addresses this challenge, as amino acids exhibit two distinct patterns in isotopic enrichment: trophic amino acids (i.e., glutamic acid, alanine, proline) become enriched in $\delta^{15}N$ with each trophic transfer and source amino acids (i.e., phenylalanine, lysine, methionine) show minimal change and thus are reflective of the base of the food web (Chikaraishi et al., 2009; McClelland & Montoya, 2002; N. Ohkouchi et al., 2017).

Similar to the nitrogen stable isotope composition of amino acids as a proxy for nitrogen sources, carbon isotopic composition has emerged as a useful tool for assessing historic

changes in phytoplankton (Lorrain et al., 2020; McMahon et al., 2019). However, cellular growth rates, phytoplankton community composition, the isotopic composition of carbon in CO₂, and CO₂ concentration all affect the $\delta^{13}C$ (¹³C/¹²C) values of phytoplankton in tandem (Burkhardt, Riebesell, & Zondervan, 1999; Lorrain et al., 2020). The relative effects of these factors remain difficult to discern from carbon isotope data alone. Nonetheless, carbon stable isotope data is highly correlated with copepod biomass in the northeast Pacific and thus can be a useful combined index of ocean productivity (Espinasse, Hunt, Batten, Pakhomov, & Tittensor, 2020). While both source amino acid $\delta^{15}N$ and bulk $\delta^{13}C$ values can be influenced by a number of biogeochemical and physiological processes (Figure 2.1), they are useful indicators of nitrogen utilization (source amino acid $\delta^{15}N$) and phytoplankton dynamics (bulk $\delta^{13}C$), despite the difficulty in identifying specific mechanisms of fractionation.

Here we use source amino acid $\delta^{15}N$ and bulk $\delta^{13}C$ values of consumer bone collagen as indicators of change in food web-assimilated nitrogen (nitrogen utilization and isotopic composition at the base of the food web) and food web-assimilated production (phytoplankton composition, [CO₂], cellular growth, and physiology). These definitions assume major changes in nitrogen utilization and phytoplankton dynamics are recorded in the stable isotope composition of nitrogen and carbon in phytoplankton (McMahon et al., 2019; N. Ohkouchi et al., 2017; Owen A. Sherwood et al., 2011; Vega et al., 2021), scaled to the spatial and temporal resource use of consumers, and conserved with minimal trophic fractionation (Chikaraishi et al., 2009). Bulk $\delta^{13}C$ and $\delta^{15}N$ values of source amino acids such as phenylalanine ($\delta^{15}N_{Phe}$) from long-lived, generalist consumers provide ecosystem-level information of carbon and nitrogen dynamics that are integrated over space, time, and multiple energy pathways in the food web (K. S. McCann, Rasmussen, & Umbanhowar, 2005; Vega et al., 2021). As a result, these data sources are more relevant to questions of food web responses to large-scale environmental forcing than discrete measurements of inorganic nutrients or phytoplankton. Ultimately these data can be used to understand how ecosystems have responded to environmental variability in the past and glean insights into food web responses to oceanic

conditions in the future.

Harbor seals (*Phoca vitulina*) are a particularly well-suited predator to understand food web shifts through time because of their primarily piscivorous diet, generalist foraging strategies, high site fidelity, and frequent occurrence in museum specimen collections. Adult harbor seals typically forage 5 - 10 km from haul out sites and at depths < 200 m and are opportunistic feeders (M. M. Lance, Chang, Jeffries, Pearson, & Acevedo-Gutierrez, 2012). Therefore, the nitrogen and carbon stable isotope composition of harbor seals offer a robust representation of the isotopic composition of carbon and nitrogen assimilated into coastal food webs. Harbor seal specific trophic enrichment factors for nitrogen have been quantified in controlled feeding studies, confirming minimal trophic enrichment for phenylalanine between seals and their prey (Germain, Koch, Harvey, & McCarthy, 2013). Environmentally induced shifts in foraging patterns, specifically nearshore verse offshore feeding, has the potential to affect the carbon isotope composition in harbor seal tissues (Figure 2.1). We assume these behavioral effects are minimal on annual time scales compared to changes in the carbon and nitrogen isotope composition at the base of the food web given their restricted foraging ranges.

We aim to identify how archived $\delta^{15}N_{Phe}$ and bulk $\delta^{13}C$ values vary regionally across the northeast Pacific on ecologically relevant scales (integrated annually and regionally) and through time using museum harbor seal specimens from 1928-2014 (Figure 2.2). Additionally, we characterize abiotic factors that influence harbor seal $\delta^{15}N_{Phe}$ and bulk $\delta^{13}C$ values to identify ocean conditions important for food web assimilation of nitrogen and carbon. The effect of regional ocean condition on the stable isotope signature of source amino acids limits the application of short-term datasets for productivity studies, as short-term environmental perturbations are difficult to decouple from longer term trends such as climate regimes (Vokhshoori & McCarthy, 2014). We therefore identify long-term environmental drivers that are important for interpreting reconstructed isotope data.

2.3 Methods

2.3.1 Sample Collection and Analysis

Harbor seal bone samples were obtained from specimens curated at the Burke Museum (University of Washington), the Slater Museum (University of Puget Sound), the Museum of the North (University of Alaska Fairbanks), the Royal British Columbia Museum, the Smithsonian Institute, and the National Marine Mammal Laboratory (NOAA). Specimens were either treated by maceration in warm water or cleaned by beetles and soaked in a dilute ammonia solution then stored in acid free boxes. Adult specimens were sampled from three regions: eastern Bering Sea, the Gulf of Alaska, and Washington state, which also included 18 specimens from the southern British Columbia coast (Figure 2.2). We further stratified samples from the Gulf of Alaska into two subregions (northern and southeast) and Washington state into two subregions (coastal and Salish Sea) for a total of five subregions. Sampling prioritized long-term temporal coverage, specifically focusing on climate regimes shifts (i.e., PDO). Additionally, samples with sex and size metadata were prioritized, although it was not available for most specimens. Metadata was accessed through [VertNet](#) using catalogue numbers and institution codes.

Bone samples were decalcified with the resulting collagen acid hydrolyzed, derivatized, and analyzed for compound-specific nitrogen stable isotope analysis (CSIA) of 11 individual amino acids, including one source amino acid, phenylalanine (phe). Of the 11 amino acids, phenylalanine was the only discernable source amino acid and phenylalanine is the only amino acid data are reported in this manuscript (Appendix S1). CSIA samples were analyzed by GC-C-irMS at the University of Washington Facility for Compound-Specific Stable Isotope Analysis of Environmental Samples using a Thermo Scientific Trace GC + GC IsoLink coupled to a Delta V irMS following the procedures developed by Y. Chikaraishi, Kashiyama, Ogawa, Kitazato, & Ohkouchi (2007) and protocols by Rachel Jeffrey's lab at University of Liverpool UK (full analytical details are provided in Appendix 1). Individual collagen

samples were analyzed in triplicate along with a mixed amino acid standard of known isotopic composition (Sigma-Aldrich Co.) (mean precision of analytical standard for phenylalanine = 0.3‰). Internal and external standards were used and data processing included a drift correction. A total of 215 specimens were sampled from the time period of 1928-2014 for CSIA, making this the largest CSIA dataset of a mammal to date. Decalcified collagen of 190 specimens was analyzed for bulk $^{13}\text{C}/^{12}\text{C}$ and bulk $^{15}\text{N}/^{14}\text{N}$ at the University of Washington's IsoLab using a Costech ElementalAnalyzer, ConFlo III, MAT253 for continuous flow-based measurements. $^{15}\text{N}/^{14}\text{N}$ and $^{13}\text{C}/^{12}\text{C}$ are reported in standard delta notation:

$$\delta^{15}\text{N}(\text{\%vs.air}) = [(\frac{^{15}\text{N}/^{14}\text{N}_{\text{Sample}}}{^{15}\text{N}/^{14}\text{N}_{\text{Air}}} - 1) * 1000] \quad (2.1)$$

$$\delta^{13}\text{C}(\text{\%vs.VPBD}) = [(\frac{^{13}\text{C}/^{13}\text{C}_{\text{Sample}}}{^{13}\text{C}/^{13}\text{C}_{\text{VPBD}}} - 1) * 1000] \quad (2.2)$$

Internal laboratory standards (Bristol Bay salmon and glutamic acid) were interspersed with samples for a two-point calibration and blank correction (mean standard precision 0.09‰ for $\delta^{15}\text{N}$ and 0.04‰ for $\delta^{13}\text{C}$). A linear drift correction was also applied using IsoDat software. The collagen C:N ratio was used to verify the integrity of collagen for stable isotope analysis following specimen treatment and storage (Klinken, 1999).

The isotopic composition of marine dissolved organic carbon has been steadily depleted in ^{13}C over the past 100 years due to increases in anthropogenic CO₂ in the atmosphere (referred to as the Oceanic Seuss Effect) (P. D. Quay, Tilbrook, & Wong, 1992). $\delta^{13}\text{C}$ data were therefore corrected for the Seuss Effect using the following equation (Misarti, Finney, Maschner, & Wooller, 2009):

$$\text{Seuss Effect Correction Factor} = d * e^{0.027*(t-1850)} \quad (2.3)$$

Where d is the maximum annual rate of $\delta^{13}\text{C}$ decrease specific to the North Pacific (-0.014 derived from P. D. Quay et al. (1992)), t is the year represented by the year of specimen collection with a one-year lag. The Seuss effect varies regionally (Tagliabue & Bopp, 2008) and we applied a northeast Pacific parameterization (Misarti et al., 2009).

Standard linear models were used to identify whether size (standard length, cm), sex, and subregion of the harbor seals sampled were related to isotopic composition and to test whether these parameters needed to be standardized in environmental models. $\delta^{15}N_{Phe}$ and $\delta^{13}C$ values were modelled independently as univariate continuous response variables using the following equation:

$$y_i \sim N(\boldsymbol{\alpha} + \boldsymbol{\beta}\mathbf{X}_i, \sigma_y^2) \quad (2.4)$$

where y is the mean triplicate value for each individual i for either $\delta^{15}N_{Phe}$ or $\delta^{13}C$ values. \mathbf{X} represents the matrix of predictors (sex, length, subregion), $\boldsymbol{\alpha}$ is a scalar and $\boldsymbol{\beta}$ is a vector of coefficients for the predictors. Length ($n = 116$) was modelled as a continuous variable and was natural log transformed; subregion and sex ($n = 190$) were modelled as factors. Individual models were used to test whether a predictor was significant as opposed to a multivariate framework because, 1) sample sizes for $\delta^{15}N_{Phe}$ ($n = 215$) and $\delta^{13}C$ ($n = 190$) data varied, and 2) predictor metadata was incomplete for specimens. A pairwise t-test using the Bonferroni correction and non-pooled standard deviation was also used to compare differences in mean isotope signature between subregions and sex (Figure 2.3, Tables 2.4 & 2.5).

To understand the extent of coupling between indices of food web assimilated production and nitrogen resources, a linear model representing the basin wide relationship was fit to $\delta^{15}N_{Phe}$ and $\delta^{13}C$ values as continuous variables assuming normal errors. To understand spatial variation in this relationship, a hierarchical model was fit to the same dataset with varying slope and varying intercept based on subregion as a random effect. This model took the following form:

$$y_i \sim N(\boldsymbol{\alpha}_{j[i]} + \boldsymbol{\beta}_{j[i]}\mathbf{x}_i, \sigma_y^2) \quad (2.5)$$

Where y represents $\delta^{13}C$ values as a continuous variable and x represents $\delta^{15}N_{Phe}$ values as a continuous variable and j represents the group level predictor, subregion. $\boldsymbol{\alpha}$ and $\boldsymbol{\beta}$ are each vectors of coefficients that vary by subregion.

2.3.2 Quantifying effects of ocean condition on food web isotope indices

Linear models were used to identify environmental drivers of $\delta^{13}C$ and $\delta^{15}N_{Phe}$ values using a suite of environmental indices as covariates. A total of 42 environmental time series were compiled as potential predictor variables (Table 2.2) based on previous evidence for food web importance in the northeast Pacific (Di Lorenzo et al., 2008; Stachura et al., 2014). Each environmental time series was standardized around a mean of 0 and standard deviation of 1 and discharge data was also natural log transformed. We divided these environmental covariates a priori into four main mechanistic properties based on the expected effect on nutrient assimilation into the food web: climate regime, freshwater discharge, circulation (wind and upwelling), and sea surface temperature (Figure 2.1). Given the three regions in our analysis, each of these hypotheses were also divided according to our regional geographic breaks (eastern Bering Sea, Gulf of Alaska, and Washington). To reduce collinearity between environmental time series and reduce the total number of candidate models, a subset of 7 environmental times series were selected for each region based on the temporal overlap with stable isotope data. Each subset contained at least one time series for each of the four mechanistic properties and all possible combinations of predictors were tested (Table 2.3). While reduction of the number of times series provides analytical benefits, it comes at the cost of potentially conservative estimates of which covariates are important, meaning important components of ocean condition to the food webs may be missed.

$\delta^{15}N_{Phe}$ and $\delta^{13}C$ values were independently considered as response variables to evaluate relationships between predictors (environmental indices and location) and stable isotope data using Figure (2.4) where X is a matrix of predictors using the 7 standardized environmental time series (continuous) and subregion (factor) as covariates. We treated carbon and nitrogen isotopes as response variables separately in linear models, rather than in a combined multivariate model due to differences in sample size and differences in the strength of correlation between for $\delta^{15}N_{Phe}$ and $\delta^{13}C$ values for each subregion. Time series data prior to 1950 and after 2014 was excluded from this analysis as data for some covariates did not extend

beyond 1950. Candidate models ($n = 53$) were compared using Akaike Information Criteria with a small sample size correction [AICc] and included all combinations of the environmental indices. In addition, a subregion factor was included with two levels for Washington (Salish Sea and coastal Washington) and the Gulf of Alaska (southcentral and southeast) and a null model (intercept only) was also tested. Tissue turnover time of bone collagen has not been measured in mammals of this size to our knowledge but is approximately 173 days for birds (K. A. Hobson & Clark, 1992). Thus, a lag of one year was applied to the stable isotope datasets to account for the timing of tissue turnover in bone collagen. To validate this approach of applying a 1-year lag, 0- and 2-year lags were also applied to the best models of each region and compared to the 1-year lag using AIC. Additionally, month was tested as a smoothed predictor with 12 knots for stable isotope data in Washington samples using a generalized additive model (GAM). Support for a significant smoothing term would identify and seasonality in the data, which would be expected if tissue turnover time is less than a year. A one-year tissue turnover time was confirmed as a suitable assumption for harbor seal bone collagen, as 0- and 2- year lags had similar or less model support. There was no support for a smoothing effect by month in generalized additive models of $\delta^{15}N_{Phe}$ and $\delta^{13}C$ which would have indicated any seasonal variability in isotope composition and thus a turnover time of less than or greater than a year ($p < 0.05$; Figure 2.9) and thus a 1-year lag was applied to isotope data for all temporal analyses.

For each model with relatively high support ($\Delta\text{AICc} < 2$) the AICc weight and the coefficient for each covariate is reported (Figure 2.3). To confirm collinearity was not problematic in the candidate models that included more than one environmental covariate, matrix scatterplots and variance inflation factors (vif) were used from the car package (Fox et al. 2019) in R (R Development Core Team, 2020).

2.3.3 Gaussian Process Dynamic Factor Analysis (GPDFA)

To further understand how the environment, $\delta^{13}C$, and $\delta^{15}N_{Phe}$ values covary through time in the Northeast Pacific, we developed a novel extension of conventional Dynamic Factor Analysis (DFA). DFA is a dimension reduction technique that identifies common processes underlying a set of multivariate time series. This technique has been applied to multivariate time series problems in fisheries and ecology to identify patterns of oceanographic variability that drive Pacific salmon stocks (Jorgensen, Ward, Scheuerell, & Zabel, 2016; Ohlberger, Scheuerell, Schindler, & Peters, 2016; Stachura et al., 2014).

DFA models identify common trends across multiple time series (“latent trends”) and estimates the importance of that trend for each individual time series as a coefficient (“factor loading”). The two equations describing DFA take on the following form:

$$\mathbf{y}_t = \mathbf{Z}\mathbf{x}_t + \mathbf{v}_t, \text{ where } \mathbf{v}_t \sim MVN(0, \mathbf{R}) \quad (2.6)$$

$$\mathbf{x}_t = \mathbf{x}_{t-1} + \mathbf{w}_t, \text{ where } \mathbf{w}_t \sim MVN(0, \mathbf{I}) \quad (2.7)$$

The observed data \mathbf{y}_t are modeled as combinations of latent trends \mathbf{x}_t at time t (the dimensions of \mathbf{x}_t matching the number of trends which are also referred to as states) and factor loadings (\mathbf{Z}) (a coefficient for each time series for each trend) at time t , which are modeled as a random walk (Zuur et al. 2003). In addition there is an optional random observation error (\mathbf{v}_t) and process error (\mathbf{w}_t) which are multivariate normal

Our extension of DFA adopts an alternative model of the latent trends, modeling them with Gaussian Processes rather than random walks. Gaussian Processes (GP) have been widely used in fisheries and other fields (S. B. Munch, Giron-Nava, & Sugihara, 2018). Instead of modeling a time series as an autoregressive process, GPs model a time series via a mean and variance function, $x \sim MVN(u, \Sigma)$ where u represents an optional mean vector and Σ a covariance matrix. For GPDFA, we assume the mean to be zero, letting just the covariance function determine the GP smoothing. GPs are flexible in that the covariance matrix can be described by a wide range of flexible functions; for this application we use a Gaussian

kernel (squared exponential) so that $\Sigma_{i,j} = \sigma^2 \exp(-d_{i,j}/\sigma)$, where σ^2 is a variance parameter controlling the magnitude, σ is a shape parameter controlling how quickly covariance declines, and $d_{i,j}$ is the known distance between time points i and j . A benefit of modeling Σ with a covariance function is that regardless of the dimensionality, all elements of Σ can be described by a small number of parameters. For GPDFA, we choose to use a GP predictive process model, because the number of time points may be large (Latimer, Banerjee, Sang Jr, Mosher, & Silander Jr, 2009). This predictive model estimates the function values at a subset of locations (knots), and combines these estimates with the distance to locations at which data are observed to make predictions. More specifically, the values of the time series at the knot locations are $x^* \sim MVN(0, \Sigma^*)$. Given the known distances between the locations of knots and locations of data, the covariance matrix between the two can be calculated, $\Sigma_{(x,x^*)}$. Finally, the predictions of the time series at the observed data can be calculated as $\hat{x} = \Sigma'_{(x,x^*)} \Sigma^{*-1} x^*$. In this extension of DFA, all other model components are identical to the conventional time series version with latent trends modeled as a random walk.

With the Gaussian Process DFA model, a decision needs to be made a priori about selecting the number and location of knots, where the function parameters are estimated at. There are multiple approaches for doing this; we adopted a model with 15 knots (more knots resulting in a smoother function), and estimated the knot location by performing a clustering approach of the years corresponding to the raw observations (partitioning around medoids, using the ‘pamk’ function in the fpc library in R).

With conventional DFA using an autoregressive model, long gaps in time series data result in large, overestimations of the variance of the latent trends. Gaussian Processes model time series as a multivariate normal distribution, with estimated mean vector \mathbf{u} and covariance matrix Σ (S. B. Munch et al., 2018). To constrain the number of estimated parameters, elements of Σ were modeled with a Gaussian or squared covariance exponential function such that $\Sigma_{(i,j)} = \sigma^2 \exp(-(t_i - t_j)^2/\theta)$. In this parameterization, σ^2 controls the variability of the stochastic process, θ controls the rate of decay in correlation between time steps, and

t_i and t_j are the time variables (e.g. years) for locations i and j .

We considered models with 1- 4 underlying trends. Each trend was modelled separately (different means) but models with multiple trends to have a shared covariance matrix amongst trends. The GPDFA approach was applied to time series from each region and the best model was selected using leave-one-out cross-validation (LOOIC) from the loo package in R (Vehtari, Gelman, & Gabry, 2017). The choice of knots affects the degree of smoothness, with more knots creating more smooth functions. We tested several different numbers of knots and found results to be qualitatively similar. Similar to the previous analysis, time series data prior to 1948 for Washington state and prior to 1940 and after 2008 for the Gulf of Alaska was excluded from this analysis. We fit GPDFA to data from each region including all of the initial 42 identified environmental time series for that region (Table 2.2), $\delta^{15}N_{Phe}$ and $\delta^{13}C$ values, with location as a factor. We implemented GPDFA using the Stan language (Stan Development Team 2019, B. Carpenter et al., 2017), and R (R Core Development Team 2019, version 3.6.2) via R package rstan (Stan Development Team 2019, version 2.21.2). Code to implement GPDFA is available [here](#)

2.4 Results

$\delta^{15}N_{Phe}$ and bulk $\delta^{13}C$ values did not vary by sex ($p > 0.05$, Figure 2.3 or size for the individuals sampled ($p > 0.05$; Figure 2.9). Spatial variation in harbor seal $\delta^{15}N_{Phe}$ and $\delta^{13}C$ values were observed on subregional scales. $\delta^{15}N_{Phe}$ values were similar for harbor seals in the northern Gulf of Alaska (11.9 ± 2.9 , mean \pm 1SD), southeast Gulf of Alaska (10.8 ± 1.7), and coastal Washington (11.3 ± 1.9). The eastern Bering Sea had significantly higher $\delta^{15}N_{Phe}$ values compared to other subregions (15.2 ± 1.8) followed by the Salish Sea (12.2 ± 2.3) which had similar $\delta^{15}N_{Phe}$ values compared to the northern Gulf of Alaska (Figure 2.3, Table 2.4). $\delta^{13}C$ values varied by subregion ($p < 0.05$) with the exception of the Gulf of Alaska, where the northern (-14.6 ± 0.9) and southeast (-14.4 ± 1.1) subregions were not significantly different, and the eastern Bering Sea (-13.4 ± 0.9) and coastal Washington

(-13.6 ± 0.9) were not significantly different (Figure 2.3, Table 2.5). The variation between subregions appeared to follow a latitudinal gradient, where harbor seal mean $\delta^{13}C$ values were most enriched in ^{13}C in the Salish Sea (-12.2 ± 1.5), became more depleted from coastal Washington and into the Gulf of Alaska (Table 2.1).

The relationship between harbor seal $\delta^{15}N_{Phe}$ and $\delta^{13}C$ values also varied on subregional scales. There was positive linear association between harbor seal $\delta^{15}N_{Phe}$ and $\delta^{13}C$ values in the combined northeast Pacific basin and Bering Sea model with a slope of 0.12 (Figure 2.4A). For the hierarchical subregion model, the eastern Bering Sea and coastal Washington demonstrated similar relationship, with slopes of 0.08 (95% CI [0.05, 0.11]) and 0.07 (95% CI [0.05, 0.09]) respectively. Similarly, harbor seals in both Gulf of Alaska subregions demonstrated comparable coupling of $\delta^{15}N_{Phe}$ and $\delta^{13}C$, with slopes of 0.13 (95% CI [0.11, 0.14]) for the northern subregion and 0.12 (95% CI [0.10, 0.14]) for the southeastern subregion. Salish Sea harbor seals had a distinct relationship between $\delta^{15}N_{Phe}$ and $\delta^{13}C$ values relative to other subregions with a slope of only 0.02 that was not significantly different from 0 (95% CI [0.0, 0.04]) (Figure 2.4B).

For both $\delta^{15}N_{Phe}$ and $\delta^{13}C$ values there was substantial support for models including environmental indices rather than null or subregion only models. The relationship between environmental indices and harbor seal $\delta^{15}N_{Phe}$ and $\delta^{13}C$ values in the northeast Pacific varied on regional scales. For Washington, the best model to predict harbor seal $\delta^{15}N_{Phe}$ values included Columbia River discharge in high flow months, summer upwelling, and subregion. There was substantial model uncertainty for $\delta^{15}N_{Phe}$ values in the Washington region, however 90% of model weight supported the inclusion of Columbia River discharge (Figure 2.5A). The model for harbor seal $\delta^{13}C$ values with the most support indicated a positive association between PDO, spring upwelling, and freshwater discharge in the Washington region (Figure 2.5B). In the Gulf of Alaska, the summer upwelling model had the most support as a predictor of harbor seal $\delta^{15}N_{Phe}$ values with some model support for inclusion of the NPGO (North Pacific Gyre Oscillation), although the coefficients for this covariate did not differ

substantially from 0 (Figure 2.5C). The best model for harbor seal $\delta^{13}C$ values for the Gulf of Alaska included subregion, PDO (Pacific Decadal Oscillation), and NPGO (Figure 2.5D). In contrast to Washington, the Gulf of Alaska models supported a negative association between $\delta^{13}C$ values and PDO. The null model for $\delta^{15}N_{Phe}$ values in the eastern Bering Sea had the most support (Figure 2.5E). Lack of model support for environmental covariates in the eastern Bering Sea may have been a result of the small sample size in the region. Cross-shelf wind was included as a predictor in the best model (Figure 2.5F) for $\delta^{13}C$ values in the eastern Bering Sea and was supported by 76% of the model weight.

PDO and Kuskokwim river discharge during high flow months were found to be highly collinear ($VIF > 10$) and PDO was omitted from the candidate model set for the eastern Bering Sea analysis. All other models containing multiple environmental predictors with relative support had variance inflation factors of less than 2 indicating only moderate collinearity across covariates. Model residuals for the best models did not show trends through time (Figure 2.14). This indicates that there were no trends associated with other potential ecosystem changes, such as harbor seal foraging strategy for example, after accounting for ocean condition. Model results did not change when using $\delta^{13}C$ data that were not corrected for the regional Seuss Effect.

The GPDFA analysis showed temporal synchronies and shared trends across environmental conditions and stable isotope values in the northeast Pacific. In the Gulf of Alaska, the data supported three latent trends (Figure 2.6). Both $\delta^{15}N_{Phe}$ and $\delta^{13}C$ values had the highest loadings for trend 1, which showed an increase starting in 1965 until 1980 followed by the trend oscillating at approximately 25% above the long-term average. The harbor seal $\delta^{15}N_{Phe}$ values for the southeast subregion, harbor seal $\delta^{13}C$ values, and spring upwelling had negative loadings on trend 1; loadings of $\delta^{15}N_{Phe}$ values were generally weaker relative to loadings of $\delta^{13}C$ values. For the other two trends (2-3), loadings were clustered by environmental driver category. Latent trend 2 oscillated around the long-term average and was uninformative. Trend 3 was below average starting in 1985 with strong loadings for climate time series,

spring and summer upwelling, and discharge in high flow months (Figure 2.6). Annual discharge, autumn upwelling, Oceanic Niño Index and Northern Oscillation Index did not demonstrate strong loadings for any trend. In Washington, there was support for two latent trends. Latent trend 1 shows a rapid increase in the 1940's to 25% above the long-term mean then a gradual decline until 1986 to approximately 40% below the long-term mean, with values below the mean starting in 1977 (Figure 2.7). Trend loadings for harbor seal $\delta^{15}N_{Phe}$ and $\delta^{13}C$ values were stronger for coastal seals and trend 1 had stronger loadings for freshwater discharge than trend 2. Trend 2 had strong loadings for $\delta^{15}N_{Phe}$ and $\delta^{13}C$ values for both Salish Sea and coastal Washington harbor seals. Trend 2 oscillated above and below the long-term mean and had large loadings for sea surface temperature, summer upwelling, Fraser River discharge and climate indices (Figure 2.7).

To validate this approach of applying a 1-year lag, 0- and 2-year lags were also applied to the best models of each region and compared to the 1-year lag using AIC. Additionally, month was tested as a smoothed predictor with 12 knots for stable isotope data in Washington samples using a generalized additive model (GAM). Support for a significant smoothing term would identify and seasonality in the data, which would be expected if tissue turnover time is less than a year. A one-year tissue turnover time was confirmed as a suitable assumption for harbor seal bone collagen, as 0- and 2- year lags had similar or less model support. There was no support for a smoothing effect by month in generalized additive models of $\delta^{15}N_{Phe}$ and $\delta^{13}C$ which would have indicated any seasonal variability in isotope composition and thus a turnover time of less than or greater than a year ($p < 0.05$; Figure 2.9) and thus a 1-year lag was applied to isotope data for all temporal analyses.

2.5 Discussion

We analyzed bone collagen $\delta^{15}N_{Phe}$ and bulk $\delta^{13}C$ values from harbor seal museum specimens collected between 1928 and 2014 as indices of change in food web assimilated nitrogen and carbon. Based on previous research (Lorrain et al., 2020; Owen A. Sherwood et al., 2014;

Vega, Jeffreys, Tuerena, Ganeshram, & Mahaffey, 2019), we interpret $\delta^{15}N_{Phe}$ and bulk $\delta^{13}C$ values as primarily representing nitrogen and carbon resource utilization, and growth and community composition of primary producers at the base of the food web. Our data show the relationship between indices of primary production and nitrogen resources assimilated into food webs varies regionally across the northeast Pacific. By pairing these data with environmental time series data, we provide new insights into large scale environmental forcing that impacts the base of the food web and is transferred to higher trophic levels. Specifically, oceanic conditions associated with climate regimes and upwelling explain significant temporal variation in $\delta^{15}N_{Phe}$ and bulk $\delta^{13}C$ values of coastal predators in northeast Pacific (Figure 2.5; Figure 2.14). This analysis demonstrates $\delta^{15}N_{Phe}$ and bulk $\delta^{13}C$ values are useful indicators of resources assimilated by coastal food webs.

2.5.1 Spatial variation in stable isotope indices

The geographically widespread association between harbor seal $\delta^{15}N_{Phe}$ and bulk $\delta^{13}C$ values indicates food web assimilated primary production is coupled with nitrogen resources in most regions of the northeast Pacific, with the Salish Sea as a notable exception (Figure 2.4). Short-term studies in coastal Washington showed phytoplankton respond considerably to nitrogen inputs and are frequently nitrogen limited (Dortch & Postel, 1989; R. M. Kudela & Peterson, 2009). Similarly, short term studies of the inner Gulf of Alaska shelf demonstrated primary production is generally nitrogen limited, and size, growth rates, and community composition are all tightly coupled with nutrient availability (S. L. Strom, Olson, Macri, & Mord, 2006). A significant relationship between bulk $\delta^{15}N$ and $\delta^{13}C$ values was also observed in the tissues of some gorgonian corals over the same time period in coastal Gulf of Alaska (B. Williams, Risk, Stone, Sinclair, & Ghaleb, 2007). Given the evidence of nitrogen limitations and its relationship with phytoplankton growth and community composition in these coastal environments, the association between $\delta^{15}N_{Phe}$ and bulk $\delta^{13}C$ values could be the result of nitrogen limiting growth at the base of the food web. Alternatively, the $\delta^{15}N_{Phe}$ and bulk

$\delta^{13}C$ coupling could be driven by covariance with an untested environmental variable that impacts most of the northeast Pacific but not the Salish Sea.

The coastal Washington and the Salish Sea food webs assimilate different nitrogen and carbon sources (Figure 2.5 A & B). Salish Sea harbor seals have higher $\delta^{15}N_{Phe}$ and bulk $\delta^{13}C$ values compared to individuals on the outer coast, which is likely due to significant contributions of intertidal producers and the legacy of anthropogenic N in the Salish Sea food web. Intertidal macrophytes (seagrass and algae) have similar ^{13}C values ($\sim -10\text{\textperthousand}$) compared to harbor seals in the Salish Sea, while other potential sources are much lower (i.e., marine derived sources $\sim -20\text{\textperthousand}$, terrestrial derived sources $\sim -30\text{\textperthousand}$) (Conway-Cranos et al., 2015; Howe & Simenstad, 2015). Incorporation of intertidal producers into the Salish Sea food web explains the difference in carbon stable isotope signatures between Salish Sea and coastal Washington harbor seals ($\sim 1.4\text{\textperthousand}$, Figure 2.5A). However, it does not explain the higher $\delta^{15}N_{Phe}$ values (Figure 2.5B, Table 2.1). Surface nitrate was observed to be $8\text{\textperthousand} - 12\text{\textperthousand}$ off the coast of Washington in spring 1993 (J. Wu, Calvert, & Wong, 1997) which was exceeded by harbor seals in both coastal Washington and the Salish Sea (Table 2.1). It is likely anthropogenically derived nitrogen sources contribute to the higher observed $\delta^{15}N_{Phe}$ values both directly and indirectly, particularly in the Salish Sea where harbor seal $\delta^{15}N_{Phe}$ values were up to $2.4\text{\textperthousand}$ higher than coastal Washington seals. Wastewater treatment facilities and agriculture runoff contribute substantial amounts ($\sim 32\%$) of nitrogen in the Salish Sea (Mohamedali et al. 2011) and are enriched in ^{15}N . In recent decades, Salish Sea waters have also been characterized by low dissolved oxygen and hypoxic events (PSEMP 2019) from human derived nitrogen loading. Anoxic conditions are conducive to denitrification, another potential indirect source of ^{15}N from human activities in the region.

2.5.2 Ocean condition and stable isotope indices

Washington state food webs exhibit environmentally induced changes in assimilated primary production and nitrogen sources. The isotope-ocean condition relationship in the region can

be explained by introduction of terrestrial derived nutrients and climatically induced changes in phytoplankton community structure observed in previous studies (Du & Peterson, 2014; R. Kudela et al., 2008; 2015). For example, the PDO has been associated with phytoplankton community shifts between dinoflagellates and diatoms in the northern California Current (2015). Similarly, the phytoplankton community composition is distinct in the early (spring) upwelling season compared to the late (summer) upwelling season (Du & Peterson, 2014). This could explain the inversely related associations between bulk $\delta^{13}C$ values and summer and spring upwelling (Figure 2.5B). Shifts in phytoplankton community structure are therefore a mechanism to explain the relationship between harbor seal bulk $\delta^{13}C$ values and ocean condition. In addition, freshwater discharge explains 16% of variation observed in both $\delta^{15}N_{Phe}$ and bulk $\delta^{13}C$ values in Washington. The Columbia River Plume introduces terrestrial derived nutrients, including nitrogen, and has been associated with increased primary production and fish production (R. Kudela et al., 2008). The covariation between $\delta^{15}N_{Phe}$, bulk $\delta^{13}C$, and discharge indicates isotopically distinct nitrogen resources introduced by freshwater discharge alters primary production which is then assimilated into the Washington food web, and ultimately harbor seals.

In the eastern Bering Sea, our results suggest ice-born algae and ^{15}N enriched nitrogen from the inner shelf are important for supporting the coastal food web. Recent evidence supports that consumer $\delta^{15}N_{Phe}$ values reflect nitrate $\delta^{15}N$ values in the arctic (de la Vega et al. 2020). However, our $\delta^{15}N_{Phe}$ values from harbor seals of the eastern Bering Sea were high relative to previous studies of summer nitrate (5 to 9‰) (Lehmann et al., 2005) and plankton nitrogen isotope signatures (6-12‰) (S. L. Smith, Henrichs, & Rho, 2002) from the outer and mid Bering Sea shelf. Morales et al. (2014) subsequently found the stable isotope composition of nitrogen in diatoms ranged from 5-21‰ in late winter and early spring. These values also increased in association to sea ice with a positive shoreward gradient (Morales et al., 2014). The range of sea-ice algae $\delta^{15}N$ values observed by Morales et al. (2014) are consistent with our observed $\delta^{15}N_{Phe}$ values in harbors seals (2.1). Furthermore, the

harbor seals in this study were located near the inner shelf in an area that has been partially covered by sea ice from January to May during the past century (Stabeno, Bond, & Salo, 2007). Together this indicates ice algae as a significant contributor to the coastal food web. The disconnect between the $\delta^{15}N$ values of offshore nitrate (Lehmann et al., 2005) and harbor seals also highlights the problem in assuming spatially and temporally discrete nitrate or phytoplankton measurements are representative of resources utilized by, and assimilated into, coastal food webs. Consumer $\delta^{15}N_{Phe}$ measurements by their nature represent the N assimilated into the food web and integrated over relatively long time scales, while discrete measurements of nitrate may be spatially or temporally biased.

A short term (1998-2011) study of abiotic drivers in the Gulf of Alaska found chlorophyll-a anomalies were positive when downwelling favorable winds were low and had a negative relationship with sea level (Waite & Mueter, 2013). Similarly, Espinasse et al. (2020) found chlorophyll-a, SST, and sea level anomalies were the best predictors of carbon and nitrogen isotope data for secondary consumers over the past two decades. Our results agree with these studies as NPGO (an index of sea level) is negatively associated with both harbor seal $\delta^{15}N_{Phe}$ (Figure 2.5C) and $\delta^{13}C$ values (Figure 2.5 D) in the Gulf of Alaska. Similarly, summer upwelling is positively associated with our $\delta^{15}N_{Phe}$ values (Figure 2.5C). Based on our results, these environmentally induced changes represent long-term ecosystem dynamics that extend beyond merely the base of the food web and ultimately impact resources assimilated by top predators. In addition, regional climate indices characterize nutrient and primary production assimilated annually into the food web better than sea surface temperature data alone. It is possible that other untested abiotic factors such as cross-shelf exchanges via eddy propagation or local wind stress (Waite & Mueter, 2013) may be important to food web assimilated nitrogen and primary production in the Gulf of Alaska. Regardless, local variability in upwelling and basin scale indices of sea surface height and temperature (i.e., NPGO) ultimately determine resource assimilation in Gulf of Alaska food web in which harbor seals forage.

By comparing consumer stable isotope values against environmental covariates across multiple sub basins we show environmental forcing on coastal food webs is regionally distinct. For example, climate indices (i.e., PDO) in the Gulf of Alaska were inversely associated with food web-assimilated primary production (Figure 2.5D, Figure 2.6 Trend 1-2) and positively associated in Washington (Figure 2.5B, Figure 2.7 Trends 1-2). This agrees with previous studies where the Pacific Decadal Oscillation has been associated with alternating salmon production in the northeast Pacific (Mantua, Hare, Zhang, Wallace, & Francis, 1997). In cool phase years (i.e., 1947-1977), Washington stocks experience above average production and Alaska stocks experience below average production. Our results show that $\delta^{13}C$ values for Washington and Gulf of Alaska also indicate alternating primary production between the two regions in association with PDO. Surprisingly, $\delta^{13}C$ values are higher in cool phase years for the Gulf of Alaska (Figure 2.5D) and lower in cool phase years for Washington (Figure 2.5B). This suggests there is lower phytoplankton growth in Washington and higher in Gulf of Alaska in cool phase years. This is contrary to results of previous studies, assuming 1) higher $\delta^{13}C$ values represent higher growth rates and 2) PDO is inhibiting growth at the base of the food web and indirectly constraining higher trophic levels such as salmon (Mantua et al., 1997). It is likely the relationship between PDO, salmon production, and $\delta^{13}C$ values of harbor seals is instead caused by phytoplankton community structure constraining higher trophic levels rather than growth.

Common temporal trends in harbor seal stable isotopes and ocean condition empirically derived from the GPDFA analysis (Figures 6 & 7) show changes in biogeochemical cycling and food web-assimilated production in recent decades that are associated with climatic variables. Since 1975, shared trends in environmental time series and stable isotope data in the Gulf of Alaska are above average for temperature, discharge, and NPGO and below average for assimilated $\delta^{13}C$ values (as indicated by its negative loadings; Figure 2.6). Trends 2 and 3 in the Gulf of Alaska (Figure 2.6) show a distinct change in environmental indices starting in 1988. Loadings on these trends were higher for environmental indices than stable isotope

data, suggesting a decoupling of environment-food web relationship in the region starting around 1988, which has also been observed between climate regimes and fish species (Litzow et al., 2020). This environmental-food web decoupling was not observed in Washington (Figure 2.7) in our study or others (Litzow et al., 2020).

2.5.3 Using stable isotopes as food web indicators

Previous research has shown lower trophic levels are sensitive to environmental variation in bottom-up drivers of productivity (Frank et al., 2015; Jennings & Brander, 2010), but few studies have demonstrated how the impact of these changes span entire food webs on long time scales. By applying CSSIA to museum specimens of a generalist predators, we provide a novel piece of the ecological puzzle not previously available. First, these data provide a measure of changing nitrogen resources and phytoplankton dynamics that are spatially and temporally integrated for food web resource assimilation, rather than measuring the availability of inorganic nutrients or lower trophic level biomass and assuming an associated food web response. Dominant species of marine zooplankton exhibit selective foraging, particularly when resources are highly available (Bi & Sommer, 2020; Boersma et al., 2016; Jungbluth, Selph, Lenz, & Goetze, 2017) thus discrete measures of resources are not necessarily representative of what is utilized by the food web. Second, studies directly measuring primary production are often temporally limited to short time scales and recent decades. CSSIA of historic specimens allows for retrospective analyses that span long time scales (McMahon et al., 2019; Owen A. Sherwood et al., 2011) and thus identify long-term environmental forcing on food webs.

Despite these benefits, CSSIA (and stable isotope analysis data more generally) is limited in its ability to discern different mechanistic processes for isotopic enrichment in observational studies. Multiple mechanisms of fractionation often operate in tandem (Figure 2.1) and can be both additive and subtractive. For example, both the isotopic composition of dissolved inorganic nitrogen sources (primarily NO_3^- , but also urea and NH_4^+) and the relative uptake

of these sources impact the isotopic composition of nitrogen in primary producers (N. Ohkouchi et al., 2017; 2009). As a result, these data on their own are limited in their ability to track exact mechanisms of fractionation and specific biogeochemical changes through time or space. Regardless, stable isotope signatures of nitrogen from source amino acids and bulk carbon can be used to trace variations in nitrogen sources at the base of the food web (Owen A. Sherwood et al., 2014; Vega et al., 2019) and changes in phytoplankton dynamics (i.e., production) (Lorrain et al., 2020; Vega et al., 2019) broadly. In addition, CSSIA of carbon is also emerging as reliable proxy for phytoplankton community composition (Larsen et al., 2013). We also assume a constant and small trophic enrichment factor for both bulk $\delta^{13}C$ and $\delta^{15}N_{Phe}$ values. While trophic enrichment in $\delta^{13}C$ and $\delta^{15}N_{Phe}$ values is minimal (Bocherens & Drucker, 2003; Germain et al., 2013; K. A. Hobson, Schell, Renouf, & Noseworthy, 1996; N. Ohkouchi et al., 2017), and thus unlikely to impact overall correlations between datasets, it can produce enriched absolute isotope values and increased variation between observations, which was not accounted for in this study. Nonetheless, ours is among a number of supporting studies that show food webs are impacted by changing environmental conditions in the northeast Pacific (C. J. Cunningham et al., 2018; Puerta et al., 2019; Stachura et al., 2014).

Climate change will alter nutrient distributions and primary production throughout the worlds' oceans (Kwiatkowski et al., 2017; Marinov, Doney, & Lima, 2010). Based on analysis of historical patterns of consumer isotopic variation with environmental forcing, we anticipate there will be region-specific spatial variability in how primary production and its dependent food webs respond to environmental change throughout the northeast Pacific over the next century. As environmental conditions (i.e., sea surface temperature, discharge, anthropogenic nitrogen) continue to change, so will resources available to and assimilated by food webs. Given both resource availability and community composition of resources impact the function and stability of food webs (Narwani & Mazumder, 2012) it is likely that ecosystem interactions will change in response to environmentally induced shifts in resources.

Understanding dynamics influencing food web responses to their environment is important, as it provides information useful for predicting climate change impacts to aquatic resources and the communities and economies that depend on them.

2.6 Tables

Table 2.1: Range of $\delta^{13}C$ and $\delta^{15}N_{phe}$ values observed in harbor seals for each of the five northeast Pacific subregions.

Table 2.1: Ranges of stable isotope data

Subregion	$\delta^{15}N_{phe}$	$\delta^{13}C$
Coastal WA	6.0 – 15.8	-15.6 – -11.8
Salish Sea	5.9 – 18.2	-16.6 – -6.8
Northern Gulf of Alaska	6.2 – 21.5	-16.7 – -12.5
Southeast Gulf of Alaska	8.0 – 15.2	-17.3 – -12.1
Eastern Bering Sea	12.4 – 18.9	-15.0 – -12.1

Table 2.2: Environmental datasets. SST data was obtained from NOAA ERSST V5 data provided by the NOAA/OAR/ESRL PSD, Boulder, Colorado, USA, from their Web site at <https://www.esrl.noaa.gov/psd/>

Table 2.2: Environmental Datasets

Environmental Driver Category	Eastern Bering Sea	Gulf of Alaska	Washington
Discharge	Total discharge from the Kuskokwim River at Crooked Creek, AK during the winter months of low discharge (Nov-Apr) and summer months of high discharge (May-Oct) from monthly U.S. Geological Survey discharge data. 1951-2018. N = 3	Estimates of total freshwater discharge for a location near Seward, Alaska during winter months of low discharge (Jan-Jul) and summer months of high discharge (Aug-Dec) from monthly data. 1931-2011. N= 3.	Total discharge from the Columbia River at Dalles, WA and Fraser River at Hope during the winter months of low discharge (Nov-Apr) and summer months of high discharge (May-Oct) from monthly U.S. Geological Survey discharge data. 1879-2018 and 1913-2016. N = 6.
	Data Source: USGS 15304000	Data Source: Tom Royer, Royer and Grosch 2007	Data Source: USGS 14105700; BC Fraser 08MF005
Sea Surface Temperature (SST)	Average of monthly NOAA Extended Reconstructed SST for winter (Jan-Mar), spring (Apr-Jun), summer (Jul-Sep), and fall (Oct-Dec) and annually at 60°N, 170°W. 1854-2019. N = 5	Average of monthly NOAA Extended Reconstructed SST for winter (Jan-Mar), spring (Apr-Jun), summer (Jul-Sep), and fall (Oct-Dec) and annually in southcentral AK (60°N 149°W). 1854-2019. N = 5	Average of monthly NOAA Extended Reconstructed SST for winter (Jan-Mar), spring (Apr-Jun), summer (Jul-Sep), and fall (Oct-Dec) and annually in coastal Washington (48°N, 125°W). 1854-2019. N=5
Upwelling/Circulation	Data Source: NOAA ERSST V5 Average winter (Oct-Apr) cross-shelf and along-shelf wind at 60°N, 170°W from monthly NCEP/NCAR reanalysis data. 1949-2011. N = 2	Data Source: NOAA ERSST V5 Mean coastal upwelling index (CUI) the Gulf of AK (60°N, 149°W and 60°N, 147°W) using Bakun upwelling calculation based on Ekman's theory of mass transport due to transport due to wind stress, for spring and summer. 1946-2019. N = 4	Data Source: NOAA ERSST V5 Mean coastal upwelling index (CUI) the coastal Washington (45°N, 125°W) using Bakun upwelling calculation based on Ekman's theory of mass transport due to wind stress, for spring, summer, winter and annual. 1946-2019.
	Data Source: Megan Stachura, Stachura et al. 2014 from NOAA ESRL	Data Source: NOAA ERD SWFSC	Data Source: NOAA ERD SWFSC

Climate Regime	Multivariate ENSO Index (1950-2019), Oceanic Nino Index (1950-2019), Pacific Decadal Oscillation Index (1900-2018), the Northern Oscillation Index (1928-2019), North Pacific Gyre Oscillation (1950-2019). N = 5	Same as eastern Bering Sea
	Data Sources: PDO; NPGO; NOI; MEI; ONI	
		Total upwelling magnitude Index (TUMI, 45°N). 1965-2019. Data Source: NOAA CCIEA Same as eastern Bering Sea

Table 2.3: Reduced time series for linear models by regions.

Table 2.3: Reduced Time Series

Mechanism	Washington	Gulf of Alaska	Eastern Bering Sea
Climate Regime	Pacific Decadal Oscillation	Pacific Decadal Oscillation	Pacific Decadal Oscillation
Climate Regime	Multivariate ENSO Index	Multivariate ENSO Index	Multivariate ENSO Index
Climate Regime	North Pacific Gyre Oscillation	North Pacific Gyre Oscillation	North Pacific Gyre Oscillation
Temperature	Mean summer sea surface temperature (Jul-Sep) at 48°N, 125°W	Mean summer sea surface temperature (Jul-Sep) at 60°N 149°W	Mean summer sea surface temperature (Jul-Sep) at 60°N, 170°W
Circulation	Mean summer coastal upwelling (Jul-Sep) at 48°N, 125°W	Mean summer coastal upwelling (Jul-Sep) at 60°N 149°W	Mean winter (Oct-Apr) cross-shelf wind vector at 60°N, 170°W
Circulation	Mean Coastal Upwelling (Spring)	Mean Coastal Upwelling (Spring)	Average winter (Oct-Apr) along-shelf wind vector at 60°N, 170°W
Discharge	Columbia River Discharge during summer months of high discharge (May-Oct)	Total freshwater discharge for a location near Seward during summer months of high discharge (May-Oct)	Total discharge from the Kuskokwim River at Crooked Creek during summer months of high discharge (May-Oct)

Table 2.4: Pairwise t-test by sub region with bonferroni correction and pooled standard deviation for $\delta^{15}N_{Phe}$.

Table 2.4: Nitrogen Phenylalanine T-Test

Subregion	Eastern Bering Sea	Coastal WA	Salish Sea	Southcentral GoA
Coastal WA	p < 0.05*	-	-	-
Salish Sea	p < 0.05*	p < 0.05*	-	-
Southcentral GoA	p < 0.05*	0.93	1	-
Southeast GoA	p < 0.05*	1	p < 0.05*	0.28

Table 2.5: Pairwise t-test by sub region with bonferroni correction and pooled standard deviation for $\delta^{13}C$.

Table 2.5: Bulk Carbon T-Test

Subregion	Eastern Bering Sea	Coastal WA	Salish Sea	Southcentral GoA
Coastal WA	1	-	-	-
Salish Sea	p < 0.05*	p < 0.05*	-	-
Southcentral GoA	p < 0.05*	p < 0.05*	p < 0.05*	-
Southeast GoA	p < 0.05*	p < 0.05*	p < 0.05*	1

2.7 Figures

Figure 2.1: Mechanisms of environmentally induced changes in resources (A-D) assimilated into stable isotope ratios of primary producers (1-2), which are conserved when assimilated into higher trophic levels in the food web (3).

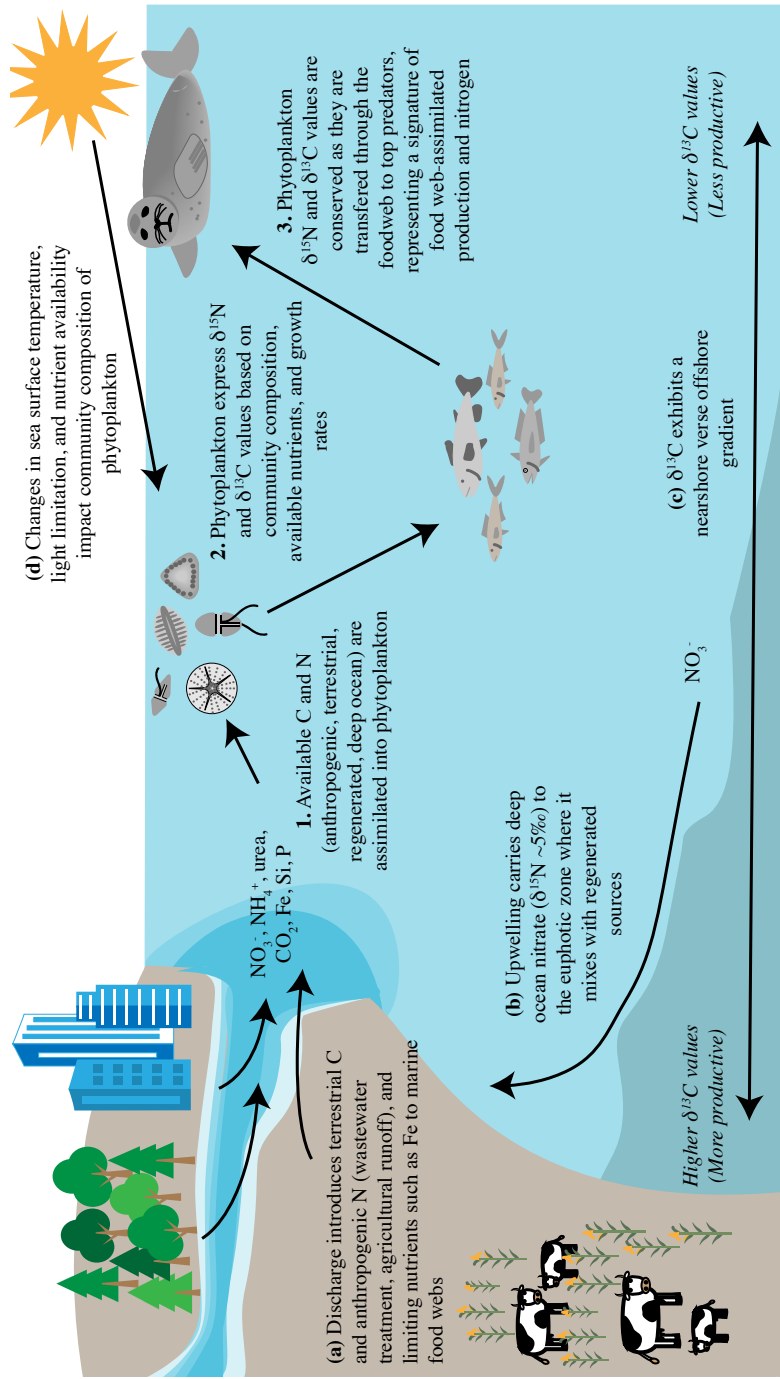


Figure 2.1: Mechanisms of stable isotope change

Figure 2.2: Spatial and temporal distributions of northeast Pacific harbor seal specimens by subregion analyzed for $\delta^{15}N_{Phe}$ and bulk $\delta^{13}C$ values. Subplot colors correspond to map locations and x-axis (years) is the same for each subplot.

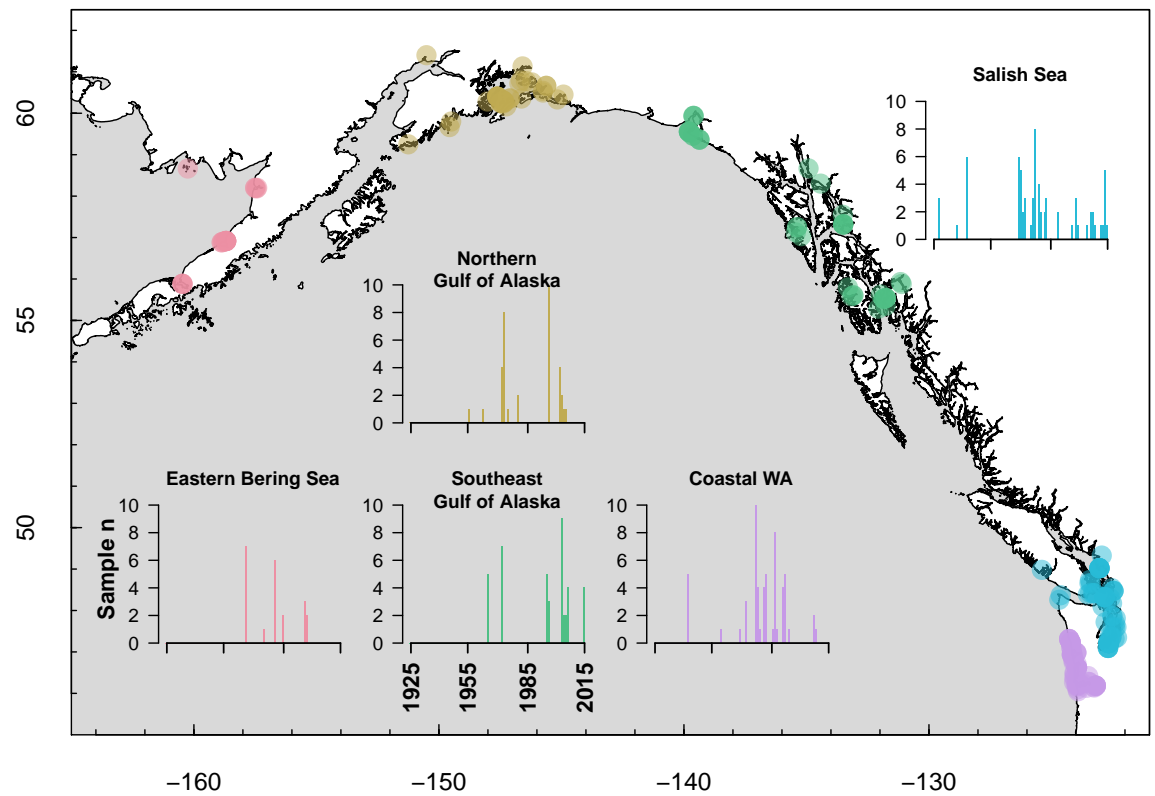


Figure 2.2: Distribution of harbor seal specimens

Figure 2.3: Variability in $\delta^{15}\text{N}_{\text{Phe}}$ and $\delta^{13}\text{C}$ values based on sub region and sex. * denotes a significant difference in isotopic signature between males and females for that region (colors correspond to 2.2).

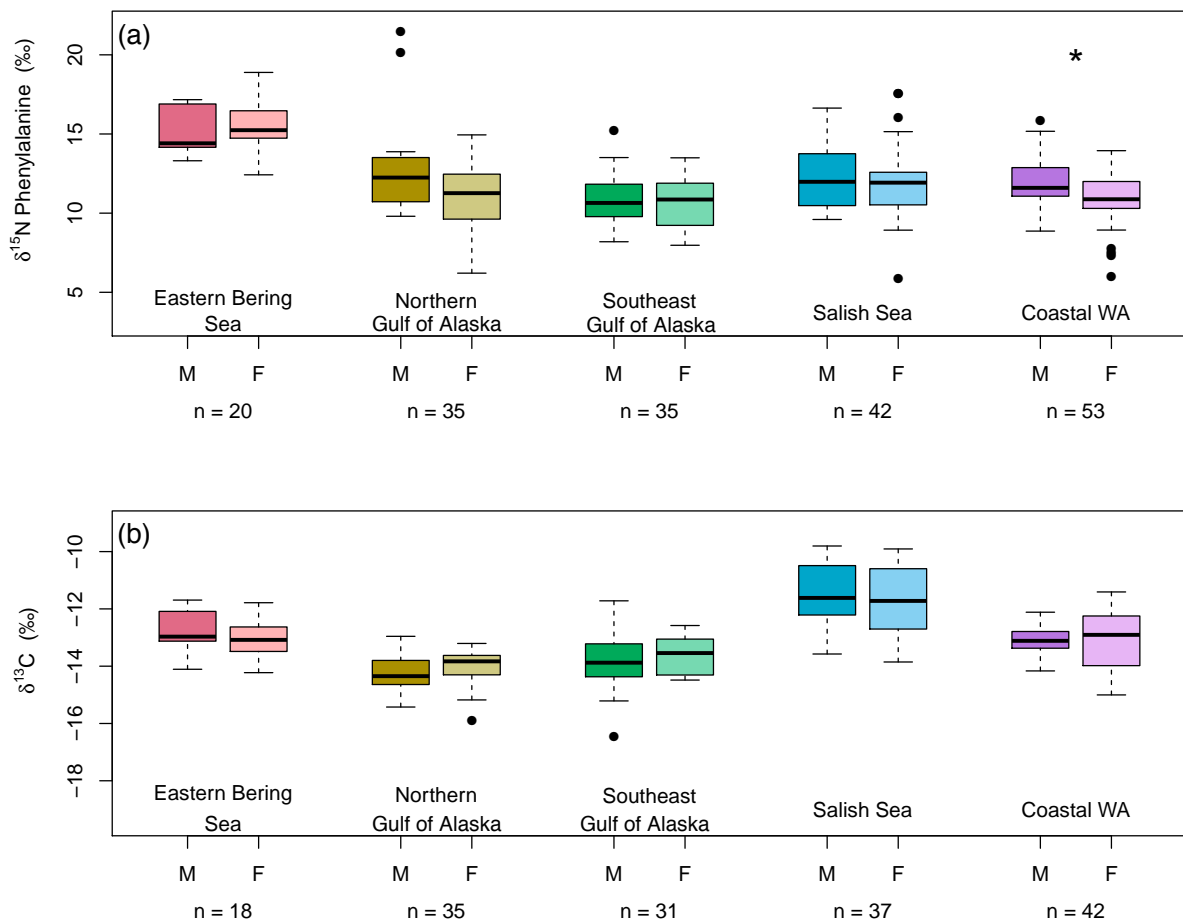


Figure 2.3: Sex and Region based differences

Figure 2.4: Relationship between nitrogen sources ($\delta^{15}N_{Phe}$) and primary production ($\delta^{13}C$) assimilated into the food web for A. a single linear model for the combined data across the northeast Pacific and eastern Bering Sea and B. a mixed effects model with random slope and intercept by sub region (colors correspond to 2.2).

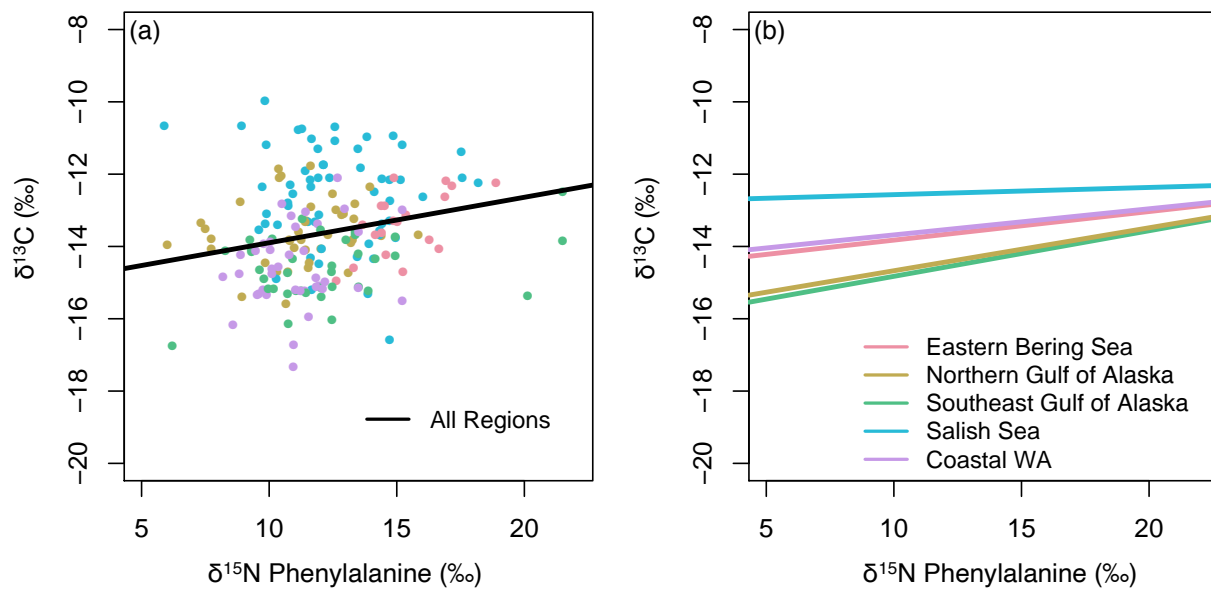


Figure 2.4: Hierarchical $\delta^{15}N_{Phe}$ and $\delta^{13}C$ Models

Figure 2.5: Coefficients of environmental covariates for models with relative support ($\Delta AIC_c < 2$) for harbor seal $\delta^{15}N_{Phe}$ and $\delta^{13}C$ values in three regions of the northeast Pacific: Washington, Gulf of Alaska, and the eastern Bering Sea. Color indicates model support based on AIC_c weight, points are the coefficient estimates for each environmental covariate included in an individual model, and bars show two standard deviations from the coefficient estimate.

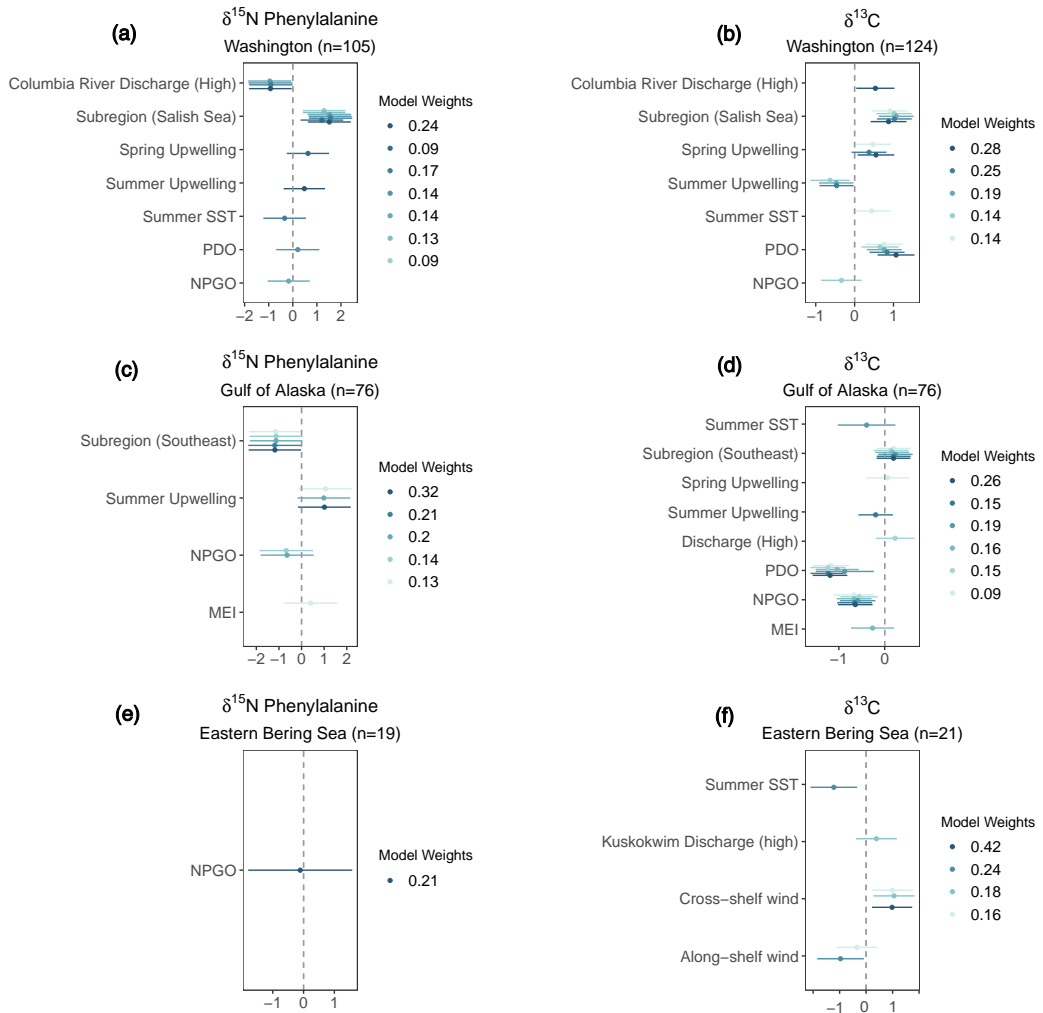


Figure 2.5: Coefficients of Environmental Covariates

Figure 2.6: Common trends in environmental condition and food web assimilated stable isotope values for the regional Gulf of Alaska gaussian-dynamic factor analysis model. The solid lines represent the modelled trends, where 0 is the long-term average and 1 and -1 represent the maximum and minimum possible values respectively; the dash line is the 90% credible interval. Factor loadings can be interpreted as coefficients, representing the strength of association between the modelled trend and each observed environmental time series (colors represent a priori driver category). Values close to 0 mean the observed time series did not correlate to the corresponding trend, while values close to 1 show the observed time series closely matched the modelled trend. Negative loadings indicate an inverse relationship between the observed time series and modelled trend. Stable isotope times series are modelled separately for the northern ($N. \delta^{15}N_{Phe}$; $N. \delta^{13}C$) and southeast ($S. \delta^{15}N_{Phe}$; $S. \delta^{13}C$) subregions.

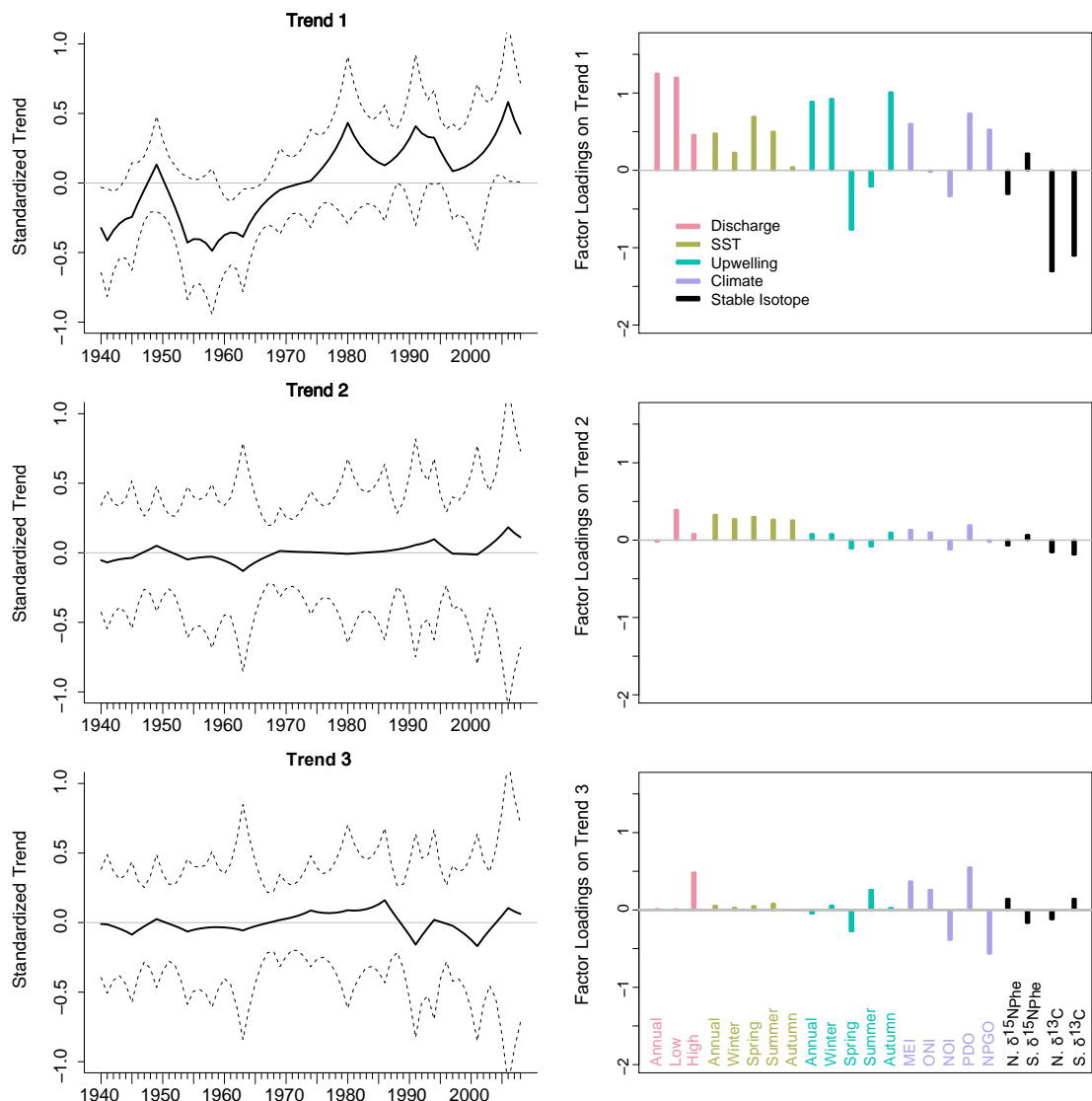


Figure 2.6: Alaska GDFA Results

Figure 2.7: Common trends in environmental condition and food web assimilated stable isotope values for the regional Washington gaussian-dynamic factor analysis model. Stable isotope times series are modelled separately for the coastal ($C. \delta^{15}N_{Phe}$; $C. \delta^{13}C$) and Salish Sea (S.S. $\delta^{15}N_{Phe}$; S.S. $\delta^{13}C$) subregions. See 2.6 caption for further interpretation.

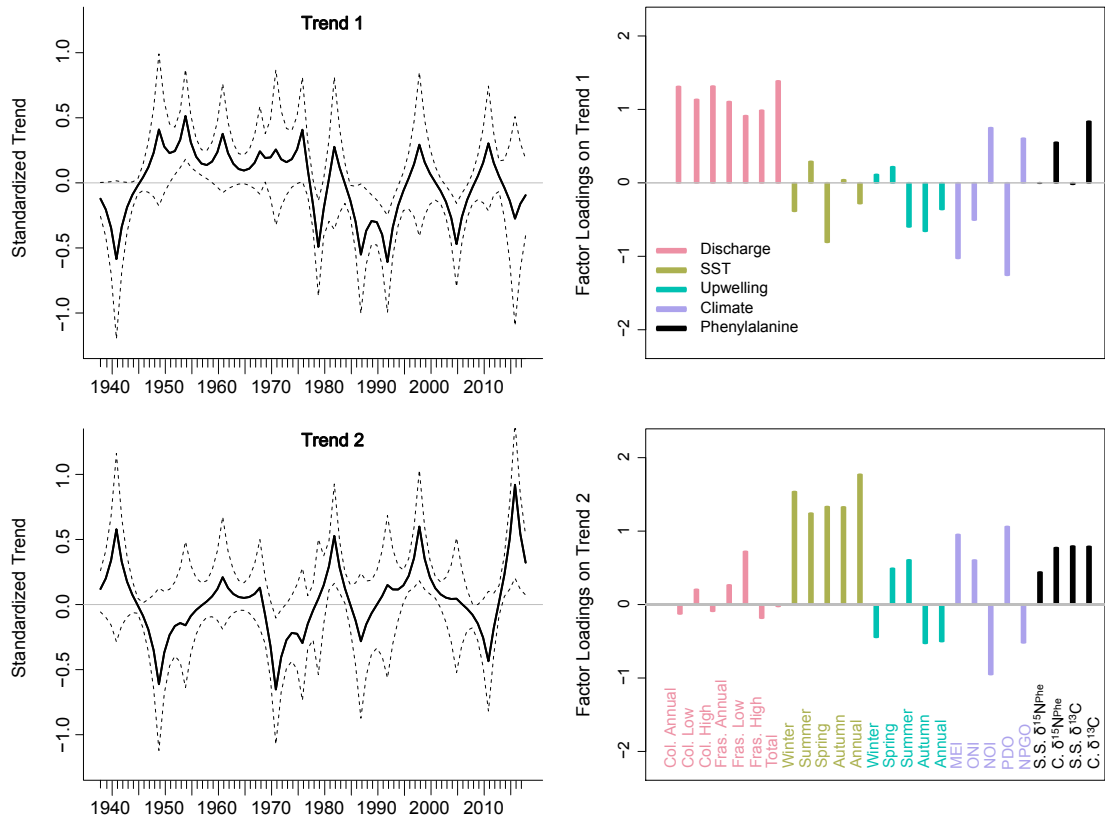


Figure 2.7: Washington GDFA Results

Figure 2.8: Analysis of a) $\delta^{15}N_{Phe}$ and b) $\delta^{13}C$ values by month. For both models, $s(\text{month})$ $p > 0.1$ indicating no seasonality of harbor seal bone collagen stable isotope signature.

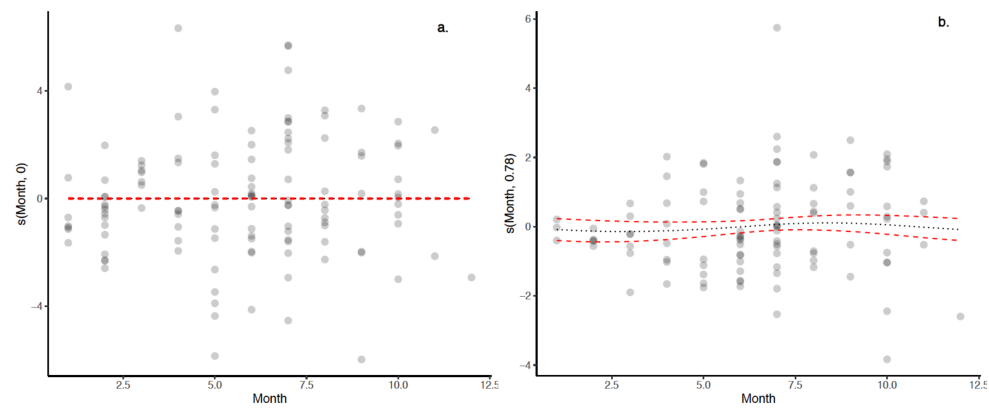


Figure 2.8: Bone collagen stable isotope seasonality analysis

Figure 2.9: Analysis of a) $\delta^{15}\text{N}_{\text{Phe}}$ and b) $\delta^{13}\text{C}$ values by length. For both models, there was no significant slope ($p>0.1$)

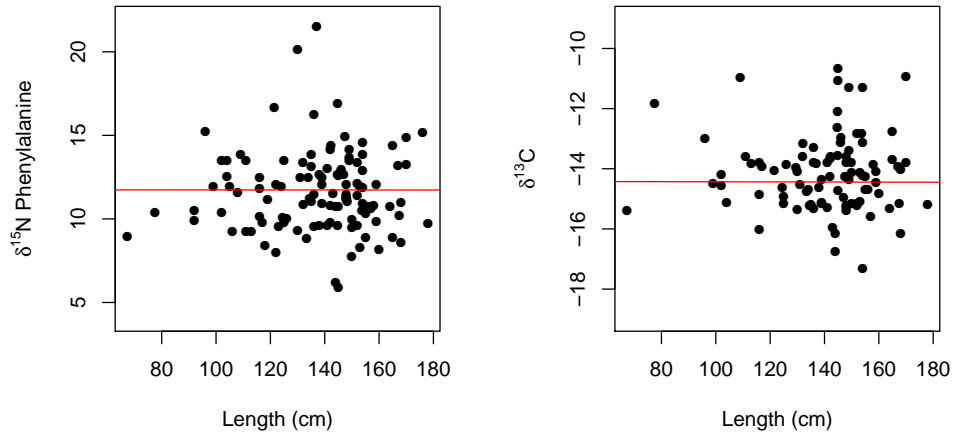


Figure 2.9: Bone collagen stable isotope length analysis

Figure 2.10: Bone collagen $\delta^{15}N$ values of phenylalanine from archival harbor seal specimens collected in the northeastern Pacific in five subregions.

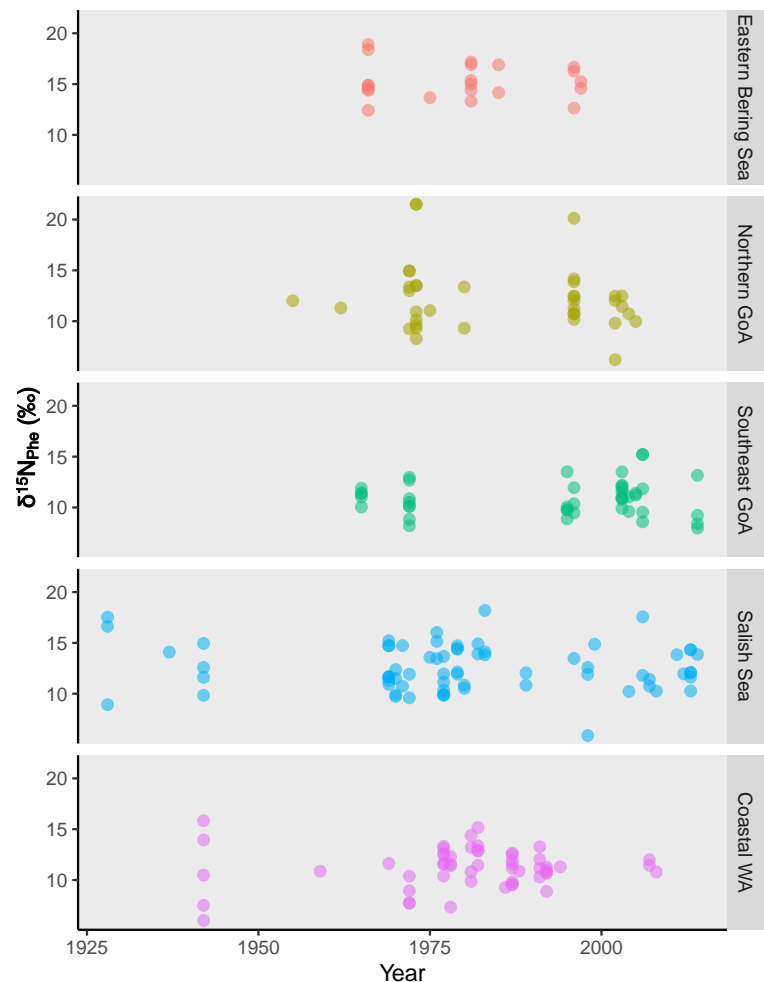


Figure 2.10: Time series of $\delta^{15}N_{Phe}$ data

Figure 2.11: Bone collagen bulk $\delta^{13}C$ values of archival harbor seal specimens collected in the northeastern Pacific in five subregions. These values are not corrected for the Suess effect.

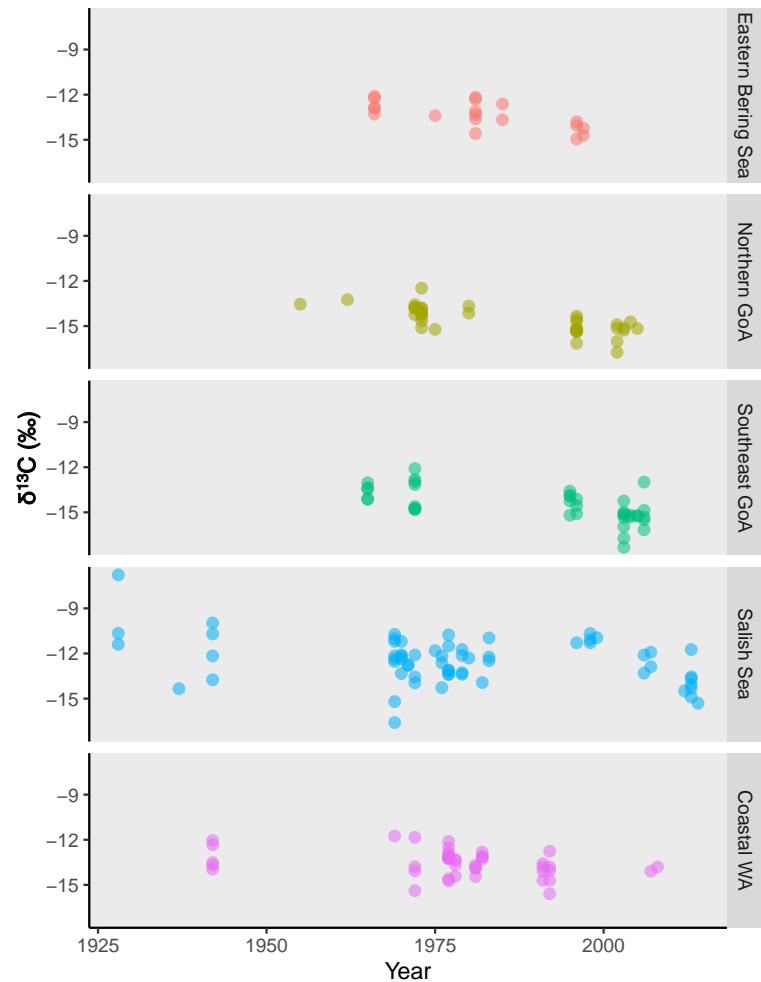


Figure 2.11: Time series of $\delta^{13}C$ data

Figure 2.12: Bone collagen bulk $\delta^{13}\text{C}$ values of archival harbor seal specimens collected in the northeastern Pacific in five subregions. These values are corrected for the Suess effect.

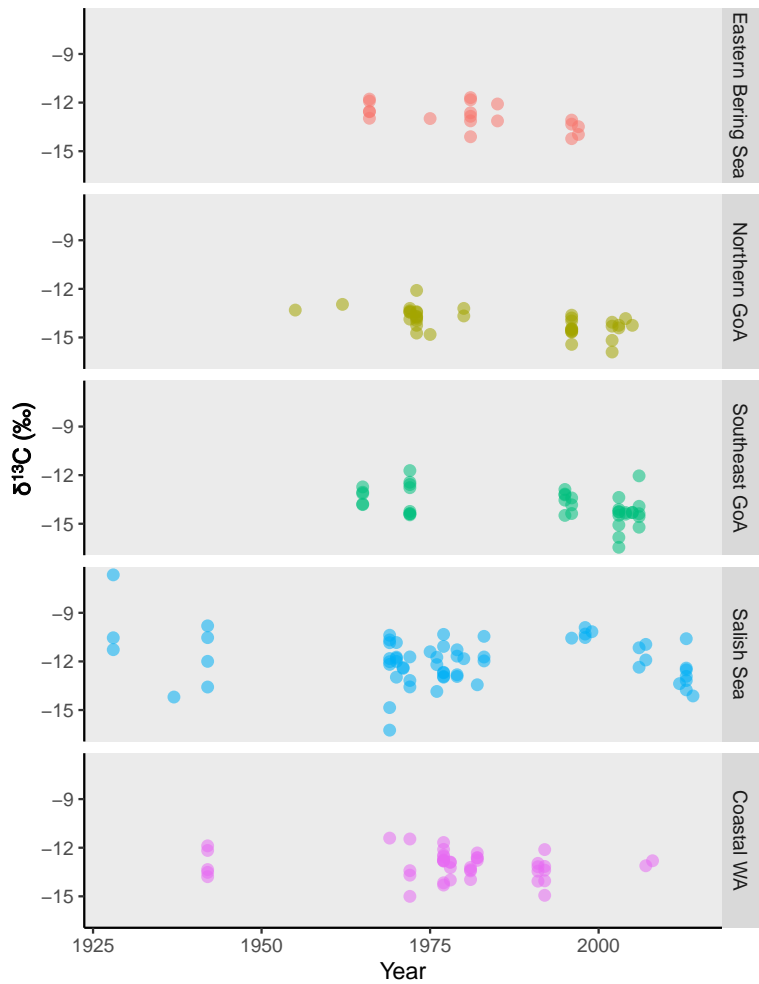


Figure 2.12: Time series of $\delta^{13}\text{C}$ data corrected for Suess effect

Figure 2.13: Bone collagen bulk $\delta^{15}N$ values of archival harbor seal specimens collected in the northeastern Pacific in five subregions.

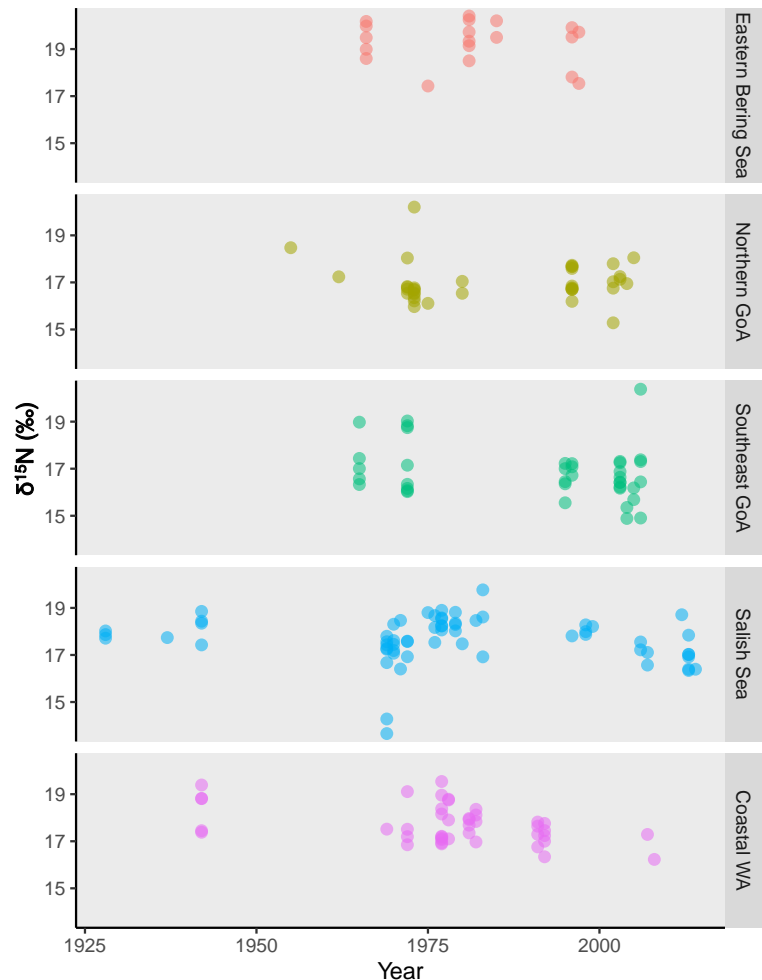


Figure 2.13: Time series of bulk $\delta^{15}N$ data

Figure 2.14: Residuals for the model with the most support (2.5) plotted by year. A trend in model residuals would indicate environmental variables do not account for all temporal variation in harbor seal $\delta^{15}N_{Phe}$ and $\delta^{13}C$ values.

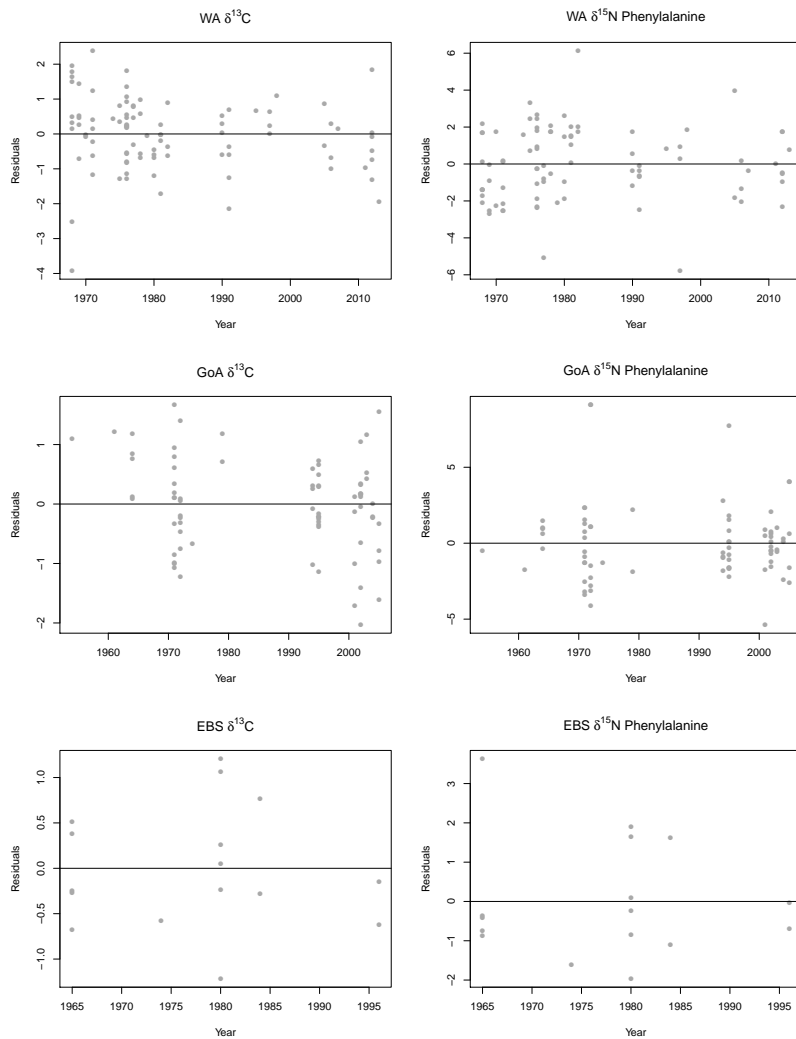


Figure 2.14: Residuals trends for linear models with the most support

Figure 2.15: Model residual plots for the models with the most support from the candidate model set. Note: EBS phenylalanine is an intercept only model, GOA phenylalanine only contains a 2-factor location as a covariate.

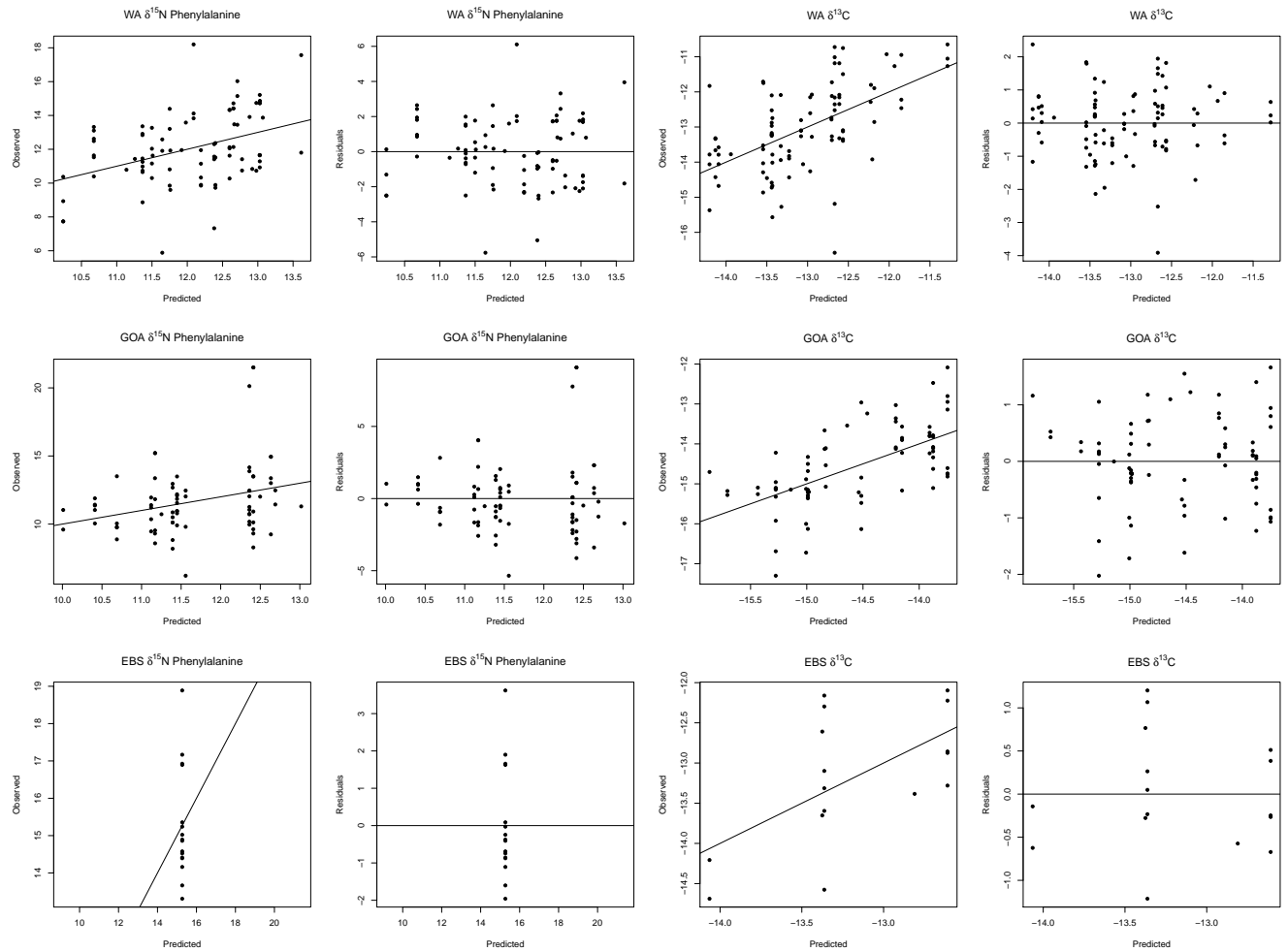


Figure 2.15: Residuals for linear models with the most support

Chapter 3

DELAYED TROPHIC RESPONSE OF A MARINE PREDATOR TO OCEAN CONDITION AND PREY AVAILABILITY DURING THE PAST CENTURY

3.1 Abstract

Understanding the response of predators to ecological change at multiple temporal scales can elucidate critical predator-prey dynamics that would otherwise go unrecognized. We performed compound-specific nitrogen stable isotope analysis (CSIA) of amino acids on 153 harbor seal museum skull specimens to determine how this marine predator has responded to ecosystem change over the past century. The relationships between harbor seal trophic position, ocean condition, and prey abundance, were analyzed using hierarchical modelling of a multi-amino acid framework and applying 1-, 2-, and 3- year temporal lags. We identified delayed responses of harbor seal trophic position to both physical ocean conditions (upwelling, sea surface temperature, freshwater discharge) and prey availability (Pacific hake, Pacific herring and Chinook salmon). However, the magnitude and direction of the trophic response to ecological changes depended on the temporal delay. For example, harbor seal trophic position was negatively associated with summer upwelling, but had a 1- year delayed response to summer sea surface temperature, indicating some predator responses to climate extremes are not immediately observable. These results highlight the importance of considering dynamic responses of predators to their environment as multiple ecological factors are often changing simultaneously and predator response occurs at multiple temporal scales.

3.2 Introduction

The regulation of food web structure by resources (bottom-up control) and the presence of top predators (top-down control) is fundamental for understanding food web responses to environmental, ecological, and anthropogenic change (S. R. Carpenter, Kitchell, & Hodgson, 1985; Estes, Tinker, Williams, & Doak, 1998; Hunter & Price, 1992). Ecological communities are continuously experiencing both biotic and abiotic disturbances (Paine, Tegner, & Johnson, 1998) and the ability of food webs to dynamically respond to these changes is crucial for ecosystem stability (Ghedini, Russell, & Connell, 2015). In marine food webs, physical ocean conditions can impact primary production and ultimately constrain energy availability and thus biomass at higher trophic levels (Emmanuel Chassot et al., 2010; J. K. Moore et al., 2018; Ware & Thomson, 2005). Similarly, the removal of top predators from an ecosystem as a result of human activities such as fishing can decrease predation pressure and alter abundance in both adjacent and non-adjacent trophic levels (Heithaus, Frid, Wirsing, & Worm, 2008; Steneck, 2012). However, large-scale changes in nutrient availability (Rykaczewski & Dunne, 2010), primary productivity (Emmanuel Chassot et al., 2010), and top predator abundance over the past century (Magera, Flemming, Kaschner, Christensen, & Lotze, 2013) means many food webs are experiencing shifts in multiple mechanisms of regulation in tandem, making it challenging to identify dominant drivers structuring ecosystems over the long term.

Marine predators respond to multiple types of bottom-up drivers (i.e., ocean condition, prey availability) and the different temporal scales over which they respond is crucial for understanding community stability. However, delayed predator responses to environmental perturbations are prevalent in marine system, as impacts do not immediately propagate through the complete food web (Duguid et al., 2019; R. S. Smith, Weldon, Hayward, & Henson, 2017). Given communities can shift from bottom-up to top-down control, particularly in response to changing climate conditions (Kratina, Greig, Thompson, Carvalho-Pereira, & Shurin, 2012), delayed predator responses to climate conditions has implications for abun-

dance and mortality rates of prey.

Historical marine predator data that span multiple environmental, ecological, and anthropogenic contexts are useful for identifying time scales over which predators respond to ecosystem drivers. Compound-specific stable isotope analysis (CSIA) of amino acid nitrogen can serve as a tracer of historical predator response to ecological and environmental change by deriving retrospective trophic position estimates from museum specimens (Feddern, Holtgrieve, & Ward, 2021; McMahon et al., 2019). Source amino acids (i.e., phenylalanine, lysine, methionine) exhibit minimal trophic discrimination (the difference in $^{15}\text{N}/^{14}\text{N}$ between trophic and source amino acids in consumers from a trophic transfer) and thus are a proxy for the isotopic signature of primary producers at the base of the food web. In contrast, trophic amino acids (i.e., alanine, glutamic acid, valine, proline) demonstrate trophic enrichment (Kelton & Matthew, 2016) that varies for individual amino acids. Combined, this approach allows for reconstruction of historic trophic position estimates under changing environmental conditions when characterizing the isotopic baseline of past ecosystems may not be possible (McMahon et al., 2019). Thus, CSIA is well suited to identify long-term drivers of food web dynamics when analyzed with historic indices of ocean condition and prey availability.

Reconstructing time series of predator trophic position requires careful consideration of physiological and ecological parameters that contribute to stable isotope signatures. First, taxa exhibit different trophic enrichment factors based on excretion pathways, diet type (omnivory, herbivory, carnivory), and growth (J. M. Nielsen, Popp, & Winder, 2015). Second, the nitrogen production pathway of vascular (i.e., seagrasses) versus nonvascular (i.e., marine diatoms) primary producers impart distinct stable isotope fractionation factors (β) as inorganic sources of nitrogen are converted to tissues (H. B. Vander Zanden et al., 2013). Assumptions about the relative contributions of vascular versus nonvascular plants can therefore impact trophic position estimates (Choi et al. 2017). Finally, there is a delay between the time a prey source is consumed and when that prey source has been fully assimilated into the consumer, referred to as the ‘turnover time’. Turnover times must be considered when

comparing trophic position data to ocean condition and prey availability covariates, as the consumer response to an ecological change will not be immediately observable in consumer tissues.

Nearshore coastal ecosystems provide a model system to assess long-term changes of food web drivers using archival museum specimens of a marine predator by applying CSIA. Food webs of coastal Washington and the Salish Sea have experienced dramatic restructuring over the past century due to declines and subsequent recoveries of marine predators (S. Jeffries, Huber, Calambokidis, & Laake, 2003; Ohlberger, Schindler, Ward, Walsworth, & Essington, 2019). Decades of state-financed population control programs resulted in harbor seals (*Phoca vitulina*) reaching a historic low in the 1970's, with an estimated abundance of approximately 1,000 individuals (S. Jeffries et al., 2003). Following the cessation of bounties in 1960 and the passage of the Marine Mammal Protection Act in 1972, top-predator abundance increased dramatically. Benefiting from a relatively short life history, generalist diet, and legislation restricting mortality, harbor seal populations increased 10-fold between 1970 and 2003 (S. Jeffries et al., 2003). The dramatic increase in abundance of this top predator has been implicated in the declines in economically and ecologically important prey species in the region (Chasco et al., 2017; Nelson, Walters, Trites, & McAllister, 2019), specifically, Chinook salmon (*Oncorhynchus tshawytscha*). Chinook salmon are listed as endangered in the region (WDFW 2017) and are an important prey species for the endangered southern resident orca (Marshall, Stier, Samhouri, Kelly, & Ward, 2016). Simultaneously, the region has also experienced changes in nutrients (Mohamedali et al. 2011), climate regimes (Corwith & Wheeler, 2002; Mantua & Hare, 2002) and abundances of other important prey species such as Pacific herring (*Clupea pallasii*, Siple & Francis (2015)).

Here we examined a century of harbor seal trophic position data in coastal Washington and the Salish Sea. The objective of this work is to identify the time scales at which physical ocean conditions and prey availability exert bottom-up control on marine predator trophic ecology. We assumed a correlation between trophic position and prey species abundance is

the result of increased or decreased consumption of that species. Additionally, we established a multi-amino acid framework for measuring trophic position that improves precision and ecological accuracy by applying a species-specific trophic discrimination factor (McMahon et al., 2019; J. M. Nielsen et al., 2015). We also included a system specific β value rather than a universal value, and applied temporal lags to account for both physiological and ecological delays in consumer response.

3.3 Methods

3.3.1 Sample collection and analysis

Samples were obtained using methods described in Feddern et al. (2021). Briefly, harbor seal bone was obtained from four museum institutions (the Burke Museum, the Slater Museum, the Royal British Columbia Museum, and the Smithsonian Institute) and the National Marine Mammal Laboratory (NOAA). Specimens were treated by maceration in warm water and stored in acid free boxes. Sampling targeted adult specimens and prioritized long-term temporal coverage in two main regions: coastal Washington and the Salish Sea (which included 18 specimens from British Columbia). Specimens with sex, length, and age data were also prioritized but this information was not available for all sampled specimens. A total of 153 specimens were sampled with field collection dates ranging 1928-2014 (Figure 3.1).

3.3.2 Trophic position determination

Bone collagen was decalcified, acid hydrolyzed, derivatized, and analyzed for nitrogen CSIA ($\delta^{15}N$) of 12 individual amino acids. Collagen samples were measured in triplicate with a laboratory standard containing a 12 amino acid mixture of known isotopic composition and a linear drift correction was applied. Full analytical details are described in Appendix 1: Text 1. Previous controlled feeding studies have determined the trophic enrichment factor (TEF) for harbor seals is substantially lower than the conventional literature value of 7.6‰ (Germain

et al., 2013) and thus applying a harbor seal-specific TEF is more accurate (McMahon, Polito, Abel, McCarthy, & Thorrold, 2015). Therefore, trophic position was calculated using a harbor seal-specific TEF, described by McMahon et al. (2015) as a “multi-TEF” approach, using the following equation:

$$\text{TrophicPosition} = \frac{\delta^{15}N_{(i-o)} - TEF_{(i-o),j} - \beta_{(i-o),N}}{\overline{TEF}_{(i-o)}} + 2 \quad (3.1)$$

where $\delta^{15}N_i$ is the measured stable isotope composition of a trophic amino acid i in a sample and $\delta^{15}N_o$ is the stable isotope composition of a source amino acid o in a sample. $\delta^{15}N_{(i-o)}$ represents the total trophic enrichment that has occurred throughout the food web measurable from predator tissues. $TEF_{(i-o),j}$ is the trophic enrichment factor between trophic amino acid i and source amino acid o of a specific consumer j (in this study, harbor seals) which occurs when consumer j assimilates prey. $\beta_{(i-o),N}$ is the difference in enrichment between a specific trophic amino acid i and source amino acid o for non-vascular primary producers N that occurs when primary producers assimilate inorganic nitrogen (J. M. Nielsen et al. (2015); Table 3.1). $\overline{TEF}_{(i-o)}$ represents the mean trophic enrichment that occurs at other trophic levels in the food web, and is calculated from the mean difference between trophic amino acid i and source amino acid o across all consumers described in J. M. Nielsen et al. (2015).

The β parameter differs substantially between vascular and nonvascular primary producers (Ramirez, Besser, Newsome, & McMahon (2021); Table 3.1). In food webs that assimilate organic matter from both vascular and nonvascular plants, including many nearshore food webs, β will be intermediate. In addition to testing a value that represents nonvascular primary producers exclusively $\beta_{(i-o),N}$, we also applied a two-source mixing model using carbon stable isotope data similar to B. Choi et al. (2017). This generates a β that is weighted $\beta_{(i-o),NV}$ based on the contributions of both vascular and nonvascular plants specific to the Washington nearshore ecosystem by first calculating the percent contribution of vascular plants to the food web:

$$\%V = \frac{\delta^{13}C_H - \delta^{13}C_N}{\delta^{13}C_V - \delta^{13}C_N} / 100 \quad (3.2)$$

where $\delta^{13}C_H$ is the mean observed $\delta^{13}C$ value for Washington harbor seals. $\delta^{13}C_V$ is the carbon stable isotope end member for vascular plants, v (-9.5 ‰, derived from seagrasses *Zostera spp.*); and $\delta^{13}C_N$ is the carbon stable isotope end member for nonvascular plants, n (-19.5 ‰, derived from phytoplankton). Carbon end members were specific to the Washington nearshore ecosystems (Howe & Simenstad, 2015). Percent V is the percent contribution of vascular plants to the food web in which harbor seals forage. This assumes the trophic enrichment of ^{13}C is generally negligible (0–1 ‰, Deniro & Epstein 1978). $\beta_{(i-o),NV}$ was then derived by:

$$\beta_{(i-o),NV} = (\beta_{(i-o),V} * \%V) + (\beta_{(i-o),N} * (1 - \%V)) \quad (3.3)$$

where $\beta_{(i-o),N}$ is the enrichment between an individual trophic amino acid i and source amino acid o for aquatic phytoplankton and $\beta_{(i-o),V}$ represents the trophic enrichment of seagrass which are vascular plants (Table 3.1).

3.3.3 Quantifying bottom-up drivers of foraging

To identify the most important explanatory variables of ocean condition and prey availability on predator trophic position, we fit two sets of candidate models using a multi-amino acid (glutamic acid, aspartic acid, alanine, proline, valine) hierarchical model. We selected 12 putative explanatory variables based on the length of the time series and divided them *a priori* into our two categories of interest, ocean condition and prey availability, representing our expected primary forcing mechanisms (Tables 3.2 & 3.4). We fit candidate models to the trophic position and covariate data, and the candidate model set included a null and location-only model (Tables 3.4 & 3.5). Location (Salish Sea or coastal Washington) was included as a factor in all candidate models except the null model. Due to the correlation between the multivariate El Niño Southern Oscillation index and the Pacific Decadal Oscillation only one of these covariates were included in a single model. All timeseries were standardized around a mean of 0 and standard deviation of 1. To avoid collinearity, no more than four covariates (including location) were included in an individual model.

J. M. Nielsen et al. (2015) determined that the use of multiple amino acids improves estimates of trophic position. Therefore, we used multiple trophic amino acids i (alanine, glutamic acid, valine and proline) and one source amino acid o (phenylalanine) to calculate trophic position. We selected amino acids based on: their prevalence in previous studies to derive parameters for equation 1; tissue turnover time relative to the source amino acid, phenylalanine; and their concentrations in bone collagen. The hierarchical linear model took the following structure:

$$\mathbf{y}_t = \alpha_k + \boldsymbol{\beta} \mathbf{X}_{t-d} + \epsilon, \quad (3.4)$$

where y represents harbor seal trophic position from year t and k represents four different trophic amino acids (factors) used to calculate trophic position included as a random effects. \mathbf{X} is a matrix of continuous bottom-up drivers in year t . $\boldsymbol{\beta}$ is a vector of predicted effects (coefficients) of bottom-up drivers included in the model (Tables 3.4 & 3.5) on harbor seal trophic position, and a is the predicted trophic position when all included bottom-up drivers are at an average value (represented by 0) in the coastal region of Washington. The variable d is the temporal lag between a change in bottom-up drivers and when that change is reflected in harbor seal bone collagen. This lag can be due to both physiological (tissue turnover) or ecological effects (rate of propagation through the food web). Time (year, Figure 3.2), sex, size (Figures 3.3 & 3.4), and seasonality (month, Figure 3.5), were also considered as predictors of trophic position but no significant associations were identified and thus these parameters were not included in the hierarchical modeling (Appendix Text 2). The best performing models for both of these approaches were selected using Akaike's Information Criterion (Akaike 1973) with a correction for small sample size (AIC_c). Inclusion of predictors in the model with the most support is indicative of ecological parameters that alter harbor seal foraging ecology or food web dynamics. Additionally, magnitude and sign of the coefficients for included predictors can be interpreted as the degree of trophic change induced by consuming different species, life stages of species, or groups of species, caused by a given predictor.

Stable isotope composition of bone collagen is assumed to reflect diet over the past 1-2

years of the individual's life (K. A. Hobson & Clark, 1992; Newsome, Koch, Etnier, & Aurioles-Gamboa, 2006; Riofrío-Lazo & Aurioles-Gamboa, 2013). A 1-year lag (d) was applied to all harbor seal trophic position estimates to account for the physiological delay from tissue turnover time of bone collagen, where the collagen in a harbor seal collected in year t reflects what the individual ate in the previous year, $t-1$. Delayed harbor seal foraging response to ecosystem dynamics was also tested by applying additional 2-year and 3-year lags to trophic position data; these models represent a 1-year and 2-year ecological delay in addition to the 1-year physiological delay for tissue turnover time. For example, the association between harbor seal trophic position and environmental conditions 2 years before the collection year would indicate that there was a 1-year delay between when the environmental change happened and when the resultant changes propagated through the food web, after accounting for the 1-year tissue turnover time. To check the assumption of no collinearity in predictors in the models with most support ($\Delta AIC_c < 2$), we consulted matrix scatterplots using the car package (Fox and Weisberg 2019) in R (R Development Core Team, 2020) and calculated variance inflation factors.

3.4 Results

3.4.1 Drivers of predator trophic position

Among the physical variables tested, summer upwelling, sea surface temperature and Columbia River discharge during high flow months all impacted harbor seal trophic position but on different temporal scales. There was model selection uncertainty at all three temporal lags (Tables 3.6, 3.7 & 3.8) but covariates and their coefficient estimates were consistent across the most supported models ($\Delta AIC_c < 2$) (Figure 3.8). There were five physiological delay models (Figure 3.8c) with substantial support ($\Delta AIC_c < 2$) all of which included location (Salish Sea versus coastal Washington) as a factor with a coefficient of -0.29 (95% CI [-0.40, -0.19]) and a negative coefficient for summer upwelling (-0.04[-0.07, -0.02]). There were four models with substantial support for the 1-year ecological delay

(Figure 3.8b) all of which included a negative coefficient for summer sea surface temperature (-0.2 [-0.28, -0.11]) and a positive coefficient for spring upwelling (0.03 [0.0, 0.05]). Columbia River discharge during high flow months was included in the five 2-year ecological delay models with the most support (Figure 3.8a) and had the highest impact on harbor seal trophic position with a coefficient of 0.4 [0.22, 0.57]. All other coefficients did not differ substantially from 0 (Figure 3.8). Summer upwelling exhibited an immediate impact on harbor seal trophic position that resulted in overall lower trophic position during the same year (after accounting for tissue turnover; Figure 3.8c). Summer sea surface temperature showed a delayed impact, where harbor seals foraged lower in the food web the year following summers with higher-than-average sea surface temperatures (-0.2 [-0.28, -0.11], Fig. 2). The coefficients for upwelling (Figure 3.8a-c) in all models were small compared to sea surface temperature (Figure 3.8b) and Columbia River discharge (Figure 3.8a). Location had an ecologically significant coefficient of ~ -0.3 [-0.40, -0.19] which was similar across all supported models at all three lags, demonstrating harbor seals in the Salish Sea feed lower in the food web than their coastal Washington counterparts.

Location, Chinook salmon abundance, and hake and herring spawning biomass were the biological variables strongly associated with harbor seal trophic position. Similar to the ocean condition analysis, there was model selection uncertainty but covariates and their coefficients were similar across supported models ((Tables 3.9, 3.10, 3.11 & Figure 3.9)). Chinook smolt production (0.08 [0.02, 0.16]), and hake (0.13 [0.05, 0.21]) and herring spawning biomass (-0.06 [-0.14, 0.02]) were correlated with harbor seal trophic position in the two physiological delay models with substantial support ($\Delta AIC_c < 2$) but the effect of herring spawning biomass on harbor seal trophic position was not significantly different from 0 (Figure 3.8f). Hake spawning biomass and Chinook salmon escapement were included in three out of four 1-year ecological delay models with substantial support (Figure 3.8f) and both were included in the best model. Chinook salmon smolt production (combined index of hatchery releases and wild production of Chinook salmon) was included in all four models with substantial support

at the same lag (Figure 3.8f). Both Chinook salmon smolt production (0.12 [0.06, 0.20]) and hake spawning biomass (0.06 [-0.0, 0.14]) in the 1-year ecological delay model were positively correlated with harbor seal trophic position (Figure 3.8f). Thus, harbor seals fed higher in the food web one year after hake spawning biomass and Chinook salmon smolt production was high (Figure 3.9). In contrast, Chinook escapement counts were negatively correlated at the same time lag (-0.07 [-0.14,0.0]). Covariates and the magnitude and direction of their coefficients were similar in the 2-year ecological delay model (Figure 3.8d) compared to the 1-year ecological delay model (Figure 3.8e) but only three models had substantial support (Figure 3.8d).

3.4.2 Parameterization of the trophic position equation

Inclusion of multiple trophic enrichment factors (Appendix 1: Text 4), multiple trophic amino acids, and a system-specific β value in the trophic position equation improved trophic position estimates (Figures 3.10 & 3.11) compared to the more commonly applied single trophic enrichment factor, nonvascular β parameter, and using only the canonical trophic amino acid, glutamic acid (Appendix 1: Text 4). Harbor seals are known to consume both adult and juvenile hake, Pacific herring, and Pacific salmon, thus a trophic position of 3.5 – 5 would be considered ecologically realistic based on known foraging strategies. Seventy-six % of observations were considered ecologically realistic when applying a system-specific $\beta_{(i-o),V}$, harbor seal-specific trophic enrichment factor, and including glutamic acid, valine, alanine, aspartic acid, and proline (Figure 3.11.2). This parameterization offered a substantial improvement over other parameterizations of the trophic position equation, which ranged from 15% to 80% of observations being ecologically realistic, and was more parsimonious than similarly performing equations (Figures 3.10.4). However, aspartic acid was more variable than other trophic amino acids in all parameterizations and thus was omitted from the hierarchical modelling analysis (Appendix 1: Text 4).

3.5 Discussion

Harbor seals occupy different trophic positions depending on ecological conditions and exhibit delayed trophic responses to ecological perturbations. We found that both ocean conditions and prey availability impact predator trophic position, however, the magnitude and time scale at which predators exhibited trophic responses to these bottom-up drivers varied. In fact, some of the most influential drivers of predator trophic position (i.e., freshwater discharge) had a multi-year delay in predator trophic response. Some effects of ecosystem change on nearshore marine predators will not be immediately observable based on our results and others (R. S. Smith et al., 2017). Furthermore, changes in ocean conditions can alter top-down pressure on the ecological community in subsequent years, as generalist top predators shift their trophic ecology in response to their environment. Our results suggest that following years with extreme ocean conditions, ecological responses will continue to manifest for multiple years into the future as impacts propagate through the food web.

3.5.1 Delayed trophic position response to environmental conditions

Multiple studies have shown that ocean conditions such as sea surface temperature, upwelling, and freshwater discharge impact abundance and recruitment of nearshore fishes in coastal Washington (C. Greene, Kuehne, Rice, Fresh, & Penttila, 2015; Reum, Essington, Greene, Rice, & Fresh, 2011). For some species of seabirds in the region, breeding success also responds to ocean conditions but exhibits a temporally lagged response (Duguid et al., 2019). Our results show trophic position of top predators (harbor seals) can also have delayed responses to bottom-up forcing of ocean conditions with up to a 2-year ecological delay. Reum et al. (2011) found age-0 Pacific herring abundance in Puget Sound was also positively correlated with annual upwelling in the Strait of Georgia. Consumption of a greater proportion of these low-trophic level juvenile fishes by harbor seals could explain the negative correlation between trophic position and upwelling in the physiological delay model (Figure

3.8c).

3.5.2 Delayed trophic position response to prey abundance

Harbor seal trophic position responds to the abundance of multiple prey species and the magnitude and direction of the response depends on both the individual species and temporal delay. Pacific hake and Pacific herring have frequently been documented as common prey sources in Washington harbor seal diet (M. M. Lance et al., 2012; A. C. Thomas, Lance, Jeffries, Miner, & Acevedo-Gutierrez, 2011). For some species of hake, trophic level can differ by as much as 0.6 among individuals of different size classes (Iitembu, Miller, Ohmori, Kanime, & Wells, 2012). In years when Pacific hake spawning biomass is high, and the years following high spawning biomass, harbor seal trophic position increases, indicating harbor seals are opportunistically feeding on large, adult-stage hake (Figure 3.9d). In contrast to Pacific hake, harbor seal trophic position exhibited a negative relationship with herring spawning biomass. The relative abundance of adult to juvenile herring in harbor seal diet varies between years (M. M. Lance et al., 2012) and harbor seals are known to preferentially consume juveniles during herring spawning season and adult herring during the non-spawning season (A. C. Thomas et al., 2011). Our results agree with these findings and indicate a trophic shift in response to herring spawning biomass (Figure 3.8c), which is likely a result of increased juvenile consumption during the spawning season. Alternatively, this result may be due to covariation with a third variable. For example, upwelling was also correlated to harbor seal trophic position in the physiological delay model and is known to impact herring abundance (Reum et al., 2011).

Harbor seals opportunistically consume more low-trophic level smolts when they are abundant which occurs in the two years after high spawner abundance (Figure 3.9). Escapement counts represent the number of adult salmon that return to freshwater to spawn after they have been both fished and predated on and serve as a strong predictor of out migrating smolts during the next two years. After hatching, fry and parr reside in freshwater for 12-18

months before migrating to estuaries. The 1- and 2- year delayed negative response of harbor seal trophic position to Chinook salmon escapements counts agrees with previous studies documenting harbor seal consumption of out-migrating smolts (Figure 3.9d, A. C. Thomas, Nelson, Lance, Deagle, & Trites (2017), M. M. Lance et al. (2012)). In contrast, a combined index of hatchery Chinook smolt production and wild Chinook smolt production offers the best predictor of adult salmon availability to harbor seals (Figure 3.9). The positive relationship between harbor seal trophic position and smolt production indicates smolt production is a better indicator of adult Chinook salmon prey availability to harbor seals than escapement counts. Chinook salmon spend 1-7 years the ocean before returning to freshwater to spawn, and escapement counts only represents the age class of fish that are returning to spawn in a given year. In contrast, smolt production in the current year and during the previous two years provides an index of adult salmon abundance that are available to and predated upon by harbor seals (Figure 3.9d). Notably, the salmon abundance estimates in this study were specific to Washington Chinook salmon. It is possible that harbor seal trophic position estimates have stronger associations with metrics of total abundance of all species of Pacific salmon if harbor seals are not selective of the salmon they species consume. However, data available for other species in the region did not provide enough temporal overlap with the trophic position data and thus were omitted. Regardless, this analysis indicates both adult and juvenile Chinook salmon contribute to harbor seal trophic ecology and predation on both age classes may be an important component for at sea survival of Washington Chinook salmon.

Management of predators that consume threatened, economically important prey species such as harbor seals requires extensive tradeoffs (Marshall et al., 2016). Harbor seals demonstrate large variations in trophic ecology in response to location, prey availability, and ocean condition thus, they exert dynamic top-down effects on the community in which they forage. The balance of top-down versus bottom-up effects on food webs in response to resource perturbations is determined by a top predator's ability to exploit subsidies (McCary et al.,

2021). Our results also show the response of trophic position (and assumed predation) change is often delayed on the order of 1-2 years in response to ecological conditions. Currently, model estimates of total biomass of Chinook salmon consumed by harbor seals is assumed to be static through time (Chasco et al., 2017). Based on our results and others (M. M. Lance et al., 2012; K. Wilson, Lance, Jeffries, & Acevedo-Gutierrez, 2014) this is likely inaccurate as seasonality, spatial location, and individual behavior impact harbor seal predation. This variability in foraging ecology should be carefully considered when assessing tradeoffs of predator management decisions to ensure realized expectations for stakeholders. Spatially distinct management strategies that are reevaluated in the context of changing ecological conditions will likely be important for managing harbor seal prey given their dynamic foraging strategies and trophic responses.

3.5.3 Advances in the application of amino acid based trophic position calculations

CSIA is a powerful tool for reconstructing historical ecological data that requires consideration for system specific dynamics for accurate trophic position estimates. Despite its benefits compared to traditional bulk stable isotope analysis, CSIA is sensitive to the parameterization of trophic position equation (Germain et al., 2013; McMahon et al., 2019) (Figure 3.10 & 3.11). Application of a multi-TEF approach has led to consistent underestimates of trophic position compared to known feeding ecology (Germain et al., 2013; McMahon et al., 2019, 2015) despite its more realistic representation of metabolic pathways compared to a single-TEF approach. Thus, the utility and reliability of CSIA for trophic position studies for retrospective analyses requires careful consideration of the trophic enrichment factors, tissue turnover, and β values applied. Harbor seals are expected to exhibit a trophic position ranging from approximately 3.5 to 5 and only 12%-66% of data fell within this range when applying $\beta_{(i-o),N}$ (Figure 3.10). Seagrasses are abundant in coastal Washington and the Salish Sea and there is evidence of food web coupling in these coastal environments (Howe & Simenstad, 2015) therefore vascular primary producers are expected to contribute to these

food webs requiring a system specific β value. Variation in vascular plant abundance over time could result in temporal changes to the relative contribution of these primary producers to the food web which would require the application of a time-varying β value. We did not find evidence of temporal trends in $\delta^{13}C$ data in harbor seals (Feddern et al., 2021) which would be expected if seagrass contribution to the food web was time-varying and therefore a temporally static β value was appropriate for this study. By applying a system specific β value based on expected proportions of primary producer ecophysiology types entering the food web, we significantly improved the realism of our trophic position estimates. We therefore recommend using a multi-trophic enrichment factor approach with taxa specific trophic enrichment factors and system-specific β when there is evidence of vascular plant contributions to the food web.

More research is needed to investigate the degree to which top predator trophic position change can serve as an indicator of top-down control on the community, which undoubtedly depends on food web structure of a given system (i.e., degree of omnivory, connectance). Regardless, delayed predator dynamics are not limited to marine or nearshore environments, although the temporal scales for delayed trophic responses for other predators and systems warrants investigation. Anticipating delayed responses may be equally important for identifying long-term ecological consequences in response to future climate perturbations, especially as extreme climate events become frequent and more severe.

The regulation of food web structure by resources is foundational for understanding ecosystem response to perturbations. Based on our findings, nearshore marine predators exhibit a trophic response to ecological change on multiple temporal scales, as different ecological perturbations propagate through the food web at different rates. As such, changes to predator trophic ecology can have consequences throughout the food web that are not immediately realized especially following environmental perturbations. Impacts of the 2014-2016 marine heatwave in the Gulf of Alaska (the longest lasting event of the past decade) are still being observed and some ecological responses have persisted for up to 5 years (Suryan et al., 2021).

Delayed responses of marine predators should be considered when anticipating ecological responses following extreme environmental and ecological events as top-down pressure on the community in subsequent years is likely to change as predators shift their trophic ecology in response to their environment.

(Figure 3.8d)

3.6 Tables

Table 3.1: Trophic amino acid specific parameter values for β and trophic enrichment factors (TEF) to test parameterization of trophic position calculations using multiple TEFs and β values. The source amino acid (o) for all parameters was phenylalanine.

Table 3.1: Trophic position parameter values

Trophic Amino Acid (i)	$\beta_{(i-o),N}$	$\beta_{(i-o),V}$	$\beta_{(i-o),NV}$	$TEF_{(i-o),j}$	$\overline{TEF}_{(i-o)}$
Glutamic acid (Glu)	2.9	-8.7	-3.9	3.4	6.6
Alanine (Ala)	2.8	-8	-3.6	2.5	6.8
Aspartic Acid (Asp)	1.8	-7.3	-4.2	3.5	5.4*
Valine (Val)	3.4	-6.8	-2.6	7.5	4.6
Proline (Pro)	2.7	-7.7	-3.9	5.5	5
Data Source	Nielsen et al. 2015	Vander Zanden et al. 2013	This study	Germain et al. 2013	Nielsen et al. 2015

Table 3.2: Datasets used to test ocean condition as a bottom-up driver of harbor seal trophic ecology. Total number of models tested = 35.

Table 3.2: Environmental Datasets

Covariate	Time Series Description	Length	Source
Discharge	Total discharge from the Columbia River at Dalles, WA during summer months of high discharge (May-Oct) from monthly U.S. Geological Survey discharge data.	1879-2018	Data Source: USGS 14105700
Sea Surface Temperature (SST)	Average of monthly NOAA Extended Reconstructed SST for summer (Jul-Sep) in coastal Washington (48°N, 125°W).	1854-2019	Data Source: NOAA ER SST V5
Upwelling	Mean coastal upwelling index (CUI) coastal Washington (45°N, 125°W) using Bakun upwelling calculation based on Ekman's theory of mass transport due to wind stress, for spring (Apr-Jun) and summer (Jun-Sep).	1946-2019.	Data Source: NOAA ERD SWFSC
North Pacific Gyre Oscillation	2nd dominant mode of sea surface height variability in the northeast Pacific. Correlates with fluctuations in salinity nutrients and chlorophyll-a.	1950-2019	Data Source: Di Lorenzo et al. 2008, NPGO
Multivariate ENSO Index	The extended Multivariate ENSO Index (MEI) uses Principle Component analysis on six variables: sea-level pressure, u and v component of the surface wind vector, sea surface temperature and cloudiness fraction in the tropical Pacific.	1950-2019	Data Source: NOAA/ESRL via California Current Integrated Ecosystem Assessment MEI
Pacific Decadal Oscillation	Same as eastern Bering Sea	1900-2018	Data Sources: PDO; Zhang et al. 1997; Mantua et al 1997

Table 3.4: Datasets used to test prey availability as a bottom-up driver of harbor seal trophic ecology. Total number of models tested = 26.

Table 3.3: Prey Datasets

Covariate	Time Series Description	Length	Source
Herring Biomass	Adult herring spawning biomass from egg deposition surveys for the estimated from Washington State Department of Fish and wildlife by Siple and Francis 2015.(MARSS output section S5, Figures S11 & S12)	1973-2012	Siple, M.C. and T.B. Francis. 2015. Population diversity in Pacific herring of the Puget Sound, USA.
Hake Biomass	Pacific Hake (whiting) relative spawning biomass in US and Canadian waters.	1973-2012	Berger et al. 2017. Table 8 total spawning biomass.
Chinook Salmon Spawners	Chinook salmon spawner summary data including all populations with a time series with data from at least 1973. Includes: Cedar River, Coweeman River, Elochoman River, Grays and Chinook Rivers, Green River, Kalama River, Lewis River, Lower Cowlitz River, Lower and Upper Sauk River, Lower and Upper Skagit River, McKenzie River, Mid-Hood Canal, Nisqually River, Puyallup River, Skokomish River, Skykomish River, Snoqualmie River, Suiattle River, Toutle River, Upper Gorge Tributaries, White River and White Salmon River.	1973-2012	Northwest Fisheries Science Center, 2020: SPS Abundance - Salmon spawner abundance data compilation and database management
Chinook Salmon Smolt Production	Hatchery release data from the Regional Mark Information System and Wild Salmon Production data summarized by Chasco et al. 2017. Data was summed across both datasets for total juvenile salmon production.	1973-2012	RMIS, summarized at https://github.com/bchasco/COAST_WIDE

Harbor Seal Abundance	Harbor seal population estimates based on coastal estuary, eastern Bays, Hood Canal, Olympic Peninsula, Puget Sound, San Juan Islands, and the Strait of Juan de Fuca counts. (MARSS output section S5, Figures S13 & S14)	1975-2012	Jeffries, S., H. Huber, J. Calambokidis and J. Laake. 2003. Trends and status of harbor seals in Washington state: 1978-1999. <i>The Journal of Wildlife Management</i> 67: 207-218.
-----------------------	--	-----------	--

Table 3.4: Full candidate model set ($n = 35$) for ocean condition modelling. The same candidate models were used for the physiological delay, 1-year ecological delay, and 2-year ecological delay models

Table 3.4: Ocean Condition Candidate Models

Covariates
1. Null
2. Location Only
3. PDO, Location
4. NPGO, Location
5. MEI, Location
6. Upwelling (Spring), Location
7. NPGO, PDO, Location
8. PDO, Upwelling (Spring), Location
9. NPGO, Upwelling (Spring), Location
10. MEI, Upwelling (Spring), Location
11. SST (Summer), Location
12. SST (Summer), PDO, Location
13. SST (Summer), NPGO, Location
14. SST (Summer), MEI, Location
15. SST (Summer), Upwelling (Spring), Location
16. SST (Summer), PDO, Upwelling (Spring), Location
17. SST (Summer), NPGO, Upwelling (Spring), Location
18. SST (Summer), MEI, Upwelling (Spring), Location
19. Upwelling (Summer), Location
20. Upwelling (Summer), PDO, Location
21. Upwelling (Summer), NPGO, Location
22. Upwelling (Summer), MEI, Location
23. Upwelling (Summer), NPGO, Upwelling (Spring), Location
24. Columbia Discharge (High), Location
25. Columbia Discharge (High), PDO, Location
26. Columbia Discharge (High), NPGO, Location
27. Columbia Discharge (High), MEI, Location
28. Upwelling (Spring), Location
29. Columbia Discharge (High), PDO, Upwelling (Spring), Location
30. Columbia Discharge High, NPGO, Upwelling (Spring), Location

31. Columbia Discharge High, MEI, Upwelling (Spring), Location
 32. Columbia Discharge (High), SST (Summer), Location
 33. Columbia Discharge (High), Upwelling (Summer), Location
 34. SST (Summer), Upwelling (Summer), Location
 35. SST (Summer), Upwelling (Summer), Columbia Discharge (High), Location
-

Table 3.5: Full candidate model set ($n = 26$) for prey availability modelling. The same candidate models were used for the physiological delay, 1-year ecological delay, and 2-year ecological delay models.

Table 3.5: Prey Availability Candidate Models

Covariates
1. Null
2. Location Only
3. Herring Spawning Biomass, Location
4. Chinook Escapements, Location
5. Chinook Smolt Production, Location
6. Hake Spawning Biomass, Location
7. Herring Spawning Biomass, Chinook Escapements, Location
8. Herring Spawning Biomass, Hake Spawning Biomass, Location
9. Herring Spawning Biomass, Chinook Smolt Production, Location
10. Chinook Escapements, Hake Spawning Biomass, Location
11. Chinook Escapements, Chinook Smolt Production, Location
12. Chinook Smolt Production, Hake Spawning Biomass, Location
13. Chinook Escapement, Chinook Smolt Production, Hake Spawning Biomass, Location
14. Herring Spawning Biomass, Chinook Smolt Production, Hake Spawning Biomass, Location
15. Chinook Escapements, Chinook Smolt Production, Herring Spawning Biomass, Location
16. Herring Spawning Biomass, Hake Spawning Biomass, Chinook Escapements, Location
17. Harbor Seal Abundance, Location
18. Harbor Seal Abundance, Herring Spawning Biomass, Location
19. Harbor Seal Abundance, Chinook Escapements, Location
20. Harbor Seal Abundance, Chinook Smolt Production, Location
21. Harbor seal Abundance, Hake Spawning biomass, Location
22. Harbor Seal Abundance, Herring biomass, Chinook Escapements, Location
23. Harbor Seal Abundance, Herring Spawning Biomass, Hake Spawning Biomass, Location
24. Harbor Seal Abundance, Herring Spawning Biomass, Chinook Smolt Production, Location
25. Harbor Seal Abundance, Chinook Escapements, Hake Spawning Biomass, Location
26. Harbor Seal Abundance, Chinook Smolt Production, Hake Spawning Biomass, Location

Table 3.6: Top ten ocean condition models with the most support (lowest AIC_c) with a physiological delay applied.

Table 3.6: Physiological delay top 10 models (ocean condition)

Covariates	AIC_c	ΔAIC_c
23. Upwelling (Summer), NPGO, Upwelling (Spring), Location	742.75	0.00
35. SST (Summer), Upwelling (Summer), Columbia Discharge (High), Location	743.39	0.63
33. Columbia Discharge (High), Upwelling (Summer), Location	744.12	1.36
19. Upwelling (Summer), Location	744.30	1.55
34. SST (Summer), Upwelling (Summer), Location	744.70	1.95
21. Upwelling (Summer), NPGO, Location	745.25	2.50
22. Upwelling (Summer), MEI, Location	745.55	2.80
20. Upwelling (Summer), PDO, Location	746.11	3.36
26. Columbia Discharge (High), NPGO, Location	754.16	11.41
30. Columbia Discharge High, NPGO, Upwelling (Spring), Location	754.71	11.96
	NA	NA

Table 3.7: Top ten ocean condition models with the most support (lowest AIC_c) with a 1-year ecological delay applied.

Table 3.7: 1-year ecological delay top 10 models (ocean condition)

Covariates	AIC_c	ΔAIC_c
15. SST (Summer), Upwelling (Spring), Location	734.84	0.00
16. SST (Summer), PDO, Upwelling (Spring), Location	736.55	1.70
18. SST (Summer), MEI, Upwelling (Spring), Location	736.65	1.81
17. SST (Summer), NPGO, Upwelling (Spring), Location	736.80	1.95
14. SST (Summer), MEI, Location	738.91	4.07
11. SST (Summer), Location	740.21	5.37
32. Columbia Discharge (High), SST (Summer), Location	741.30	6.46
12. SST (Summer), PDO, Location	741.34	6.49
34. SST (Summer), Upwelling (Summer), Location	741.99	7.15
13. SST (Summer), NPGO, Location	742.04	7.20
	NA	NA

Table 3.8: Top ten ocean condition models with the most support (lowest AIC_c) with a 2-year ecological delay applied.

Table 3.8: 2-year ecological delay top 10 models (ocean condition)

Covariates	AIC_c	ΔAIC_c
24. Columbia Discharge (High), Location	742.09	0.00
33. Columbia Discharge (High), Upwelling (Summer), Location	742.83	0.74
26. Columbia Discharge (High), NPGO, Location	743.06	0.97
25. Columbia Discharge (High), PDO, Location	743.54	1.45
28. Upwelling (Spring), Location	743.86	1.77
27. Columbia Discharge (High), MEI, Location	744.04	1.95
32. Columbia Discharge (High), SST (Summer), Location	744.07	1.98
35. SST (Summer), Upwelling (Summer), Columbia Discharge (High), Location	744.48	2.38
29. Columbia Discharge (High), PDO, Upwelling (Spring), Location	744.56	2.47
30. Columbia Discharge High, NPGO, Upwelling (Spring), Location	745.06	2.97
	NA	NA

Table 3.9: Top ten prey availability models with the most support (lowest AIC_c) with a physiological delay applied.

Table 3.9: Physiological Delay Top 10 Models (Prey Availability)

Covariates	AIC_c	ΔAIC_c
14. Herring Spawning Biomass, Chinook Smolt Production, Hake Spawning Biomass, Location	547.29	0.00
12. Chinook Smolt Production, Hake Spawning Biomass, Location	547.58	0.29
26. Harbor Seal Abundance, Chinook Smolt Production, Hake Spawning Biomass, Location	549.48	2.20
13. Chinook Escapement, Chinook Smolt Production, Hake Spawning Biomass, Location	549.50	2.21
23. Harbor Seal Abundance, Herring Spawning Biomass, Hake Spawning Biomass, Location	549.54	2.25
6. Hake Spawning Biomass, Location	549.55	2.27
21. Harbor seal Abundance, Hake Spawning Biomass, Location	551.18	3.89
10. Chinook Escapements, Hake Spawning Biomass, Location	551.46	4.18
5. Chinook Smolts Production, Location	552.72	5.43
16. Herring Spawning Biomass, Hake Spawning Biomass, Chinook Escapements, Location	552.97	5.69
	NA	NA

Table 3.10: Top ten prey availability models with the most support (lowest AIC_c) with a 1-year ecological delay applied.

Table 3.10: 1-Year Ecological Top 10 Models (Prey Availability)

Covariates	AIC_c	ΔAIC_c
13. Chinook Escapement, Chinook Smolt Production, Hake Spawning Biomass, Location	554.76	0.00
12. Chinook Smolt Production, Hake Spawning Biomass, Location	555.28	0.53
11. Chinook Escapements, Chinook Smolt Production, Location	555.56	0.80
14. Herring Spawning Biomass, Chinook Smolt Production, Hake Spawning Biomass, Location	555.91	1.15
26. Harbor Seal Abundance, Chinook Smolt Production, Hake Spawning Biomass, Location	556.78	2.03
5. Chinook Smolts Production, Location	557.22	2.47
15. Chinook Escapements, Chinook Smolt Production, Herring Spawning Biomass, Location	557.50	2.74
20. Harbor Seal Abundance, Chinook Smolt Production, Location	559.09	4.33
9. Herring Spawning Biomass, Chinook Smolt Production, Location	559.22	4.46
24. Harbor Seal Abundance, Herring Spawning Biomass, Chinook Smolt Production, Location	560.99	6.23
NA	NA	

Table 3.11: Top ten prey availability models with the most support (lowest AIC_c) with a 2-year ecological delay applied.

Table 3.11: 2-Year Ecological Top 10 Models (Prey Availability)

Covariates	AIC_c	ΔAIC_c
11. Chinook Escapements, Chinook Smolt Production, Location	480.69	0.00
10. Chinook Escapements, Hake Spawning Biomass, Location	481.41	0.72
7. Herring Spawning Biomass, Chinook Escapements, Location	484.20	3.51
4. Chinook Escapements, Location	484.90	4.21
12. Chinook Smolt Production, Hake Spawning Biomass, Location	485.17	4.48
5. Chinook Smolts Production, Location	486.50	5.81
6. Hake Spawning Biomass, Location	486.56	5.87
19. Harbor Seal Abundance, Chinook Escapements, Location	486.74	6.05
9. Herring Spawning Biomass, Chinook Smolt Production, Location	487.91	7.22
1. Null	488.12	7.43
	NA	NA

3.7 Figures

Figure 3.1: Spatial distribution of harbor seal specimens (a) collected in the Salish Sea (yellow) and coastal Washington (blue) with the year of specimen collection and total number of specimens (n) for each year from 1928-2014 in the Salish Sea (b) and coastal Washington (c).

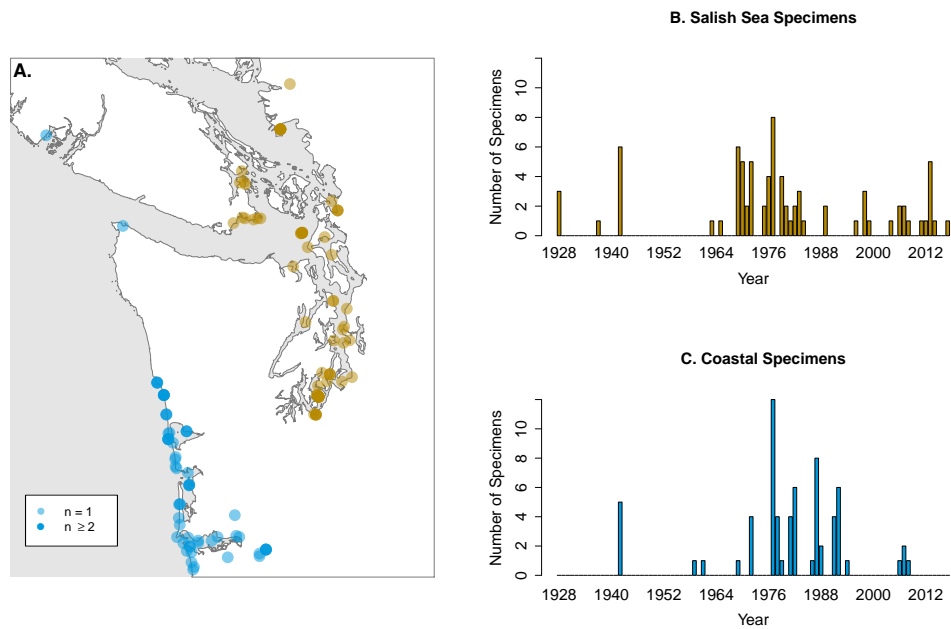


Figure 3.1: Spatial and temporal distribution of specimens

Figure 3.2: Time series of harbor seal trophic position in a) coastal Washington and b) the Salish Sea for five different trophic amino acids (glutamic acid, alanine, aspartic acid, valine, and proline) calculated using the source amino acid phenylalanine. Color corresponds to trophic amino acid, while line shows the fit of a generalized additive model with a smoothed term by year and a k of 6. * denotes a significant smoothed term.

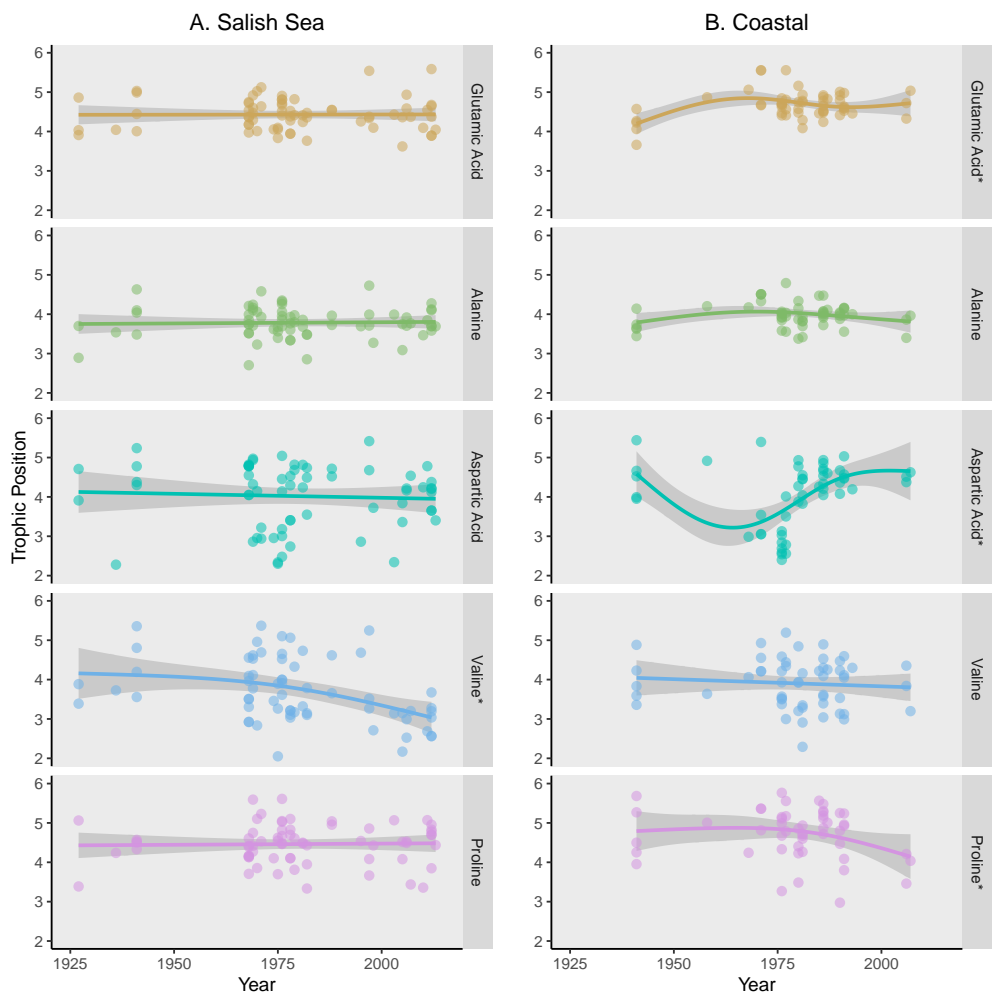


Figure 3.2: Temporal trends of harbor seal trophic position

Figure 3.3: Sex specific trophic position for male (M) and female (F) harbor seals pooled over the past century and calculated using five different trophic amino acids (glutamic acid, alanine, aspartic acid, valine, and proline) for a) Salish Sea and b) coastal Washington specimens.

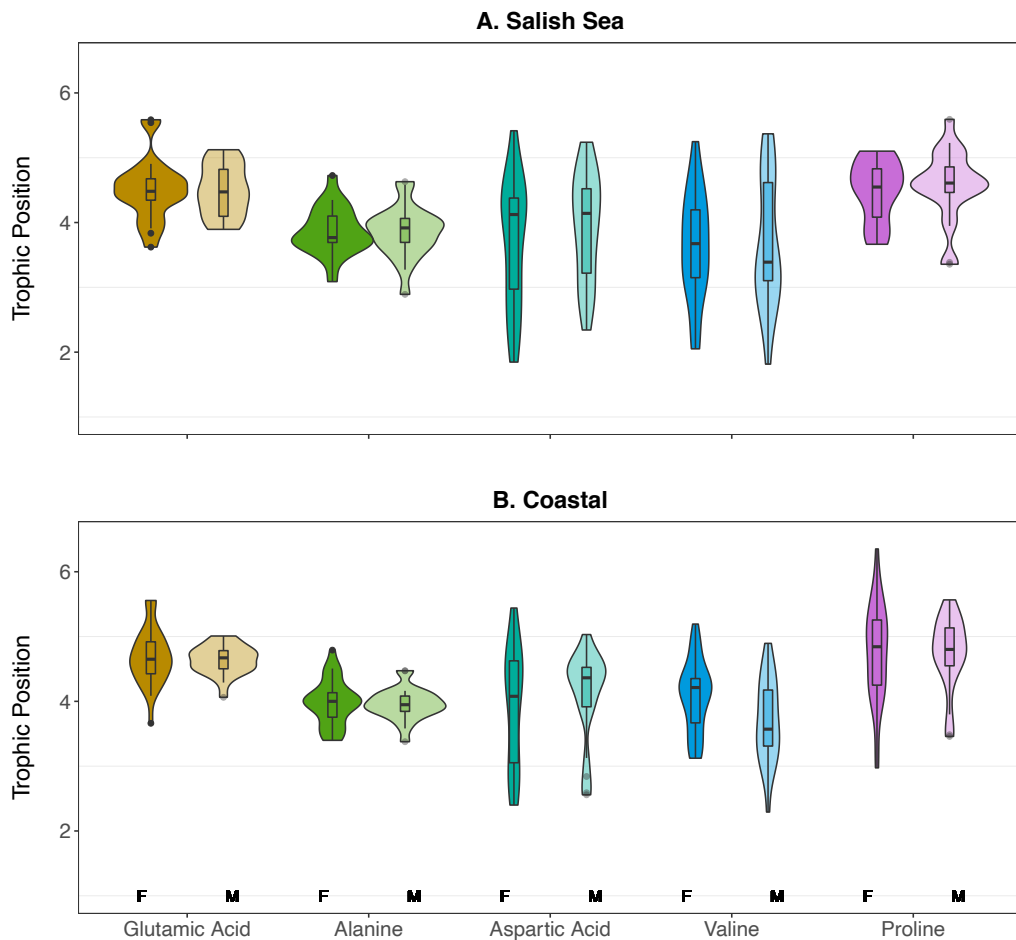


Figure 3.3: Sex differences of harbor seal trophic position

Figure 3.4: Relationship between harbor seal size (standard length, cm) and trophic position calculated using five different trophic amino acids (glutamic acid, alanine, aspartic acid, valine, and proline).

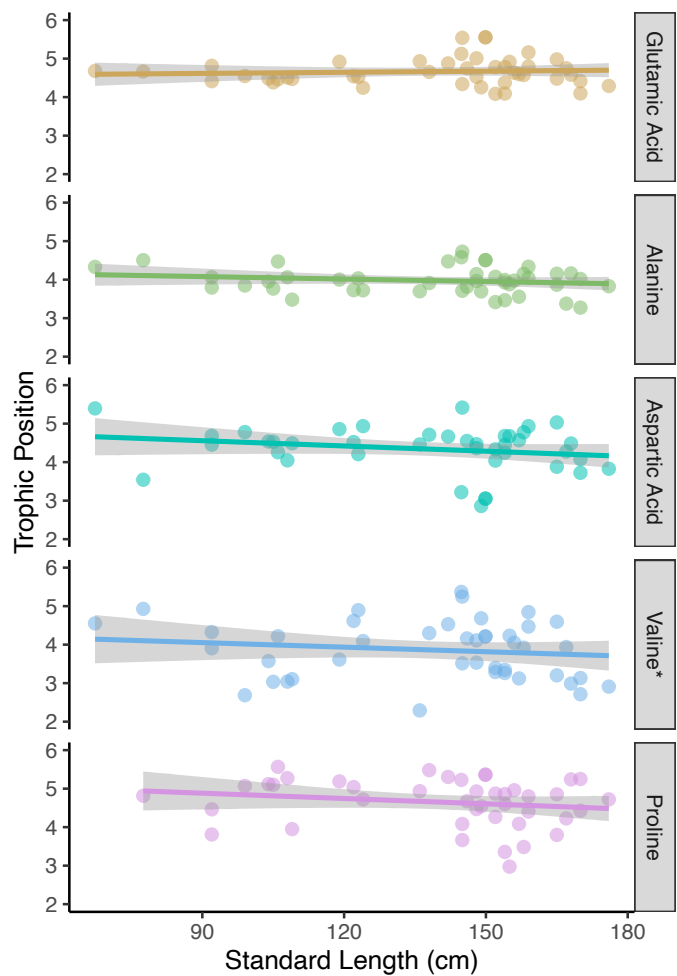


Figure 3.4: Size trends of harbor seal trophic position

Figure 3.5: Analysis of seasonality of harbor seal trophic position for five different trophic amino acids (glutamic acid, alanine, aspartic acid, valine, and proline) calculated using with $\beta_{(i-o),NV}$, line shows the fit of a generalized additive model with a smoothed term by month (1 = January, 12 = December). Smoothed terms were not significant.

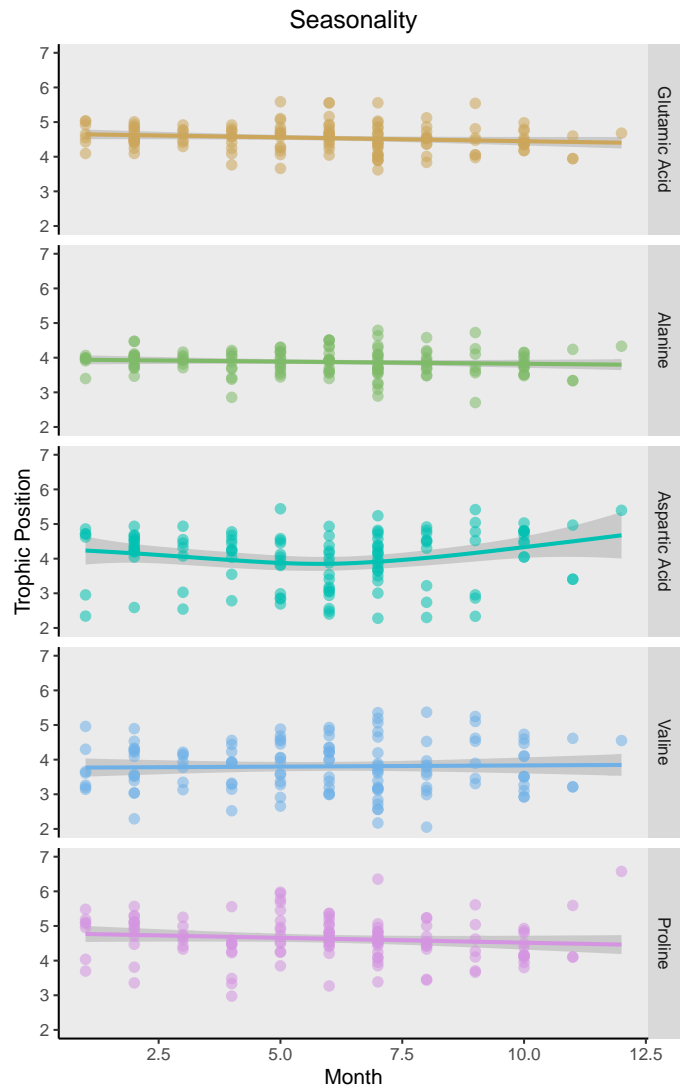


Figure 3.5: Seasonality of harbor seal trophic position

Figure 3.6: Time series of residuals by year for the three ocean condition models (physiological delay, 1-year ecological delay, 2-year ecological delay) with the most support for the four different trophic amino acids used in the models (glutamic acid, alanine, valine, and proline) with trophic position calculated using the source amino acid phenylalanine. Color corresponds to trophic amino acid, line shows the fit of a generalized additive model with a smoothed term by year and a k of 6. * denotes a significant smoothed term.

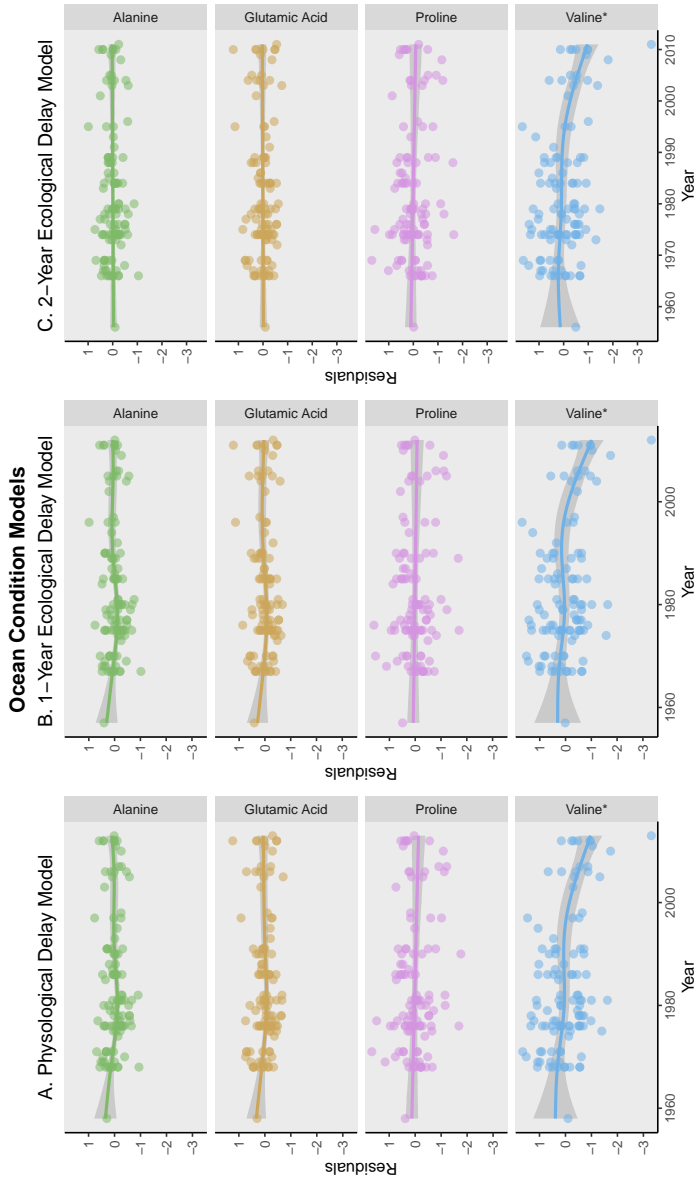


Figure 3.6: Temporal trends in ocean condition model residuals

Figure 3.7: Time series of residuals by year for the three food web models (physiological delay, 1-year ecological delay, 2-year ecological delay) with the most support for the four different trophic amino acids used in the models (glutamic acid, alanine, valine, and proline) with trophic position calculated using the source amino acid phenylalanine. Color corresponds to trophic amino acid, line shows the fit of a generalized additive model with a smoothed term with year and a k of 6. * denotes a significant smoothed term.

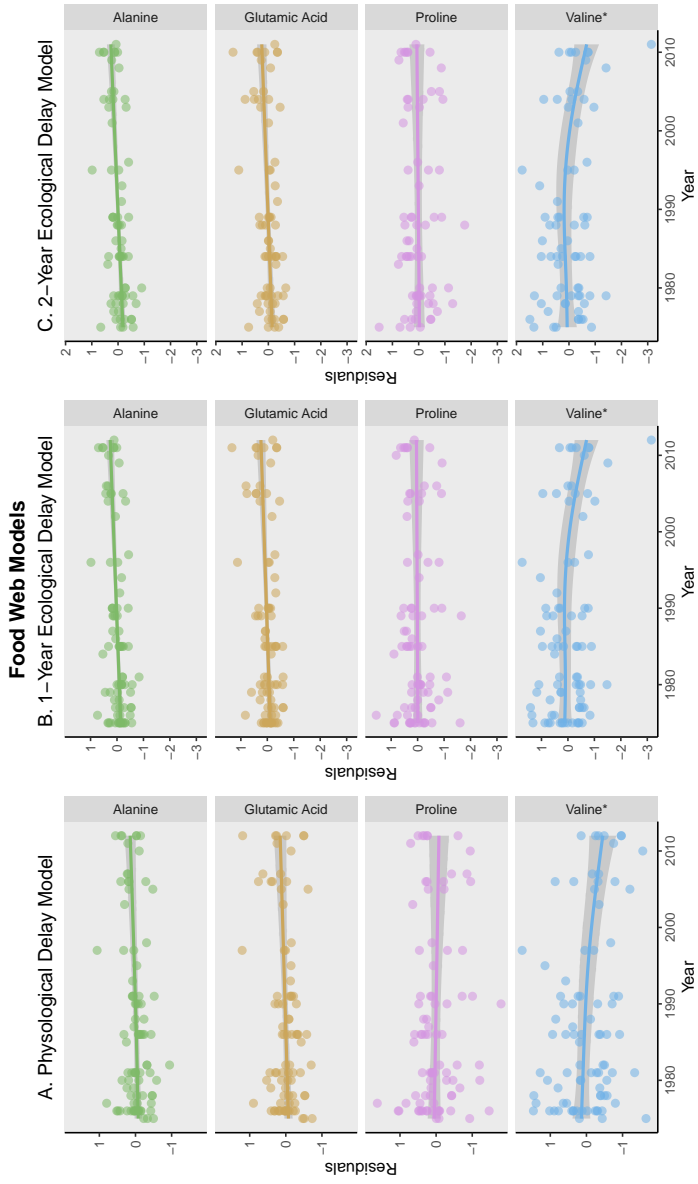


Figure 3.7: Temporal trends in prey availability model residuals

Figure 3.8: Coefficient estimates (dots) for the best ocean condition (a-c) and prey availability (d-f) hierarchical models with 95% confidence intervals (whiskers). Y-axis labels describe each covariate for supported models ($\Delta AIC_c < 2$) and x-axis is the coefficient estimate for each covariate (magnitude of trophic level change in response to the covariate). Colors correspond to the temporal lags applied to the 2-year ecological delay models (pink, a and f), 1-year ecological delay models (blue, b and e) and physiological delay models (green, c and d).

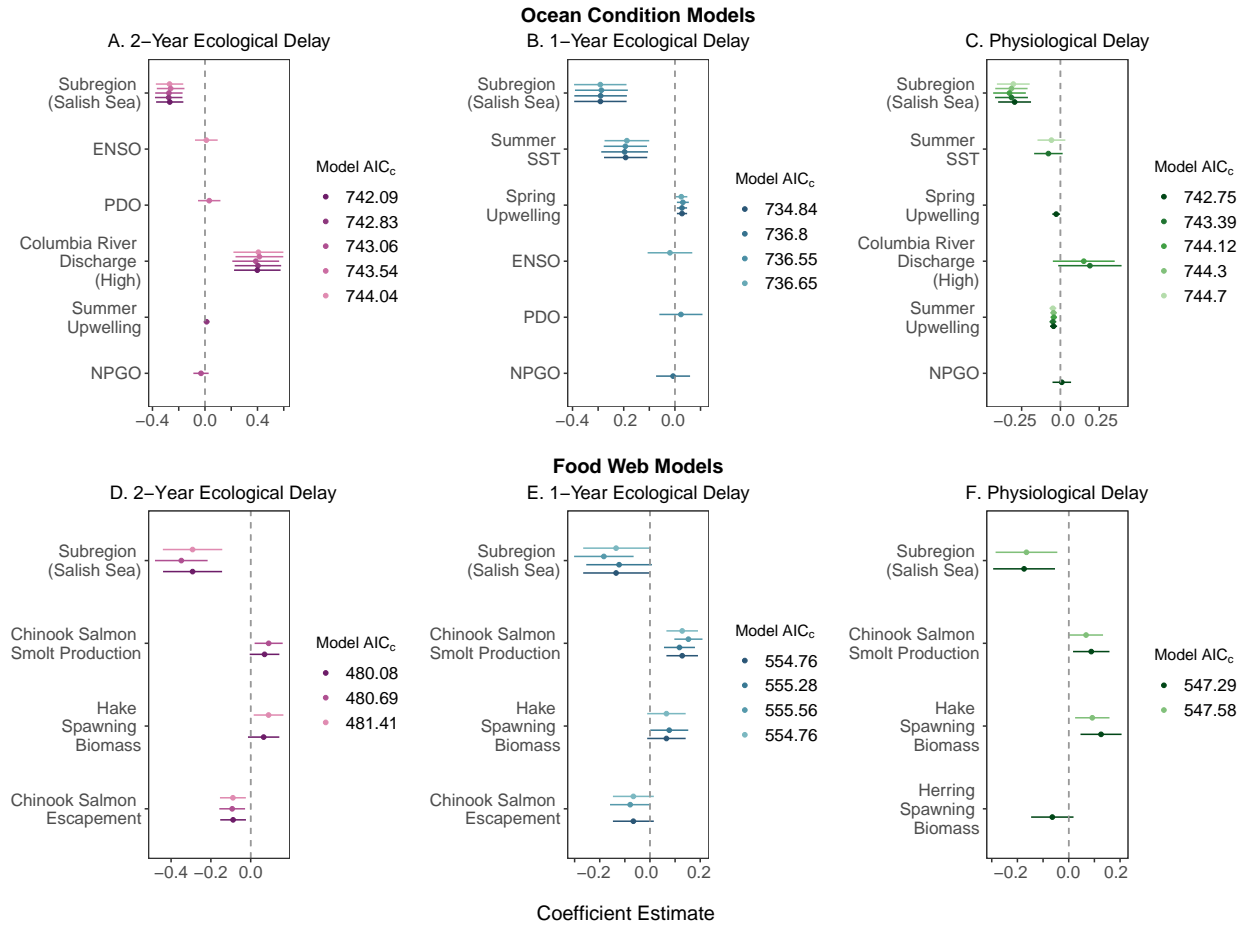


Figure 3.8: Coefficients of harbor seal trophic position models

Figure 3.9: Conceptual diagram interpreting the mechanism of trophic position response (d) to estimated model coefficients (Fig. 2d-f) included in the best food web models ($\Delta AIC_c < 2$) for the 2-year ecological delay models (a, pink arrows), 1-year ecological delay models (b, blue arrows) and the physiological delay models (c, green arrows). Solid arrows indicate indirect effects of covariates on harbor seal trophic position, signs indicate the direction of trophic position response based on coefficient estimates, and dashed arrows conceptually represent the mechanism directly impacting harbor seal trophic position.

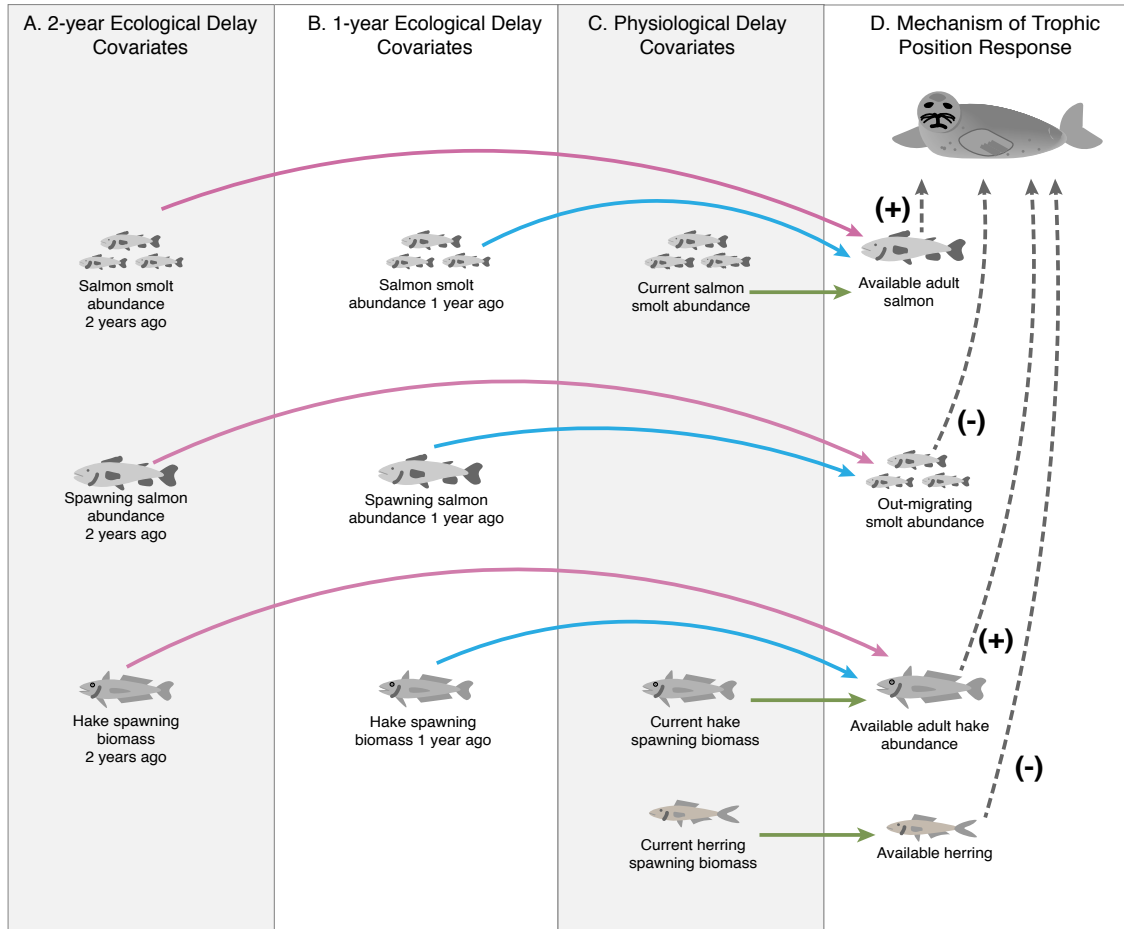


Figure 3.9: Conceptual representation of trophic position response to prey

Figure 3.10: Distributions (density of probability, y-axis) of calculated trophic position (x-axis) for harbor seals in this study. Parameter values are described in Table 3.1. Colors correspond to trophic amino acids (Tr) and the grey box represents ecologically realistic trophic positions for harbor seals if they were to predate 1 trophic position above herring (trophic position of 2.5, minimum expected value) and one trophic position below killer whales (trophic position of 6, maximum). The value within the grey box corresponds to the percentage of observed trophic position values that fell within the ecologically realistic range.

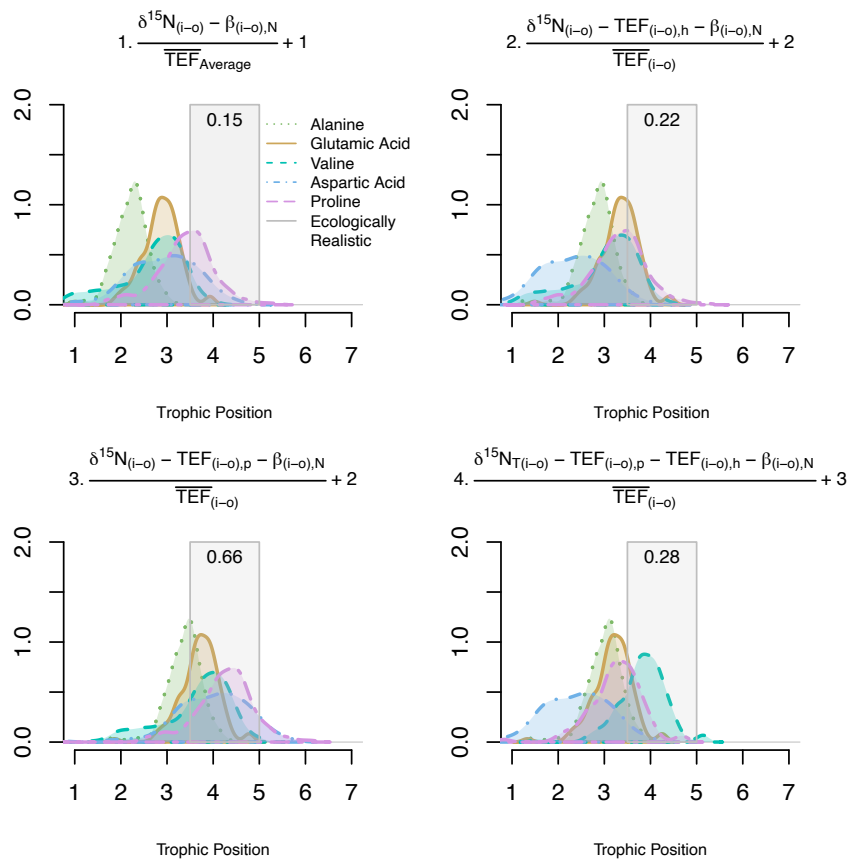


Figure 3.10: Trophic position estimates applying $\beta_{(i-o),N}$

Figure 3.11: Distributions (density of probability, y-axis) of calculated trophic position (x-axis) for harbor seals in this study applying four trophic position equation parameterizations and $\beta_{(i-o),NV}$ instead of $\beta_{(i-o),N}$.

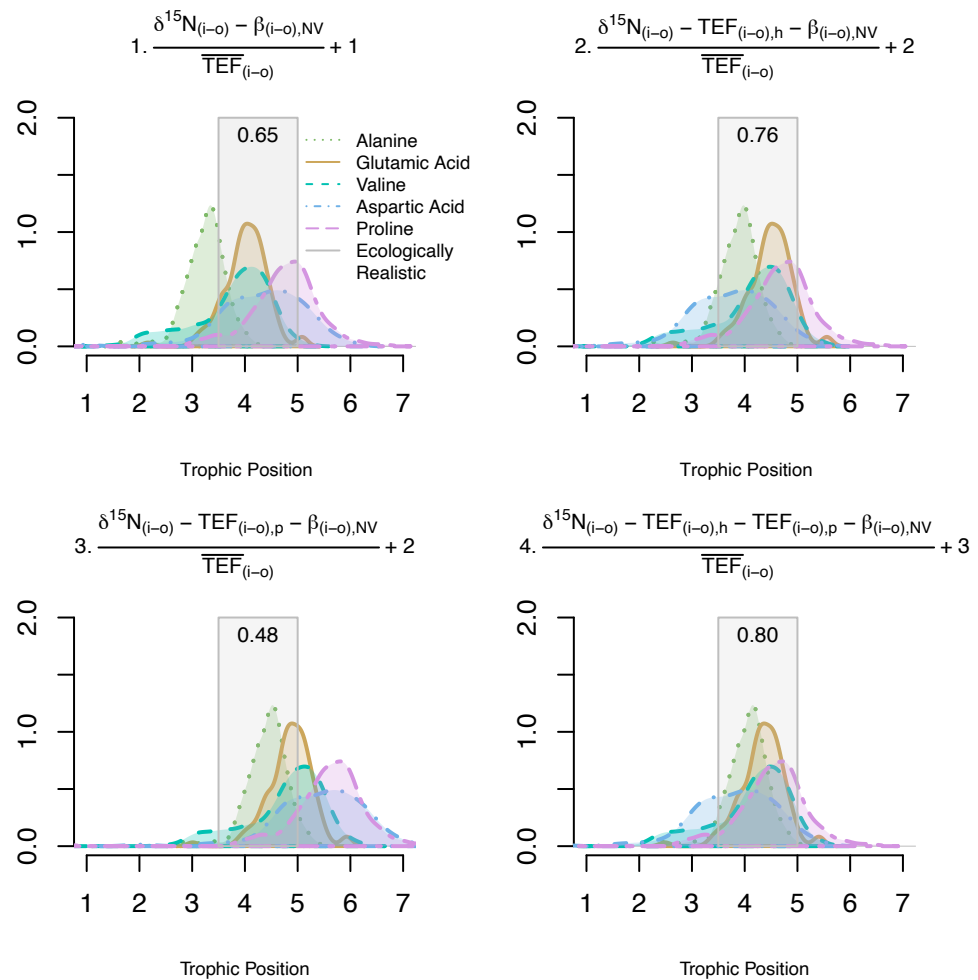


Figure 3.11: Trophic position estimates applying $\beta_{(i-o),NV}$

Chapter 4

RECENT DIVERGENT CHANGES IN ALASKAN PINNIPED TROPHIC POSITION DETECTED USING COMPOUND-SPECIFIC STABLE ISOTOPE ANALYSIS

4.1 Abstract

Over the past century Alaskan pinnipeds have experienced dramatic changes in abundance, but these changes have been highly variable across species and region. In recent decades, changes in atmospheric forcing and sea surface temperature have been particularly pronounced in the Gulf of Alaska and eastern Bering Sea, impacting the food webs in which Alaskan pinnipeds forage. We used compound-specific stable isotope analysis of nitrogen in amino acids to estimate historic and modern trophic position of harbor seals and Steller sea lions in the Gulf of Alaska and Bristol Bay. We applied a Bayesian hierarchical framework to determine whether shared trends through time exist across pinnipeds (classified by species and region) on decadal scales. Model results identified both shared trends through time and classification-specific decadal changes in pinniped trophic position. The largest change in trophic position occurred in the 2000s and 2010s and was observed in both Steller sea lions and harbor seals in the Gulf of Alaska, but not harbor seals in Bristol Bay or Iliamna Lake. Divergent trophic position patterns in the 2000s were identified in the western stock of Steller sea lions, which increased in trophic position, and sympatric harbor seals in the northern Gulf of Alaska, which decreased in trophic position. Our results indicate that these species have begun exploiting distinct trophic niches or experiencing unique food web conditions in recent decades in the Gulf of Alaska, likely in response to recent climate-induced ecological change in the region.

4.2 Introduction

Over the past century, pinniped populations in the northeast Pacific Ocean have experienced changes in adult and pup abundances (Muto et al., 2020). Understanding specific drivers of these population trends is important for management, as multiple stocks have been listed as threatened or endangered over the past two decades (Muto et al., 2020). The observed population dynamics have also corresponded with shifts in both the physical and ecological marine environment, which frequently occur simultaneously. As a result, disentangling drivers of population trends is complex, as multiple factors (environmental conditions, prey availability, anthropogenic disturbances) can change in tandem and potentially act synergistically on pinniped populations.

Data on long-term trends in trophic position across regions, species, and populations is one potential way to assess how food web changes have impacted pinnipeds in Alaska. This approach can identify how broad shifts in foraging ecology correspond to changes in abundance and population dynamics. More specifically, examining trophic position during periods of declining versus increasing predator abundance can provide insight into whether foraging behavior and prey availability are important drivers of population dynamics. In this study, we aim to identify whether common temporal trends in trophic ecology exist across harbor seals (*Phoca vitulina*) and Steller sea lions (*Eumetopias jubatus*) and their locations by deriving 70-years of trophic position data from compound-specific stable isotope analysis (CSIA) of museum specimens.

Following climatic changes in the 1970s that altered ocean currents and sea surface temperature (Hare & Mantua, 2000), most Gulf of Alaska and Bering Sea pinniped populations experienced declines that persisted through the 1990s (Muto et al., 2020). However, these responses differed across populations and species. For example, the western stock of Steller sea lions (located west of 144°W) decreased from approximately 240,000 animals in the late 1970s to 50,000 in 2000 (Burkanov & Loughlin, 2005). Similarly, harbor seal populations in

Prince William Sound and Glacier Bay declined by approximately 60% between the 1980s and 2000 (K. J. Frost, Lowry, & Ver Hoef, 1999; Womble et al., 2010). In contrast, the eastern stock of Steller sea lions (located east of 144°W) increased by 3-4% per year over the same time period (Figure 4.2) (Muto et al., 2020; K. W. Pitcher et al., 2007). More recently, atmospheric circulation anomalies in the northeast Pacific Ocean have resulted in unprecedently warm sea surface temperatures during the past decade (Walsh et al., 2018) and this environmental shift has altered fish abundances (N. A. Bond et al., 2015; Litzow et al., 2020). For example, the unprecedented marine heatwave that occurred in 2014 - 2016 triggered dramatic ecosystem change, including a 71% decline in Pacific cod in the Gulf of Alaska (Barbeaux et al., 2020). Declines in phytoplankton biomass, forage fish abundance, and changes in community structure as a whole were also observed (Suryan et al., 2021). During this recent period of environmental change, many pinniped populations have experienced increases or stabilization of population abundance (Muto et al., 2020) (Figure 4.2), although declines in some Gulf of Alaska Steller sea lion populations were observed following the marine heat wave (Suryan et al., 2021).

These variable changes in Alaskan pinniped populations over the past 50 years cannot be attributed to a single cause, as multiple environmental, anthropogenic, and ecological factors have changed simultaneously. For example, the rapid decline of the western stock of Steller sea lions between the 1970s and 1990s has been attributed to myriad factors, including change to the physical environment, competition with fisheries for common prey, predation, disease, and human-caused mortality (S. Atkinson, Demaster, & Calkins, 2008). Glacier Bay harbor seal populations have primarily, but not exclusively, been impacted by the decline of sea ice, which provides a majority of their haulout sites (Womble et al., 2010). Population declines have also been associated with increased numbers of tour vessels, particularly in glacier fjords that provide important nursing and whelping habitat (Jansen, Boveng, Ver Hoef, Dahle, & Bengtson, 2015; Mathews et al., 2016). The differences in pinniped population trends across the Gulf of Alaska and Bering Sea suggest varied environmental and ecological

drivers underlying these dynamics. Interestingly, harbor seals and Steller sea lions that occur in the same geographic region (sympatric) have experienced different population trends over similar time period (Figure 4.2). Identifying trophic position trends through time that are shared, compared to changes that only impact a specific species or region, can elucidate how widespread ecological forcing versus localized change influence top predators and potentially explain variable population abundance trends.

Both harbor seals and Steller sea lions exhibit generalist, piscivorous foraging strategies, although differences in foraging range, body size, and diet exist. Adult harbor seals have high site fidelity, opportunistically forage 5 - 10 km from haulout sites and at depths < 200 m (M. M. Lance et al., 2012; Lowry, Frost, Ver Hoep, & Delong, 2001), and weigh up to 300 pounds. Steller sea lions are central place foragers known to migrate to prey aggregations on the continental shelf and oceanographic boundary zones (E. H. Sinclair & Zeppelin, 2002; Womble & Sigler, 2006). Foraging trips can last 1-3 days (Maniscalco, Parker, & Atkinson, 2006) with average distances of 133 km for adult females (Merrick & Loughlin, 1997), although foraging trips are shorter in the breeding season (Maniscalco et al., 2006). Adult females can weigh up to 800 pounds whereas adult males can exceed 2,500 pounds, indicating a higher energetic demand compared to harbor seals. Diet studies of Steller sea lions and harbor seals are spatially and temporally limited, and primarily utilize scat samples. In the Gulf of Alaska, gadids, cephalopods, and forage fishes are prevalent in both harbor seal and Steller sea lion diet (Geiger et al., 2013; E. H. Sinclair & Zeppelin, 2002), whereas salmonids are also important for harbor seals in Bristol Bay and Iliamna lake (Hauser, Allen, Rich, & Quinn, 2008).

Stable isotopes have been used to reconstruct historical differences in diet and trophic position in Alaskan pinnipeds (Brennan et al., 2019; Hirons, Schell, & Finney, 2001; Keith A. Hobson, Sease, Merrick, & Piatt, 1997). These previous studies utilized bulk stable isotope analysis exclusively and were therefore limited in their inferential strength. Differences in the bulk $^{15}\text{N}/^{14}\text{N}$ of consumer tissues can indicate either a trophic level change of the con-

sumer or a change in nitrogen resources at the base of the food web. The specific cause of the isotopic variation cannot be ascertained from consumer bulk stable isotope values unless the data are paired with temporal information on $^{15}\text{N}/^{14}\text{N}$ in primary producers. Lack of consistent, concurrent sampling of nitrogen stable isotope composition of primary producers therefore presents a challenge for previous long-term studies of the trophic dynamics of consumers from bulk stable isotope data. CSIA data address this challenge, as amino acids exhibit two distinct patterns in isotopic enrichment: trophic amino acids (i.e., glutamic acid, alanine, proline) become enriched in ^{15}N with each trophic transfer and source amino acids (i.e., phenylalanine) show minimal change and thus are reflective of the base of the food web (Chikaraishi et al., 2009; McClelland & Montoya, 2002; N. Ohkouchi et al., 2017). With the ability to internally correct for expected changes in $^{15}\text{N}/^{14}\text{N}$ at the base of the food web [Feddern et al. (2021); Ramirez et al. 2021], CSIA allows for a more robust retrospective analysis of consumer trophic dynamics on decadal and century scales.

The objective of this work is to describe and compare changes in trophic ecology for Alaskan pinnipeds throughout the past century and investigate trophic position differences for sympatric populations. We apply hierarchical Bayesian analyses to 70 years of trophic position data derived from CSIA from pinnipeds (harbor seal and Steller sea lion) in the Gulf of Alaska, Bristol Bay, and a small population of freshwater harbor seals in Iliamna Lake, Alaska which is adjacent to Bristol Bay. We build on previous research examining pinniped nitrogen stable isotope composition (Brennan et al., 2019; Hiron et al., 2001; Keith A. Hobson et al., 1997; Misarti et al., 2009) by adding two decades of data to the record (2000s and 2010s) and incorporating a broad spatial scope (Bristol Bay, Iliamna Lake, Gulf of Alaska). Additionally, by analyzing nitrogen stable isotopes derived from amino acids, we were able to control for known changes in nitrogen resources and phytoplankton composition at the base of the food web that can confound trophic position interpretations from bulk stable isotope data collected over decadal scales (Feddern et al., 2021). Furthermore, by comparing trophic position dynamics across species and region through time, regional and

location-specific ecological responses to a changing ecosystem can be identified.

4.3 Methods

4.3.1 Sample collection and analysis

Samples were obtained using methods described in Feddern et al. (2021). Briefly, harbor seal and Steller sea lion bones were sampled from specimens curated at the University of Alaska Museum of the North (Supplementary Information Table S1). Specimens were treated by maceration in warm water and soaked in a dilute ammonia solution then stored in acid free boxes. Adult specimens were sampled exclusively to avoid dietary differences between adults and juveniles. Specimens were classified based on species and region. We prioritized long-term temporal coverage in four regional classifications of harbor seals (Iliamna Lake, southeast Gulf of Alaska, northern Gulf of Alaska, eastern Bering Sea) and two regional classifications of Steller sea lions (eastern and western stocks) for a total of 6 species x region classifications. Specimens were extremely limited for the eastern Steller sea lion stock ($n = 2$) and Iliamna Lake harbor seas ($n = 3$). We also prioritized specimens with sex and age identifications, but these data were not available for some specimens. A total of 106 harbor seal and 21 Steller sea lion specimens were sampled representing the 1950s to 2010s (Figure 4.1).

Steller sea lions were classified according to the National Oceanic and Atmospheric Administration's (NOAA) distinct population segments, where Steller sea lions east of 144°W are considered the eastern stock and west of 144°W are considered the western stock (Figure 4.1). NOAA has identified twelve stocks of harbor seals in Alaska and, due to limitations of archived specimens, harbor seals were not able to be classified according to NOAA stocks. Instead, they were classified based on their range relative to the Steller sea lion stocks and utilization of marine versus freshwater habitats. Harbor seals that were west of 144°W, which included samples from the Prince William Sound and Cook Inlet/Shelikof

Strait stocks (Figure 4.1), were classified as northern Gulf of Alaska harbor seals. Harbor seals that were located east of 144°W, which included samples from the Glacier Bay/Icy Strait, Sitka/Chatham Strait, Lynn Canal/Stephens Passage, Dixon/Capes Decisions, and Clarence Strait stocks (Figure 4.1), were classified as southeast Gulf of Alaska harbor seals. The Bristol Bay harbor seal stock was divided into two classifications, Bristol Bay referring to marine harbor seals, and Iliamna Lake referring to freshwater harbor seals (Figure 4.1). This allowed for comparison of three pairs of geographically overlapping classifications: western stock of Steller sea lions and northern Gulf of Alaska harbors seals, eastern stock of Steller sea lions and southeast Gulf of Alaska harbor seals, and Bristol Bay and Iliamna Lake harbor seals.

4.3.2 Trophic position calculation

Bone collagen within the samples was decalcified, acid hydrolyzed, derivatized and analyzed for compound-specific stable isotope analysis (CSIA) of nitrogen ($\delta^{15}N$) for 12 individual amino acids following the protocol described in Feddern et al. (2021). $\delta^{15}N$ was measured as:

$$\delta^{15}N(\text{\%vs.air}) = [(\frac{^{15}\text{N}/^{14}\text{N}_{\text{Sample}}}{^{15}\text{N}/^{14}\text{N}_{\text{Air}}} - 1) * 1000] \quad (4.1)$$

Collagen samples were measured in triplicate with a laboratory standard containing a 12 amino acid mixture of known isotopic composition. Full analytical details are described in Appendix S1.

Trophic position was calculated using a harbor seal-specific trophic discrimination factor (difference in $^{15}\text{N}/^{14}\text{N}$ between trophic and source amino acids in consumers for a trophic transfer; Germain et al. (2013)). This approach assumed trophic discrimination factors (TDF) derived from controlled feeding studies of harbor seals were similar to Steller sea lions. Applying a “multi-TDF” approach that combines both average and taxa-specific TDF can improve trophic position estimates in marine predators including pinnipeds (Germain et al., 2013; McMahon et al., 2019). The following equation was used to determine the trophic

position of each sampled individual:

$$TrophicPosition = \frac{\delta^{15}N_i - \delta^{15}N_o - TDF_{(i-o),j} - \bar{\beta}_{(i-o)}}{TDF_{(i-o)}} + 2 \quad (4.2)$$

where, $\delta^{15}N_i$ is the measured stable isotope composition of a trophic amino acid i in a sample and $\delta^{15}N_o$ is the stable isotope composition of a source amino acid o in a sample. $\overline{TDF}_{(i-o)}$ is the mean difference between given trophic amino acid i and source amino acid o across all consumers described in J. M. Nielsen et al. (2015). $TDF_{(i-o),j}$ is the trophic discrimination factor between trophic amino acid i and source amino acid o from a controlled feeding study of a specific consumer j ; here we use harbor seals from Germain et al. (2013) (Table 4.1). $\bar{\beta}_{(i-o)}$ is the mean difference in $\delta^{15}N$ across aquatic phytoplankton between a specific trophic amino acid i and source amino acid o [J. M. Nielsen et al. (2015); Table 4.1]. J. M. Nielsen et al. (2015) also determined using multiple amino acids to estimate trophic position improves precision. Therefore, we used multiple trophic amino acids i (alanine, glutamic acid, aspartic acid and proline) and one source amino acid o (phenylalanine) to calculate trophic position (Table 4.1). These amino acids were chosen based on their prevalence in previous studies to derive parameters for equation 2, and their concentrations in bone collagen (see Appendix S1).

4.3.3 Model framework

Sex was considered as a predictor for trophic position, however, sex metadata were not available for all specimens. In order to evaluate difference in trophic position by sex, we fit linear statistical models to each individual trophic amino acid, by classification (species x region). These models took the following form:

$$y_i = \alpha + \beta x_i + \epsilon_i, \epsilon \sim N(0, \sigma) \quad (4.3)$$

where, y_i is trophic position for an individual amino acid and β is a vector of coefficients for the predictor, in this case sex, and ϵ are residual errors assumed to be normally distributed

with mean 0 and standard deviation σ . There was not sufficient metadata for the eastern stock Steller sea lion population or the Iliamna Lake population and these two classifications were omitted from this analysis.

A Bayesian hierarchical mixed effects model was used to identify decadal change across pinniped classifications (species x region), and the degree to which these changes were shared by testing the effects of classification, decade, and a classification-decade interaction as either population-level (fixed) or group-level (random) effects (see candidate models in Table 4.1). Hierarchical models share information across ‘groups’ to identify common responses, which refers to both decade and classification in this study. The interaction term allows for increased flexibility, letting each classification have slight departures from the group-level means. The mean and variance of pinniped trophic position for each region-species classification and decade were estimated using a generalized linear Bayesian hierarchical model with decade, population, and trophic amino acid as predictors:

$$y_i = \boldsymbol{\alpha} + \boldsymbol{\beta}x_i + \epsilon_i, \epsilon \sim N(0, \sigma_y) \quad (4.4)$$

$$\boldsymbol{\alpha}_{k=1:k} \sim N(\mu_{\alpha,k}, \sigma_{\alpha,k}) \quad (4.5)$$

where, for data point i , $\boldsymbol{\beta}$ is a vector of coefficients for the unpooled predictors (fixed effects, Table 4.1) and $\boldsymbol{\alpha}$ is a vector of coefficients for the partially pooled group-level predictors (random effects, Table 4.1) for group k (amino acid, decade or classification). At minimum, the $\boldsymbol{\alpha}$ included a random term for the amino acid corresponding to data point i , and depending on the model included up to a total of 4 random effects (also effects of decade, classification, and their interaction, Model 6 in Table 4.1). For each random effect included, $\mu_{\alpha,k}$ and $\sigma_{\alpha,k}$ are hyperparameters representing the mean and standard deviation of group-level effects on trophic position, for random effect k . For models with more than one random effect, we assumed the deviations to be independent and uncorrelated. We considered models that included decade, classification, and the interaction between decade and classification either as fixed or random effects (e.g. Model 4 v Model 6, Table 4.1), but did not consider models that included both as fixed and random (Table 4.1). Parameter estimates were obtained

using the `brms` package (Burkner et al. 2017, version 2.14.4) in R (R Core Development Team 2021, version 3.6.2), which implements a Hamiltonian Monte Carlo sampler and its extension no-U-turn sampler (Hoffman and Gelman 2014) through Stan (Stan Development Team 2020). Minimally informative priors were used for random effects (normal distributions with a mean of 0 and variance of 10) and fixed effects (Student's t-distribution with a mean of 0, standard deviation of 2.5 and 3 degrees of freedom). Trophic amino acid was included as a random effect for all models (Table 4.1). Selection of the best models (Table 4.1) given the data was based on approximate leave-one-out cross-validation (LOOIC) using the `loo` package (Veharti et al. 2017, version 2.4.1).

4.4 Results

We found no differences between the average male and female pinniped trophic position over the 50-year study period (Figure 4.3) for the four tested species-region classifications. This finding was consistent for all trophic amino acids-source amino acid pairs (Figure 4.3). Based on glutamic acid trophic position estimates, both western stock Steller sea lions (2.6 ± 0.5 ; mean \pm sd) and eastern stock Steller sea lions (2.7 ± 0.16) had similar trophic positions. Harbor seals in the Gulf of Alaska foraged higher in the food web than their Steller sea lion counterparts (Figure 4.3). Harbor seals in the southeast region had a higher trophic position on average than any other pinniped in this study (3.5 ± 0.3) but were similar to harbor seals in the northern region (3.3 ± 0.5). Bristol Bay (3.1 ± 0.4) and Iliamna lake (3.0 ± 0.3) harbor seals had a lower trophic position than their Gulf of Alaska counterparts on average (Figure 4.3).

4.4.1 Common trends in Alaskan pinniped trophic position

The best performing model (Table 4.1, model 6) of pinniped trophic position included both species-region classification and decade as random effects (shared trends) along with an interaction between population and decade (Table 4.1). Based on the support for decade

and classification to be included as group-level effects, these data support consistent differences between classifications over time, as well as differences between trophic position for all classifications. The supported interaction between population and decade (Table 4.1) indicates distinct decadal changes in trophic position for species-region classifications exist. The model that included decade, classification, and the interaction between decade and classification as fixed effects (model 4) was also supported based on the models LOOIC (Table 4.1). Therefore, the inclusion of the interaction term was more important for improving model performance than inclusion of decade and classification as fixed versus random effects.

There were consistent differences in trophic position that varied by species and ocean basin for the model with the most support. Harbor seals in the Gulf of Alaska had higher trophic position than their Steller sea lion counterparts. The mean difference of the posterior distributions indicated southeast Gulf of Alaska harbor seals have historically fed at 0.32 [-0.01, 0.61] (highest density 80% credible interval) trophic levels higher than sympatric eastern stock Steller sea lions (Figure 4.4). Similarly, the mean difference of posterior distributions showed northern Gulf of Alaska harbor seals fed 0.28 [-0.03, 0.50] trophic levels higher than the sympatric western stock Steller sea lions. Within the Gulf of Alaska, the posterior distributions for trophic position overlapped 39% between harbor seals and Steller sea lions in both the eastern and western regions (Figure 4.4). Iliamna Lake harbor seals have historically fed at a lower trophic level (mean posterior difference 0.16 [-0.11, 0.41]) than harbor seals in Bristol Bay, but these two classifications have 66% overlap of the group-level posterior distributions for trophic position (Figure 4.4). The 80% credible intervals included 0 for most region-species classifications thus the posterior probabilities support marginal evidence for consistent differences in trophic position between classifications. Regardless, the differences in posterior means were large, although the distributions were wide.

There were no consistent decadal differences in trophic position across the region-species classification (Figure 4.5). Pinniped trophic position in the 2000s was slightly higher for all classifications (mean posterior difference 0.03 [-0.09, 0.16]) on average compared to 1990

and the posterior distributions for 1990 and 2000 had an 85% overlap (Figure 4.5). Similarly, posterior distributions in between 2000 and 2010 had a mean difference of -0.1 [-0.27, 0.08] with a 65% overlap (Figure 4.4). Overall, decadal differences in pinniped trophic position through time were smaller than the region-species classification effects and were likely ecologically inconsequential.

4.4.2 Spatial and temporal differences in pinniped trophic structure

Distinct decadal changes in trophic position were observed for each species-region classification and varied more than the shared decadal changes (Figure 4.6) as indicated by the decade-classification interaction. Most, but not all, pinniped classifications experienced substantial trophic level change in 2000 or 2010 but the magnitude and direction of this change varied by region-species classification based on the combined effects of decade, classification, and the decade-classification interaction (Figure 4.6). The recent decadal change in trophic position was most prominent for the western stock of Steller sea lions which had a mean trophic level decrease of 0.43 [-0.25, -0.60] from 1990 to 2000 (a percent decrease of 0.15) with only a 21% overlap between the posterior distributions (Figure 4.6 E). This decline in trophic position remained in the 2010s. A similar decline was observed in the southeast Gulf of Alaska harbor seals. This population experienced relatively stable trophic position from 1960-1990, which then declined on average by 0.31 [-0.19, -0.45] trophic levels in 2000 (33% posterior overlap) (Figure 4.6 C). In contrast, harbor seals in the northern Gulf of Alaska had variable trophic position across decades and had the highest trophic position in 2000 in contrast to their southeast Gulf of Alaska harbor seals and Steller sea lion counterparts (Figure 4.6 B). Data were only available for 2000 and 2010 for the eastern stock Steller sea lions, and trophic position was similar for this population during both of these decades (Figure 4.6 F). Both Bristol Bay and Iliamna Lake harbor seals had relatively stable trophic position from 1950s until 2010s (Figure 4.6 A & B). Bristol Bay harbor seals experienced their lowest trophic level in the 1990s with a 0.24 [-0.54, 0.00] trophic level decrease com-

pared to the 1970s and 2000s, but the posterior distribution still overlapped 54% with other decades (Figure 4.6 A).

4.5 Discussion

Over the past 70 years, Alaskan pinnipeds have exhibited both common and distinct differences in trophic position across region-species classification on decadal scales (Table 4.1). While potential drivers of change in trophic position were not tested in this study due to data limitations, our results support a combination of local-scale (i.e., vessel traffic, reduction of glacial ice, local foraging) and regional-scale (i.e., environmental condition, basin-wide prey abundance) changes may be influencing pinniped trophic ecology. Furthermore, the largest decadal changes in pinniped trophic position were distinct for each region-species classification and were most apparent during the most recent two decades (2000s and 2010s). These patterns are more pronounced in the Gulf of Alaska compared to Bristol Bay (Figures 5 & 6).

4.5.1 Regional and species trends in harbor seal trophic position

Both Steller sea lions and harbor seals exhibit generalist foraging patterns (Geiger et al., 2013; M. M. Lance et al., 2012). Diets of Alaskan pinnipeds consist of similar prey species but vary between species, population, and local availability of prey (Hirons et al., 2001; Iverson, Frost, & Lowry, 1997). Bulk stable isotope studies in the Gulf of Alaska have shown that Steller sea lions feed lower in the food web compared to harbor seals (Iverson et al., 1997). Our CSIA analysis confirms the interpretation of these previous studies that isotopic differences can be attributed to trophic position changes and not isotopic shift of basal phytoplankton resources. Both western and eastern stock Steller sea lions have lower trophic position compared to sympatric harbor seal populations but have similar trophic position compared to other populations such as Iliamna Lake. However, despite known differences in both diet (Geiger et al., 2013; E. H. Sinclair & Zeppelin, 2002) and nearshore versus offshore

foraging (Lowry et al., 2001; Merrick & Loughlin, 1997) between the two species, our results also show historical overlap in trophic position, indicating potential trophic redundancy between harbor seals and Steller sea lions in the Gulf of Alaska.

Harbor seals in Bristol Bay and Iliamna Lake are managed as a single population (Muto et al., 2020) despite lack of evidence of migration by the freshwater population and utilization of different resources (Brennan et al., 2019). A previous study of strontium and carbon stable isotopes showed Iliamna Lake harbor seals utilize freshwater-derived resources (resident lake fishes), particularly early in life, and exhibit an ontogenetic shift to more marine resources (returning sockeye salmon) later in life (Brennan et al., 2019). Based on CSIA nitrogen data, Iliamna Lake harbor seals also forage lower in the food web compared to Bristol Bay harbor seals. In addition, both classifications exhibited trophic stability, with the Bristol Bay harbor seals only experiencing a trophic shift in the 1990s relative to the 1960s and 1970s. This coincided with the lowest sockeye salmon returns to Iliamna Lake on record (Hilborn, Quinn, Schindler, & Rogers, 2003). Interestingly, the decrease in trophic position in the 1990s occurred simultaneously with decreases in basin wide Bristol Bay harbor seal abundance in the late 1990s, which then stabilized and increased in the 2000s and 2010s (Figure 4.2). Data were not available for the freshwater harbor seals between 1990 and 2000 and thus it is unclear whether the freshwater population also experienced a trophic position change during the 1990s when sockeye salmon returns were low. While quantitative comparisons to salmon abundance were not made in this study, salmon population abundance and harbor seal trophic ecology and population trends are seemingly interrelated.

4.5.2 Recent trophic position changes in the Gulf of Alaska

Trophic position changes were observed in all pinniped classifications in the Gulf of Alaska during the past two decades, although the direction of these changes varied on more local scales. During the past two decades (2000-2020), harbor seals in the Gulf of Alaska have experienced stabilization of most monitored populations following long-term declines that

persisted from the 1950s through the 1990s (Figure 4.2, Muto et al. (2020)). During this same time period, harbor seals in both southeast and northern Gulf of Alaska experienced a shift in trophic position that was particularly prominent in the 2000s compared to historic estimates of trophic position (Figure 4.6 B & C). It is possible that the observed trophic position shift may have contributed to the population stabilization of Gulf of Alaska harbor seals, either by an increase in prey availability or opportunistically foraging on a novel prey source. Gagne, Hyrenbach, Hagemann, & Van Houtan (2018) observed similar trophic position declines in seabird populations, which were attributed to a shift in diet from fish to squid. A similar dietary shift could explain the observed trophic position shift in southeast Gulf of Alaska harbor seals and western stock Steller sea lions.

Recent regional change in the Gulf of Alaskan food webs has been well documented in other species and primarily attributed to bottom-up effects of climate (Barbeaux et al., 2020; Litzow et al., 2020). These region-wide trends likely altered prey availability for pinniped populations in the Gulf of Alaska. How pinniped populations have adapted their foraging ecology, however, indicates regional and species trophic divergence, which could be attributed to either local-scale foraging adaptations or differences in prey availability. Pinniped groups that overlap in space (Figure 4.1) revealed divergent trends in trophic position between Steller sea lions and harbor seals in recent decades (Figure 4.6 B & E). For example, trophic position of northern Gulf of Alaska harbor seals increased in the 2000s while the western stock of Steller sea lions decreased. For western stock Steller sea lions, this shift also persisted into the 2010s (Figure 4.6 E). Posterior distributions of western stock Steller sea lions and northern Gulf of Alaska harbor seals overlapped by 63% in the 1950s but only overlapped by 3% in the 2000s (Figure 4.6 B & E). The recent change in pinniped trophic position within the Gulf of Alaska coincided with population abundance stabilization, albeit at lower than historical abundance for most populations. This trophic divergence indicates there could be increased competition for resources between northern Gulf of Alaska harbor seals and western stock Steller sea lions resulting in diet adaptations. Similar comparisons were

challenging to make for the eastern stock of Steller sea lions and southeast Gulf of Alaska harbor seals due to limitations in historical data for the former. However, trophic position in the 2000s showed a 38% overlap (Figure 4.6 C & E) between the two species, indicating any trophic divergence between them may be less pronounced in this region, if existent.

The observed divergent trends indicate differences in how Alaskan pinnipeds are adapting to environmental and ecological changes. Trophic position changes from stable isotope data can be accounted for by: 1) prey switching between different species, 2) consuming different sizes of the same prey, or 3) consuming different quality prey. These changes can occur at the consumer level (pinnipeds) or lower in the food web and still be reflected in consumer stable isotope signature and thus trophic position. In recent decades, Pacific salmon and halibut in Alaska have both declined in size (K. K. Holsman et al., 2019; Oke et al., 2020). These changes in size distributions of prey have been attributed to changes in marine mammal populations (Groskreutz et al. 2019) and likely contributed to the observed trophic position declines in western Steller sea lion and southeast Gulf of Alaska harbor seals. In contrast, consuming low-quality prey with lower protein content and greater amino acid imbalance between consumer and prey increases the amino acid trophic enrichment factor of nitrogen (McMahon et al., 2015). If not accounted for in trophic position equations, this increase in trophic enrichment factor can result in erroneously high trophic position estimates. This may explain the observed increase in estimated trophic position in northern Gulf of Alaska harbor seals where this population may be consuming a greater proportion of lower quality prey (i.e., crustaceans, shrimp, cephalopods) in recent decades rather than feeding on prey species that are higher in the food web.

4.5.3 Considerations and limitations for CSIA analyses

The data in this study were limited in sample size primarily due to the availability of archived specimens. As a result, we were not able to discern between known fine scale differences in populations or annual trends. For example, harbor seals in the southeast Gulf of Alaska

consist of 13 individual stocks. Due to limitations in the number of archived specimens, these stocks were pooled and analyzed as a single classification despite known differences in genetic structure (Muto et al., 2020). Given the observed broad range in trophic position of these generalist predators, it is unlikely that inclusion of finer spatial dynamics would have changed the supported model, although variation in temporal trends within a classification may have been identified. Similarly, data were only available for eastern stock Steller sea lions for 2000s and 2010s. As a result, no historical comparisons were possible and the conclusions about this population are tentative. Nonetheless, this dataset offers historic documentation of pinniped trophic position that can be updated with future samples or additional archived specimens.

Trophic position estimates in this study were low compared to known foraging strategies of these pinnipeds. For example, Steller sea lions eat primarily walleye pollock and Atka mackerel (Keith A. Hobson et al., 1997; Trites, Calkins, & Winship, 2007), which would indicate a trophic position of 3 or higher. Mean trophic position for Steller sea lions was closer to 2.7 in this study, which is lower than expected based on known foraging ecology. It is common for CSIA to underestimate trophic position of marine predators (Germain et al., 2013; McMahon et al., 2019) and the inclusion of multiple amino acid pairs and a multi-trophic enrichment factor framework did not fully resolve this issue. J. M. Nielsen et al. (2015) found trophic position estimates can be highly sensitive to the applied β values in equation 2. In our trophic position calculation, we assumed a constant β represented by marine diatoms. However, β values differ by more than 11 per mille between seagrasses and diatoms (H. B. Vander Zanden et al., 2013) which has been attributed to differences between vascular and nonvascular plants (B. Choi et al., 2017, Ramirez et al. 2021). If vascular plants, such as seagrasses, contribute to the food web in addition to non-vascular algae, the applied β would be too high and would result in underestimation of trophic position of marine consumers (B. Choi et al., 2017, Ramirez et al. 2021). Even a 10% contribution of vascular plant-derived nitrogen to the food web would result in an underestimation of

0.2 trophic position. It is likely that vascular plants at least partially contribute to the Alaskan food web, as seagrass beds provide essential habitat and food for many fish species and invertebrates. Consideration for variable β values may be helpful in resolving trophic position underestimation of future studies, especially in cases where consumer carbon stable isotope data is available and contributions of seagrasses to the food web are well documented.

4.5.4 Conclusions and Implications

Marine ecosystems in Alaska are experiencing unprecedented environmental change that has altered abundance and size distributions of many fish species consumed by pinnipeds (Barbeaux et al., 2020; K. K. Holsman et al., 2019; Oke et al., 2020; Suryan et al., 2021). Heterogeneity in diet and foraging locations allow top predators to adjust to availability of resources by altering their foraging. Based on the observed region-species specific changes in trophic position over the past two decades, pinnipeds are experiencing different food web conditions than in the past, even those that occur in similar geographic regions. This may be the result of adapting foraging strategies to exploit other prey resources or a change that is occurring lower in the food web and is measurable in predators. While our results cannot discern between these two mechanisms of trophic level change, we can conclude that recent food web dynamics have impacted pinniped trophic ecology in Alaska. Future responses of pinnipeds to food web change will likely be locally variable between species, even those that occur within similar geographic regions.

4.6 Tables

Table 4.1: Parameter values for trophic discrimination factors between a trophic amino acid (i) and phenylalanine (o) for harbor seals ($TDF_{(i-o),j}$), for an average consumer ($TDF(i-o)$), and for primary producers ($\beta_{(i-o)}$) derived from previous studies to apply a multi amino acid framework to equation 2.

Table 4.1: Trophic position parameter values for Equation 2

Trophic Amino Acid (i)	$\bar{\beta}_{(i-o)}$	$TDF_{(i-o),j}$	$\overline{TDF}_{(i-o)}$
Glutamic acid (Glu)	2.9	3.4	6.6
Alanine (Ala)	2.8	2.5	6.8
Aspartic Acid (Asp)	1.8	3.5	5.4*
Proline (Pro)	2.7	5.5	5
Data Sources	Nielsen et al. 2015	Germain et al. 2013	Nielsen et al. 2015

Table 4.2: Candidate models for identifying spatial and temporal trophic structure of Alaskan pinnipeds. Assumptions define how the model describes trophic structure with regards to decade and classification and LOOIC describes the support of each candidate models. The best model (6) is italicized.

Table 4.2: Candidate Models

Model	Fixed Effects	Random Effects	Assumption	LOOIC Standard error
1	Decade	Trophic Amino Acid	Trophic position varies by decade but not classification	878.8 (52.3)
2	Classification	Trophic Amino Acid	Trophic position varies by classification but not decade	816.5 (52.3)
3	Classification, Decade	Trophic Amino Acid	Trophic position varies by both classification and decade	816.6 (52.1)
4	Classification*Decade	Trophic Amino Acid	Trophic position varies by classification and decade; decadal change is distinct for each classification	797.9 (53.1)
5	-	Classification, Decade, Trophic Amino Acid	Trophic position varies with classification and decade but common trends exist across classification and decade	813.7 (52.6)
6	-	<i>Classification*Decade,</i> <i>Trophic Amino Acid</i>	<i>Trophic position varies by classification and decade;</i> <i>decadal change is distinct for each classification.</i> <i>Common trends exist across classification and decade</i>	<i>771.4 (53.1)</i>

4.7 Figures

Figure 4.1: Spatial and temporal distribution of harbor seal and Steller sea lion specimens. ‘n’ denotes the number of specimens sampled for each decade. The dashed line shows 144°W, which delineates the distinct population segments of eastern and western Steller sea lion stocks.

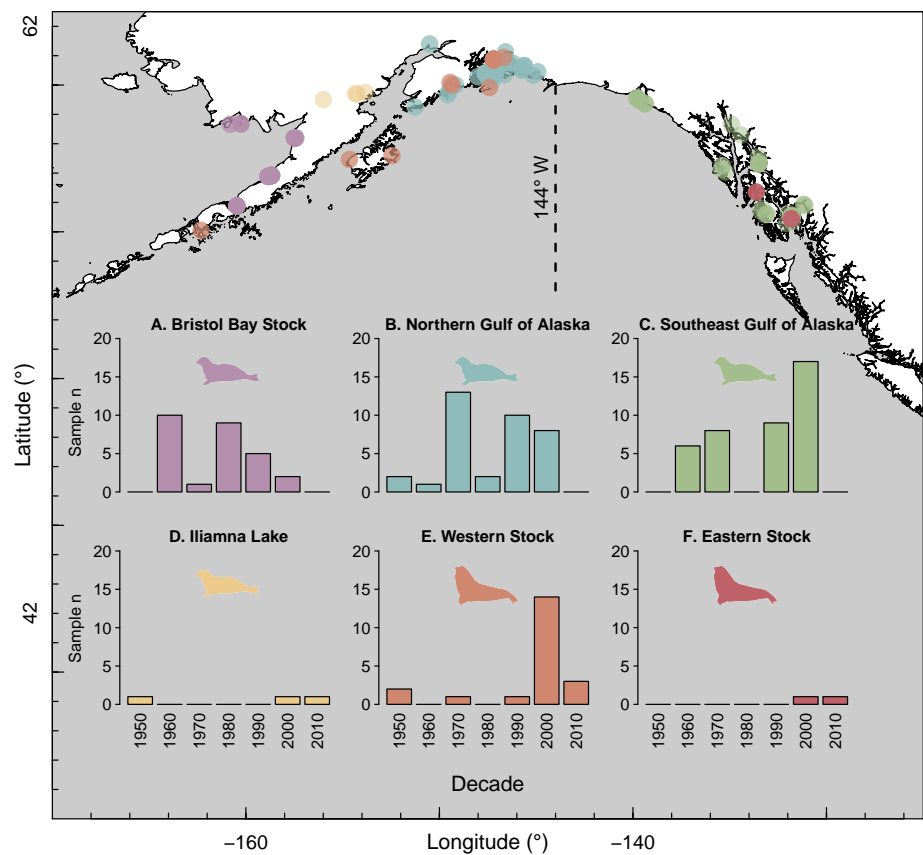


Figure 4.1: Spatial and temporal distribution of specimens

Figure 4.2: General trends in pinniped population abundance summarized by the six species-region classifications described in this study.

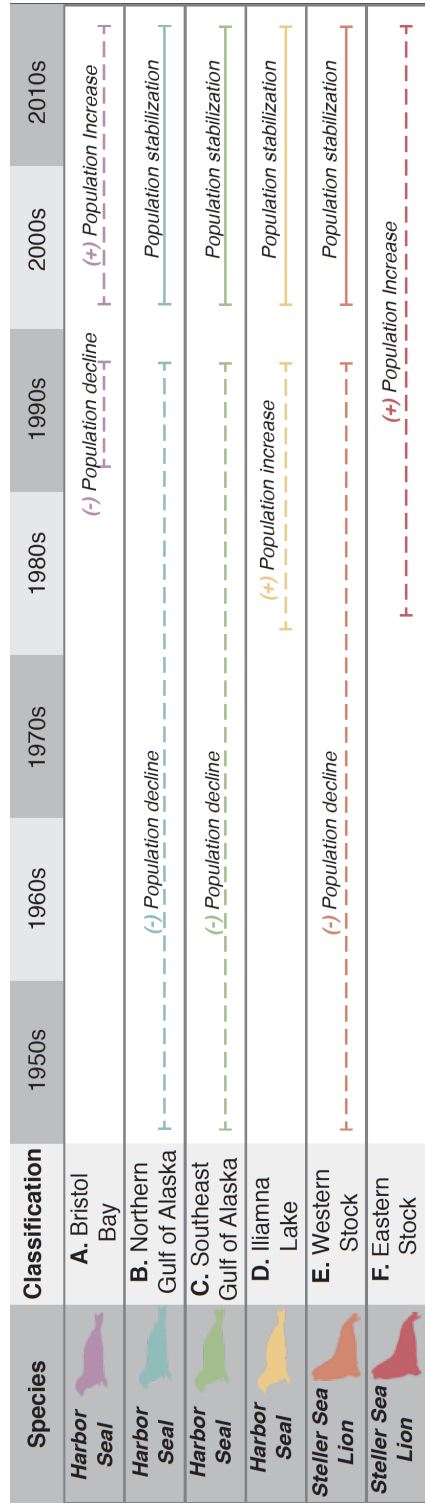


Figure 4.2: General trends in pinniped population abundance

Figure 4.3: Distribution of harbor seal trophic position data for male (M) and female (F) pinnipeds pooled over the past century and calculated using five different trophic amino acids (glutamic acid, alanine, aspartic acid, valine, and proline) for a) Bristol Bay harbor seals, b) northern Gulf of Alaska harbor seal, c) southeast Gulf of Alaska harbor seals and d) western Steller sea lion stock. Eastern Steller sea lion stock and Iliamna Lake harbor seals did not have sufficient sample sizes; no significant differences between males and females were observed ($\alpha = 0.05$).

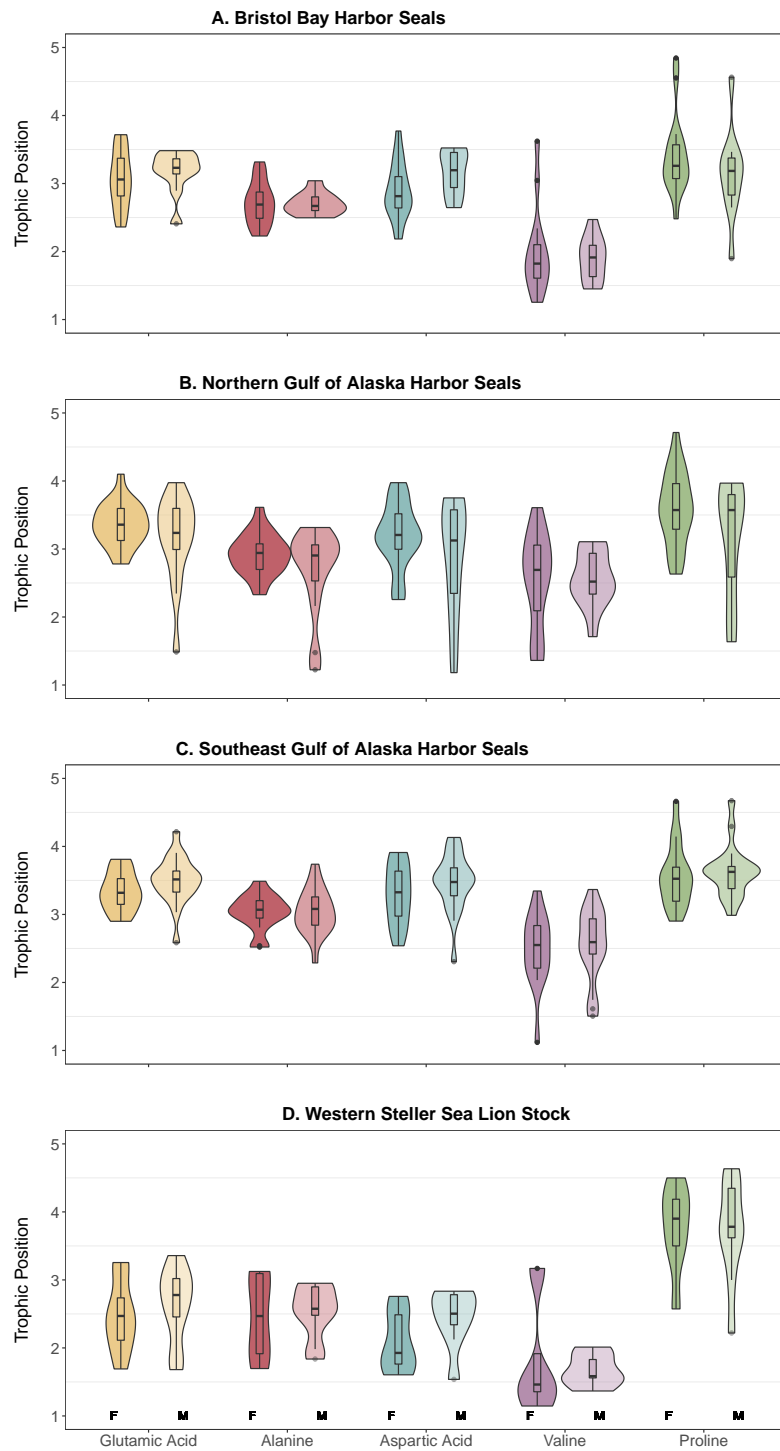


Figure 4.3: Distribution of harbor seal trophic position data for male (M) and female (F) pinnipeds

Figure 4.4: Model estimated posterior distributions for group-level effects of the region-species classification included as a random effect (k) in the best performing model (Model 6, Table 4.1). Distributions denote medians (black bold line) and 80% credible intervals (colored shaded region) in units of trophic position (x-axis).

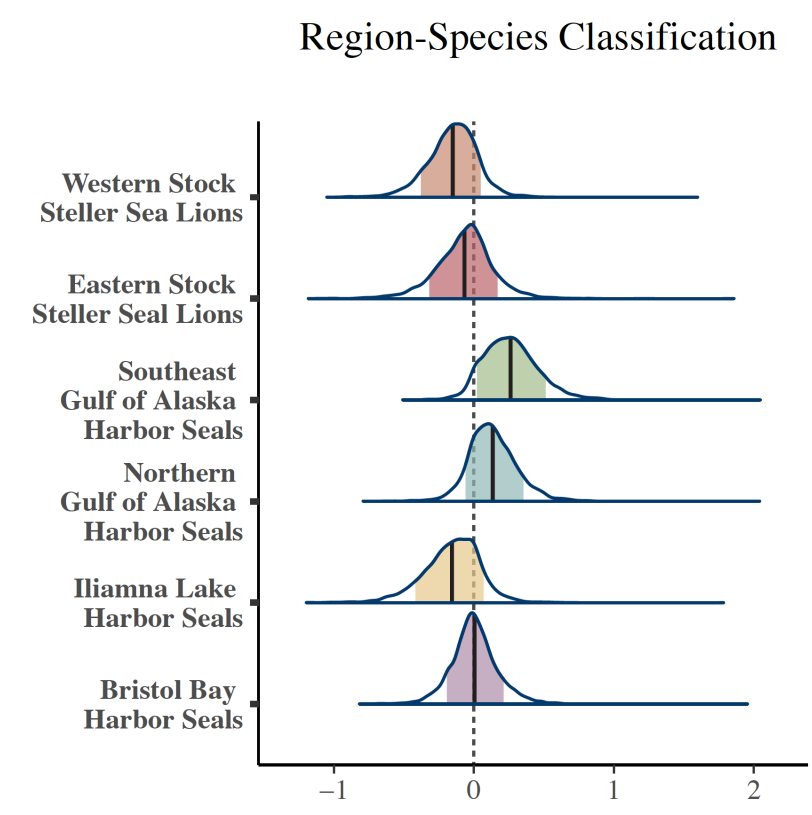


Figure 4.4: Region-species classification included as a random effect (k)

Figure 4.5: Model estimated posterior distributions for group-level effects of decade included as a random effect (k) in the best performing model (Model 6, Table 4.1). Distributions denote medians (black bold line) and 80% credible intervals (colored shaded region) in units of trophic position (x-axis).

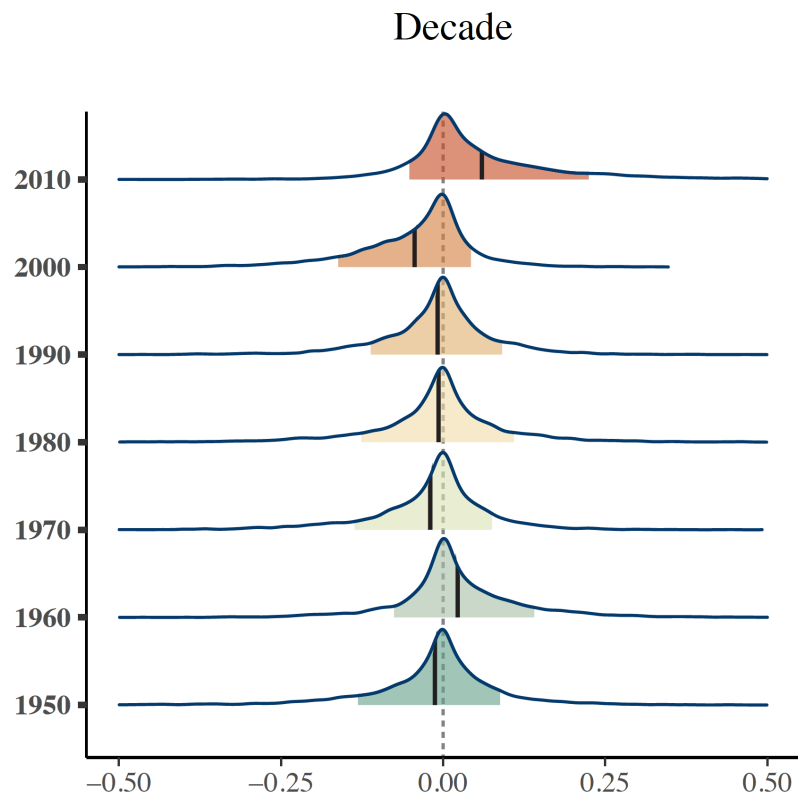


Figure 4.5: Decade included as a random effect (k)

Figure 4.6: Median of the posteriors for combined decade, classification, and the decade-classification interaction effect on pinniped trophic position from the best performing model (Model 6, Table 4.1). Tails denote 80% credible interval and dashed line is the long-term mean for each pinniped classification.

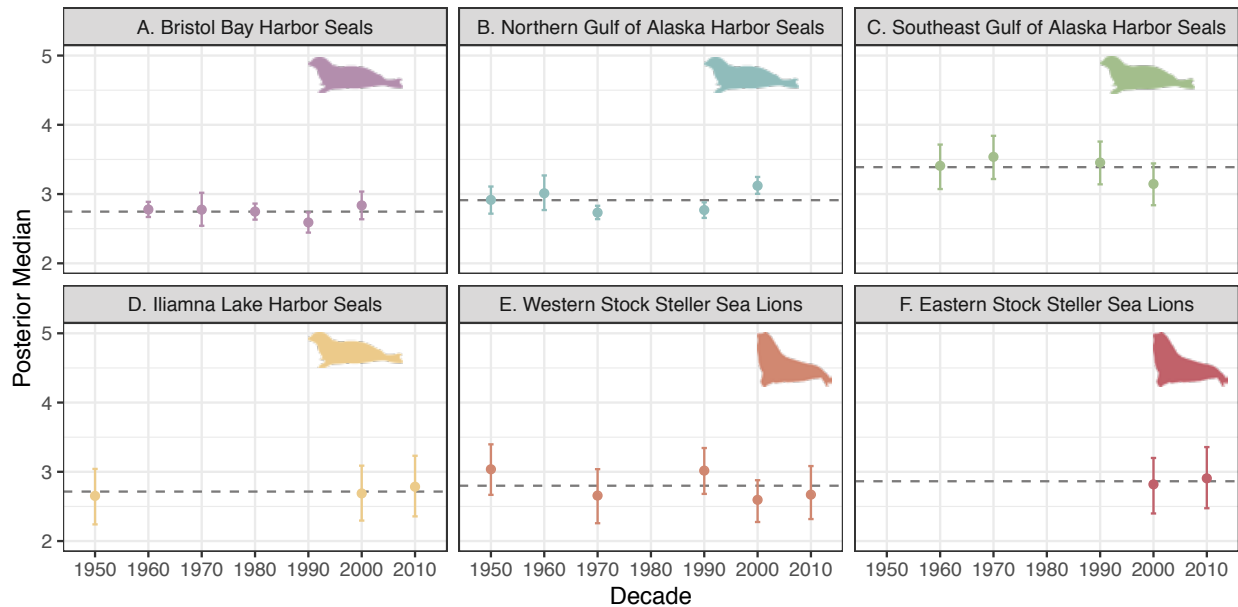


Figure 4.6: Combined decade, classification, and the decade-classification interaction effect

Chapter 5

THE INFLUENCE OF TEMPORAL ISOTOPE HETEROGENEITY AND ISOTOPE INCORPORATION RATES ON CONSUMER TROPHIC POSITION ESTIMATION

5.1 *Abstract*

Nitrogen stable isotope ratios are frequently used to estimate Nitrogen stable isotope ratios are frequently used to estimate trophic position of consumers. A key assumption in this application of stable isotope data is that the food webs in which consumers forage are in isotopic equilibrium with nitrogen resources. However, isotopic heterogeneity in the food web, which can arise from seasonal nutrient fluctuations, spatial variability in primary production, or variability in available prey, exists in most systems. Given resources are not immediately assimilated into the tissues of consumers, it is likely that the assumption of isotopic equilibrium is frequently violated in most systems. We tested the degree to which the violation of this assumption impacts consumer stable isotope ratios and trophic position estimates from those ratios. We constructed a compartment model to explore consumer stable isotope incorporation rates and their effect on trophic position calculations using bulk and compound-specific stable isotope data from previous experimental and observational studies derived from a variety of aquatic systems. We also tested how different parameterizations of the stable isotope baseline in trophic position calculations can improve accuracy. We found trophic position estimates of higher trophic level consumers are less accurate than lower trophic level consumers when applying bulk stable isotope analysis (BSIA) with particulate organic matter as the stable isotope baseline in trophic position equations. Accuracy of consumer trophic position improved for tertiary consumers when applying a 90-day lag between the consumer

stable isotope measurement compared to baseline measurements, but this was at the expense of decreased accuracy for lower trophic level consumers. Compound-specific stable isotope analysis (CSIA) of individual amino acids was more accurate in estimating trophic position for all consumers and systems compared to BSIA. Overall, our results show consideration of stable isotope heterogeneity and stable isotope incorporation rates of consumers is important for accurate trophic position estimates and should be carefully considered when designing stable isotope studies.

5.2 Introduction

In most ecosystems, seasonality drives food web structure and function (McMeans, McCann, Humphries, Rooney, & Fisk, 2015). Nutrients, such as phosphorus, nitrogen, and silicon, can be seasonally limited in their availability, which can determine the timing and amount of primary production (Kolzau et al., 2014; Moon & Carrick, 2007; Søndergaard, Lauridsen, Johansson, & Jeppesen, 2017) in aquatic systems. Nutrient availability can be influenced by oceanographic conditions, due to upwelling (J. A. Barth et al., 2007; Ferreira et al., 2020), resource pulses (Benbow, Receveur, & Lamberti, 2020; Verspoor, Braun, Stubbs, & Reynolds, 2011), or anthropogenic inputs (Khangaonkar, Nugraha, Xu, & Balaguru, 2019; McCrackin, Jones, Jones, & Moreno-Mateos, 2017), allowing for increased resource sequestration as primary producers are released from growth-limiting constraints. In addition, the impact of nutrient limitation can propagate to the rest of the food web, as primary production can alter abundance in both adjacent and non-adjacent trophic levels (Ware & Thomson, 2005) by controlling the energy available for higher trophic level consumers.

Stable isotope analysis of nitrogen ($^{15}\text{N}/^{14}\text{N}$) serves as a useful tool for identifying trophic interactions and nutrient sources in food webs. The nitrogen stable isotope values ($\delta^{15}\text{N}$) of consumers within a food web are governed by nitrogen availability, contributions of distinct nitrogen sources (i.e., anthropogenically fixed; M. J. Vander Zanden, Vadeboncoeur, Diebel, & Jeppesen (2005)), and trophic position. Trophic position of a consumer may be calculated based on marked isotope enrichment between consumer and prey (typically 2 to 4 per mille, Deniro & Epstein (1981)) referred to as the trophic enrichment factor. However, these calculations also require, and are highly sensitive to, the stable isotope baseline (stable isotope ratio of primary producers or inorganic nitrogen sources) within the food web, which can vary through space and time (C. Anderson & Cabana, 2007; Possamai, Hoeinghaus, & Garcia, 2021; Post, 2002). There is no consistent methodology to measure isotope baselines (Kjeldgaard, Hewlett, & Eubanks, 2021; Possamai et al., 2021) although recommendations for best practices have been made (Jardine et al., 2014; Possamai et al., 2021; Post, 2002).

Typically, the isotope baseline is estimated from primary producers, particulate organic matter (POM), or primary consumers that were measured at the same time as the consumer of interest (Kjeldgaard et al., 2021). However, baseline values averaged over time or generic values that may not be from the same environment or time period are also used (i.e. Estrada, Rice, Lutcavage, & Skomal (2003); Ruiz-Cooley, Markaida, Gendron, & Aguíñiga (2006); Chiang et al. (2020)] and fail to represent heterogeneity within and across systems.

A fundamental assumption of trophic position calculations from stable isotope data is that a consumer is in close equilibrium or ‘isotopic steady state’ with its dietary resources (Deniro & Epstein, 1981; Martinez del Rio, Wolf, Carleton, & Gannes, 2009; Phillips et al., 2014) and the isotope baseline used to calculate consumer trophic position. This means the stable isotope inputs (consumed resources) are in balance with outputs (excretion) such that consumer tissues represent the stable isotope value consumed resources plus a trophic enrichment factor. However, in nature such steady state do not necessarily occur, and while such assumption violations are often acknowledged, they are rarely quantified. The ecosystem heterogeneity created by seasonal fluctuations in both physical, chemical, and biological processes influence the isotopic values of primary producers and primary consumers (the isotope baseline) which varies both seasonally (Woodland, Magnan, Glémet, Rodríguez, & Cabana, 2012) and spatially (Vokhshoori & McCarthy, 2014). For example, seasonal variability in the nitrogen isotope values of seston or particulate organic matter are common in aquatic systems (B. Gu, 2009; Matthews & Mazumder, 2007a; Rolff & Elmgren, 2000; (Sylväranta, Hamalainen, & Jones, 2006; Vokhshoori & McCarthy, 2014; J. P. Wu, Calvert, & Wong, 1999). Such isotope variation at the base of the food web has been detected in higher trophic level consumers (Dale, Wallsgrove, Popp, & Holland, 2011; Feddern et al., 2021; Olson et al., 2010; Popp et al., 2007). However, isotope incorporation into consumer tissues typically occurs at a slower rate than that of the prey, as the rate of isotope turnover increases with animal size (S. M. Thomas, Crowther, & Bearhop, 2015; M. J. Vander Zanden, Clayton, Moody, Solomon, & Weidel, 2015) in addition to temperature, growth rate, and the type of

tissue studied [Dalerum & Angerbjörn (2005); Figure 5.11]. As a result of slower incorporation times, consumers can dampen short-term temporal stable isotope heterogeneity relative to algae or particulate organic matter (Woodland et al., 2012). The temporal mismatches created by differences in isotope incorporations rates between diet and consumer result in non-equilibria that violate stable isotope assumptions and can affect the calculation of animal trophic position.

A recent methodological advancement in stable isotope analysis, compound-specific stable isotope analysis (CSIA) of amino acid nitrogen ($\delta^{15}N$), provides researchers with a powerful new tool to estimate the stable isotope values of the base of the food web (Feddern et al., 2021; McMahon et al., 2015; Owen A. Sherwood et al., 2011) which can be applied for trophic position calculations of a consumer (Popp et al., 2007). A key advantage of estimating trophic position using CSIA is the distinct properties of source and trophic amino acids. Source amino acids do not exhibit isotopic enrichment with each trophic transfer and thus depict the nitrogen stable isotope baseline of a system. In contrast, trophic amino acids track the apparent trophic position of the animal through trophic enrichment. This allows estimation of baseline values directly in the consumer organism of interest. Furthermore, the baseline value of the source amino acids represents an integrated dietary contribution relating directly to the physiology and thus stable isotope turnover of the consumer itself. That, in principle, results in a smaller temporal mismatch and standardization across a heterogenous environment between the source and trophic amino isotope values.

Incorporation rates of individual amino acids vary [Bradley, Madigan, Block, & Popp (2014); Downs, Popp, & Holl (2014); Figure 5.11] and whether source and trophic amino acids are incorporated at similar rates is currently not well studied. Downs et al. (2014) showed that the amino acid incorporation rates of glutamic acid (trophic) and phenylalanine (source), which are the most commonly applied amino acids for trophic position calculations due to their trophic enrichment factors, in shrimp appear similar (Figure 5.11). However, it is not known if this is a persistent pattern between glutamic acid and phenylalanine across

animal groups or tissue types because controlled feeding studies measuring turnover rates of individual amino acids are currently limited. There is evidence that turnover time of amino acids may also vary with diet quality for some but not all amino acids (Chikaraishi, Steffan, Takano, & Ohkouchi, 2015). Furthermore, the same study found both faster and slower turnover rates for other trophic (aspartic acid, proline) and source (lysine, methionine) amino acids, motivating an analysis of how temporal isotope integration in amino acids influences the accuracy of trophic position estimates.

Here we evaluate the consequences of biologically-plausible consumer isotope incorporation rates under baseline variability for estimating trophic position using bulk stable isotope analysis (BSIA) and CSIA. We approach this by constructing a simulation model using stable isotope data from previous experimental and observational studies. The objectives of this work are to:

1. Explore how mismatches in isotope turnover rates between food web baseline and consumers influence trophic position calculations from bulk $\delta^{15}\text{N}$ values among various trophic levels, tissue types, and aquatic systems.
2. Examine how variability of source amino acid and trophic amino acid turnover rates can influence trophic position calculations.
3. Consider how different trophic position calculations and isotope baseline sampling strategies for both BSIA and CSIA can improve accuracy in trophic position estimations.

5.3 Methods

Nitrogen stable isotope values of primary, secondary, and tertiary consumers were modelled using a first order-kinetics compartment model (Cerling et al., 2007; Del Rio & Carleton, 2012). Different stable isotope baselines and incorporation rates were modelled to understand

how they impact stable isotope values and trophic position accuracy of consumers for distinct food web scenarios. To represent biologically plausible parameters, stable isotope baselines were compiled from observational studies and tissue turnover times for BSIA and CSIA were compiled from controlled feeding experiments. Trophic position estimates were calculated from model simulations and accuracy of trophic position estimates were quantified for each consumer and each model simulation.

5.3.1 Tissue Turnover Modelling Structure

The stable isotope values of consumers were modeled using a first order kinetics model as described by Del Rio & Carleton (2012) and modified from Cerling et al. (2007). Many controlled feeding studies use an exponential fit model to estimate tissue turnover where:

$$\delta X_t = b e^{-\lambda t} + c \quad (5.1)$$

δ is the stable isotope value of a consumer's tissues for a given element X that has been measured at time t before and after the consumer has been switched to an isotopically distinct diet. The parameters b , δ , and c are each estimated empirically from a best fit of the exponential model to the data, where the parameter c is the asymptotic value of the isotope composition of tissue after the diet switch once tissues have reached steady state. The parameter b represents the magnitude of isotopic change in tissues or the difference between the initial isotopic steady state before the diet switch and the final isotopic steady state after the diet switch. The parameter λ is a first order data-derived rate constant referred to as the turnover rate, which can be derived the isotopic half-life or time to reach steady state after a diet switch:

$$t_\alpha = \frac{\ln(1 - \alpha)}{\lambda}. \quad (5.2)$$

In most controlled feeding studies t_α is reported as the isotopic half-life where α is 0.5 which represents the amount of time (in days or hours) required for 50% equilibration with a new diet source. $t_{0.95}$ values are also frequently reported and denote 95% equilibrium and are

commonly accepted as the amount of time to reach isotopic steady state. Chemically, this representation of the first order rate constant, λ , assumes a first order reaction given for a trace isotope where the concentration of the rare isotope (^{15}N) is significantly less than that of the abundant isotope (^{14}N). Thus, the system can be closely approximated by changes in only the rare isotope. In the case of controlled feeding experiments the food source is treated as a reservoir where the isotopic value of the food supply is unaffected by consumption (Criss, 1999).

We apply this approach but with a modified representation of equation (5.1) as presented in Del Rio & Carleton (2012) with more biologically meaningful set of parameters:

$$\delta X_t = \delta X_\infty - (\delta X_\infty - \delta X_0)e^{\lambda t}, \quad (5.3)$$

where x represents a particular element (in this case nitrogen), δX_∞ is the asymptotic isotope value a consumer will reach at steady state with a new diet (or the final diet isotopic value plus the trophic enrichment factor). δX_0 is the initial isotope value of the tissue, and λ is the empirically derived rate constant as described above.

5.3.2 Bulk Stable Isotope Model

Using observed stable isotope baseline data derived from particulate organic matter (POM) (Table 5.1) we modelled the stable isotope composition of primary, secondary and tertiary consumers associated with a particular food web scenario (Figure 5.1). The number of trophic transfers is a known component of the model structure and for all model simulations the true trophic level was 2 for the primary consumer, 3 for the secondary consumer, and 4 for the tertiary consumer. Equation (5.3) was modified to describe each trophic level as:

$$\delta X_{t,\hat{tp}} = (\delta X_{t-1,\hat{tp}-1} + TEF) - [(\delta X_{t-1,\hat{tp}-1} + TEF) - \delta X_{t-1,\hat{tp}}]e^{-\lambda}, \quad (5.4)$$

where, $\delta X_{t,\hat{tp}}$ is $\delta^{15}N$ at time t with a true trophic position of \hat{tp} of a modelled consumer. TEF is the trophic enrichment factor of consumers which was assumed to be known and the

canonical value of 3.4 per mille was applied for all consumers in the BSIA models. Trophic position was then calculated from modelled stable isotope date $\delta X_{t,\hat{tp}}$ from equation (5.4) as:

$$tp = \frac{\delta X_{t,\hat{tp}=2:4} - \delta X_{t,\hat{tp}=1}}{TEF} + 1, \quad (5.5)$$

where tp is the estimated trophic position. $\delta X_{t,\hat{tp}=1}$ represents the $\delta^{15}N$ of primary producers at the base of the food web and $\delta X_{t,\hat{tp}=2:4}$ represents the modelled consumers (primary, secondary, and tertiary). Finally, an effect size was estimated as the magnitude and duration the estimated trophic position, tp , deviated from the true trophic position \hat{tp} (Figure 5.3):

$$d = tp - \hat{tp}, \quad (5.6)$$

where d is the trophic position estimation error of a consumer based on the estimated trophic position tp calculated from equation (5.5), where \hat{tp} represents the true trophic position ($\hat{tp} = 2:4$) of primary, secondary, and tertiary consumers. Duration of deviation was determined by summing the number of days where d was ± 0.5 for each consumer (Figure 5.3), meaning tp was within 0.5 of the true trophic position, \hat{tp} . We assumed the stable isotope signature of the base of the food web, TEF , and λ were known.

5.3.3 Compound-specific Stable Isotope Model

Diet switching studies that report the isotope turnover rates for individual amino acids are currently uncommon in the stable isotope literature. For the CSIA model simulations we applied our modelling framework to two consumers with known isotope turnover rates for individual amino acids, bluefin tuna (*Thunnus orientalis*; Bradley et al. (2014)) and Pacific white shrimp (*Litopenaeus vannamei*; Downs et al. (2014)). For each consumer, four trophic amino acids (glutamic acid, alanine, proline, valine) and a single source amino were modelled (Figure 5.11). The canonical source amino acid for trophic position calculations, phenylalanine, was modelled for shrimp however a phenylalanine half-life value was not reported in Bradley et al. (2014) and lysine was used as the source amino acid for tuna

instead of phenylalanine. Tuna and shrimp were modelled as a single food web (Figure 5.2) for each of the four baseline case studies (Table 5.1) where shrimp was the primary consumer and tuna was the secondary consumer. Equation 4 was modified to model each of the 5 amino acids for each consumer:

$$\delta X_{t,\hat{tp},a} = (\delta X_{t-1,\hat{tp}-1,a} + TEF) - [(\delta X_{t-1,\hat{tp}-1,a} + TEF) - \delta X_{t-1,\hat{tp},a}]e^{-\lambda_a}, \quad (5.7)$$

where $\delta X_{t,\hat{tp},a}$ is the estimated stable isotope composition of nitrogen, X , at a given time t for a specific consumer, \hat{tp} , for each amino acid a . As such, λ was distinct for each amino acid, a including the source amino acid. The trophic position equation was also modified to calculate the trophic position of shrimp and tuna from amino acids, with source amino acids instead of the measured baseline:

$$tp_t = \frac{\delta X_{t,\hat{tp}=2:3,(i-o)} - \beta_{(i-o)}}{TEF_{(i-o)}} + 1, \quad (5.8)$$

where trophic position tp for time t is estimated from simulated stable isotope data from equation (5.7). $\delta X_{t,\hat{tp}=2:3,(i-o)}$ is the stable isotope value of compound X (nitrogen for this study) for each trophic amino acid i and source amino acid o in a consumer with a known trophic position \hat{tp} . δX_{i-o} represents the total trophic enrichment that has occurred throughout the food web measurable from consumer tissues at a given trophic level (\hat{tp}). β_{i-o} is the difference of enrichment between a specific trophic amino acid i and source amino acid o for primary producers derived from laboratory experiments (Y. Chikaraishi et al. (2007)). TEF_{i-o} represents the mean trophic enrichment factors for consumers, and is calculated from the mean difference between trophic amino acid i and source amino acid o across all consumers described in J. M. Nielsen et al. (2015). Equation (5.6) was applied to the CSIA models calculate trophic position deviation d with $\hat{tp} = 2$ for shrimp and $\hat{tp} = 3$ for tuna.

5.3.4 Data Compilation

Data used for case studies was compiled from previous research that measured the stable isotope signature of nitrogen in particulate organic matter (POM) in both marine and fresh-

water systems and laboratory experiments that measured nitrogen stable isotope turnover rates in different taxa, tissues, and amino acids. These studies were used to obtain realistic estimates of the natural variation of ^{15}N at the base of the food web over the course of a year. We prioritized studies that 1) collected data at least monthly and 2) represented a range of aquatic systems (Table 5.1). Four diverse ecosystem studies were used as case studies; a moderately eutrophic urban lake ((Syväranta, Tirola, & Jones, 2008), a shallow subarctic lake in interior Alaska (Binhe Gu, Schell, & Alexander, 1994), a pristine oligotrophic lake (Matthews & Mazumder, 2007b) and a marine upwelling site near Vancouver Island (J. P. Wu et al., 1999). The rate of tissue turnover for nitrogen isotopes is typically measured on the time scale of hours or days and thus daily values of the nitrogen isotope baseline is necessary to model isotopic incorporation by consumers. However, studies collect stable isotope data from POM and primary producers on weekly and monthly scales. Therefore, we linearly interpolated nitrogen stable isotope values between observations in order to approximate daily changes in the isotopic baseline (Table 5.1).

Six theoretical food web scenarios were constructed for BSIA that contain primary, secondary, and tertiary consumers and that could be associated with the baseline values for each of the four case studies (Table 5.1& Figure 5.1). Data for bulk nitrogen stable isotope turnover rates are available for a variety of taxa and tissues (M. J. Vander Zanden et al., 2015). Food web scenarios were constructed by matching consumers' half-life values with isotope baseline data from an ecosystem in which they could reasonably forage. A marine food web was constructed from half-life values for an amphipod, a herring and a great skua and a freshwater food web was constructed from half-life values for a water strider, a steelhead or small mouth bass, and a black bear (Figure 5.1). The selected species did not represent a specific food web, but rather were selected based on whether they could reasonably be found within the same food web and if their tissue turnover times could be representative of other species within their trophic level. These scenarios were used to make specific comparisons regarding stable isotope baseline and the half-life values of the consumers. As a first comparison, the half-life value of

the secondary consumer was increased between scenario a and b to represent different tissues (liver versus muscle), an increase in temperatures, or an increase in size, all of which can alter isotope incorporation rates. Comparison 2 decreased the half-life of the secondary consumer and increased the half-life of the tertiary consumer between scenarios c and d (Figure 5.1). The objective of this comparison was to identify how dietary differences of the tertiary consumer can impact its stable isotope composition and how sampling different tissues of the tertiary consumer can impact trophic position estimates. Finally, comparison 3 examined how two isotope basslines with distinct shapes can impact trophic position estimates of the same food web (Figure 5.1, Table 5.1).

For CSIA of amino acid nitrogen models, half-life data from two aquatic consumers (shrimp and tuna) were used to construct a single food web with four trophic amino acids and one source amino acid modelled for each consumer (Figure 5.2). The stable isotope values for each amino acid for both consumers were modelled for all four of the stable isotope baselines derived from particulate organic matter (Table 5.1). The stable isotope values for each amino acid were then compared for each baseline and both consumers to assess the performance of trophic amino acids in trophic position estimations.

5.3.5 Comparison to recommended methodologies

Guidance on baseline sampling for BSIA suggests primary consumers should be used as the stable isotope baseline rather than particulate organic matter or primary producers (Post, 2002), and consumers of interest should be sampled 90 days after sampling the stable isotope baseline (Possamai et al., 2021). These two approaches can minimize baseline isotope variability or account for disconnect between the baseline and consumer due to tissue turnover. We assessed the utility of these approaches to improve trophic position accuracy across a variety of systems by applying them to our simulated food webs. To calculate trophic position using the primary consumer we applied:

$$tp = \frac{\delta X_{\hat{tp}} - \delta X_{\hat{tp}=2}}{TEF} + 2. \quad (5.9)$$

Using the stable isotope values of the simulated primary consumer, $\delta X_{\hat{tp}=2}$. To calculate the trophic position using a 90 day delay we used:

$$tp_y = \frac{\delta X_{\hat{tp},y} - \delta X_{\hat{tp}=1,y}}{TEF} + 1, \quad (5.10)$$

where trophic position of consumers, tp , is estimated at days (y) = 90, 270 and 360 from the simulated consumer stable isotope data $\delta X_{\hat{tp},y}$ for each consumer, \hat{tp} . $\delta X_{\hat{tp}=1,y}$ is the stable isotope value of the baseline at days, (y) = 1, 90, 270, and 360. A third approach combining both of these methodologies was also applied to the model output. Trophic position estimation error for all three approaches was assessed using d from equation (5.6).

5.3.6 Sensitivity Analysis

A sensitivity analysis was performed to further explore how variability in tissue turnover time impacts trophic position estimates using BSIA and CSIA. We simulated an isotope baseline that had a rate of isotope change that varied from 0 to 0.15 (per mille per day), represented 123 days, and represented a 1 to 6 per mille isotope change which was realistic based on previous studies (Table 5.1, Figure 5.4). A primary, secondary, and tertiary consumer were modelled for BSIA (equation (5.4) - (5.6)) and CSIA (equations (5.7) - (5.8)). Half-life values ranged from 1 to 280 days which were considered reasonable estimates for most tissues, taxa, and both approaches (Figure 5.11). The model was run using the same simulated baseline for each of the 280 half-life values. To assess the sensitivity across half-life values, the mean and standard deviation of trophic position deviation was taken for each model run which represented the average deviation across the 123-day simulation. For the CSIA model, two analyses were run, one with a source amino acid half-life value of 130 days (representing the values for lysine in bluefin tuna reported by Bradley et al. (2014)) and a second of 33 days (representing the values for phenylalanine in shrimp reported by Downs et al. (2014)). The half-life value of the source amino acid was assumed to be known and the half-life value of the trophic amino acid was varied for each simulation. The half-life values of the primary,

secondary, and tertiary consumers were manipulated simultaneously, and all three consumers had the same half-life value for a single model simulation.

5.4 Results

The dynamic behavior of the stable isotope baseline impacts the BSIA values and estimation error of trophic position for simulated primary, secondary, and tertiary consumers. The four stable isotope baselines (Table 5.1) showed a range of stable isotope variability over the course of a year (Figure 5.4). The oligotrophic lake (baseline 4, Figure 5.4F) had the greatest variability in the stable isotope values of particulate organic matter, that ranged from 0 to over 10‰, but was relatively stable (fluctuations within 2‰ range) until day 300. In contrast, the two other freshwater systems exhibited fluctuations within a 5‰ range, but oscillated more frequently between values (Figure 5.4C – E) within that range. Of the two eutrophic lakes, the heavily polluted lake (baseline 3; Figure 5.4E) had the greatest range in stable isotope values. The marine upwelling system showed baseline isotope values characteristic of seasonal nutrient fluctuations and spring phytoplankton blooms. Nitrogen stable isotope values of POM were lowest in the spring and summer when upwelling is high, and higher in the winter when nutrients are more limiting (Figure 5.4A & B).

5.4.1 Bulk Stable Isotope Model

Our model showed that consumers are rarely in isotopic steady state with their available resources and the violation of this assumption resulted in trophic position estimation error by as much as one trophic level (Table 5.2; Figure 5.5C & F). We define duration of deviation as the number of simulated days that a consumer had a trophic position estimation error of greater than ± 0.5 trophic level (equivalent to $\pm 1.7\text{\textperthousand}$ deviation from steady state with resources). Primary consumers had less than 34 days duration of deviation (Table 5.2). The duration of deviation increased as you moved up the food web. For all scenarios, tertiary consumers had the longest duration of deviation, which was as high as 115 out of

365 days for scenario 4 (Table 5.2; Figure 5.4C). Based on comparison 1 (increasing half-life of the secondary consumer only), the duration of deviation also increased for tertiary consumers when half-life of secondary consumers increased, despite the same half-life of tertiary consumers and same stable isotope baseline (Table 5.2; Figure 5.4A versus B). Therefore, duration of deviation was determined by the consumers half-life, in addition to the half-life of consumers lower in the food web that serve as resources for higher trophic levels.

Similarly, the magnitude of trophic position estimation error depended on both the half-life of the consumer of interest, and the half-life of consumers lower in the food web. When a primary or secondary consumer is not in steady state with its resources, the resulting trophic position deviation propagates through the food web. In comparison 1, the magnitude of trophic position estimation error for the tertiary consumer was higher when the half-life value of the secondary consumer (Figure 5.5A) was higher, despite the half-life value of the tertiary consumer being the same in both scenarios. Sampling a tissue of a tertiary consumer with extremely rapid turnover time (i.e., blood plasma Figure 5.5C) did not prevent trophic position estimation error, despite the tertiary consumer being as close to isotopic steady state with its prey as possible. Sampling the blood plasma of a tertiary consumer that has prey with slow tissue turnover (i.e., adult steelhead muscle), results in substantial trophic position estimation error ranging from -1.1 to 0.8 ($\hat{tp} = 4$, Figure 5.5C). This deviation is similar to sampling a tissue with a longer isotopic half-life from a tertiary consumer that eats prey with a faster half-life (i.e., juvenile small mouth bass muscle) ($\hat{tp} = 4$, Figure 5.5D) which ranges from -0.9 to 0.8.

In addition to half-life value of the consumers in a food web, the dynamic behavior of the stable isotope baseline (rate of isotopic change, inflection points, magnitude of change) also impacts the stable isotope values of the consumers, and as a result, the magnitude and duration of trophic position estimation error. The eutrophic urban lake ((Syvääranta et al., 2008) had a stable isotope baseline that demonstrated a slow rate of change that

reached a high magnitude (Figure 5.4E). By comparison, the pristine oligotrophic lake showed frequent, low magnitude, rapid, fluctuations followed by a rapid increase of 10‰ (Figure 5.4D). The eutrophic lake had a much longer duration of deviation for all consumers (Table 5.2) compared to the oligotrophic lake (Figure 5.5E & D). For almost the entire model simulation, the oligotrophic food web was within ± 0.5 trophic levels until day 310 when all consumers experienced a rapid, high-magnitude, deviation from their true values (Figure 5.5D). In comparison, the trophic position of the consumers in the eutrophic lake were consistently underestimated but experienced a lower magnitude of deviation (Figure 5.5E).

5.4.2 CSIA Model

The magnitude of trophic position estimation error and the duration of deviation was lower using CSIA compared to BSIA and varied across trophic amino acids. Baseline 3, the moderately eutrophic urban lake, had the highest magnitude of estimation error for all stable isotope baselines for the CSIA model (Figure 5.7E & F) but did not exceed ± 0.4 estimation error for primary or secondary consumers. In contrast, for the BSIA model secondary consumers exceeded ± 0.5 estimation error for all scenarios (Figure 5.5). For the BSIA model, estimation error always propagated up the food web and was greatest for higher level consumers in all scenarios. This was not necessarily the case for the CSIA model. In fact, for most baselines and amino acids, both shrimp and tuna performed similarly (Figure 7) despite tuna being modelled as a higher trophic level consumer (secondary) than shrimp (primary). No amino acids for the primary and secondary consumers in the CSIA model exceeded an estimation error of greater than 0.4 trophic levels and for most trophic amino acids it did not exceed ± 0.2 trophic levels, with glutamic acid and alanine preforming particularly well across consumers and baseline scenarios. In comparison, the secondary consumer in scenario 3 of the bulk stable isotope model had an estimation error of 0.8 trophic levels (Figure 5.5C) which was twice as high as the largest trophic position estimation error for the CSIA model.

All amino acids used in the CSIA model performed better in terms of the magnitude of

trophic position estimation error (Figure 5.7) and duration of deviation compared to BSIA analysis (Figure 5.5). Of the tested trophic amino acids, proline had the greatest magnitude of estimation error for both shrimp, the primary consumer (maximum estimation error = 0.4, Figure 5.7G), and tuna, the secondary consumer (maximum estimation error = 0.4; Figure 5.7F). In comparison, the canonically used trophic amino acid for CSIA trophic position calculations, glutamic acid, only had a maximum estimation error of 0.04 for shrimp and 0.2 for tuna for the same baseline, and lower magnitude of estimation error for all other baselines (Figure 5.7E). Both glutamic acid and alanine performed similarly in terms of estimation error for both consumers in the CSIA model and as a result were the best suited trophic amino acids for minimizing trophic position estimation error when paired with phenylalanine and lysine as source amino acids.

5.4.3 Sensitivity Analysis

Sensitivity of trophic position estimation error to consumer half-life was similar across consumer trophic level for BSIA of nitrogen. For all consumers, the mean and standard deviation of trophic position estimation error was similar at half-life values greater than 100 days. For higher trophic level consumers, trophic position was slightly more sensitive to half-life values less than 100 days (Figure 5.8C & D). Initially the deviation and variability increased at a higher rate than consumers lower in the food web, but eventually leveled off at a half-life of approximately 100 days, at which point the mean and standard deviation of the tertiary consumer was similar to that of lower trophic level consumers (Figure 5.8D).

Trophic position deviation for BSIA was more sensitive to consumer half-life than CSIA. Sensitivity of trophic position deviation was minimized when the half-life of the trophic amino acid was equal to the half-life of the source amino acid, which was 130 days (Figure 5.9) and 33 days (Figure 5.10) for these model simulations. Mean trophic position deviation and its distribution decreased in magnitude initially before intersecting with the half-life of source amino acid. At half-life value greater than the source amino acid variability increased slightly

but did not deviate substantially from zero for any of the three trophic level consumers (Figure 5.9D). The greatest sensitivity of trophic position estimation error occurs when the half-life values of trophic amino acids are less than source amino acid half-life values.

5.4.4 Comparison to recommended methodologies

Alternative recommended methods to calculate trophic position from stable isotope data produced only moderate improvements for trophic position accuracy. The 90-day lag between the stable isotope baseline and tertiary consumers improved accuracy for trophic position, although estimates ranged ± 0.6 trophic levels for the eutrophic, arctic lake (Table 5.4A, Scenario 4). The range in trophic position estimates for secondary consumers were similar for the 90-day lag compared to a simultaneous sampling approach. In contrast the range in primary consumer trophic position was much greater with a 90-day lagged sampling strategy compared to a simultaneous strategy, with overestimates as high as two trophic levels in some systems (Table 5.4A). Using primary consumers as a stable isotope baseline improved trophic position estimation error for all consumers in all systems (Figure 5.12) compared to the particulate organic isotope baseline model (Figure 5.5) although estimation error still exceeded ± 0.5 for substantial amounts of time for most scenarios. Applying the 90-day lagged equation with the primary consumer as the stable isotope baseline further improved trophic position accuracy for the tertiary consumer (Table 5.4B) although accuracy for the secondary consumer was similar to the simultaneously measured model with the primary consumer as the stable isotope baseline (Figure 5.12).

5.5 Discussion

Temporal heterogeneity in the bulk nitrogen stable isotope baseline results in erroneous trophic position estimates when heterogeneity and tissue turnover are not accounted for. Based on our results, this error can even occur when the isotope baseline can be sampled continuously and simultaneously with the consumer and is considered known. Both the shape

of the heterogeneity of the stable isotope baseline and the trophic level of the consumers are important factors in the magnitude and duration of trophic position estimation error for a given aquatic food web. Notably, for BSIA, trophic position estimation error propagates up the food web with greater error in estimation for consumers feeding at higher trophic levels. Using CSIA to sample consumers provides the best approach for minimizing trophic position estimation error due to temporal heterogeneity and tissue turnover rates however the relative rate of turnover between the source amino acid and the trophic amino acid used to calculate trophic position should be considered. When CSIA is not feasible, using primary consumers as the stable isotope baseline or sampling the consumer 90 days after sampling the baseline can provide moderate improvement to trophic position estimation error of high trophic level consumers, but does not eliminate it entirely and the improvement comes with decreased accuracy for lower trophic level consumers.

The duration of trophic position deviation is substantial for all of the modelled consumers using BSIA. However, no consumer had a trophic position deviation of greater than ± 0.5 for the entire modelled time period. In fact, for at least 30% of the model time for all consumers in all food webs trophic deviation was less than ± 0.5 trophic positions. Based on this result, there are substantial time periods within each food web when trophic deviation can be minimized simply based on sampling time. For most modelled food webs, days 0 - 100 (January 1 – April 10) and 200 - 250 (July 19 – September 7) produced accurate trophic position estimations for secondary and tertiary consumers (Figure 5.5 A-F), although the moderately eutrophic, urban lake (scenario 5; Figure 5.5E) was an exception. Sampling consumers during early winter or late summer when estimation error is lowest could improve accuracy of trophic position estimation. Consideration for the shape of the stable isotope baseline is necessary for this approach. Specifically, researchers should identify how nitrogen resources are expected to change through time in their system of interest and anticipate how this may impact the stable isotope values of consumers. However, this approach may not be appropriate for all research questions, as trophic position measurements during the spring

or autumn may be of particular interest. The applicability of this strategy across systems also warrants additional research as the food web baselines modelled in this study represent temperate systems.

Notably, estimation errors associated with turnover and heterogeneity propagate up food webs and are more pronounced and occur for a longer duration (Table 5.2) in higher trophic level consumers when using BSIA to estimate trophic position (Figure 5.5). The sensitivity of trophic position to stable isotope half-life also propagates up the food web (Figure 5.8), such that higher trophic level consumers experience more trophic position deviation at higher half-life values than their lower trophic level counterparts. This is a result of tertiary consumers being even further from isotopic steady state with the sampled isotope baseline, in this case POM, compared to lower trophic level consumers. G. Cabana & Rasmussen (1996) observed that $\delta^{15}N$ values of phytoplankton are ten times more variable than primary consumers. Due to the short life span of primary producers, they only represent a short-term measure of the isotope baseline (S. Vizzini & Mazzola, 2003). By sampling primary consumers as the stable isotope baseline isotope heterogeneity is time averaged as nitrogen is assimilated into primary consumer tissues. This results in a dampening of baseline stable isotope heterogeneity. Our results agree with this, while trophic position estimation error is higher in secondary and tertiary consumers, variability in the magnitude of trophic position estimation error is dampened relative to the stable isotope values observed lower in the food web (Figure 5.4). This indicates that when consumer tissues are sampled is less impactful for the overall magnitude of trophic position deviation than when and how the baseline is sampled. Modifications to the timing of stable isotope baseline sampling is the most fruitful approach for minimizing trophic position estimation error (compared to adjusting consumer sampling).

Previous research has provided guidance to improve accuracy of trophic position estimation from bulk stable isotope data. Our analysis utilized stable isotope data of particulate organic matter because it is prevalent and longer-term data was available for a greater variety of

systems. It also allowed us to manipulate the tissue turnover time of all of the consumers in the modelled food web. However, Kjeldgaard et al. (2021) found that there were 10 methods to quantify stable isotope baseline in the literature, of which particulate organic matter was only one. Guidance on stable isotope sampling strategy has included increasing sample size (Kjeldgaard et al., 2021), using primary consumers as the stable isotope baseline rather than particulate organic matter or primary producers (Post, 2002), and sampling consumers of interest and the stable isotope baseline 90 days apart (Possamai et al., 2021). With our model, we explored these options and found that applying a 90-day lag or using the primary consumer as the stable isotope baseline offered only moderate improvement of the accuracy in trophic position estimation (Table 5.4; Figure 5.12). Accuracy in trophic position estimation improved the most for tertiary consumers for both methods but was worse for primary consumers when applying the 90-day delay. This result indicates the steady-state assumption is more accurate for higher trophic level consumers when applying a 90-day sampling delay and using primary consumers as the stable isotope baseline. When applying both of the sampling strategies at once, the trophic position deviation of tertiary consumers was only ± 0.3 trophic levels for most systems (Figure 5.4B). Using a 90-day lag between the consumer of interest and isotope baseline, using primary consumers as the stable isotope baseline, or both, could be a useful strategy for minimizing error in trophic position estimation for tertiary consumers or higher but will decrease the accuracy of lower trophic level consumers.

To further improve this strategy, a different time lag could be applied for lower trophic level consumers that is less than 90 days and aligns more closely with their isotopic turnover rates. This strategy would be particularly useful for studies where large sample size or CSIA is impractical or cost prohibitive. It is important to note that in order to utilize primary consumers as the isotopic baseline as opposed to primary producers, the trophic level of the primary consumers must be known with certainty, or it could introduce another component of error into the trophic position estimates. This can be particularly challenging when

employing a method such as plankton tows, which frequently include mixture of planktonic taxa (i.e., microbial heterotrophs, detritus, microzooplankton) in different life stages, and as a result can impact trophic position estimates of consumers of any trophic level (Hannides, Popp, Choy, & Drazen, 2013; McCarthy, Benner, Lee, & Fogel, 2007). In addition, omnivory is common in zooplankton (A. Atkinson, 1996; Castellani, Irigoien, Mayor, Harris, & Wilson, 2008) making it challenging to know their trophic level absolutely if they are used as the stable isotope baseline for trophic position calculations of other consumers. Using sessile filter feeders (i.e. mussels, barnacles) as the stable isotope baseline when possible would be the best practice, as suggested by other research (Mancinelli, Vizzini, Mazzola, Maci, & Basset, 2013; Post, 2002; Zanden & Joseph, 1999; Zanden & Rasmussen, 2001).

CSIA substantially reduces the trophic position estimation error and duration of trophic position deviation relative to BSIA. Some trophic amino acids performed better than others, specifically, proline had the highest trophic position estimation error compared to glutamic acid and alanine which had the lowest. Based on our sensitivity analysis, trophic position estimation error is less sensitive to longer trophic amino acid half-life values (Figures 5.9 & 5.10). Calculating trophic position using a source amino acid with a longer half-life (Figure 5.9) also reduced sensitivity of estimation error to trophic amino acid half-life values compared to a shorter half-life of the source amino acid (Figure 5.10).

CSIA allows researchers to measure the stable isotope value of multiple amino acids from a single sample. Phenylalanine and glutamic acid have become the canonical source and trophic amino acids applied in CSIA because phenylamine demonstrates the lowest trophic enrichment while glutamic acid has the highest (Y. Chikaraishi et al., 2007; Chikaraishi et al., 2009; Hannides, Popp, Landry, & Graham, 2009; McClelland & Montoya, 2002). Recent studies have shown using multiple amino acids can improve trophic position estimates (J. M. Nielsen et al. (2015), Feddern et al. in prep) but there is little guidance in the literature quantifying which amino acids are best and why. Best practices in CSIA should focus on utilizing source - trophic amino acid pairs where the amino acids have similar half-life values.

When researchers are choosing between pairs, it is best to select source amino acids with longer half-life values, and generally, selecting a trophic amino acid that has a longer half-life than the selected source amino acid will produce the best results. Based on our results, glutamic acid and alanine are the best trophic amino acids to use and are suitable to be paired with either lysine or phenylalanine as source amino acids.

While our results show CSIA reduces error in trophic position estimation relative to BSIA, CSIA is can be cost prohibitive and half-life values of individual amino acids are not well studied across taxa and tissues. Studies examining nitrogen stable isotope half-life values of individual amino acids are limited, and the field of CSIA would greatly benefit from more half-life values reported in the literature. Our results show lysine, phenylalanine, glutamic acid, and alanine perform well based on half-life values of tuna white muscle and shrimp tail muscle. Similarly, Feddern et al. in prep found that using both alanine and glutamic acid paired with phenylalanine from harbor seal bone offered the most improvement to model certainty compared to using either amino acid alone or other trophic amino acids. This indicates that the best CSIA amino acid pairs may be fairly consistent across taxa and tissues, but additional studies of tissue turnover rates would verify this result, particularly in animals that utilize urea-excretion (Germain et al., 2013) and in tissues commonly used for historical CSIA studies such as bone or coral (Feddern et al., 2021; Misarti et al., 2009; O. A. Sherwood et al., 2005; Owen A. Sherwood, Jamieson, Edinger, & Wareham, 2008; Owen A. Sherwood et al., 2011).

Here we focused on seasonal, temporal heterogeneity, but other types of stable isotope heterogeneity exist within aquatic systems and impact trophic position calculations. Spatial heterogeneity is common in stable isotope baselines (Lorrain et al., 2015) and changes with latitude (Lorrain et al., 2015; Vokhshoori & McCarthy, 2014) and depth (L. Peters, Faust, & Traunspurger, 2012; D. M. Sigman, Karsh, & Casciotti, 2009; J. P. Wu et al., 1999) within ocean basins. As a result, mobile consumers are frequently integrating distinct stable isotope baselines, that may not reflect the baseline where they were caught for sampling.

Stable isotope values of primary producers also vary based on taxa in both freshwater (Vuorio, Meili, & Sarvala, 2006) and marine habitats (Lorrain et al., 2015; Ramirez et al., 2021; D. M. Sigman et al., 2009). On smaller scales in freshwater lakes, habitat availability and population abundance can also influence isotopically distinct basal resource use of aquatic consumers (Stiling, Holtgrieve, & Olden, 2021). Changes in diet that impact resource use can result in changes in the stable isotope baseline that is assimilated by a consumer of interest. Similar considerations for tissue turnover times and its implications for trophic position estimates should be made for mobile consumers in spatially heterogenous systems as well as the temporally heterogenous systems examined in this study.

This study examined temporal isotope heterogeneity, tissue turnover times and their impact of estimating trophic position from stable isotope data. While we focused on the assumption of isotopic steady state between consumers and their prey, this is not the only assumption for calculating stable isotope values that impacts the interpretation of stable isotope data. Trophic enrichment factors are often assumed to be equal for consumers but is known to be vary based on taxa, tissues, excretion pathway, and diet (Blanke et al., 2017; Caut, Angulo, & Courchamp, 2008; Deniro & Epstein, 1981; Vanderklift & Ponsard, 2003). We did not model the effect of variable trophic enrichment factors, though this value is known to influence trophic position calculations and resource estimates (A. L. Bond & Diamond, 2011). Variability in trophic enrichment factors and baseline heterogeneity can act both synergistically and antagonistically on trophic position estimates. The scope of this study was to understand error associated with heterogeneity and tissue turnover specifically. While our model is limited in the number of parameters that vary, it fulfills this crucial knowledge gap.

Stable isotope heterogeneity and stable isotope turnover of consumer tissues impact the accuracy of trophic position estimates. Based on our results CSIA reduces trophic position estimation error more than any of the tested trophic position equations for BSIA. Using primary consumers as the stable isotope baseline or applying a 90-day lag between baseline

and consumer sampling can improve accuracy of trophic position estimation for tertiary consumers or higher, although it does not eliminate it. Thus, stable isotope heterogeneity and its potential effects on trophic position estimates should be considered when interpreting stable isotope values. Our results agree with the recommendations made by Possamai et al. (2021), when possible, trophic position studies should use CSIA for at least a subset of samples. Researchers applying stable isotope data to calculate consumer trophic position should carefully consider heterogeneity in baseline isotope values expected in their system, isotope turnover rates for their consumers of interest, and isotope turnover rates of the resources of their consumers of interest. We caution researchers against a one size fits all approach for improving trophic position estimation, and it may be beneficial to apply different approaches for different consumers in the same system.

5.6 Tables

Table 5.1: Summary of observational nitrogen stable isotope baseline data used for modelling case studies.

Table 5.1: Baseline environments

Study	Taxa	Season of Data	Range of Isotopic Change	Ecosystem	Location
1. Wu et al. 1999	POM	January - December 1989	4.11	Marine upwelling zone	Coast of Vancouver Island, Canada
2. Gu et al. 1994	POM	January - December 1989	4.20	Eutrophic, subartic lake	Smith Lake, Fairbanks, Alaska, USA
3. Syvaranta et al. 2008	POM	May - September 2004	5.68	Moderately eutrophic, urban lake	Jyväsjärvi Lake, Jyväskylä, Finland
4. Matthews and Mazumder 2007	POM	February 2002 - April 2003	10.40	Pristine oligotrophic lake	Council Lake, Vancouver Island, Canada,

Table 5.2: Duration of trophic position deviation (number of days the magnitude of trophic position estimation error is greater than ± 0.5 trophic levels from (\hat{tp}) for each of the six, bulk stable isotope food web scenarios (Figure 5.1).

Table 5.2: Trophic Position Duration of Deviation

Trophic Position	Scenario 1	Scenario 2	Scenario 3	Scenario 4	Scenario 5	Scenario 6
Primary Consumer	0 (0.0)	0 (0.35)	0 (0.0)	0 (0.0)	9 (0.0)	34 (0.10)
Secondary Consumer	55 (0.15)	89 (0.24)	94 (0.26)	35 (0.10)	43 (0.18)	44 (0.13)
Tertiary Consumer	106 (0.29)	114 (0.31)	101 (0.28)	115 (0.31)	44 (0.70)	43 (0.12)

Table 5.3: Duration of trophic position deviation (number of days the magnitude of trophic position estimation error is greater than ± 0.5 trophic levels from (\hat{tp}) for each of the two CSIA food web scenarios (Figure 5.2).

Table 5.3: Duration of Trophic Position Deviation (days)

Amino Acid	Baseline 1 (365)	Baseline 2 (365)	Baseline 3 (233)	Baseline 4 (351)	NA
Glutamic Acid	Shrimp (primary consumer)	0	0	0	0
Alanine	Shrimp (primary consumer)	0	0	0	0
Proline	Shrimp (primary consumer)	0	0	0	0
Valine	Shrimp (primary consumer)	0	0	0	0
Glutamic Acid	Tuna (secondary consumer)	0	0	0	0
Alanine	Tuna (secondary consumer)	0	0	0	0
Proline	Tuna (secondary consumer)	0	0	0	0
Valine	Tuna (secondary consumer)	0	0	0	0

Table 5.4: Range of trophic position estimates applying a 90-day lag between baseline sampling and consumer sampling for calculations A) trophic position estimates using POM as the stable isotope baseline and B) trophic position estimates using the primary consumer as the stable isotope baseline

Table 5.4: Range of Trophic position estimates with different baselines

Scenario	Baseline	Primary	Secondary	Tertiary
		Consumer (tp = 2)	Consumer (tp = 3)	Consumer (tp = 4)
2	A. POM	1.4 – 2.4	2.8 – 3.2	3.9 – 4.4
3	A. POM	0.8 – 2.9	2.2 – 3.6	3.2 – 4.6
4	A. POM	0.8 – 2.9	2.1 – 3.9	3.4 – 4.7
5	A. POM	2 – 3.1	3.0 – 3.8	3.9 – 4.4
6	A. POM	1.9 – 4.0	2.9 – 3.9	3.9 – 4.2
1	B. Primary Consumer	–	2.5 – 3.4	3.7 – 4.3
2	B. Primary Consumer	–	2.7 – 3.3	3.8 – 4.2
3	B. Primary Consumer	–	2.5 – 3.4	3.5 – 4.3
4	B. Primary Consumer	–	2.4 – 3.6	3.7 – 4.5
5	B. Primary Consumer	–	3.1 – 4.1	4.0 – 4.7
6	B. Primary Consumer	–	2.9 – 4.0	3.9 – 4.3

5.7 Figures

Figure 5.1: Six theoretical food web scenarios for BSIA model constructed from consumer experimental stable isotope half-life ($t_{0.5}$) studies and observed nitrogen stable isotopes values of particulate organic matter (baselines 1-4; Table 5.2) from four distinct aquatic systems. Three comparisons were made between two food web scenarios: 1) different $t_{0.5}$ of the secondary consumer 2) different $t_{0.5}$ of the secondary and tertiary consumer 3) different baseline from particulate organic matter.

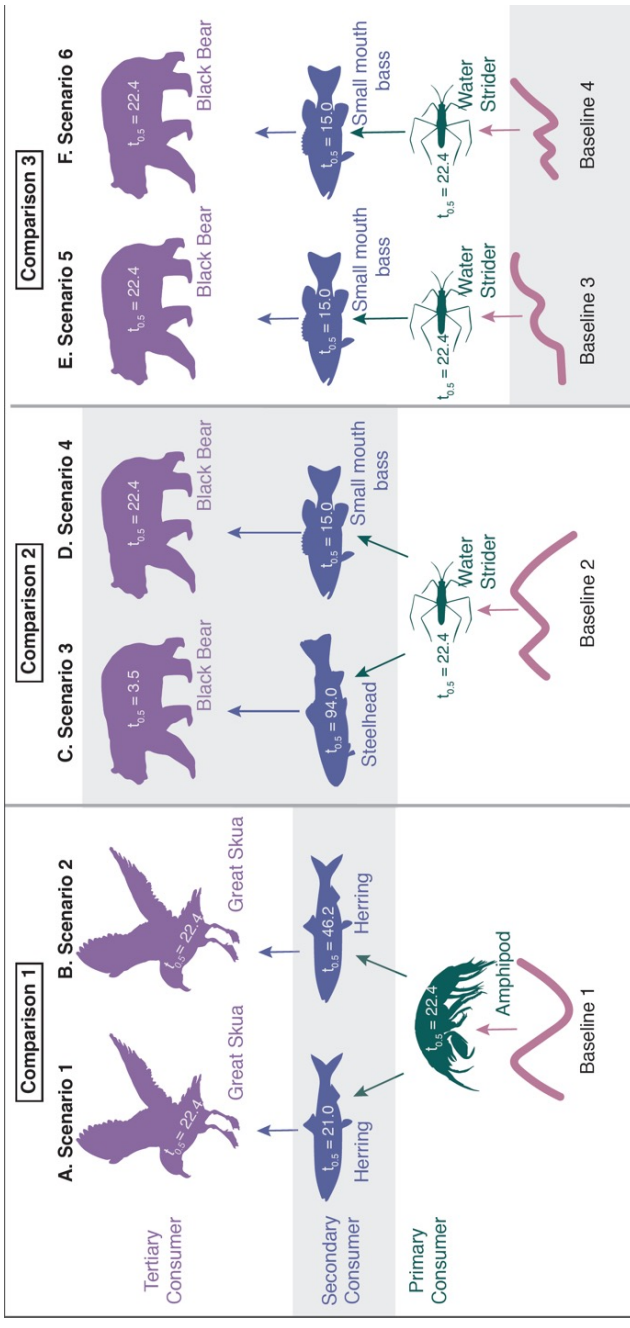


Figure 5.1: BSIA theoretical food web scenarios

Figure 5.2: A theoretical food web for CSIA model constructed from consumer experimental stable isotope half-life ($t_{0.5}$) studies and applied to observed nitrogen stable isotopes values of particulate organic matter from all four distinct aquatic systems (baselines 1- 4, Table 5.2).

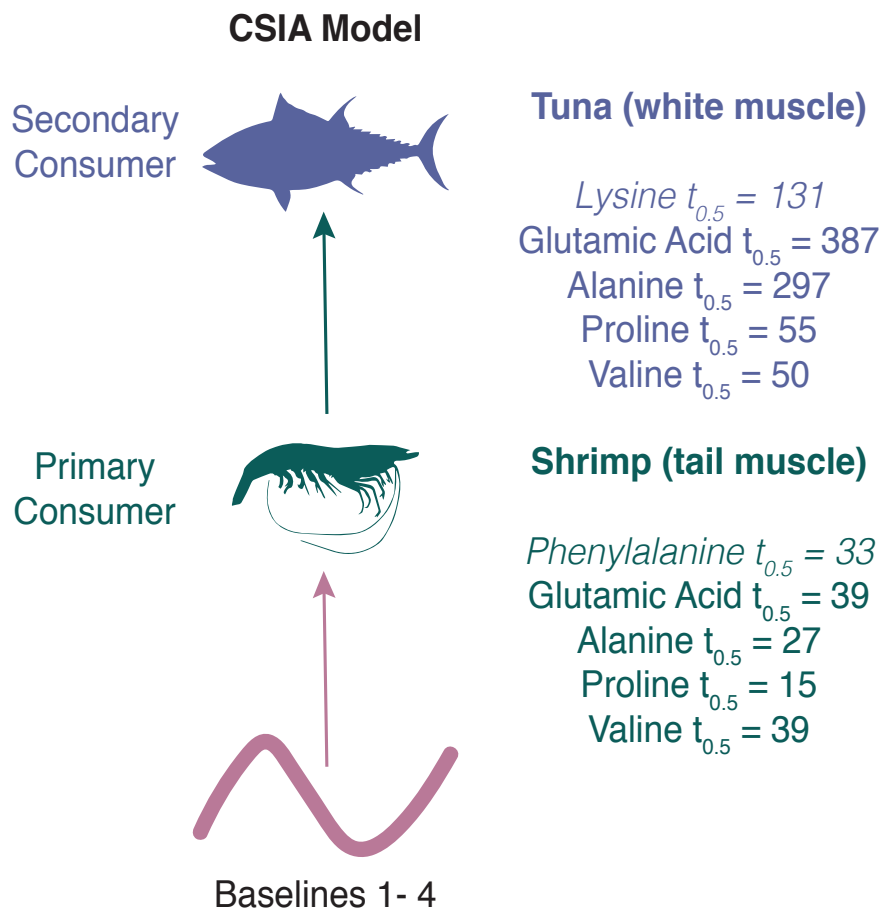


Figure 5.2: CSIA theoretical food web scenarios

Figure 5.3: Depiction of the two effect sizes used to assess accuracy of trophic position estimation in this study 1) the magnitude of trophic position estimation error which describes the degree to which trophic position is over or under estimated and 2) the duration of deviation which describes the length of time over the course of the model simulation that trophic position was erroneously estimated by ± 0.5 trophic levels.

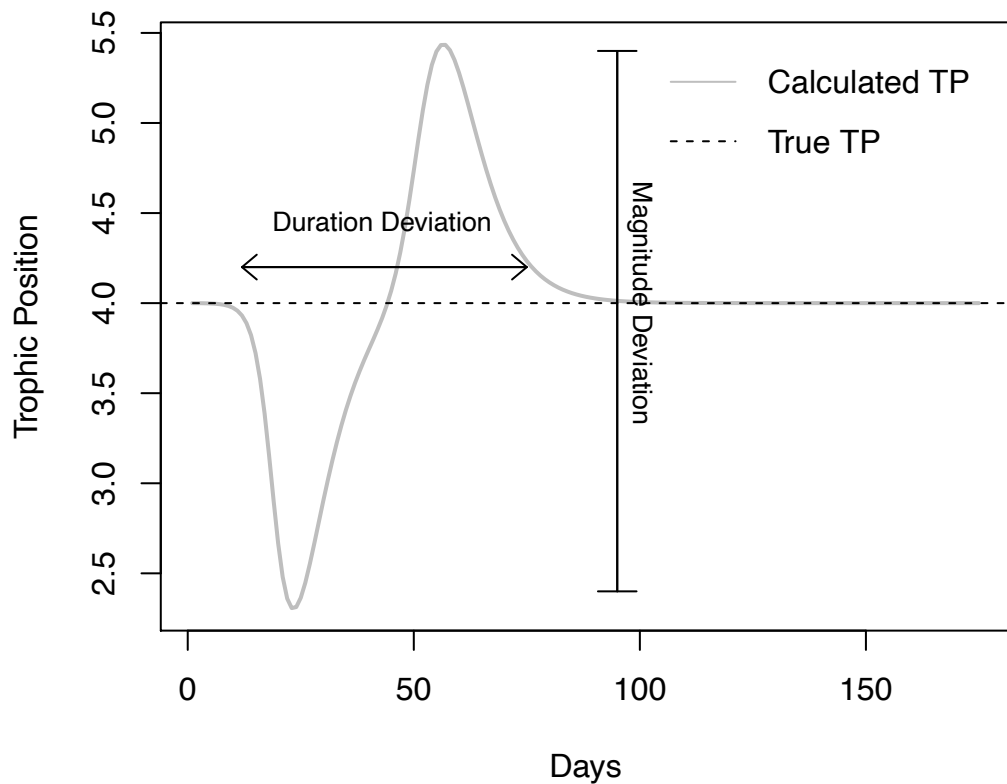


Figure 5.3: Trophic position estimation error effect sizes

Figure 5.4: Simulated primary, secondary, and tertiary consumer bulk nitrogen stable isotope values ($\delta^{15}\text{N}$) for six (A-F) food web scenarios (Figure 5.1) using $\delta^{15}\text{N}$ of particulate organic matter from observational studies as the stable isotope baseline (Table 5.1).

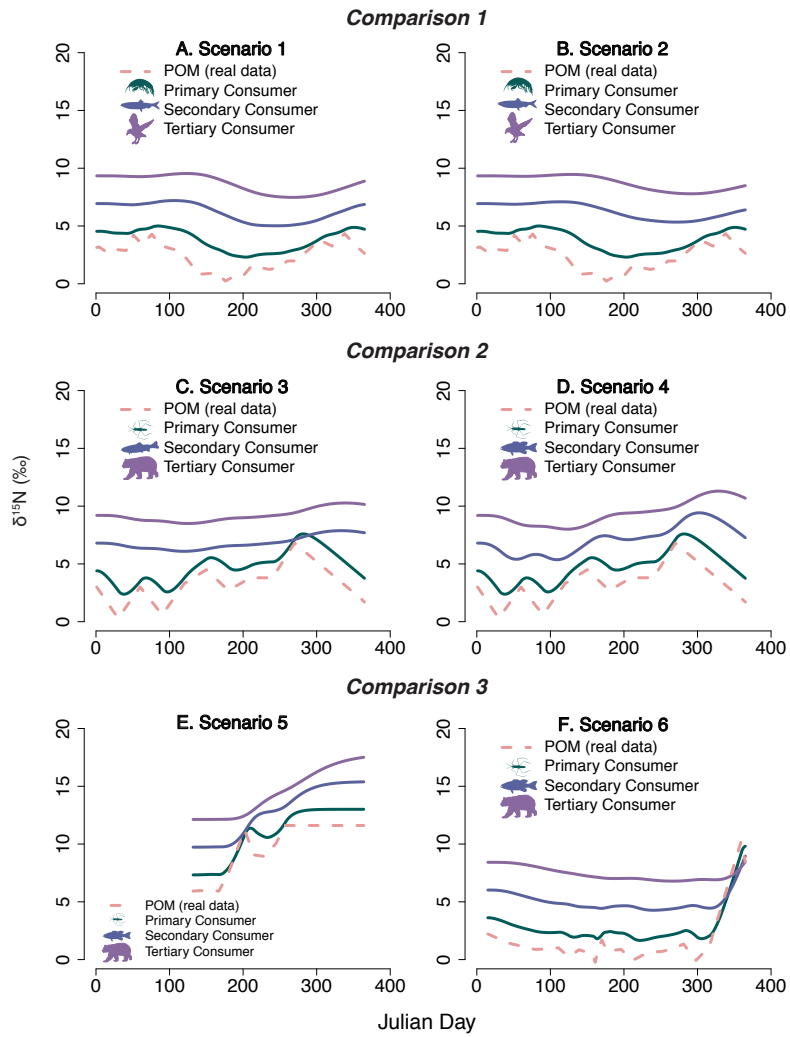


Figure 5.4: BSIA simulted $\delta^{15}\text{N}$

Figure 5.5: Trophic position estimation error based on simulated primary, secondary, and tertiary consumer bulk nitrogen stable isotope values ($\delta^{15}\text{N}$) for six (A-F) food web scenarios (Figure 5.1) and three main comparisons using POM stable isotope values to calculate trophic position. 0 denotes the true trophic level of a given consumer and grey box denotes trophic position deviation of ± 0.5 trophic levels and used to calculate duration of deviation.

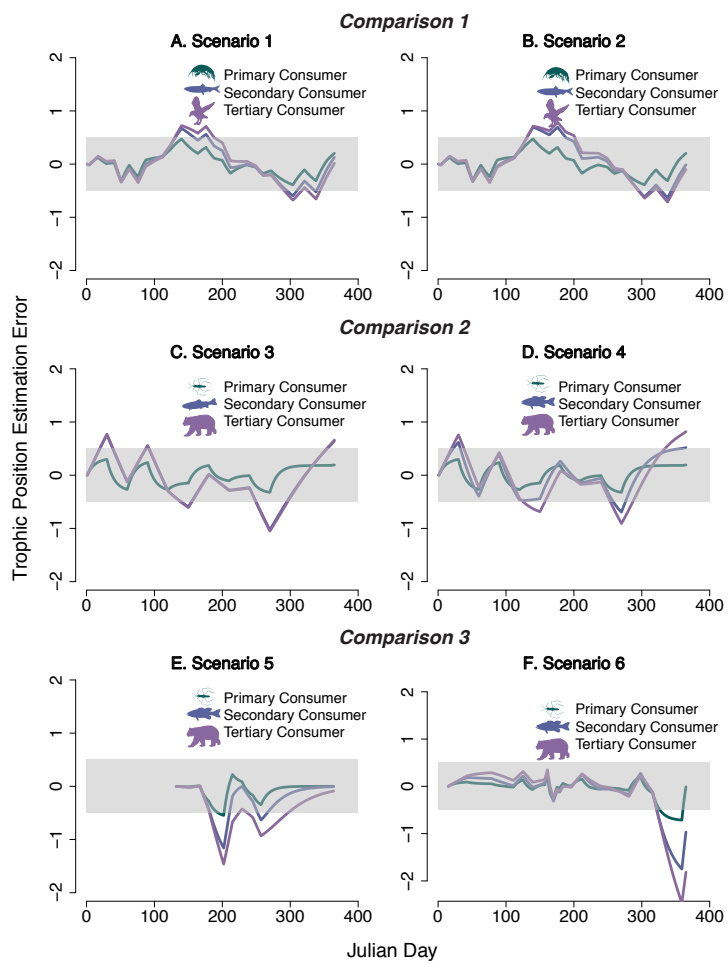


Figure 5.5: BSIA simulated trophic position

Figure 5.6: Simulated amino acid (color) nitrogen CSIA values ($\delta^{15}N$) for primary (A, C, E, G) and secondary (B, D, F, H) consumers using four stable isotope baselines derived from observational particulate organic matter studies (Table 5.1, Figure 5.2).

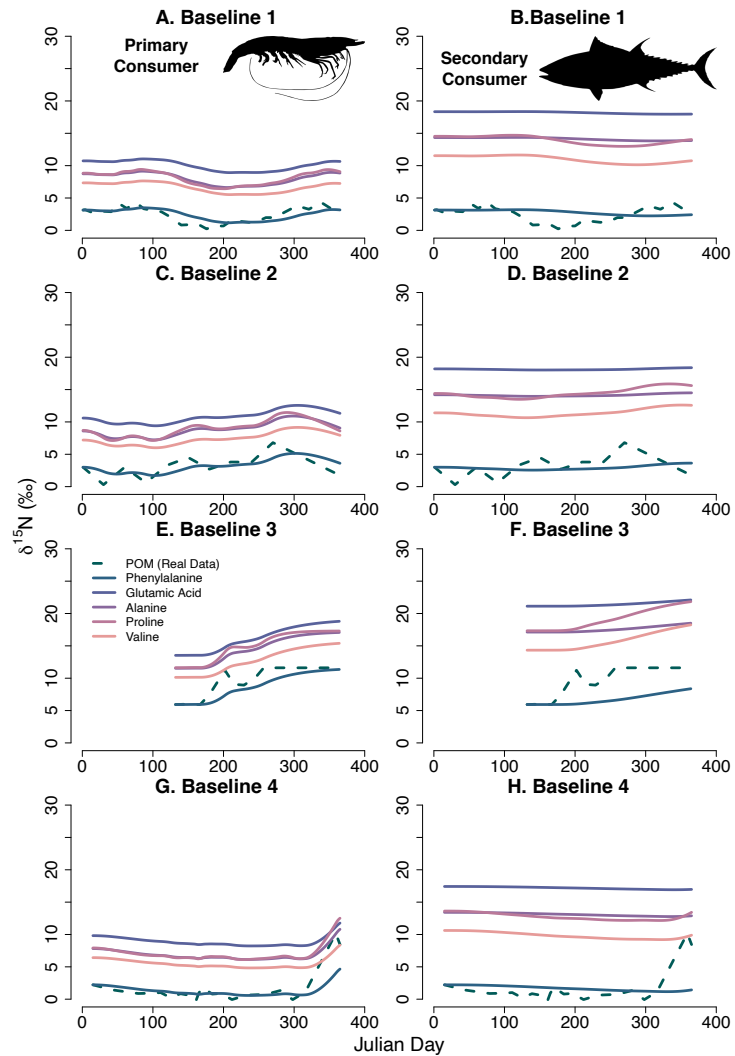


Figure 5.6: CSIA simulated $\delta^{15}N$

Figure 5.7: Trophic position estimation error from simulated amino acid (color) nitrogen CSIA values ($\delta^{15}N$) for primary (A, C, E, G) and secondary (B, D, F, H) consumers using four stable isotope baselines derived from observational particulate organic matter studies (Table 1, Figure 5.2). 0 denotes the true trophic level of a given consumer and grey box denotes trophic position deviation of ± 0.5 trophic levels and used to calculate duration of deviation.

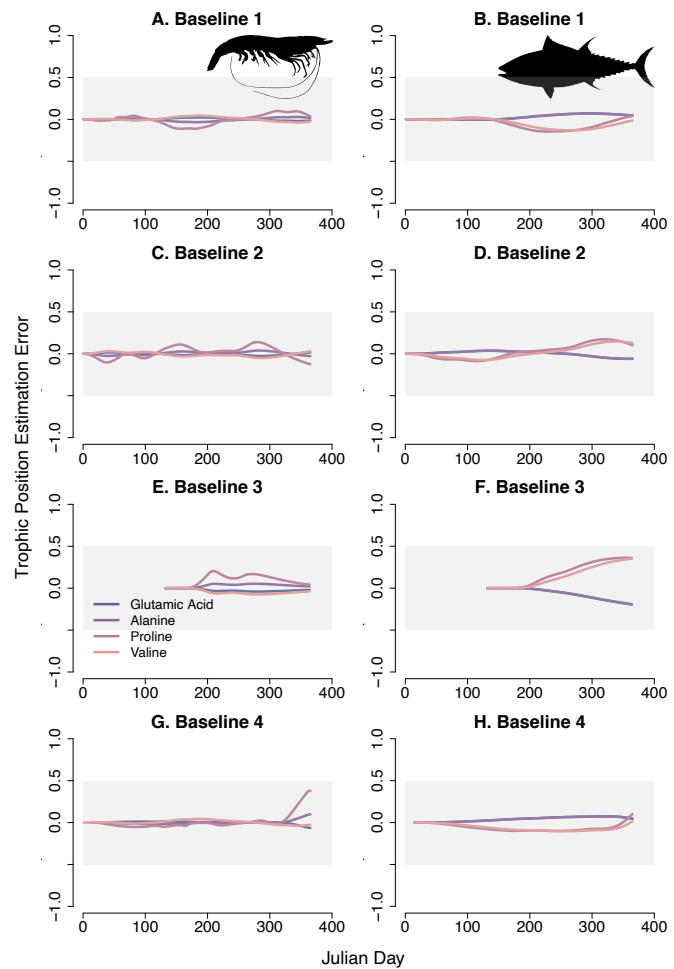


Figure 5.7: CSIA simulated trophic position

Figure 5.8: Sensitivity analysis of the magnitude of trophic position estimation error from bulk stable isotope values in response to primary, secondary, and tertiary (color) consumer stable isotope half-life values for a single simulated stable isotope baseline (a). Solid line denotes mean magnitude of estimation error across the 125-day baseline simulation (A) for a given half-life and shaded region denotes 1 standard deviation from the mean. 0, in B-D, represents the true trophic level of a consumer.

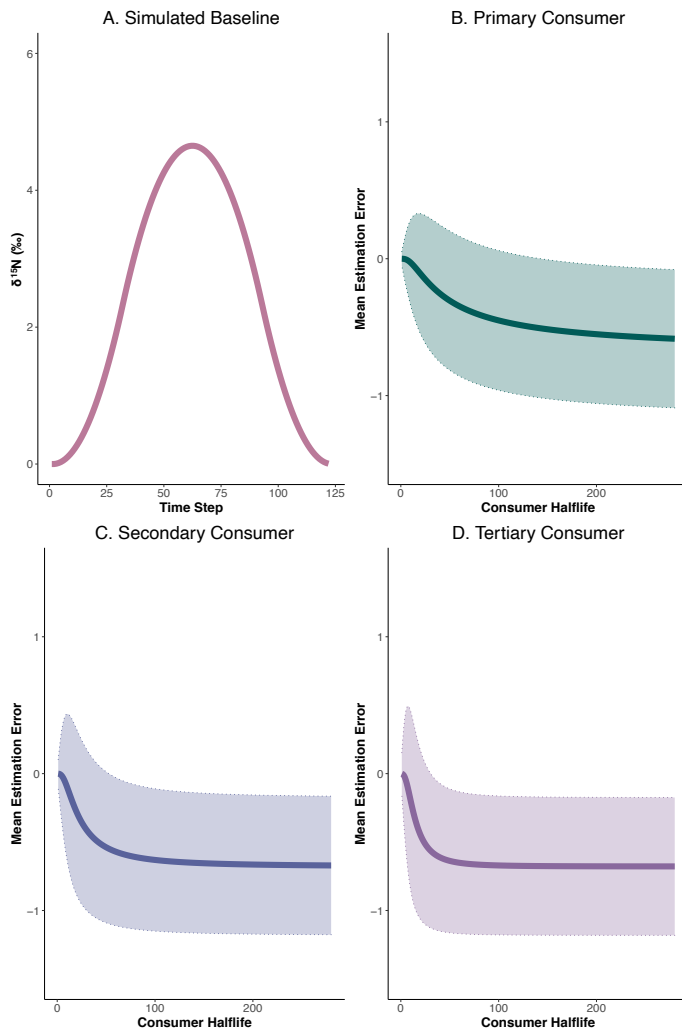


Figure 5.8: BSIA tissue turnover sensitivity analysis

Figure 5.9: Sensitivity analysis of the magnitude of trophic position estimation error from CSIA for primary, secondary, and tertiary (color) consumer stable isotope half-life values for a single simulated stable isotope baseline (a). The source amino acid line denotes the single half-life value (130 days, lysine tuna) of the source amino acid modelled in this analysis. Solid line denotes mean magnitude of estimation error across the 125-day baseline simulation (A) for a given half-life and shaded region denotes 1 standard deviation from the mean. 0, in B-D, represents the true trophic level of a consumer.

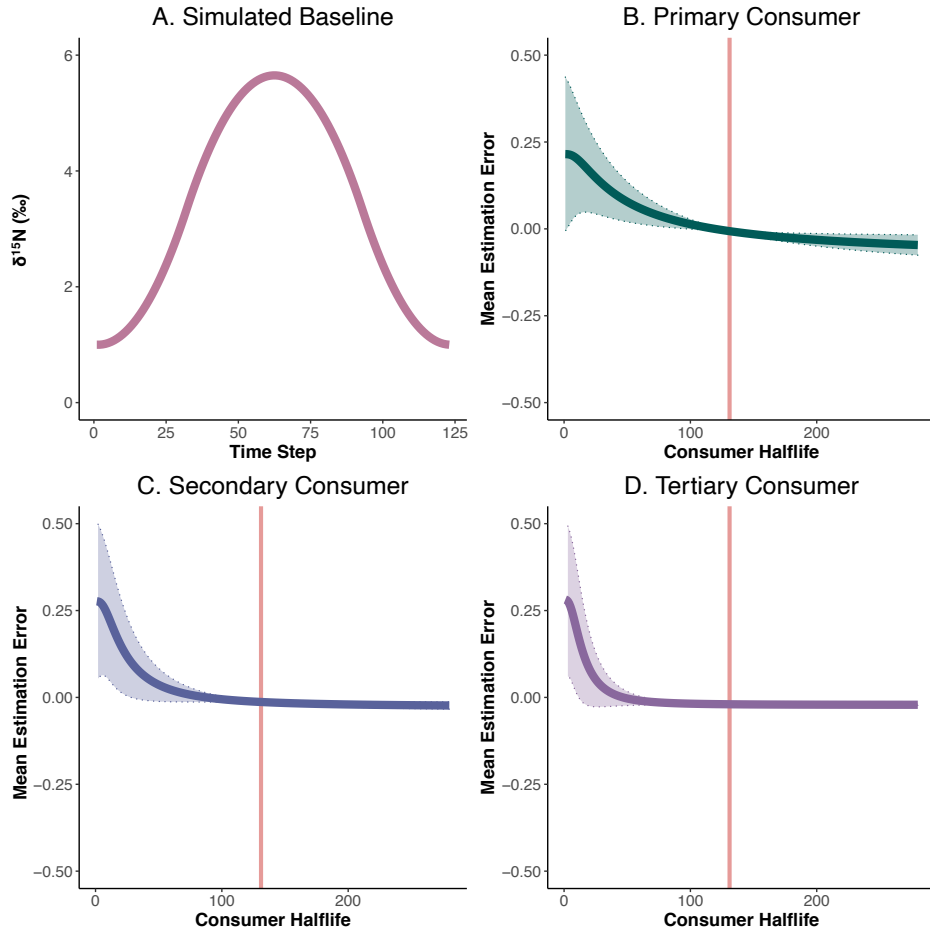


Figure 5.9: CSIA tissue turnover sensitivity analysis: lysine

Figure 5.10: Sensitivity analysis of the magnitude of trophic position estimation error from CSIA for primary, secondary, and tertiary (color) consumer stable isotope half-life values for a single simulated stable isotope baseline (a). The source amino acid line denotes the single half-life value (33 days, phenylalanine in shrimp) of the source amino acid modelled in this analysis. Solid line denotes mean magnitude of estimation error across the 125-day baseline simulation (A) for a given half-life and shaded region denotes 1 standard deviation from the mean. 0, in B-D, represents the true trophic level of a consumer.

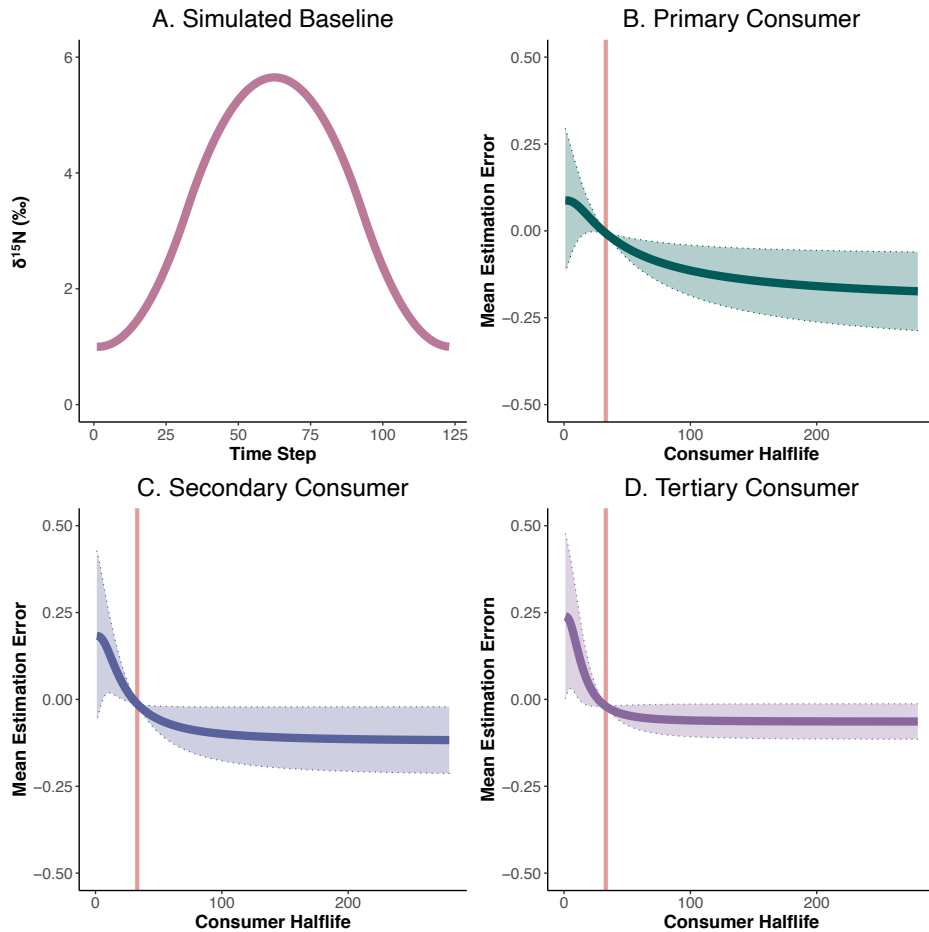


Figure 5.10: CSIA tissue turnover sensitivity analysis: phenylalanine

Figure 5.11: Nitrogen stable isotope half-life values (days) experimentally derived for a) bulk stable isotope analysis (M. J. Vander Zanden et al., 2015) for different species (label) and tissues (color) and b) CSIA half-life values of individual amino acids (Downs et al. and Popp et al.) for different species (color) and amino acids (label).

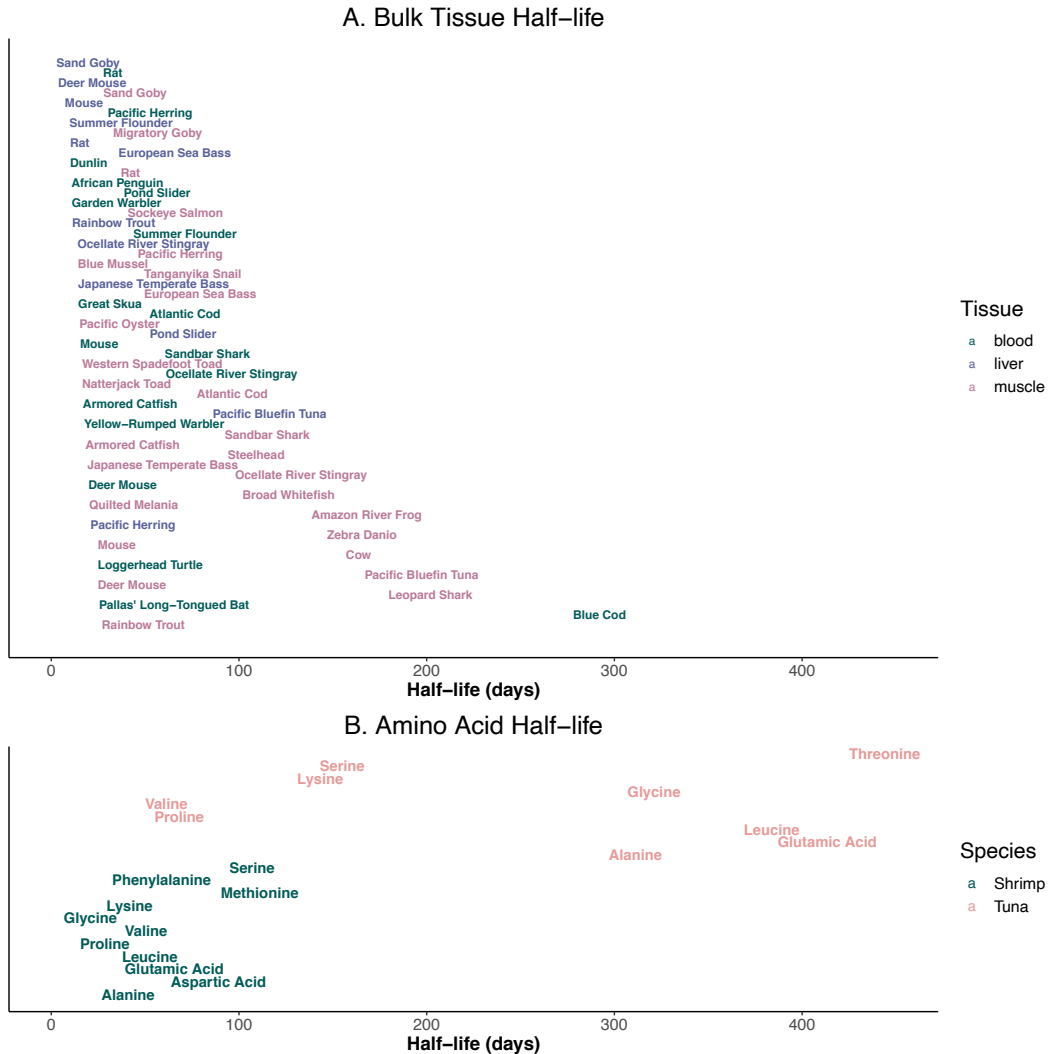


Figure 5.11: Observed tissue half-life values

Figure 5.12: Trophic position estimation error based on simulated primary, secondary, and tertiary consumer bulk nitrogen stable isotope values ($\delta^{15}\text{N}$) for six (A-F) food web scenarios (Figure 5.1) using the primary consumer stable isotope values to calculate trophic position. 0 denotes the true trophic level of a given consumer and grey box denotes trophic position deviation of ± 0.5 trophic levels used to calculate duration of deviation.

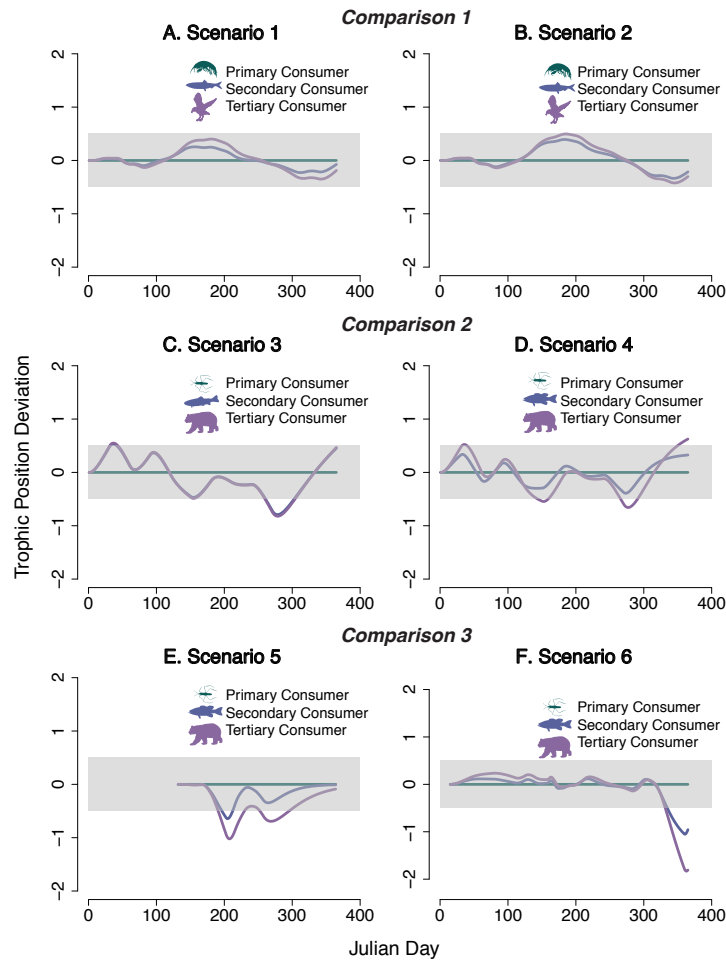


Figure 5.12: BSIA simulated trophic position: primary consumer baseline

CONCLUSION

This dissertation identified novel applications CSIA. In many studies, the physiological challenges of measuring stable isotope data (i.e., tissue turnover time) are often framed as a hindrance for data interpretation. In this dissertation I demonstrated that incorporating the physiological and biogeochemical conditions that influence stable isotope chemistry in consumers into study design can elucidate more information for a system of interest. For example, applying temporal lags based on tissue turnover times can identify delayed food web responses to ecological change. This research provides a detailed framework for incorporating stable isotope fractionation, tissue turnover time, beta values, and resource use into the study design and interpretation of CSIA data. Without consideration for each of these components of stable isotope chemistry, there will be errors in trophic position estimation and mixing model results that will hinder data interpretation and potentially result in misleading conclusions.

Without accurate representation of the nitrogen fractionation that occurs when organic nitrogen is transformed to inorganic sources (mineralization, nitrification) contributions of salmon as a nutrient source to vegetation will be overestimated and is likely overestimated in previous marine derived nitrogen studies. The application of stable isotope mixing models requires accurate stable isotope end members to estimate dietary sources to consumers. When mixing models are applied to vegetation, consideration for the direct sources of nitrogen that plants “consume” are necessary (i.e., ammonium, nitrate, amino acids). My finding that soil ammonium is substantially enriched in ^{15}N compared to salmon tissue demonstrates salmon should not be used as an end member in mixing models applied to plants because it does not consider fractionation that occurs in soils. Understanding the contributions of salmon to the riparian environment also requires careful selection of a study site that has

salmon present and a second control site without salmon. Control sites usually consider the composition of tree and vegetation community, but do not typically consider soil composition. I observed substantial site variability with distance from the same stream for sites previously used as controls. Slope, aspect, gravimetric water content, and soil type are just a few conditions that can alter nutrient content, fractionation in soil, and tree growth, and if not accounted for can lead to misinterpretations of marine derived nutrient studies. Conclusions from studies that do not confirm soil conditions are comparable between ‘salmon’ and ‘control’ sites should be interpreted with caution. Finally, marine derived nutrient studies should focus on measuring ecological responses to salmon presence rather than measuring the presence of marine derived nutrients from stable isotopes and assuming the presence of enriched nitrogen equates to increased nitrogen availability that will elicit an ecological response. My results found differences in marine derived nutrients with salmon presence but not increases in long-term nitrogen availability or transformation rates. Studies should focus on the ecological response (i.e., increased nitrogen transformation rates, increased tree growth) between ‘salmon’ and ‘control’ sites and apply stable isotopes to support the interpretation that ecological responses are due to salmon contributions.

I demonstrated source amino acids provide novel information about how nitrogen moves through and is utilized by food webs, particularly for retrospective analyses. Studies focused on understanding nitrogen resources directly measure phytoplankton blooms or nitrogen concentrations and datasets are only available for small areas and short periods of time. This presents a challenge of scale, both spatially and temporally, when trying to understand how these measurements contribute to mobile, large bodied, slow growing, marine consumers that integrate resources from over broader spatial ranges and longer time scales. The unique qualities of source amino acids that make them useful as an indicator of stable isotope baseline for consumers, also means they can serve as an important tracer on their own. Notably, source amino acids are still susceptible to the challenges in interpreting stable isotope values of nitrogen that occur from fractionation from nitrogen transformations, phytoplankton

assimilation, and trophic enrichment. Therefore, the most interpretable and useful applications of source amino acid studies will trace long-term contributions of nitrogen sources with distinct stable isotope values. Sea ice derived algae is one example of a nitrogen sources that is enriched in ^{15}N and measurable in consumer tissues based on our results. Measuring the nitrogen stable isotope values of source amino acids from historic and contemporary samples from environments where sea ice derived algae has been known to change due sea ice decline and oceanic warming such as Baffin Bay, could inform how food webs adapt their resource use in a changing world.

Measuring trophic position in consumers such as harbor seals is useful for understanding general ecosystem change but identifying the specific mechanism that caused the trophic position change requires additional information. Some climate drivers were strong predictors of both source amino acid stable isotope values and trophic position estimates, but others were only good predictors of trophic position estimates. This is particularly relevant when trying to identify mechanisms of climate forcing on the food web. One approach for identifying whether the mechanisms of climate forcing is constraining nutrients at the base of the food web or is acting on recruitment and growth higher in the food web, is to combine analyses of both trophic position and source amino acids. For example, freshwater discharge impacts harbor seal trophic position and source amino acid stable isotope values. Therefore, climate variables are directly influencing nitrogen at the base of the food web which then is propagating through the food web and altering harbor seal trophic level. In contrast, sea surface temperature only impacted harbor seal trophic position, meaning it was altering abundance of mid trophic level species (likely forage fish) and that was the mechanism that was ultimately causing a trophic shift. Applying CSIA to mid trophic level species in addition to a top predator would provide a more complete picture of causal mechanisms of trophic level change of top predators. Specifically, it could identify if the trophic level change was occurring in the top predator (if the lower trophic level species did not also have a shift) or if it was occurring lower in the food web (if both species experienced a trophic level change).

Trophic position change can be difficult to interpret, particularly for high trophic level, generalist predators like harbor seals. Trophic position can change due to a dietary shift by the consumer of interest, a shift lower in the food web, or a shift in protein quality of prey. These mechanisms are more easily resolved when applying CSIA to specialist species compared to a generalist. One potential application would be the southern resident killer whale (SRKW) in Washington, that consumes exclusively salmon. Applying CSIA to SRKW would eliminate the potential of protein quality influencing data interpretation (due to the exclusively piscivorous diet) therefore a trophic level change in SRKW would indicate consumption of smaller salmon. This could be the result of eating a greater number of smaller species such as pink salmon, or smaller individuals of Chinook salmon. While the exact mechanism would still not be identified from CSIA data alone, it would identify a change in the SRKW – salmon relationship and if combined with pacific Salmon abundance and size data which are collected annually, it would offer a more complete picture of the dynamics of this relationship through time than abundance data alone.

Ecological integrity indicators have been incorporated into the California Current Integrated Ecosystem Assessment and include indicators of trophic structure such as mean groundfish trophic level. Harbor seal trophic position could be a useful addition to these datasets. This dissertation provides a historic baseline which contemporary data can be compared to. In addition, contemporary mean groundfish trophic level is collected annually. Combined, these two datasets are a powerful tool for measuring ecological integrity. The addition of harbor seal data would determine whether changes in ecological integrity span the entire food web and identify whether observed changes are confined to certain parts of the food web. For example, if changes were observed in harbor seals but not groundfish that would indicate predators were modifying their foraging strategies. If a change was observed in both groundfish and harbor seals, then it would indicate a bottom-up effect propagating through the entire food web. Collection of harbor seal trophic position data for indicators would ideally occur annually, but data that is pooled over 1-5 years should be sufficient

for identifying widespread ecological change, as this dissertation shows harbor seal trophic position response to food web and climate conditions are often delayed by multiple years. A continuous sampling strategy may be able to be incorporated into marine mammal stranding networks. Pooling data on decadal scales may be more feasible, but it comes with the risk of overlooking potential food web responses based on how the decadal breakpoints correspond temporally relative to the ecological change. Alternatively, samples could be collected in the two years following major climate perturbations. Given the lagged response due to both tissue turnover and propagation of ecological conditions up the food web, and the increase in extreme climate events over the past two decades, it would be possible to retroactively analyze the effects of extreme climate conditions on the food web by measuring predator tissues in the 1-3 years following the event.

Compound-specific stable isotope analysis can provide novel information regarding ecological and biogeochemical responses to climate change. An important component to the application and interpretation of this type of data is the physiological and biogeochemical parameters that influence stable isotope fractionation. With my dissertation as a foundation future work can better constrain assumptions of stable isotope parameters to reconstruct historic datasets and apply CSIA data to understand delayed food web responses and resource assimilation into food webs.

Appendix A

APPENDIX 1

A.1 *Text 1: Full analytical details for stable isotopes*

Collagen samples have been analyzed for both CSSIA and bulk $\delta^{15}N$ which require 10 mg of purified collagen (100 mg of bone). Preliminary analyses were conducted to determine the highest rate of collagen return from bone sampled from different parts of the skull to minimize destruction. Samples were taken from the internal occipital shelf to maintain external integrity. Bone was decalcified using 0.2 M HCl for 24-72 hours depending on bone thickness, followed by centrifugation and nanopure water rinse. Removal of humic acids was conducted using 0.125 M NaOH for 20 hours. Samples were washed to a neutral pH, then solubilized in 0.01N HCl. Once solubilized samples were blown down under N2 to prevent isotopic fractionation, and freeze dried. Freeze dried collagen was be analyzed for bulk isotopic composition of nitrogen by the UW IsoLab (isolab.ess.washington.edu) using a coupled elemental analyzer-isotope ratio mass spectrometer following the standard protocols of the laboratory. C:N ratios were calculated from this data, which is a measure of the quality for carbon and nitrogen analyses of bone collagen for isotopic analysis. Only three observations were outside of the acceptable rang of 2.7-3.6; indicating there was no substantial loss of glycine or addition of nitrogen due to microbial processing from mortality, decay, curation, and analysis.

$\delta^{15}N$ of eleven amino acids were measured in the UW Facility for Compound-Specific Isotope Analysis of Environmental Samples. Samples were prepared following the procedures developed by Popp Marine Lab at University of Hawaii Manoa. Briefly, proteins were hydrolyzed in 6N HCl and purified using a cation exchange column. Amino acids were esterified using

isopropanol acetyl chloride, and derivatized via acylation with 4:1 toluene: pivaloyl chloride. Samples were brought up in ethyl acetate and analyzed using a coupled gas chromatography-combustion-isotope ratio mass spectrometer system (GC-C-irMA; Thermo Scientific Trace GC + GC IsoLink coupled to a Delta V irMS) in continuous flow mode monitoring masses (m/z) 28 and 29 using a db-35 column. For each run a 12 amino acid external standard with known isotopic composition was injected three times followed by sample injections. Samples were injected in triplicate, with the 12 amino acid standard injected every two samples (or six injections). A two-hour column oxidation was performed after 6 samples (25 injections). Samples and standards included norleucine as an internal standard.

For each machine run, a linear model was fit for each individual amino acid using the following equation:

$$Std_{aa} = m_{aa}t + b_{aa} \quad (\text{A.1})$$

Where m represents the slope of the precision drift, t represents the injection number since last column oxidation, and Std represents the $\delta^{15}\text{N}$ of an individual amino acid for a standard observation. The data was then corrected using the following equations:

$$D_{aa,t} = Std_{aa,t} - True \quad (\text{A.2})$$

Where $D_{aa,t}$ is the difference between an observed standard $\delta^{15}\text{N}$ of $Std_{aa,t}$ for a given amino acid at a given injection number and the true $\delta^{15}\text{N}$ for that standard. Then:

$$Sample_{corrected,aa,t} = Sample_{obs,aa,t} - D_{aa,t} \quad (\text{A.3})$$

Where the drift value, $D_{aa,t}$, is subtracted from the sample value for a given amino acid and a given injection to correct the observed sample values for precision drift since last column oxidation. Mean sample corrected values for the triplicate injections were used for all amino acid $\delta^{15}\text{N}$.

A.2 Text 2: Identifying size and sex-based trends in harbor seal trophic position

Only a subset of the samples included month of collection, sex, and length metadata and therefore separate month, length, and sex specific analyses were fit to the data to test whether they should be considered as predictors for the ocean condition and prey availability data. Standard linear models with: 1) sex as a factor, 2) length as a continuous covariate and 3) month as a continuous covariate were fit to both Salish Sea and coastal WA for each individual trophic amino acid. These models were used to test whether trophic position varies with length and sex, whether these trends are consistent between amino acids, and whether one year was an appropriate approximation for tissue turnover of bone collagen. The standard linear models took the following structure:

$$y_i \sim N(\alpha_{j[i]} + \beta_{j[i]} \mathbf{x}_i, \sigma_y^2) \quad (\text{A.4})$$

where y represents harbor seal trophic position calculated from phenylalanine and a trophic amino acid i , \mathbf{X} is a matrix of bottom-up drivers for a given model, β is a vector of covariates (sex, length, month, location), and a is the intercept. There were no significant differences in trophic position between male and female harbor seals in either the Salish Sea (Figure 3.3A) or coastal Washington (Figure 3.3B); this relationship was consistent across amino acids. Similarly, trophic position did not change based on harbor seal length (Figure 3.4). Interestingly, the exception to this finding was trophic position calculated by proline, which showed a significant decline with size. Mean harbor seal trophic position calculated from proline for harbor seals ranging from 150 - 180 cm in standard was 0.6 lower than harbors seals that were less than 120 cm of standard length (Figure 3.4). Trophic position calculated from alanine, aspartic acid and valine also showed negative trends with size, although the trend was not statistically significant, while trophic position calculated from glutamic acid was positive but also not statistically significant. There was also no observed ‘seasonality’ in harbor seal trophic position (Figure 3.5) indicating 1-year physiological delay was a reasonable approximation for tissue turnover time of skull bone collagen.

Harbor seals in Washington do not have distinct trophic ecology based on adult size (Figure 3.3) or sex (Figure 3.4). Bjorkland et al. (2015) did not observe sex or size (weight) based differences in bulk $\delta^{15}N$ values in harbor seals in the San Juan Islands in the Salish Sea between 2007 and 2008. Our results agree with this finding and with similar studies of other Pacific pinniped species (Dehn et al., 2007; Drago, Cardona, Crespo, & Aguilar, 2009). While both male and female harbor seals have a similar trophic position, it is possible sex and size-based differences in foraging strategies within a similar trophic position exist (Bjorkland et al., 2015; K. Wilson et al., 2014). Additionally, this study focused on adult harbor seals and changes in trophic position between juveniles, sub adults and adults are possible as indicated by pinniped studies (Zhao, Castellini, Mau, & Trumble, 2004). Regardless, our results show long-term consistencies in the trophic niche exploited by both male and female harbor seals regardless of adult size in Washington.

A.3 Text 3: Identifying temporal trends in harbor seal trophic position

To understand any changes through time to harbor seal foraging ecology over the past 100 years that were not explained by the tested environmental and food web covariates (Tables 3.4 & 3.5), generalized additive models (GAMs) were fit the residuals for the best ocean condition-prey model with a smooth term by year and a k term of 5. These analyses (Figures 3.6 & 3.7) were compared to the raw time series of harbor seal trophic position data (Figure 3.2) to identify trends through time that are unexplained by the covariates included in this analysis.

Trends in harbor seal trophic position through time were different between the Salish Sea and coastal Washington (Figure 3.2). The time series of the glutamic acid trophic position in coastal Washington had a significant positive trend through time (Figure 3.2b) that increased from 1948-1968 and remained relatively constant following 1975. Trophic position calculated from alanine and proline showed similar trends, although the alanine trophic position trend was not statistically significant (Figure 3.2a). In contrast, harbor seal trophic position in

the Salish Sea calculated from glutamic acid, alanine, aspartic acid, and proline has been relatively stable over the past century, but the trophic position calculated from valine showed a significant decline since 1968.

There were no trends through time for the model residuals for any amino acid after accounting for environmental (Figure 3.6) and food web (Figure 3.7) conditions at all three time lags. This indicates that prey availability and ocean conditions account for most temporal variation observed in the trophic position time series (Figure 3.2). However, valine was a notable exception, which demonstrated a decreasing trend through time in model residuals for all of the models with the most support.

A.4 Text 4: Accounting for variability in trophic enrichment factors

Trophic enrichment factors are variable based on animal diet (omnivory, carnivory, herbivory), pathways of nitrogen excretion, and trophic level (McMahon et al., 2015; J. M. Nielsen et al., 2015) with omnivory, carnivory and higher trophic levels demonstrating the lowest trophic enrichment for most amino acids. Trophic enrichment has ultimately been attributed to diet quality (similarity in tissues between consumer and prey) and mode of nitrogen excretions, although the relative impacts of each is difficult to discern, especially considering most controlled feeding studies include low-trophic level ammonia excretion but not high trophic level species (i.e., adult hake or salmon). In coastal Washington, most trophic transfers are between high diet quality, piscivorous fish (ammonia excretion) with a high-quality transfer between fish and harbor seal (urea excretion). Studies using multiple trophic enrichment factors based on the food web structure and consumption type produce more accurate trophic position estimations especially for higher level consumers (Kelton & Matthew, 2016; McMahon et al., 2019, 2015).

We applied multiple trophic position calculation frameworks for harbor seals to determine the best approach (Table 3.1) by identifying the percentage of data that fell within an ecologically realistic trophic position range for harbor seals. We also applied these approaches to herring,

a known harbor seal prey species, with data from Germain et al. (2013). Based on known foraging patterns, we anticipate harbor seals have an average trophic position of 3.5 to 5 and herring will have an average trophic position of 2.5-2.9. Equation 2 from (Figure 3.11.2) produced the most accurate herring trophic position estimates for most amino acids, however valine produced an impossibly low estimate of trophic position. In contrast, equation 3 (Figure 3.11.3) produced the most accurate results for most amino acids compared to harbor seals, but these estimates were still unrealistically low for some amino acids (proline, valine), which is common for CSIA (Kelton & Matthew, 2016). Additionally, this is not the most ecologically accurate parameterization, as it assumes all trophic transfers are of high prey quality, where there must be at least one herbivorous-low quality trophic transfer in the food web from phytoplankton to zooplankton (parameterization of equation 4, Figure 3.11.4). It also assumes prey quality (carnivorous) and trophic level of the consumer is more important than nitrogen excretion pathway (urea versus ammonia) for some amino acids but not others. Seemingly, these assumptions impact trophic position estimates from individual trophic amino acids differently which will likely be an important consideration for future studies applying a multi-amino acid framework. It is possible that these reflect biases in conventional trophic position estimates (i.e., stomach content analysis) as proposed by McMahon et al. (2015) or there may be biases in controlled feeding studies. For example, growth rate of individuals in controlled feeding studies may not accurately reflect those in natural ecosystems which may lead to overestimates in trophic enrichment if they are higher in natural systems compared to controlled feeding experiments. This may be plausible in the Washington food web as consumption of juvenile fish is common at multiple trophic levels, and juveniles presumably have higher growth rates than adults.

Mean harbor seal trophic position estimates were similar across trophic amino acids however some were more variable than others. The standard deviation of trophic position was higher for proline (4.6 ± 0.7 , mean \pm 1SD), and valine (3.7 ± 0.8) and included more ecologically unrealistic values compared to glutamic acid (4.5 ± 0.4) and alanine (3.9 ± 0.4). Trophic

position calculated from aspartic acid (4.1 ± 1.0) had the highest standard deviation and also demonstrated a trend through time compared to other amino acid trophic position calculations (Figure 3.2).

Application of a multi-amino acid trophic position calculation 1) offered a more realistic parameterization of the trophic position equation, 2) improved model certainty and 3) produced similar covariate coefficients compared to a glutamic acid only parameterization. Examination of the distribution of trophic position calculations for each individual trophic amino acid shows variability in accuracy and variance for single trophic amino acid calculations (Figures 3.10 & 3.11). For example, aspartic acid had a much wider variance compared to other amino acids (Figures 3.10 & 3.11) and also produced different trends through time (Figure 3.2).

It is likely differences in tissue turnover time between individual amino acids and phenylalanine contribute to the variance of the trophic position estimates derived from individual trophic amino acids. Downs et al. (2014) found phenylalanine takes 780 hours to reach 50% turnover in shrimp. This is comparable to glutamic acid, alanine, and valine which take 940, 642, and 942 hours respectively which are substantially lower than aspartic acid which requires 1530 hours. The discrepancy between tissue turnover times between aspartic acid and phenylalanine is likely the cause of the broad distribution for aspartic acid derived trophic position compared to other trophic amino acids, as aspartic acid is incorporating the nitrogen isotope signature over a substantially larger time period relative to phenylalanine and thus may incorporate more prey switching and/or changes in the isotopic signature of primary producers.

Addition of alanine to the glutamic acid only model resulted in the largest difference in model certainty. A glutamic acid – alanine model supported the same best models for both the environmental and prey models at all time lags. The combined tissue turnover of glutamic acid and alanine of shrimp (791 hours) is very similar to that of phenylalanine (780 hours) ensuring both the trophic and source amino acids were incorporated over a similar time

scale (albeit the trophic amino acids were a wider time scale). Benefits of a multi-amino acid trophic position equation may not require four amino acids as previously suggested (J. M. Nielsen et al., 2015) but rather carefully selected trophic amino acids to ensure the trophic amino acids are incorporated over a similar time scale as the source amino acids. If tissue turnover times are unable to be approximated, utilizing four trophic amino acids or two source amino acids as suggested by J. M. Nielsen et al. (2015) would likely provide the same benefit as fewer, carefully selected amino acids based on tissue turnover times.

COLOPHON

This document is set in **EB Garamond**, **Source Code Pro** and **Lato**. The body text is set at 11pt with *lmr*.

It was written in R Markdown and *LATEX*, and rendered into PDF using **huskydown** and **bookdown**.

This document was typeset using the XeTeX typesetting system, and the **University of Washington Thesis class** class created by Jim Fox. Under the hood, the **University of Washington Thesis LaTeX template** is used to ensure that documents conform precisely to submission standards. Other elements of the document formatting source code have been taken from the **Latex**, **Knitr**, and **RMarkdown** templates for UC Berkeley's graduate thesis, and **Dissertate: a LaTeX dissertation template** to support the production and typesetting of a PhD dissertation at Harvard, Princeton, and NYU

The source files for this thesis, along with all the data files, have been organised into an R project, **Dissertation**, which is available at <https://github.com/mfeddern/Dissertation>. A hard copy of the dissertation can be found in the University of Washington library.

This version of the thesis was generated on 2021-12-01 12:41:02. The repository is currently at this commit:

The computational environment that was used to generate this version is as follows:

```
- Session info -----
  setting  value
  version  R version 4.0.2 (2020-06-22)
  os       macOS Catalina 10.15.6
```

```

system x86_64, darwin17.0
ui      X11
language (EN)
collate en_US.UTF-8
ctype   en_US.UTF-8
tz      America/Los_Angeles
date   2021-12-01

```

- Packages -----

package	*	version	date	lib	source
assertthat	0.2.1	2019-03-21	[1]	CRAN	(R 4.0.0)
backports	1.1.6	2020-04-05	[1]	CRAN	(R 4.0.0)
bookdown	0.22.3	2021-05-22	[1]	Github	(rstudio/bookdown@aa75b5f)
callr	3.7.0	2021-04-20	[1]	CRAN	(R 4.0.2)
cli	2.5.0	2021-04-26	[1]	CRAN	(R 4.0.2)
colorspace	1.4-1	2019-03-18	[1]	CRAN	(R 4.0.0)
crayon	1.3.4	2017-09-16	[1]	CRAN	(R 4.0.0)
desc	1.2.0	2018-05-01	[1]	CRAN	(R 4.0.0)
devtools	* 2.3.1	2020-07-21	[1]	CRAN	(R 4.0.2)
digest	0.6.27	2020-10-24	[1]	CRAN	(R 4.0.2)
dplyr	1.0.2	2020-08-18	[1]	CRAN	(R 4.0.2)
ellipsis	0.3.0	2019-09-20	[1]	CRAN	(R 4.0.0)
evaluate	0.14	2019-05-28	[1]	CRAN	(R 4.0.0)
fs	1.5.0	2020-07-31	[1]	CRAN	(R 4.0.2)
generics	0.0.2	2018-11-29	[1]	CRAN	(R 4.0.0)
ggplot2	3.3.0	2020-03-05	[1]	CRAN	(R 4.0.0)
git2r	0.27.1	2020-05-03	[1]	CRAN	(R 4.0.2)
glue	1.4.2	2020-08-27	[1]	CRAN	(R 4.0.2)

gttable	0.3.0	2019-03-25	[1]	CRAN	(R 4.0.0)
htmltools	0.5.1.1	2021-01-22	[1]	CRAN	(R 4.0.2)
httr	1.4.2	2020-07-20	[1]	CRAN	(R 4.0.2)
huskydown	* 0.0.5	2021-05-16	[1]	Github	(benmarwick/huskydown@addb48e)
kableExtra	1.3.4	2021-02-20	[1]	CRAN	(R 4.0.2)
knitr	1.33	2021-04-24	[1]	CRAN	(R 4.0.2)
lifecycle	0.2.0	2020-03-06	[1]	CRAN	(R 4.0.0)
magrittr	2.0.1	2020-11-17	[1]	CRAN	(R 4.0.2)
memoise	1.1.0	2017-04-21	[1]	CRAN	(R 4.0.2)
msnse	0.5.0	2018-06-12	[1]	CRAN	(R 4.0.0)
pillar	1.4.3	2019-12-20	[1]	CRAN	(R 4.0.0)
pkgbuild	1.0.6	2019-10-09	[1]	CRAN	(R 4.0.0)
pkgconfig	2.0.3	2019-09-22	[1]	CRAN	(R 4.0.0)
pkgload	1.0.2	2018-10-29	[1]	CRAN	(R 4.0.0)
prettyunits	1.1.1	2020-01-24	[1]	CRAN	(R 4.0.0)
processx	3.5.2	2021-04-30	[1]	CRAN	(R 4.0.2)
ps	1.6.0	2021-02-28	[1]	CRAN	(R 4.0.2)
purrr	0.3.4	2020-04-17	[1]	CRAN	(R 4.0.0)
R6	2.4.1	2019-11-12	[1]	CRAN	(R 4.0.0)
remotes	2.2.0	2020-07-21	[1]	CRAN	(R 4.0.2)
rlang	0.4.11	2021-04-30	[1]	CRAN	(R 4.0.2)
rmarkdown	2.8	2021-05-07	[1]	CRAN	(R 4.0.2)
rprojroot	1.3-2	2018-01-03	[1]	CRAN	(R 4.0.0)
rstudioapi	0.11	2020-02-07	[1]	CRAN	(R 4.0.0)
rvest	0.3.6	2020-07-25	[1]	CRAN	(R 4.0.2)
scales	1.1.0	2019-11-18	[1]	CRAN	(R 4.0.0)
sessioninfo	1.1.1	2018-11-05	[1]	CRAN	(R 4.0.2)
stringi	1.6.2	2021-05-17	[1]	CRAN	(R 4.0.2)

```
stringr      1.4.0   2019-02-10 [1] CRAN (R 4.0.0)
svglite       2.0.0   2021-02-20 [1] CRAN (R 4.0.2)
systemfonts   1.0.2   2021-05-11 [1] CRAN (R 4.0.2)
testthat      3.0.2   2021-02-14 [1] CRAN (R 4.0.2)
tibble        3.0.1   2020-04-20 [1] CRAN (R 4.0.0)
tidyselect    1.1.0   2020-05-11 [1] CRAN (R 4.0.0)
usethis       * 1.6.1   2020-04-29 [1] CRAN (R 4.0.2)
vctrs         0.3.4   2020-08-29 [1] CRAN (R 4.0.2)
viridisLite   0.3.0   2018-02-01 [1] CRAN (R 4.0.0)
webshot       0.5.2   2019-11-22 [1] CRAN (R 4.0.0)
withr         2.4.2   2021-04-18 [1] CRAN (R 4.0.2)
xfun          0.23    2021-05-15 [1] CRAN (R 4.0.2)
xml2          1.3.2   2020-04-23 [1] CRAN (R 4.0.2)
yaml          2.2.1   2020-02-01 [1] CRAN (R 4.0.0)
```

```
[1] /Library/Frameworks/R.framework/Versions/4.0/Resources/library
```

REFERENCES

- Anderson, C., & Cabana, G. (2007). Estimating the trophic position of aquatic consumers in river food webs using stable nitrogen isotopes. *Journal of the North American Benthological Society*, 26(2), 273–285. Journal Article. [http://doi.org/10.1899/0887-3593\(2007\)26\[273:ETTPOA\]2.0.CO;2](http://doi.org/10.1899/0887-3593(2007)26[273:ETTPOA]2.0.CO;2)
- Atkinson, A. (1996). Subantarctic copepods in an oceanic, low chlorophyll environment: Ciliate predation, food selectivity and impact on prey populations. *Marine Ecology Progress Series (Halstenbek)*, 130(1/3), 85–96. Journal Article. <http://doi.org/10.3354/meps130085>
- Atkinson, S., Demaster, D. P., & Calkins, D. G. (2008). Anthropogenic causes of the western steller sea lion *eumetopias jubatus* population decline and their threat to recovery. *Mammal Review*, 38(1), 1–18. Journal Article. <http://doi.org/10.1111/j.1365-2907.2008.00128.x>
- Barbeaux, S. J., Holsman, K., & Zador, S. (2020). Marine heatwave stress test of ecosystem-based fisheries management in the gulf of alaska pacific cod fishery. *Frontiers in Marine Science*, 7. Journal Article. <http://doi.org/10.3389/fmars.2020.00703>
- Barth, J. A., Menge, B. A., Lubchenco, J., Chan, F., Bane, J. M., Kirincich, A. R., ... Washburn, L. (2007). Delayed upwelling alters nearshore coastal ocean ecosystems in the northern california current. *Proceedings of the National Academy of Sciences - PNAS*, 104(10), 3719–3724. Journal Article. <http://doi.org/10.1073/pnas.0700462104>
- Bartz, K. K., & Naiman, R. J. (2005). Effects of salmon-borne nutrients on riparian soils and vegetation in southwest alaska. *Ecosystems (New York)*, 8(5), 529–545. Journal Article.

- <http://doi.org/10.1007/s10021-005-0064-z>
- Benbow, M. E., Receveur, J. P., & Lamberti, G. A. (2020). Death and decomposition in aquatic ecosystems. *Frontiers in Ecology and Evolution*, 8. Journal Article. <http://doi.org/10.3389/fevo.2020.00017>
- Bi, R., & Sommer, U. (2020). Food quantity and quality interactions at phytoplankton–Zooplankton interface: Chemical and reproductive responses in a calanoid copepod. *Frontiers in Marine Science*, 7. Journal Article. <http://doi.org/10.3389/fmars.2020.00274>
- Bilby, R. E., Fransen, B. R., & Bisson, P. A. (1996). Incorporation of nitrogen and carbon from spawning coho salmon into the trophic system of small streams: Evidence from stable isotopes. *Canadian Journal of Fisheries and Aquatic Sciences*, 53(1), 164–173. Journal Article. <http://doi.org/10.1139/f95-159>
- Bilby, R. E., Fransen, B. R., Bisson, P. A., & Walter, J. K. (1998). Response of juvenile coho salmon (*oncorhynchus kisutch*) and steelhead (*oncorhynchus mykiss*) to the addition of salmon carcasses to two streams in southwestern washington, u.S.A. *Canadian Journal of Fisheries and Aquatic Sciences*, 55(8), 1909–1918. Journal Article. <http://doi.org/10.1139/cjfas-55-8-1909>
- Bjorkland, R. H., Pearson, S. F., Jeffries, S. J., Lance, M. M., Acevedo-Gutierrez, A., & Ward, E. J. (2015). Stable isotope mixing models elucidate sex and size effects on the diet of a generalist marine predator. *Marine Ecology. Progress Series (Halstenbek)*, 526, 213–225. Journal Article. <http://doi.org/10.3354/meps11230>
- Blanke, C. M., Chikaraishi, Y., Takizawa, Y., Steffan, S. A., Dharampal, P. S., & Vander Zanden, M. J. (2017). Comparing compound-specific and bulk stable nitrogen isotope trophic discrimination factors across multiple freshwater fish species and diets. *Canadian Journal of Fisheries and Aquatic Sciences*, 74(8), 1291–1297. Journal Article. <http://doi.org/10.1139/cjfas-74-8-1291>

- //doi.org/10.1139/cjfas-2016-0420
- Bocherens, H., & Drucker, D. (2003). Trophic level isotopic enrichment of carbon and nitrogen in bone collagen: Case studies from recent and ancient terrestrial ecosystems. *International Journal of Osteoarchaeology*, 13(1-2), 46–53. Journal Article. <http://doi.org/10.1002/oa.662>
- Boersma, M., Mathew, K. A., Niehoff, B., Schoo, K. L., Franco-Santos, R. M., & Meunier, C. L. (2016). Temperature driven changes in the diet preference of omnivorous copepods: No more meat when it's hot? *Ecology Letters*, 19(1), 45–53. Journal Article. <http://doi.org/10.1111/ele.12541>
- Bond, A. L., & Diamond, A. W. (2011). Recent bayesian stable-isotope mixing models are highly sensitive to variation in discrimination factors. *Ecological Applications*, 21(4), 1017–1023. Journal Article. <http://doi.org/10.1890/09-2409.1>
- Bond, N. A., Cronin, M. F., Freeland, H., & Mantua, N. (2015). Causes and impacts of the 2014 warm anomaly in the ne pacific. *Geophysical Research Letters*, 42(9), 3414–3420. Journal Article. <http://doi.org/10.1002/2015gl063306>
- Bopp, L., Resplandy, L., Orr, J. C., Doney, S. C., Dunne, J. P., Gehlen, M., ... Vichi, M. (2013). Multiple stressors of ocean ecosystems in the 21st century: Projections with cmip5 models. *Biogeosciences*, 10(10), 6225–6245. Journal Article. <http://doi.org/10.5194/bg-10-6225-2013>
- Bradley, C. J., Madigan, D. J., Block, B. A., & Popp, B. N. (2014). Amino acid isotope incorporation and enrichment factors in pacific bluefin tuna, thunnus orientalis. *PLoS One*, 9(1), e85818–e85818. Journal Article. <http://doi.org/10.1371/journal.pone.0085818>
- Brander, K. (2010). Impacts of climate change on fisheries. *Journal of Marine Systems*, 79(3), 389–402. Journal Article. <http://doi.org/10.1016/j.jmarsys.2008.12.015>

- Breitburg, D., Levin, L. A., Oschlies, A., Grégoire, M., Chavez, F. P., Conley, D. J., ... Zhang, J. (2018). Declining oxygen in the global ocean and coastal waters. *Science (American Association for the Advancement of Science)*, 359(6371), eaam7240. Journal Article. <http://doi.org/10.1126/science.aam7240>
- Brennan, S. R., Fernandez, D. P., Burns, J. M., Aswad, S., Schindler, D. E., & Cerling, T. E. (2019). Isotopes in teeth and a cryptic population of coastal freshwater seals. *Conservation Biology*, 33(6), 1415–1425. Journal Article. <http://doi.org/10.1111/cobi.13303>
- Burkanov, V. N., & Loughlin, T. R. (2005). Distribution and abundance of steller sea lions, *eumetopias jubatus*, on the asian coast, 1720's-2005. *Marine Fisheries Review*, 67(2), 1. Journal Article.
- Burkhardt, S., Riebesell, U., & Zondervan, I. (1999). Effects of growth rate, co2 concentration, and cell size on the stable carbon isotope fractionation in marine phytoplankton. *Geochimica et Cosmochimica Acta*, 63(22), 3729–3741. Journal Article. [http://doi.org/10.1016/S0016-7037\(99\)00217-3](http://doi.org/10.1016/S0016-7037(99)00217-3)
- Burnham, K. P., & Anderson, D. R. (2003). *Model selection and multimodel inference: A practical information-theoretic approach* (2. ed.). Book, New York, NY: New York, NY: Springer New York. <http://doi.org/10.1007/b97636>
- Cabana, G., & Rasmussen, J. B. (1996). Comparison of aquatic food chains using nitrogen isotopes. *Proceedings of the National Academy of Sciences - PNAS*, 93(20), 10844–10847. Journal Article. <http://doi.org/10.1073/pnas.93.20.10844>
- Carpenter, B., Gelman, A., Hoffman, M. D., Lee, D., Goodrich, B., Betancourt, M., ... Riddell, A. (2017). Stan: A probabilistic programming language. *Journal of Statistical Software*, 76(1), 1–32. Journal Article. <http://doi.org/10.18637/jss.v076.i01>
- Carpenter, S. R., Kitchell, J. F., & Hodgson, J. R. (1985). Cascading trophic interactions

- and lake productivity. *Bioscience*, 35(10), 634–639. Journal Article. <http://doi.org/10.2307/1309989>
- Castellani, C., Irigoien, X., Mayor, D. J., Harris, R. P., & Wilson, D. (2008). Feeding of calanus finmarchicus and oithona similis on the microplankton assemblage in the irminger sea, north atlantic. *Journal of Plankton Research*, 30(10), 1095–1116. Journal Article. <http://doi.org/10.1093/plankt/fbn074>
- Caut, S., Angulo, E., & Courchamp, F. (2008). Caution on isotopic model use for analyses of consumer diet. *Canadian Journal of Zoology*, 86(5), 438–445. Journal Article. <http://doi.org/10.1139/Z08-012>
- Cederholm, C. J., Houston, D. B., Cole, D. L., & Scarlett, W. J. (1989). Fate of coho salmon (*oncorhynchus kisutch*) carcasses in spawning streams. *Canadian Journal of Fisheries and Aquatic Sciences*, 46(8), 1347–1355. Journal Article. <http://doi.org/10.1139/f89-173>
- Cederholm, C. J., Kunze, M. D., Murota, T., & Sibatani, A. (1999). Pacific salmon carcasses: Essential contributions of nutrients and energy for aquatic and terrestrial ecosystems. *Fisheries (Bethesda)*, 24(10), 6–15. Journal Article. [http://doi.org/10.1577/1548-8446\(1999\)024<0006:PSC>2.0.CO;2](http://doi.org/10.1577/1548-8446(1999)024<0006:PSC>2.0.CO;2)
- Cerling, T. E., Ayliffe, L. K., Dearing, M. D., Ehleringer, J. R., Passey, B. H., Podlesak, D. W., ... West, A. G. (2007). Determining biological tissue turnover using stable isotopes: The reaction progress variable. *Oecologia*, 151(2), 175–189. Journal Article. <http://doi.org/10.1007/s00442-006-0571-4>
- Chaloner, D. T., Martin, K. M., Wipfli, M. S., Ostrom, P. H., & Lamberti, G. A. (2002). Marine carbon and nitrogen in southeastern alaska stream food webs: Evidence from artificial and natural streams. *Canadian Journal of Fisheries and Aquatic Sciences*, 59(8), 1257–1265. Journal Article. <http://doi.org/10.1139/f02-084>
- Chapin, F. S. (2006). *Alaska's changing boreal forest*. Book, New York: New York : Oxford

- University Press.
- Chapin, I., F. Stuart, Matson, P. A., Vitousek, P., & Chapin, M. C. (2011). *Principles of terrestrial ecosystem ecology* (Second Edition). Book, New York, NY: New York, NY: Springer. <http://doi.org/10.1007/978-1-4419-9504-9>
- Chappell, H. N., Prescott, C. E., & Vesterdal, L. (1999). Long-term effects of nitrogen fertilization on nitrogen availability in coastal douglas-fir forest floors. *Soil Science Society of America Journal*, 63(5), 1448–1454. Journal Article. <http://doi.org/10.2136/sssaj1999.6351448x>
- Chasco, B., Kaplan, I. C., Thomas, A., Acevedo-Gutiérrez, A., Noren, D., Ford, M. J., ... Ward, E. J. (2017). Estimates of chinook salmon consumption in washington state inland waters by four marine mammal predators from 1970 to 2015. *Canadian Journal of Fisheries and Aquatic Sciences*, 74(8), 1173–1194. Journal Article. <http://doi.org/10.1139/cjfas-2016-0203>
- Chassot, E., Bonhommeau, S., Dulvy, N. K., Mélin, F., Watson, R., Gascuel, D., & Le Pape, O. (2010). Global marine primary production constrains fisheries catches. *Ecology Letters*, 13(4), 495–505. Journal Article. <http://doi.org/10.1111/j.1461-0248.2010.01443.x>
- Chassot, E., Mélin, F., Le Pape, O., & Gascuel, D. (2007). Bottom-up control regulates fisheries production at the scale of eco-regions in european seas. *Marine Ecology. Progress Series (Halstenbek)*, 343, 45–55. Journal Article. <http://doi.org/10.3354/meps06919>
- Chiang, W.-C., Chang, C.-T., Madigan, D. J., Carlisle, A. B., Musyl, M. K., Chang, Y.-C., ... Tseng, C.-T. (2020). Stable isotope analysis reveals feeding ecology and trophic position of black marlin off eastern taiwan. *Deep-Sea Research. Part II, Topical Studies in Oceanography*, 175, 104821. Journal Article. <http://doi.org/10.1016/j.dsr2.2020.104821>

- Chikaraishi, Y., Kashiyama, Y., Ogawa, N. O., Kitazato, H., & Ohkouchi, N. (2007). Metabolic control of nitrogen isotope composition of amino acids in macroalgae and gastropods: Implications for aquatic food web studies. *Marine Ecology. Progress Series (Halstenbek)*, 342, 85–90. Journal Article. <http://doi.org/10.3354/meps342085>
- Chikaraishi, Y., Ogawa, N. O., Kashiyama, Y., Takano, Y., Suga, H., Tomitani, A., ... Ohkouchi, N. (2009). Determination of aquatic food-web structure based on compound-specific nitrogen isotopic composition of amino acids. *Limnology and Oceanography, Methods*, 7(11), 740–750. Journal Article. <http://doi.org/10.4319/lom.2009.7.740>
- Chikaraishi, Y., Steffan, S. A., Takano, Y., & Ohkouchi, N. (2015). Diet quality influences isotopic discrimination among amino acids in an aquatic vertebrate. *Ecology and Evolution*, 5(10), 2048–2059. Journal Article. <http://doi.org/10.1002/ece3.1491>
- Choi, B., Ha, S., Lee, J. S., Chikaraishi, Y., Ohkouchi, N., & Shin, K. (2017). Trophic interaction among organisms in a seagrass meadow ecosystem as revealed by bulk ^{13}C and amino acid ^{15}N analyses. *Limnology and Oceanography*, 62(4), 1426–1435. Journal Article. <http://doi.org/10.1002/lno.10508>
- Claeson, S. M., Li, J. L., Compton, J. E., & Bisson, P. A. (2006). Response of nutrients, biofilm, and benthic insects to salmon carcass addition. *Canadian Journal of Fisheries and Aquatic Sciences*, 63(6), 1230–1241. Journal Article. <http://doi.org/10.1139/f06-029>
- Collins, S. F., Marcarelli, A. M., Baxter, C. V., & Wipfli, M. S. (2015). A critical assessment of the ecological assumptions underpinning compensatory mitigation of salmon-derived nutrients. *Environmental Management (New York)*, 56(3), 571–586. Journal Article. <http://doi.org/10.1007/s00267-015-0538-5>
- Compton, J. E., Andersen, C. P., Phillips, D. L., Brooks, J. R., Johnson, M. G., Church, M. R., ... Shaff, C. D. (2006). Ecological and water quality consequences of nutri-

- ent addition for salmon restoration in the pacific northwest. *Frontiers in Ecology and the Environment*, 4(1), 18–26. Journal Article. [http://doi.org/10.1890/1540-9295\(2006\)004\[0018:EAWQCO\]2.0.CO;2](http://doi.org/10.1890/1540-9295(2006)004[0018:EAWQCO]2.0.CO;2)
- Conway-Cranos, L., Kiffney, P., Banas, N., Plummer, M., Naman, S., MacCready, P., ... Ruckelshaus, M. (2015). Stable isotopes and oceanographic modeling reveal spatial and trophic connectivity among terrestrial, estuarine, and marine environments. *Marine Ecology. Progress Series (Halstenbek)*, 533, 15–28. Journal Article. <http://doi.org/10.3354/meps11318>
- Corwith, H. L., & Wheeler, P. A. (2002). El niño related variations in nutrient and chlorophyll distributions off oregon: Observations of the 1997-98 el niño along the west coast of north america. *Progress in Oceanography*, 54(1-4), 361–380. Journal Article.
- Craine, J. M., Elmore, A. J., Aidar, M. P. M., Bustamante, M., Dawson, T. E., Hobbie, E. A., ... Wright, I. J. (2009). Global patterns of foliar nitrogen isotopes and their relationships with climate, mycorrhizal fungi, foliar nutrient concentrations, and nitrogen availability. *The New Phytologist*, 183(4), 980–992. Journal Article. <http://doi.org/10.1111/j.1469-8137.2009.02917.x>
- Criss, R. E. (1999). *Principles of stable isotope distribution*. Book, Cary: Cary: Oxford University Press, Incorporated.
- Cunningham, C. J., Westley, P. A. H., & Adkison, M. D. (2018). Signals of large scale climate drivers, hatchery enhancement, and marine factors in yukon river chinook salmon survival revealed with a bayesian life history model. *Global Change Biology*, 24(9), 4399–4416. Journal Article. <http://doi.org/10.1111/gcb.14315>
- Dale, J. J., Wallsgrave, N. J., Popp, B. N., & Holland, K. N. (2011). Nursery habitat use and foraging ecology of the brown stingray *dasyatis lata* determined from stomach contents, bulk and amino acid stable isotopes. *Marine Ecology. Progress Series (Halstenbek)*, 433,

- 221–236. Journal Article. <http://doi.org/10.3354/meps09171>
- Dalerum, F., & Angerbjörn, A. (2005). Resolving temporal variation in vertebrate diets using naturally occurring stable isotopes. *Oecologia*, 144(4), 647–658. Journal Article. <http://doi.org/10.1007/s00442-005-0118-0>
- Dehn, L. A., Sheffield, G. G., Follmann, E. H., Duffy, L. K., Thomas, D. L., & O'Hara, T. M. (2007). Feeding ecology of phocid seals and some walrus in the alaskan and canadian arctic as determined by stomach contents and stable isotope analysis. *Polar Biology*, 30(2), 167–181. Journal Article. <http://doi.org/10.1007/s00300-006-0171-0>
- Del Rio, C. M., & Carleton, S. A. (2012). How fast and how faithful: The dynamics of isotopic incorporation into animal tissues. *Journal of Mammalogy*, 93(2), 353–359. Journal Article. <http://doi.org/10.1644/11-MAMM-S-165.1>
- Deniro, M. J., & Epstein, S. (1981). Influence of diet on the distribution of nitrogen isotopes in animals. *Geochimica et Cosmochimica Acta*, 45(3), 341–351. Journal Article. [http://doi.org/10.1016/0016-7037\(81\)90244-1](http://doi.org/10.1016/0016-7037(81)90244-1)
- Di Lorenzo, E., Schneider, N., Cobb, K. M., Franks, P. J. S., Chhak, K., Miller, A. J., ... Rivière, P. (2008). North pacific gyre oscillation links ocean climate and ecosystem change. *Geophysical Research Letters*, 35(8), L08607–n/a. Journal Article. <http://doi.org/10.1029/2007GL032838>
- Dortch, Q., & Postel, J. R. (1989). Biochemical indicators of n utilization by phytoplankton during upwelling off the washington coast. *Limnology and Oceanography*, 34(4), 758–773. Journal Article.
- Downs, E. E., Popp, B. N., & Holl, C. M. (2014). Nitrogen isotope fractionation and amino acid turnover rates in the pacific white shrimp litopenaeus vannamei. *Marine Ecology Progress Series (Halstenbek)*, 516, 239–250. Journal Article. <http://doi.org/10.3354/meps11030>

- Drago, M., Cardona, L., Crespo, E. A., & Aguilar, A. (2009). Ontogenetic dietary changes in south american sea lions. *Journal of Zoology (1987)*, 279(3), 251–261. Journal Article. <http://doi.org/10.1111/j.1469-7998.2009.00613.x>
- Drake, D. C., Naiman, R. J., & Bechtold, J. S. (2006). FATE of nitrogen in riparian forest soils and trees: AN 15N tracer study simulating salmon decay. *Ecology (Durham)*, 87(5), 1256–1266. Journal Article. [http://doi.org/10.1890/0012-9658\(2006\)87\[1256:FONIRF\]2.0.CO;2](http://doi.org/10.1890/0012-9658(2006)87[1256:FONIRF]2.0.CO;2)
- Du, X., & Peterson, W. T. (2014). Seasonal cycle of phytoplankton community composition in the coastal upwelling system off central oregon in 2009. *Estuaries and Coasts*, 37(2), 299–311. Journal Article. <http://doi.org/10.1007/s12237-013-9679-z>
- Duguid, W. D. P., Boldt, J. L., Chalifour, L., Greene, C. M., Galbraith, M., Hay, D., ... Juanes, F. (2019). Historical fluctuations and recent observations of northern anchovy engraulis mordax in the salish sea. *Deep-Sea Research. Part II, Topical Studies in Oceanography*, 159, 22–41. Journal Article. <http://doi.org/10.1016/j.dsr2.2018.05.018>
- Espinasse, B., Hunt, B. P. V., Batten, S. D., Pakhomov, E. A., & Tittensor, D. (2020). Defining isoscapes in the northeast pacific as an index of ocean productivity. *Global Ecology and Biogeography*, 29(2), 246–261. Journal Article. <http://doi.org/10.1111/geb.13022>
- Estes, J. A., Tinker, M. T., Williams, T. M., & Doak, D. F. (1998). Killer whale predation on sea otters linking oceanic and nearshore ecosystems. *Science (American Association for the Advancement of Science)*, 282(5388), 473–476. Journal Article. <http://doi.org/10.1126/science.282.5388.473>
- Estrada, J. A., Rice, A. N., Lutcavage, M. E., & Skomal, G. B. (2003). Predicting trophic position in sharks of the north-west atlantic ocean using stable isotope analysis. *Journal*

- of the Marine Biological Association of the United Kingdom*, 83(6), 1347–1350. Journal Article. <http://doi.org/10.1017/S0025315403008798>
- Feddern, M. L., Holtgrieve, G. W., & Ward, E. J. (2021). Stable isotope signatures in historic harbor seal bone link food web-assimilated carbon and nitrogen resources to a century of environmental change. *Global Change Biology*, 27(11), 2328–2342. Journal Article. <http://doi.org/10.1111/gcb.15551>
- Ferreira, A., Sá, C., Silva, N., Beltrán, C., Dias, A. M., & Brito, A. C. (2020). Phytoplankton community dynamics in a coastal bay under upwelling influence (central chile). *Estuarine, Coastal and Shelf Science*, 245, 106968. Journal Article. <http://doi.org/10.1016/j.ecss.2020.106968>
- Finney, B. P. (2000). Impacts of climatic change and fishing on pacific salmon abundance over the past 300 years. *Science (American Association for the Advancement of Science)*, 290(5492), 795–799. Journal Article. <http://doi.org/10.1126/science.290.5492.795>
- Frank, K. T., Fisher, J. A. D., & Leggett, W. C. (2015). The spatio-temporal dynamics of trophic control in large marine ecosystems. Generic, Cambridge University Press. <http://doi.org/10.1017/CBO9781139924856.003>
- Frank, K. T., Petrie, B., Shackell, N. L., & Choi, J. S. (2006). Reconciling differences in trophic control in mid-latitude marine ecosystems. *Ecology Letters*, 9(10), 1096–1105. Journal Article. <http://doi.org/10.1111/j.1461-0248.2006.00961.x>
- Frost, K. J., Lowry, L. F., & Ver Hoef, J. M. (1999). MONITORING the trend of harbor seals in prince william sound, alaska, after the exxon valdez oil spill. *Marine Mammal Science*, 15(2), 494–506. Journal Article. <http://doi.org/10.1111/j.1748-7692.1999.tb00815.x>
- Fry, B. (2006). *Stable isotope ecology*. Book, New York: New York : Springer.

- Gagne, T. O., Hyrenbach, K. D., Hagemann, M. E., & Van Houtan, K. S. (2018). Trophic signatures of seabirds suggest shifts in oceanic ecosystems. *Science Advances*, 4(2), eaao3946–eaao3946. Journal Article. <http://doi.org/10.1126/sciadv.aao3946>
- Geiger, G. L., Atkinson, S., Waite, J. N., Blundell, G. M., Carpenter, J. R., & Wynne, K. (2013). A new method to evaluate the nutritional composition of marine mammal diets from scats applied to harbor seals in the gulf of alaska. *Journal of Experimental Marine Biology and Ecology*, 449, 118–128. Journal Article. <http://doi.org/10.1016/j.jembe.2013.09.005>
- Gende, S. M., Miller, A. E., & Hood, E. (2007). The effects of salmon carcasses on soil nitrogen pools in a riparian forest of southeastern alaska. *Canadian Journal of Forest Research*, 37(7), 1194–1202. Journal Article. <http://doi.org/10.1139/X06-318>
- Germain, L. R., Koch, P. L., Harvey, J., & McCarthy, M. D. (2013). Nitrogen isotope fractionation in amino acids from harbor seals: Implications for compound-specific trophic position calculations. *Marine Ecology. Progress Series (Halstenbek)*, 482, 265–277. Journal Article. <http://doi.org/10.3354/meps10257>
- Ghedini, G., Russell, B. D., & Connell, S. D. (2015). Trophic compensation reinforces resistance: Herbivory absorbs the increasing effects of multiple disturbances. *Ecology Letters*, 18(2), 182–187. Journal Article. <http://doi.org/10.1111/ele.12405>
- Greene, C., Kuehne, L., Rice, C., Fresh, K., & Penttila, D. (2015). Forty years of change in forage fish and jellyfish abundance across greater puget sound, washington (usa): Anthropogenic and climate associations. *Marine Ecology. Progress Series (Halstenbek)*, 525, 153–170. Journal Article. <http://doi.org/10.3354/meps11251>
- Gregg, W. W., Conkright, M. E., Ginoux, P., O'Reilly, J. E., & Casey, N. W. (2003). Ocean primary production and climate: Global decadal changes: OCEAN primary production and climate. *Geophysical Research Letters*, 30(15). Journal Article. <http://doi.org/>

- [10.1029/2003GL016889](https://doi.org/10.1029/2003GL016889)
- Gu, B. (2009). Variations and controls of nitrogen stable isotopes in particulate organic matter of lakes. *Oecologia*, 160(3), 421–431. Journal Article. <http://doi.org/10.1007/s00442-009-1323-z>
- Gu, B., Schell, D. M., & Alexander, V. (1994). Stable carbon and nitrogen isotopic analysis of the plankton food web in a subarctic lake. *Canadian Journal of Fisheries and Aquatic Sciences*, 51(6), 1338–1344. Journal Article. <http://doi.org/10.1139/f94-133>
- Hannides, C. C. S., Popp, B. N., Choy, C. A., & Drazen, J. C. (2013). Midwater zooplankton and suspended particle dynamics in the north pacific subtropical gyre: A stable isotope perspective. *Limnology and Oceanography*, 58(6), 1931–1946. Journal Article. <http://doi.org/10.4319/lo.2013.58.6.1931>
- Hannides, C. C. S., Popp, B. N., Landry, M. R., & Graham, B. S. (2009). Quantification of zooplankton trophic position in the north pacific subtropical gyre using stable nitrogen isotopes. *Limnology and Oceanography*, 54(1), 50–61. Journal Article. <http://doi.org/10.4319/lo.2009.54.1.0050>
- Hare, S. R., & Mantua, N. J. (2000). Empirical evidence for north pacific regime shifts in 1977 and 1989. *Progress in Oceanography*, 47(2-4), 103–145. Journal Article. [http://doi.org/10.1016/S0079-6611\(00\)00033-1](http://doi.org/10.1016/S0079-6611(00)00033-1)
- Hastings, A., Abbott, K. C., Cuddington, K., Francis, T., Gellner, G., Lai, Y.-C., ... Zeeman, M. L. (2018). Transient phenomena in ecology. *Science (American Association for the Advancement of Science)*, 361(6406), 990. Journal Article. <http://doi.org/10.1126/science.aat6412>
- Hauser, D. D. W., Allen, C. S., Rich, H. B., & Quinn, T. P. (2008). Resident harbor seals (*phoca vitulina*) in iliamna lake, alaska: Summer diet and partial consumption of adult sockeye salmon (*oncorhynchus nerka*). *Aquatic Mammals*, 34(3), 303–309. Journal Article. <http://doi.org/10.1126/science.aat6412>

- Article. <http://doi.org/10.1578/AM.34.3.2008.303>
- Heithaus, M. R., Frid, A., Wirsing, A. J., & Worm, B. (2008). Predicting ecological consequences of marine top predator declines. *Trends in Ecology & Evolution (Amsterdam)*, 23(4), 202–210. Journal Article. <http://doi.org/10.1016/j.tree.2008.01.003>
- Helfield, J. M., & Naiman, R. J. (2001). Effects of salmon-derived nitrogen on riparian forest growth and implications for stream productivity. *Ecology (Durham)*, 82(9), 2403–2409. Journal Article. [http://doi.org/10.1890/0012-9658\(2001\)082\[2403:EOSDNO\]2.0.CO;2](http://doi.org/10.1890/0012-9658(2001)082[2403:EOSDNO]2.0.CO;2)
- Helfield, J. M., & Naiman, R. J. (2002). Salmon and alder as nitrogen sources to riparian forests in a boreal alaskan watershed. *Oecologia*, 133(4), 573–582. Journal Article. <http://doi.org/10.1007/s00442-002-1070-x>
- Hilborn, R., Quinn, T. P., Schindler, D. E., & Rogers, D. E. (2003). Biocomplexity and fisheries sustainability. *Proceedings of the National Academy of Sciences - PNAS*, 100(11), 6564–6568. Journal Article. <http://doi.org/10.1073/pnas.1037274100>
- Hilderbrand, G. V., Schwartz, C. C., Robbins, C. T., Jacoby, M. E., Hanley, T. A., Arthur, S. M., & Servheen, C. (1999). The importance of meat, particularly salmon, to body size, population productivity, and conservation of north american brown bears. *Canadian Journal of Zoology*, 77(1), 132–138. Journal Article. <http://doi.org/10.1139/z98-195>
- Hirons, A. C., Schell, D. M., & Finney, B. P. (2001). Temporal records of ^{13}C and ^{15}N in north pacific pinnipeds: Inferences regarding environmental change and diet. *Oecologia*, 129(4), 591–601. Journal Article. <http://doi.org/10.1007/s004420100756>
- Hobbie, S. E., & Chapin, F. S. (1996). Winter regulation of tundra litter carbon and nitrogen dynamics. *Biogeochemistry*, 35(2), 327–338. Journal Article. <http://doi.org/10.1007/BF02179958>
- Hobson, K. A., & Clark, R. G. (1992). Assessing avian diets using stable isotopes i : Turnover of ^{13}C in tissues. *The Condor (Los Angeles, Calif.)*, 94(1), 181–188. Journal Article.

- Hobson, K. A., Schell, D. M., Renouf, D., & Noseworthy, E. (1996). Stable carbon and nitrogen isotopic fractionation between diet and tissues of captive seals : Implications for dietary reconstructions involving marine mammals. *Canadian Journal of Fisheries and Aquatic Sciences*, 53(3), 528–533. Journal Article. <http://doi.org/10.1139/cjfas-53-3-528>
- Hobson, K. A., Sease, J. L., Merrick, R. L., & Piatt, J. F. (1997). INVESTIGATING trophic relationships of pinnipeds in alaska and washington using stable isotope ratios of nitrogen and carbon. *Marine Mammal Science*, 13(1), 114–132. Journal Article. <http://doi.org/10.1111/j.1748-7692.1997.tb00615.x>
- Hocking, M. D., & Reynolds, J. D. (2012). Nitrogen uptake by plants subsidized by pacific salmon carcasses: A hierarchical experiment. *Canadian Journal of Forest Research*, 42(5), 908–917. Journal Article. <http://doi.org/10.1139/x2012-045>
- Hoegh-Guldberg, O., & Bruno, J. F. (2010). The impact of climate change on the world's marine ecosystems. *Science (American Association for the Advancement of Science)*, 328(5985), 1523–1528. Journal Article. <http://doi.org/10.1126/science.1189930>
- Holmes, R. M., McClelland, J. W., Sigman, D. M., Fry, B., & Peterson, B. J. (1998). Measuring $^{15}\text{N}-\text{nh}_4^+$ in marine, estuarine and fresh waters : An adaptation of the ammonia diffusion method for samples with low ammonium concentrations. *Marine Chemistry*, 60(3-4), 235–243. Journal Article.
- Holsman, K. K., Aydin, K., Sullivan, J., Hurst, T., & Kruse, G. H. (2019). Climate effects and bottom-up controls on growth and size-at-age of pacific halibut (*hippoglossus stenolepis*) in alaska (usa). *Fisheries Oceanography*, 28(3), 345–358. Journal Article. <http://doi.org/10.1111/fog.12416>
- Holtgrieve, G. W., & Schindler, D. E. (2011). Marine-derived nutrients, bioturbation, and ecosystem metabolism: Reconsidering the role of salmon in streams. *Ecology (Durham)*,

- 92(2), 373–385. Journal Article. <http://doi.org/10.1890/09-1694.1>
- Holtgrieve, G. W., Schindler, D. E., & Jewett, P. K. (2009). Large predators and biogeochemical hotspots: Brown bear (*ursus arctos*) predation on salmon alters nitrogen cycling in riparian soils. *Ecological Research*, 24(5), 1125–1135. Journal Article. <http://doi.org/10.1007/s11284-009-0591-8>
- Holtgrieve, G. W., Schindler, D. E., Gowell, C. P., Ruff, C. P., & Lisi, P. J. (2010). Stream geomorphology regulates the effects on periphyton of ecosystem engineering and nutrient enrichment by pacific salmon. *Freshwater Biology*, 55(12), 2598–2611. Journal Article. <http://doi.org/10.1111/j.1365-2427.2010.02489.x>
- Howe, E. R., & Simenstad, C. A. (2015). Using stable isotopes to discern mechanisms of connectivity in estuarine detritus-based food webs. *Marine Ecology. Progress Series (Halstenbek)*, 518, 13–29. Journal Article. <http://doi.org/10.3354/meps11066>
- HÖgberg, P. (1998). Tansley review no. 95: 15N natural abundance in soil–plant systems. *The New Phytologist*, 139(3), 595–595. Journal Article. <http://doi.org/10.1046/j.1469-8137.1998.00239.x>
- HÖgberg, P., Fan, H., Quist, M., Binkley, D. A. N., & Tamm, C. O. (2006). Tree growth and soil acidification in response to 30 years of experimental nitrogen loading on boreal forest. *Global Change Biology*, 12(3), 489–499. Journal Article. <http://doi.org/10.1111/j.1365-2486.2006.01102.x>
- Hunter, M. D., & Price, P. W. (1992). Playing chutes and ladders: Heterogeneity and the relative roles of bottom-up and top-down forces in natural communities. *Ecology (Durham)*, 73(3), 724–732. Journal Article. <http://doi.org/10.2307/1940152>
- Iitembu, J. A., Miller, T. W., Ohmori, K., Kanime, A., & Wells, S. (2012). Comparison of ontogenetic trophic shift in two hake species, *merluccius capensis* and *merluccius paradoxus*, from the northern benguela current ecosystem (namibia) using stable

- isotope analysis. *Fisheries Oceanography*, 21(2-3), 215–225. Journal Article. <http://doi.org/10.1111/j.1365-2419.2012.00614.x>
- Iverson, S. J., Frost, K. J., & Lowry, L. F. (1997). Fatty acid signatures reveal fine scale structure of foraging distribution of harbor seals and their prey in prince william sound, alaska. *Marine Ecology. Progress Series (Halstenbek)*, 151(1/3), 255–271. Journal Article. <http://doi.org/10.3354/meps151255>
- Janetski, D. J., Chaloner, D. T., Tiegs, S. D., & Lamberti, G. A. (2009). Pacific salmon effects on stream ecosystems: A quantitative synthesis. *Oecologia*, 159(3), 583–595. Journal Article. <http://doi.org/10.1007/s00442-008-1249-x>
- Jansen, J. K., Boveng, P. L., Ver Hoef, J. M., Dahle, S. P., & Bengtson, J. L. (2015). Natural and human effects on harbor seal abundance and spatial distribution in an alaskan glacial fjord. *Marine Mammal Science*, 31(1), 66–89. Journal Article. <http://doi.org/10.1111/mms.12140>
- Jardine, T. D., Hadwen, W. L., Hamilton, S. K., Hladyz, S., Mitrovic, S. M., Kidd, K. A., ... Bunn, S. E. (2014). UNDERSTANDING and overcoming baseline isotopic variability in running waters. *River Research and Applications*, 30(2), 155–165. Journal Article. <http://doi.org/10.1002/rra.2630>
- Jeffries, S., Huber, H., Calambokidis, J., & Laake, J. (2003). Trends and status of harbor seals in washington state: 1978-1999. *The Journal of Wildlife Management*, 67(1), 207–218. Journal Article. <http://doi.org/10.2307/3803076>
- Jennings, S., & Brander, K. (2010). Predicting the effects of climate change on marine communities and the consequences for fisheries. *Journal of Marine Systems*, 79(3), 418–426. Journal Article. <http://doi.org/10.1016/j.jmarsys.2008.12.016>
- Johnston, N. T., MacIsaac, E. A., Tschaplinski, P. J., & Hall, K. J. (2004). Effects of the abundance of spawning sockeye salmon (*oncorhynchus nerka*) on nutrients and algal

- biomass in forested streams. *Canadian Journal of Fisheries and Aquatic Sciences*, 61(3), 384–403. Journal Article. <http://doi.org/10.1139/f03-172>
- Jorgensen, J. C., Ward, E. J., Scheuerell, M. D., & Zabel, R. W. (2016). Assessing spatial covariance among time series of abundance. *Ecology and Evolution*, 6(8), 2472–2485. Journal Article. <http://doi.org/10.1002/ece3.2031>
- Jungbluth, M. J., Selph, K. E., Lenz, P. H., & Goetze, E. (2017). Species-specific grazing and significant trophic impacts by two species of copepod nauplii, *parvocalanus crassirostris* and *bestiolina similis*. *Marine Ecology. Progress Series (Halstenbek)*, 572, 57–76. Journal Article. <http://doi.org/10.3354/meps12139>
- Kelton, W. M., & Matthew, D. M. (2016). Embracing variability in amino acid ^{15}N fractionation: Mechanisms, implications, and applications for trophic ecology. *Ecosphere (Washington, D.C.)*, 7(12), n/a. Journal Article. <http://doi.org/10.1002/ecs2.1511>
- Khangaonkar, T., Nugraha, A., Xu, W., & Balaguru, K. (2019). Salish sea response to global climate change, sea level rise, and future nutrient loads. *Journal of Geophysical Research. Oceans*, 124(6), 3876–3904. Journal Article. <http://doi.org/10.1029/2018JC014670>
- Kirchhoff, M. D. (2003). Effects of salmon-derived nitrogen on riparian forest growth and implications for stream productivity: Comment. *Ecology (Durham)*, 84(12), 3396–3399. Journal Article. <http://doi.org/10.1890/02-3121>
- Kjeldgaard, M. K., Hewlett, J. A., & Eubanks, M. D. (2021). Widespread variation in stable isotope trophic position estimates: Patterns, causes, and potential consequences. *Ecological Monographs*, 91(3), n/a. Journal Article. <http://doi.org/10.1002/ecm.1451>
- Kline Jr, T. C., Goering, J. J., Mathisen, O. A., Poe, P. H., Parker, P. L., & Scalan, R. S. (1993). Recycling of elements transported upstream by runs of pacific salmon: II. ^{15}N and ^{13}C evidence in the kvichak river watershed, bristol bay, southwestern alaska. *Canadian Journal of Fisheries and Aquatic Sciences*, 50(11), 2350–2365. Journal Article.

- <http://doi.org/10.1139/f93-259>
- Klinken, G. J. van. (1999). Bone collagen quality indicators for palaeodietary and radiocarbon measurements. *Journal of Archaeological Science*, 26(6), 687–695. Journal Article. <http://doi.org/10.1006/jasc.1998.0385>
- Klute, A. (1986). *Methods of soil analysis. part 1. physical and mineralogical methods* (2nd ed.). Book.
- Kolzau, S., Wiedner, C., Rücker, J., Köhler, J., Köhler, A., & Dolman, A. M. (2014). Seasonal patterns of nitrogen and phosphorus limitation in four german lakes and the predictability of limitation status from ambient nutrient concentrations. *PloS One*, 9(4), e96065–e96065. Journal Article. <http://doi.org/10.1371/journal.pone.0096065>
- Kratina, P., Greig, H. S., Thompson, P. L., Carvalho-Pereira, T. S. A., & Shurin, J. B. (2012). Warming modifies trophic cascades and eutrophication in experimental freshwater communities. *Ecology (Durham)*, 93(6), 1421–1430. Journal Article. <http://doi.org/10.1890/11-1595.1>
- Kudela, R. M., & Peterson, T. D. (2009). Influence of a buoyant river plume on phytoplankton nutrient dynamics: What controls standing stocks and productivity? *Journal of Geophysical Research: Oceans*, 114(C2), C00B11–n/a. Journal Article. <http://doi.org/10.1029/2008JC004913>
- Kudela, R., Banas, N., Barth, J., Frame, E., Jay, D., Largier, J., ... Vander Woude, A. (2008). New insights into the controls and mechanisms of plankton productivity in coastal upwelling waters of the northern California current system. *Oceanography (Washington, D.C.)*, 21(4), 46–59. Journal Article. <http://doi.org/10.5670/oceanog.2008.04>
- Kwiatkowski, L., Bopp, L., Aumont, O., Caias, P., Cox, P. M., Laufkötter, C., ... Séférian, R. (2017). Emergent constraints on projections of declining primary production in the tropical oceans. *Nature Climate Change*, 7(5), 355–358. Journal Article. <http://doi.org/10.1038/nclimate3333>

- [org/10.1038/nclimate3265](http://doi.org/10.1038/nclimate3265)
- Lance, M. M., Chang, W.-Y., Jeffries, S. J., Pearson, S. F., & Acevedo-Gutierrez, A. (2012). Harbor seal diet in northern puget sound: Implications for the recovery of depressed fish stocks. *Marine Ecology. Progress Series (Halstenbek)*, 464, 257–271. Journal Article. <http://doi.org/10.3354/meps09880>
- Larsen, T., Ventura, M., Andersen, N., O'Brien, D. M., Piatkowski, U., & McCarthy, M. D. (2013). Tracing carbon sources through aquatic and terrestrial food webs using amino acid stable isotope fingerprinting. *PloS One*, 8(9), e73441–e73441. Journal Article. <http://doi.org/10.1371/journal.pone.0073441>
- Latimer, A. M., Banerjee, S., Sang Jr, H., Mosher, E. S., & Silander Jr, J. A. (2009). Hierarchical models facilitate spatial analysis of large data sets: A case study on invasive plant species in the northeastern united states. *Ecology Letters*, 12(2), 144–154. Journal Article. <http://doi.org/10.1111/j.1461-0248.2008.01270.x>
- Lehmann, M. F., Sigman, D. M., McCorkle, D. C., Brunelle, B. G., Hoffmann, S., Kienast, M., ... Clement, J. (2005). Origin of the deep bering sea nitrate deficit: Constraints from the nitrogen and oxygen isotopic composition of water column nitrate and benthic nitrate fluxes. *Global Biogeochemical Cycles*, 19(4), GB4005–n/a. Journal Article. <http://doi.org/10.1029/2005GB002508>
- Litzow, M. A., & Ciannelli, L. (2007). Oscillating trophic control induces community reorganization in a marine ecosystem. *Ecology Letters*, 10(12), 1124–1134. Journal Article. <http://doi.org/10.1111/j.1461-0248.2007.01111.x>
- Litzow, M. A., Hunsicker, M. E., Bond, N. A., Burke, B. J., Cunningham, C. J., Gosselin, J. L., ... Zador, S. G. (2020). The changing physical and ecological meanings of north pacific ocean climate indices. *Proceedings of the National Academy of Sciences - PNAS*, 117(14), 7665–7671. Journal Article. <http://doi.org/10.1073/pnas.1921266117>

- Lloyd, A. H., Duffy, P. A., & Mann, D. H. (2013). Nonlinear responses of white spruce growth to climate variability in interior alaska. *Canadian Journal of Forest Research*, 43(999), 331–343. Journal Article. <http://doi.org/10.1139/cjfr-2012-0372>
- Lorrain, A., Graham, B. S., Popp, B. N., Allain, V., Olson, R. J., Hunt, B. P. V., ... Ménard, F. (2015). Nitrogen isotopic baselines and implications for estimating foraging habitat and trophic position of yellowfin tuna in the indian and pacific oceans. *Deep-Sea Research. Part II, Topical Studies in Oceanography*, 113, 188–198. Journal Article. <http://doi.org/10.1016/j.dsr2.2014.02.003>
- Lorrain, A., Pethybridge, H., Cassar, N., Receveur, A., Allain, V., Bodin, N., ... Young, J. W. (2020). Trends in tuna carbon isotopes suggest global changes in pelagic phytoplankton communities. *Global Change Biology*, 26(2), 458–470. Journal Article. <http://doi.org/10.1111/gcb.14858>
- Lowry, L. F., Frost, K. J., Ver Hoep, J. M., & Delong, R. A. (2001). MOVEMENTS of satellite-tagged subadult and adult harbor seals in prince william sound, alaska. *Marine Mammal Science*, 17(4), 835–861. Journal Article. <http://doi.org/10.1111/j.1748-7692.2001.tb01301.x>
- Lu, M., Yang, Y., Luo, Y., Fang, C., Zhou, X., Chen, J., ... Li, B. (2011). Responses of ecosystem nitrogen cycle to nitrogen addition: A meta-analysis. *The New Phytologist*, 189(4), 1040–1050. Journal Article. <http://doi.org/10.1111/j.1469-8137.2010.03563.x>
- Magera, A. M., Flemming, J. E. M., Kaschner, K., Christensen, L. B., & Lotze, H. K. (2013). Recovery trends in marine mammal populations. *PloS One*, 8(10), e77908–e77908. Journal Article. <http://doi.org/10.1371/journal.pone.0077908>
- Mancinelli, G., Vizzini, S., Mazzola, A., Maci, S., & Bassett, A. (2013). Cross-validation of ^{15}N and fishbase estimates of fish trophic position in a mediterranean lagoon: The importance of the isotopic baseline. *Estuarine, Coastal and Shelf Science*, 135, 77–85.

- Journal Article. <http://doi.org/10.1016/j.ecss.2013.04.004>
- Maniscalco, J. M., Parker, P., & Atkinson, S. (2006). INTERSEASONAL and interannual measures of maternal care among individual steller sea lions (*eumetopias jubatus*). *Journal of Mammalogy*, 87(2), 304–311. Journal Article. <http://doi.org/10.1644/05-MAMM-A-163R2.1>
- Mantua, N. J., & Hare, S. R. (2002). The pacific decadal oscillation. *Journal of Oceanography*, 58(1), 35–44. Journal Article. <http://doi.org/10.1023/A:1015820616384>
- Mantua, N. J., Hare, S. R., Zhang, Y., Wallace, J. M., & Francis, R. C. (1997). A pacific interdecadal climate oscillation with impacts on salmon production. *Bulletin of the American Meteorological Society*, 78(6), 1069–1079. Journal Article. [http://doi.org/10.1175/1520-0477\(1997\)078<1069:APICOW>2.0.CO;2](http://doi.org/10.1175/1520-0477(1997)078<1069:APICOW>2.0.CO;2)
- Marinov, I., Doney, S. C., & Lima, I. D. (2010). Response of ocean phytoplankton community structure to climate change over the 21st century: Partitioning the effects of nutrients, temperature and light. *Biogeosciences*, 7(12), 3941–3959. Journal Article. <http://doi.org/10.5194/bg-7-3941-2010>
- Marshall, K. N., Stier, A. C., Samhouri, J. F., Kelly, R. P., & Ward, E. J. (2016). Conservation challenges of predator recovery. *Conservation Letters*, 9(1), 70–78. Journal Article. <http://doi.org/10.1111/conl.12186>
- Martinez del Rio, C., Wolf, N., Carleton, S. A., & Gannes, L. Z. (2009). Isotopic ecology ten years after a call for more laboratory experiments. *Biological Reviews of the Cambridge Philosophical Society*, 84(1), 91–111. Journal Article. <http://doi.org/10.1111/j.1469-185X.2008.00064.x>
- Mathews, E. A., Jemison, L. A., Pendleton, G. W., Blejwas, K. M., Hood, K. E., & Raum-Suryan, K. L. (2016). Haul-out patterns and effects of vessel disturbance on harbor seals (*phoca vitulina*) on glacial ice in tracy arm, alaska. *Fishery Bulletin (Washington, D.C.)*,

- 114(2), 186–202. Journal Article. <http://doi.org/10.7755/FB.114.2.6>
- Matthews, B., & Mazumder, A. (2007a). Distinguishing trophic variation from seasonal and size-based isotopic (^{15}N) variation of zooplankton. *Canadian Journal of Fisheries and Aquatic Sciences*, 64(1), 74–83. Journal Article. <http://doi.org/10.1139/f06-168>
- Matthews, B., & Mazumder, A. (2007b). Distinguishing trophic variation from seasonal and size-based isotopic (^{15}N) variation of zooplankton. *Canadian Journal of Fisheries and Aquatic Sciences*, 64(1), 74–83. Journal Article. <http://doi.org/10.1139/f06-168>
- McCann, K. S., Rasmussen, J. B., & Umbanhowar, J. (2005). The dynamics of spatially coupled food webs. *Ecology Letters*, 8(5), 513–523. Journal Article. <http://doi.org/10.1111/j.1461-0248.2005.00742.x>
- McCarthy, M. D., Benner, R., Lee, C., & Fogel, M. L. (2007). Amino acid nitrogen isotopic fractionation patterns as indicators of heterotrophy in plankton, particulate, and dissolved organic matter. *Geochimica et Cosmochimica Acta*, 71(19), 4727–4744. Journal Article. <http://doi.org/10.1016/j.gca.2007.06.061>
- McCary, M. A., Phillips, J. S., Ramiadantsoa, T., Nell, L. A., McCormick, A. R., & Botsch, J. C. (2021). Transient top-down and bottom-up effects of resources pulsed to multiple trophic levels. *Ecology (Durham)*, 102(1), e03197–n/a. Journal Article. <http://doi.org/10.1002/ecy.3197>
- McClelland, J. W., & Montoya, J. P. (2002). Trophic relationships and the nitrogen isotopic composition of amino acids in plankton. *Ecology (Durham)*, 83(8), 2173–2180. Journal Article. [http://doi.org/10.1890/0012-9658\(2002\)083\[2173:TRATNI\]2.0.CO;2](http://doi.org/10.1890/0012-9658(2002)083[2173:TRATNI]2.0.CO;2)
- McCrackin, M. L., Jones, H. P., Jones, P. C., & Moreno-Mateos, D. (2017). Recovery of lakes and coastal marine ecosystems from eutrophication: A global meta-analysis. *Limnology and Oceanography*, 62(2), 507–518. Journal Article. <http://doi.org/10.1002/lno.10441>

- McMahon, K. W., Michelson, C. I., Hart, T., McCarthy, M. D., Patterson, W. P., & Polito, M. J. (2019). Divergent trophic responses of sympatric penguin species to historic anthropogenic exploitation and recent climate change. *Proceedings of the National Academy of Sciences - PNAS*, 116(51), 25721–25727. Journal Article. <http://doi.org/10.1073/pnas.1913093116>
- McMahon, K. W., Polito, M. J., Abel, S., McCarthy, M. D., & Thorrold, S. R. (2015). Carbon and nitrogen isotope fractionation of amino acids in an avian marine predator, the gentoo penguin (*pygoscelis papua*). *Ecology and Evolution*, 5(6), 1278–1290. Journal Article. <http://doi.org/10.1002/ece3.1437>
- McMeans, B. C., McCann, K. S., Humphries, M., Rooney, N., & Fisk, A. T. (2015). Food web structure in temporally-forced ecosystems. *Trends in Ecology & Evolution (Amsterdam)*, 30(11), 662–672. Journal Article. <http://doi.org/10.1016/j.tree.2015.09.001>
- Meehan, E. P., Seminet-Reneau, E. E., & Quinn, T. P. (2005). Bear predation on pacific salmon facilitates colonization of carcasses by fly maggots. *The American Midland Naturalist*, 153(1), 142–151. Journal Article. [http://doi.org/10.1674/0003-0031\(2005\)153\[0142:BPOPSF\]2.0.CO;2](http://doi.org/10.1674/0003-0031(2005)153[0142:BPOPSF]2.0.CO;2)
- Merrick, R. L., & Loughlin, T. R. (1997). Foraging behavior of adult female and young-of-the-year steller sea lions in alaskan waters. *Canadian Journal of Zoology*, 75(5), 776–786. Journal Article. <http://doi.org/10.1139/z97-099>
- Misarti, N., Finney, B., Maschner, H., & Wooller, M. J. (2009). Changes in northeast pacific marine ecosystems over the last 4500 years: Evidence from stable isotope analysis of bone collagen from archeological middens. *Holocene (Sevenoaks)*, 19(8), 1139–1151. Journal Article. <http://doi.org/10.1177/0959683609345075>
- Mitchell, N. L., & Lamberti, G. A. (2005). Responses in dissolved nutrients and epilithon abundance to spawning salmon in southeast alaska streams. *Limnology and Oceanography*,

- 50(1), 217–227. Journal Article. <http://doi.org/10.4319/lo.2005.50.1.0217>
- Moon, J. B., & Carrick, H. J. (2007). Seasonal variation of phytoplankton nutrient limitation in lake erie. *Aquatic Microbial Ecology : International Journal*, 48(1), 61–71. Journal Article. <http://doi.org/10.3354/ame048061>
- Moore, J. K., Fu, W., Primeau, F., Britten, G. L., Lindsay, K., Long, M., ... Randerson, J. T. (2018). Sustained climate warming drives declining marine biological productivity. *Science (American Association for the Advancement of Science)*, 359(6380), 1139–1142. Journal Article. <http://doi.org/10.1126/science.aao6379>
- Moore, J. W., Schindler, D. E., Carter, J. L., Fox, J., Griffiths, J., & Holtgrieve, G. W. (2007). Biotic control of stream fluxes: Spawning salmon drive nutrient and matter export. *Ecology (Durham)*, 88(5), 1278–1291. Journal Article. <http://doi.org/10.1890/06-0782>
- Morales, L. V., Granger, J., Chang, B. X., Prokopenko, M. G., Plessen, B., Gradinger, R., & Sigman, D. M. (2014). Elevated $^{15}\text{N}/^{14}\text{N}$ in particulate organic matter, zooplankton, and diatom frustule-bound nitrogen in the ice-covered water column of the bering sea eastern shelf: Understanding ecosystem processes in the eastern bering sea iii. *Deep-Sea Research. Part II, Topical Studies in Oceanography*, 109, 100–111. Journal Article.
- Morris, M. R., & Stanford, J. A. (2011). Floodplain succession and soil nitrogen accumulation on a salmon river in southwestern kamchatka. *Ecological Monographs*, 81(1), 43–61. Journal Article. <http://doi.org/10.1890/08-2296.1>
- Munch, S. B., Giron-Nava, A., & Sugihara, G. (2018). Nonlinear dynamics and noise in fisheries recruitment: A global meta-analysis. *Fish and Fisheries (Oxford, England)*, 19(6), 964–973. Journal Article. <http://doi.org/10.1111/faf.12304>
- Muto, M. M., Helier, V. T., J., D. B., P., A. R., L., B. P., M., B. J., ... M., L. J. (2020). 2019 marine mammal stock assessment reports, 85, 46589. Generic.

- Naiman, R. J., Bilby, R. E., Schindler, D. E., & Helfield, J. M. (2002). Pacific salmon, nutrients, and the dynamics of freshwater and riparian ecosystems. *Ecosystems (New York)*, 5(4), 399–417. Journal Article. <http://doi.org/10.1007/s10021-001-0083-3>
- Narwani, A., & Mazumder, A. (2012). Bottom-up effects of species diversity on the functioning and stability of food webs. *The Journal of Animal Ecology*, 81(3), 701–713. Journal Article. <http://doi.org/10.1111/j.1365-2656.2011.01949.x>
- Nelson, B. W., Walters, C. J., Trites, A. W., & McAllister, M. K. (2019). Wild chinook salmon productivity is negatively related to seal density and not related to hatchery releases in the pacific northwest. *Canadian Journal of Fisheries and Aquatic Sciences*, 76(3), 447–462. Journal Article. <http://doi.org/10.1139/cjfas-2017-0481>
- Newsome, S. D., Koch, P. L., Etnier, M. A., & Auriolles-Gamboa, D. (2006). USING carbon and nitrogen isotope values to investigate maternal strategies in northeast pacific otariids. *Marine Mammal Science*, 22(3), 556–572. Journal Article. <http://doi.org/10.1111/j.1748-7692.2006.00043.x>
- Nielsen, J. M., Popp, B. N., & Winder, M. (2015). Meta-analysis of amino acid stable nitrogen isotope ratios for estimating trophic position in marine organisms. *Oecologia*, 178(3), 631–642. Journal Article. <http://doi.org/10.1007/s00442-015-3305-7>
- Nordin, A., Höglberg, P., & Näsholm, T. (2001). Soil nitrogen form and plant nitrogen uptake along a boreal forest productivity gradient. *Oecologia*, 129(1), 125–132. Journal Article. <http://doi.org/10.1007/s004420100698>
- Ohkouchi, N., Chikaraishi, Y., Close, H. G., Fry, B., Larsen, T., Madigan, D. J., ... Yokoyama, Y. (2017). Advances in the application of amino acid nitrogen isotopic analysis in ecological and biogeochemical studies. *Organic Geochemistry*, 113, 150–174. Journal Article. <http://doi.org/10.1016/j.orggeochem.2017.07.009>
- Ohlberger, J., Scheuerell, M. D., Schindler, D. E., & Peters, D. P. C. (2016). Population co-

- herence and environmental impacts across spatial scales: A case study of chinook salmon. *Ecosphere (Washington, D.C)*, 7(4), n/a. Journal Article. <http://doi.org/10.1002/ecs2.1333>
- Ohlberger, J., Schindler, D. E., Ward, E. J., Walsworth, T. E., & Essington, T. E. (2019). Resurgence of an apex marine predator and the decline in prey body size. *Proceedings of the National Academy of Sciences - PNAS*, 116(52), 26682–26689. Journal Article. <http://doi.org/10.1073/pnas.1910930116>
- Oke, K. B., Cunningham, C. J., Westley, P. A. H., Baskett, M. L., Carlson, S. M., Clark, J., ... Palkovacs, E. P. (2020). Recent declines in salmon body size impact ecosystems and fisheries. *Nature Communications*, 11(1), 4155–4155. Journal Article. <http://doi.org/10.1038/s41467-020-17726-z>
- Olson, R. J., Popp, B. N., Graham, B. S., López-Ibarra, G. A., Galván-Magaña, F., Lennert-Cody, C. E., ... Fry, B. (2010). Food-web inferences of stable isotope spatial patterns in copepods and yellowfin tuna in the pelagic eastern pacific ocean. *Progress in Oceanography*, 86(1-2), 124–138. Journal Article. <http://doi.org/10.1016/j.pocean.2010.04.026>
- Oltean, G. S., Comeau, P. G., & White, B. (2016). Carbon isotope discrimination by picea glauca and populus tremuloides is related to the topographic depth to water index and rainfall. *Canadian Journal of Forest Research*, 46(10), 1225–1233. Journal Article. <http://doi.org/10.1139/cjfr-2015-0491>
- Paine, R. T., Tegner, M. J., & Johnson, E. A. (1998). Compounded perturbations yield ecological surprises. *Ecosystems (New York)*, 1(6), 535–545. Journal Article. <http://doi.org/10.1007/s100219900049>
- Perakis, S. S. (2002). Nutrient limitation, hydrology and watershed nitrogen loss. *Hydrological Processes*, 16(17), 3507–3511. Journal Article. <http://doi.org/10.1002/hyp.5078>

- Perakis, S. S., & Sinkhorn, E. R. (2011). Biogeochemistry of a temperate forest nitrogen gradient. *Ecology (Durham)*, 92(7), 1481–1491. Journal Article. <http://doi.org/10.1890/10-1642.1>
- Perry, L. G., Shafrroth, P. B., & Perakis, S. S. (2017). Riparian soil development linked to forest succession above and below dams along the elwha river, washington, usa. *Ecosystems*, 20(1), 104–129. Journal Article. <http://doi.org/10.1007/s10021-016-0080-1>
- Pershing, A. J., Head, E. H. J., Greene, C. H., & Jossi, J. W. (2010). Pattern and scale of variability among northwest atlantic shelf plankton communities. *Journal of Plankton Research*, 32(12), 1661–1674. Journal Article. <http://doi.org/10.1093/plankt/fbq058>
- Peters, L., Faust, C., & Traunspurger, W. (2012). Changes in community composition, carbon and nitrogen stable isotope signatures and feeding strategy in epilithic aquatic nematodes along a depth gradient. *Aquatic Ecology*, 46(3), 371–384. Journal Article. <http://doi.org/10.1007/s10452-012-9408-x>
- Phillips, D. L., Inger, R., Bearhop, S., Jackson, A. L., Moore, J. W., Parnell, A. C., ... Ward, E. J. (2014). Best practices for use of stable isotope mixing models in food-web studies. *Canadian Journal of Zoology*, 92(10), 823–835. Journal Article. <http://doi.org/10.1139/cjz-2014-0127>
- Pitcher, K. W., Olesiuk, P. F., Brown, R. F., Lowry, M. S., Jeffries, S. J., Sease, J. L., ... Lowry, L. F. (2007). Abundance and distribution of the eastern north pacific steller sea lion population. *Fishery Bulletin (Washington, D.C.)*, 105(1), 102. Journal Article.
- Polis, G. A., Power, M. E., & Huxel, G. R. (2004). *Food webs at the landscape level*. Book, Chicago: Chicago : University of Chicago Press.
- Popp, B. N., Graham, B. S., Olson, R. J., Hannides, C. C. S., Lott, M. J., López-Ibarra, G. A., ... Fry, B. (2007). *Insight into the trophic ecology of yellowfin tuna, thunnus albacares, from compound-Specific nitrogen isotope analysis of proteinaceous amino acids*

- (Vol. 1, pp. 173–190). Book, Elsevier Science & Technology. [http://doi.org/10.1016/S1936-7961\(07\)01012-3](http://doi.org/10.1016/S1936-7961(07)01012-3)
- Possamai, B., Hoeinghaus, D. J., & Garcia, A. M. (2021). Shifting baselines: Integrating ecological and isotopic time lags improves trophic position estimates in aquatic consumers. *Marine Ecology. Progress Series (Halstenbek)*, 666, 19–30. Journal Article. <http://doi.org/10.3354/meps13682>
- Post, D. M. (2002). Using stable isotopes to estimate trophic position: Models, methods, and assumptions. *Ecology (Durham)*, 83(3), 703–718. Journal Article. [http://doi.org/10.1890/0012-9658\(2002\)083\[0703:USITET\]2.0.CO;2](http://doi.org/10.1890/0012-9658(2002)083[0703:USITET]2.0.CO;2)
- Prescott, C. E., Corbin, J. P., & Parkinson, D. (1992). Immobilization and availability of n and p in the forest floors of fertilized rocky mountain coniferous forests. *Plant and Soil*, 143(1), 1–10. Journal Article. <http://doi.org/10.1007/BF00009123>
- Prescott, C. E., Kishchuk, B. E., & Weetman, G. F. (1995). Long-term effects of repeated n fertilization and straw application in a jack pine forest. 3. nitrogen availability in the forest floor. *Canadian Journal of Forest Research*, 25(12), 1991–1996. Journal Article. <http://doi.org/10.1139/x95-215>
- Puerta, P., Ciannelli, L., Rykaczewski, R. R., Opiekun, M., & Litzow, M. A. (2019). Do gulf of alaska fish and crustacean populations show synchronous non-stationary responses to climate? *Progress in Oceanography*, 175, 161–170. Journal Article. <http://doi.org/10.1016/j.pocean.2019.04.002>
- Quay, P. D., Tilbrook, B., & Wong, C. S. (1992). Oceanic uptake of fossil fuel co₂: Carbon-13 evidence. *Science (American Association for the Advancement of Science)*, 256(5053), 74–79. Journal Article. <http://doi.org/10.1126/science.256.5053.74>
- Quinn, T. P., Helfield, J. M., Austin, C. S., Hovel, R. A., & Bunn, A. G. (2018). A multi-decade experiment shows that fertilization by salmon carcasses enhanced tree growth

- in the riparian zone. *Ecology (Durham)*, 99(11), 2433–2441. Journal Article. <http://doi.org/10.1002/ecy.2453>
- Ramirez, M. D., Besser, A. C., Newsome, S. D., & McMahon, K. W. (2021). Meta-analysis of primary producer amino acid ^{15}N values and their influence on trophic position estimation. *Methods in Ecology and Evolution*, 12(10), 1750–1767. Journal Article. <http://doi.org/10.1111/2041-210X.13678>
- Reimchen, T. E., & Fox, C. H. (2013). Fine-scale spatiotemporal influences of salmon on growth and nitrogen signatures of sitka spruce tree rings. *BMC Ecology*, 13(1), 38–38. Journal Article. <http://doi.org/10.1186/1472-6785-13-38>
- Reum, J. C. P., Essington, T. E., Greene, C. M., Rice, C. A., & Fresh, K. L. (2011). Multiscale influence of climate on estuarine populations of forage fish: The role of coastal upwelling, freshwater flow and temperature. *Marine Ecology. Progress Series (Halstenbek)*, 425, 203–215. Journal Article. <http://doi.org/10.3354/meps08997>
- Richard, G. G., Robin, S. W., James, M. M., Laurie, A. W., Gregory, J. B., Orlay, W. J., & Jeffrey, J. H. (2007). Pacific salmon extinctions: Quantifying lost and remaining diversity. *Conservation Biology*, 21(4), 1009–1020. Journal Article. <http://doi.org/10.1111/j.1523-1739.2007.00693.x>
- Riofrío-Lazo, M., & Auñóoles-Gamboa, D. (2013). Timing of isotopic integration in marine mammal skull: Comparative study between calcified tissues: Timing of isotopic integration in marine mammal skull. *Rapid Communications in Mass Spectrometry*, 27(9), 1076–1082. Journal Article. <http://doi.org/10.1002/rcm.6556>
- Rolff, C., & Elmgren, R. (2000). Use of riverine organic matter in plankton food webs of the baltic sea. *Marine Ecology. Progress Series (Halstenbek)*, 197, 81–101. Journal Article. <http://doi.org/10.3354/meps197081>
- Ruiz-Cooley, R. I., Markaida, U., Gendron, D., & Aguíñiga, S. (2006). Stable isotopes in

- jumbo squid (*dosidicus gigas*) beaks to estimate its trophic position: Comparison between stomach contents and stable isotopes. *Journal of the Marine Biological Association of the United Kingdom*, 86(2), 437–445. Journal Article. <http://doi.org/10.1017/S0025315406013324>
- Rykaczewski, R. R., & Dunne, J. P. (2010). Enhanced nutrient supply to the California current ecosystem with global warming and increased stratification in an earth system model. *Geophysical Research Letters*, 37(21), n/a. Journal Article. <http://doi.org/10.1029/2010GL045019>
- Scheuerell, M. D., Moore, J. W., Schindler, D. E., & Harvey, C. J. (2007). Varying effects of anadromous sockeye salmon on the trophic ecology of two species of resident salmonids in southwest Alaska. *Freshwater Biology*, 52(10), 1944–1956. Journal Article. <http://doi.org/10.1111/j.1365-2427.2007.01823.x>
- Schindler, D. E., Armstrong, J. B., Bentley, K. T., Jankowski, K., Lisi, P. J., & Payne, L. X. (2013). Riding the crimson tide: Mobile terrestrial consumers track phenological variation in spawning of an anadromous fish. *Biology Letters* (2005), 9(3), 20130048–20130048. Journal Article. <http://doi.org/10.1098/rsbl.2013.0048>
- Schindler, D. E., Leavitt, P. R., Brock, C. S., Johnson, S. P., & Quay, P. D. (2005). Marine-derived nutrients, commercial fisheries, and production of salmon and lake algae in Alaska. *Ecology (Durham)*, 86(12), 3225–3231. Journal Article. <http://doi.org/10.1890/04-1730>
- Schindler, D. E., Scheuerell, M. D., Moore, J. W., Gende, S. M., Francis, T. B., & Palen, W. J. (2003). Pacific salmon and the ecology of coastal ecosystems. *Frontiers in Ecology and the Environment*, 1(1), 31. Journal Article. <http://doi.org/10.2307/3867962>
- Scott M, G., Richard T, E., Mary F, W., & Mark S, W. (2002). Pacific salmon in aquatic and terrestrial ecosystems: Pacific salmon subsidize freshwater and terrestrial ecosystems

- through several pathways, which generates unique management and conservation issues but also provides valuable research opportunities. *Bioscience*, 52(10), 917–928. Journal Article. [http://doi.org/10.1641/0006-3568\(2002\)052\[0917:PSIAAT\]2.0.CO;2](http://doi.org/10.1641/0006-3568(2002)052[0917:PSIAAT]2.0.CO;2)
- Sherwood, O. A., Guilderson, T. P., Batista, F. C., Schiff, J. T., & McCarthy, M. D. (2014). Increasing subtropical north pacific ocean nitrogen fixation since the little ice age. *Nature (London)*, 505(7481), 78–81. Journal Article. <http://doi.org/10.1038/nature12784>
- Sherwood, O. A., Heikoop, J. M., Scott, D. B., Risk, M. J., Guilderson, T. P., & McKinney, R. A. (2005). Stable isotopic composition of deep-sea gorgonian corals primnoa spp.: A new archive of surface processes. *Marine Ecology. Progress Series (Halstenbek)*, 301, 135–148. Journal Article. <http://doi.org/10.3354/meps301135>
- Sherwood, O. A., Jamieson, R. E., Edinger, E. N., & Wareham, V. E. (2008). Stable c and n isotopic composition of cold-water corals from the newfoundland and labrador continental slope: Examination of trophic, depth and spatial effects. *Deep-Sea Research. Part I, Oceanographic Research Papers*, 55(10), 1392–1402. Journal Article. <http://doi.org/10.1016/j.dsr.2008.05.013>
- Sherwood, O. A., Lehmann, M. F., Schubert, C. J., Scott, D. B., & McCarthy, M. D. (2011). Nutrient regime shift in the western north atlantic indicated by compound-specific 15N of deep-sea gorgonian corals. *Proceedings of the National Academy of Sciences - PNAS*, 108(3), 1011–1015. Journal Article. <http://doi.org/10.1073/pnas.1004904108>
- Sigman, D. M., Altabet, M. A., Michener, R., McCorkle, D. C., Fry, B., & Holmes, R. M. (1997). Natural abundance-level measurement of the nitrogen isotopic composition of oceanic nitrate: An adaptation of the ammonia diffusion method. *Marine Chemistry*, 57(3-4), 227–242. Journal Article. [http://doi.org/10.1016/S0304-4203\(97\)00009-1](http://doi.org/10.1016/S0304-4203(97)00009-1)
- Sigman, D. M., Karsh, K. L., & Casciotti, K. L. (2009). Nitrogen isotopes in the ocean, 40–54. Journal Article. <http://doi.org/10.1016/B978-012374473-9.00632-9>

- Sinclair, E. H., & Zeppelin, T. K. (2002). SEASONAL and spatial differences in diet in the western stock of steller sea lions (*eumetopias jubatus*). *Journal of Mammalogy*, 83(4), 973–990. Journal Article. [http://doi.org/10.1644/1545-1542\(2002\)083<0973:SASDID>2.0.CO;2](http://doi.org/10.1644/1545-1542(2002)083<0973:SASDID>2.0.CO;2)
- Siple, M. C., & Francis, T. B. (2015). Population diversity in pacific herring of the puget sound, usa. *Oecologia*, 180(1), 111–125. Journal Article. <http://doi.org/10.1007/s00442-015-3439-7>
- Smith, R. S., Weldon, L. M., Hayward, J. L., & Henson, S. M. (2017). TIME lags associated with effects of oceanic conditions on seabird breeding in the salish sea region of the northern california current system. *Marine Ornithology*, 45(1), 39–42. Journal Article.
- Smith, S. L., Henrichs, S. M., & Rho, T. (2002). Stable c and n isotopic composition of sinking particles and zooplankton over the southeastern bering sea shelf. *Deep-Sea Research. Part II, Topical Studies in Oceanography*, 49(26), 6031–6050. Journal Article. [http://doi.org/10.1016/S0967-0645\(02\)00332-6](http://doi.org/10.1016/S0967-0645(02)00332-6)
- Sparks, D. L., Soil Science Society of, A., & American Society of, A. (1996). *Methods of soil analysis. part 3, chemical methods*. Book, Madison, Wis.: Madison, Wis. : Soil Science Society of America : American Society of Agronomy.
- Stabeno, P. J., Bond, N. A., & Salo, S. A. (2007). On the recent warming of the southeastern bering sea shelf. *Deep-Sea Research. Part II, Topical Studies in Oceanography*, 54(23), 2599–2618. Journal Article. <http://doi.org/10.1016/j.dsr2.2007.08.023>
- Stachura, M. M., Essington, T. E., Mantua, N. J., Hollowed, A. B., Haltuch, M. A., Spencer, P. D., ... Doyle, M. J. (2014). Linking northeast pacific recruitment synchrony to environmental variability. *Fisheries Oceanography*, 23(5), 389–408. Journal Article. <http://doi.org/10.1111/fog.12066>
- Steneck, R. S. (2012). Apex predators and trophic cascades in large marine ecosystems:

- Learning from serendipity. *Proceedings of the National Academy of Sciences - PNAS*, 109(21), 7953–7954. Journal Article. <http://doi.org/10.1073/pnas.1205591109>
- Steven, S. P., Joselin, J. M., & David, E. H. (2012). N₂-fixing red alder indirectly accelerates ecosystem nitrogen cycling. *Ecosystems (New York)*, 15(7), 1182–1193. Journal Article. <http://doi.org/10.1007/s10021-012-9579-2>
- Stiling, R. R., Holtgrieve, G. W., & Olden, J. D. (2021). Population structure and habitat availability determine resource use by rainbow trout in high elevation lakes. *Freshwater Science*, 40(3), 508–523. Journal Article. <http://doi.org/10.1086/716184>
- Strom, S. L., Olson, M. B., Macri, E. L., & Mord, C. W. (2006). Cross-shelf gradients in phytoplankton community structure, nutrient utilization, and growth rate in the coastal gulf of alaska. *Marine Ecology. Progress Series (Halstenbek)*, 328, 75–92. Journal Article. <http://doi.org/10.3354/meps328075>
- Suryan, R. M., Arimitsu, M. L., Coletti, H. A., Hopcroft, R. R., Lindeberg, M. R., Barbeaux, S. J., ... Zador, S. G. (2021). Ecosystem response persists after a prolonged marine heat-wave. *Scientific Reports*, 11(1), 6235–17. Journal Article. <http://doi.org/10.1038/s41598-021-83818-5>
- (Syväranta, J., Hamalainen, H., & Jones, R. I. (2006). Within-lake variability in carbon and nitrogen stable isotope signatures. *Freshwater Biology*, 51(6), 1090–1102. Journal Article. <http://doi.org/10.1111/j.1365-2427.2006.01557.x>
- (Syväranta, J., Tiirola, M., & Jones, R. I. (2008). Seasonality in lake pelagic ¹⁵N values : Patterns, possible explanations, and implications for food web baselines. *Fundamental and Applied Limnology*, 172(3), 255–262. Journal Article. <http://doi.org/10.1127/1863-9135/2008/0172-0255>
- Søndergaard, M., Lauridsen, T. L., Johansson, L. S., & Jeppesen, E. (2017). Nitrogen or phosphorus limitation in lakes and its impact on phytoplankton biomass and submerged

- macrophyte cover. *Hydrobiologia*, 795(1), 35–48. Journal Article. <http://doi.org/10.1007/s10750-017-3110-x>
- Tagliabue, A., & Bopp, L. (2008). Towards understanding global variability in ocean carbon-13. *Global Biogeochemical Cycles*, 22(1), GB1025–n/a. Journal Article. <http://doi.org/10.1029/2007GB003037>
- Tallis, H., Levin, P. S., Ruckelshaus, M., Lester, S. E., McLeod, K. L., Fluharty, D. L., & Halpern, B. S. (2010). The many faces of ecosystem-based management: Making the process work today in real places. *Marine Policy*, 34(2), 340–348. Journal Article. <http://doi.org/10.1016/j.marpol.2009.08.003>
- Templer, P. H., Mack, M. C., Iii, F. S. C., Christenson, L. M., Compton, J. E., Crook, H. D., ... Zak, D. R. (2012). Sinks for nitrogen inputs in terrestrial ecosystems: A meta-analysis of ¹⁵N tracer field studies. *Ecology (Durham)*, 93(8), 1816–1829. Journal Article. <http://doi.org/10.1890/11-1146.1>
- Thomas, A. C., Lance, M. M., Jeffries, S. J., Miner, B. G., & Acevedo-Gutierrez, A. (2011). Harbor seal foraging response to a seasonal resource pulse, spawning pacific herring. *Marine Ecology. Progress Series (Halstenbek)*, 441, 225–239. Journal Article. <http://doi.org/10.3354/meps09370>
- Thomas, A. C., Nelson, B. W., Lance, M. M., Deagle, B. E., & Trites, A. W. (2017). Harbour seals target juvenile salmon of conservation concern. *Canadian Journal of Fisheries and Aquatic Sciences*, 74(6), 907–921. Journal Article. <http://doi.org/10.1139/cjfas-2015-0558>
- Thomas, S. M., Crowther, T. W., & Bearhop, S. (2015). Predicting rates of isotopic turnover across the animal kingdom: A synthesis of existing data. *The Journal of Animal Ecology*, 84(3), 861–870. Journal Article. <http://doi.org/10.1111/1365-2656.12326>
- Trites, A. W., Calkins, D. G., & Winship, A. J. (2007). Diets of steller sea lions in southeast

- alaska, 1993-1999. *Fishery Bulletin (Washington, D.C.)*, 105(2), 234. Journal Article.
- Vander Zanden, H. B., Arthur, K. E., Bolten, A. B., Popp, B. N., Lagueux, C. J., Harrison, E., ... Bjorndal, K. A. (2013). Trophic ecology of a green turtle breeding population. *Marine Ecology. Progress Series (Halstenbek)*, 476, 237–249. Journal Article. <http://doi.org/10.3354/meps10185>
- Vander Zanden, M. J., Clayton, M. K., Moody, E. K., Solomon, C. T., & Weidel, B. C. (2015). Stable isotope turnover and half-life in animal tissues: A literature synthesis. *PloS One*, 10(1), e0116182–e0116182. Journal Article. <http://doi.org/10.1371/journal.pone.0116182>
- Vander Zanden, M. J., Vadeboncoeur, Y., Diebel, M. W., & Jeppesen, E. (2005). Primary consumer stable nitrogen isotopes as indicators of nutrient source. *Environmental Science & Technology*, 39(19), 7509–7515. Journal Article. <http://doi.org/10.1021/es050606t>
- Vanderklift, M. A., & Ponsard, S. (2003). Sources of variation in consumer-diet $\delta^{15}\text{N}$ enrichment: A meta-analysis. *Oecologia*, 136(2), 169–182. Journal Article. <http://doi.org/10.1007/s00442-003-1270-z>
- Vecchi, G. A., & Wittenberg, A. T. (2010). El niño and our future climate: Where do we stand? *Wiley Interdisciplinary Reviews. Climate Change*, 1(2), 260–270. Journal Article. <http://doi.org/10.1002/wcc.33>
- Vega, C. de la, Jeffreys, R. M., Tuerena, R., Ganeshram, R., & Mahaffey, C. (2019). Temporal and spatial trends in marine carbon isotopes in the arctic ocean and implications for food web studies. *Global Change Biology*, 25(12), 4116–4130. Journal Article. <http://doi.org/10.1111/gcb.14832>
- Vega, C. de la, Mahaffey, C., Tuerena, R. E., Yurkowski, D. J., Ferguson, S. H., Stenson, G. B., ... Jeffreys, R. M. (2021). Arctic seals as tracers of environmental and ecological

- change. *Limnology and Oceanography Letters*, 6(1), 24–32. Journal Article. <http://doi.org/10.1002/lol2.10176>
- Vehtari, A., Gelman, A., & Gabry, J. (2017). Practical bayesian model evaluation using leave-one-out cross-validation and waic. *Statistics and Computing*, 27(5), 1413–1432. Journal Article. <http://doi.org/10.1007/s11222-016-9696-4>
- Verspoor, J. J., Braun, D. C., Stubbs, M. M., & Reynolds, J. D. (2011). Persistent ecological effects of a salmon-derived nutrient pulse on stream invertebrate communities. *Ecosphere (Washington, D.C.)*, 2(2), art18–17. Journal Article. <http://doi.org/10.1890/ES10-00011.1>
- Vizzini, S., & Mazzola, A. (2003). Seasonal variations in the stable carbon and nitrogen isotope ratios ($^{13}\text{C}/^{12}\text{C}$ and $^{15}\text{N}/^{14}\text{N}$) of primary producers and consumers in a western mediterranean coastal lagoon. *Marine Biology*, 142(5), 1009–1018. Journal Article. <http://doi.org/10.1007/s00227-003-1027-6>
- Vokhshoori, N. L., & McCarthy, M. D. (2014). Compound-specific ^{15}N amino acid measurements in littoral mussels in the california upwelling ecosystem: A new approach to generating baseline ^{15}N isoscapes for coastal ecosystems. *PLoS One*, 9(6), e98087–e98087. Journal Article. <http://doi.org/10.1371/journal.pone.0098087>
- Vuorio, K., Meili, M., & Sarvala, J. (2006). Taxon-specific variation in the stable isotopic signatures (^{13}C and ^{15}N) of lake phytoplankton. *Freshwater Biology*, 51(5), 807–822. Journal Article. <http://doi.org/10.1111/j.1365-2427.2006.01529.x>
- Waite, J. N., & Mueter, F. J. (2013). Spatial and temporal variability of chlorophyll-a concentrations in the coastal gulf of alaska, 1998–2011, using cloud-free reconstructions of seawifs and modis-aqua data. *Progress in Oceanography*, 116, 179–192. Journal Article. <http://doi.org/10.1016/j.pocean.2013.07.006>
- Walker, L. R. (1989). Soil nitrogen changes during primary succession on a floodplain in

- alaska, u.S.A. *Arctic and Alpine Research*, 21(4), 341–349. Journal Article. <http://doi.org/10.2307/1551644>
- Walsh, J. E., Thoman, R. L., Bhatt, U. S., Bieniek, P. A., Brettschneider, B., Brubaker, M., ... Partain, J. (2018). The high latitude marine heat wave of 2016 and its impacts on alaska. *Bulletin of the American Meteorological Society*, 99(1), S39–S43. Journal Article. <http://doi.org/10.1175/BAMS-D-17-0105.1>
- Ware, D. M., & Thomson, R. E. (2005). Bottom-up ecosystem trophic dynamics determine fish production in the northeast pacific. *Science (American Association for the Advancement of Science)*, 308(5726), 1280–1284. Journal Article. <http://doi.org/10.1126/science.1109049>
- Wheeler, T. A., & Kavanagh, K. L. (2017). Soil biogeochemical responses to the deposition of anadromous fish carcasses in inland riparian forests of the pacific northwest, usa. *Canadian Journal of Forest Research*, 47(11), 1506–1516. Journal Article. <http://doi.org/10.1139/cjfr-2017-0194>
- Wheeler, T. A., Kavanagh, K. L., & Daanen, S. A. (2014). Terrestrial salmon carcass decomposition: Nutrient and isotopic dynamics in central idaho. *Northwest Science*, 88(2), 106–119. Journal Article. <http://doi.org/10.3955/046.088.0206>
- Whitney, N. M., Johnson, B. J., Dostie, P. T., Luzier, K., & Wanamaker, A. D. (2019). Paired bulk organic and individual amino acid ^{15}N analyses of bivalve shell periostracum: A paleoceanographic proxy for water source variability and nitrogen cycling processes. *Geochimica et Cosmochimica Acta*, 254, 67–85. Journal Article. <http://doi.org/10.1016/j.gca.2019.03.019>
- Williams, B., Risk, M., Stone, R., Sinclair, D., & Ghaleb, B. (2007). Oceanographic changes in the north pacific ocean over the past century recorded in deep-water gorgonian corals. *Marine Ecology. Progress Series (Halstenbek)*, 335, 85–94. Journal Article. <http://doi.org/10.3354/meps335085>

- [org/10.3354/meps335085](http://doi.org/10.3354/meps335085)
- Wilson, K., Lance, M., Jeffries, S., & Acevedo-Gutierrez, A. (2014). Fine-scale variability in harbor seal foraging behavior. *PLoS One*, 9(4), e92838–e92838. Journal Article. <http://doi.org/10.1371/journal.pone.0092838>
- Winder, M., & Sommer, U. (2012). Phytoplankton response to a changing climate. *Hydrobiologia*, 698(1), 5–16. Journal Article. <http://doi.org/10.1007/s10750-012-1149-2>
- Winder, M., Schindler, D. E., Moore, J. W., Johnson, S. P., & Palen, W. J. (2005). Do bears facilitate transfer of salmon resources to aquatic macroinvertebrates? *Canadian Journal of Fisheries and Aquatic Sciences*, 62(10), 2285–2293. Journal Article. <http://doi.org/10.1139/f05-136>
- Wipfli, M. S., Hudson, J. P., Caouette, J. P., & Chaloner, D. T. (2003). Marine subsidies in freshwater ecosystems: Salmon carcasses increase the growth rates of stream-Resident salmonids. *Transactions of the American Fisheries Society (1900)*, 132(2), 371–381. Journal Article. [http://doi.org/10.1577/1548-8659\(2003\)132<0371:MSIFES>2.0.CO;2](http://doi.org/10.1577/1548-8659(2003)132<0371:MSIFES>2.0.CO;2)
- Wipfli, M. S., Hudson, J., & Caouette, J. (1998). Influence of salmon carcasses on stream productivity : Response of biofilm and benthic macroinvertebrates in southeastern alaska, u.S.A. *Canadian Journal of Fisheries and Aquatic Sciences*, 55(6), 1503–1511. Journal Article. <http://doi.org/10.1139/cjfas-55-6-1503>
- Womble, J. N., & Sigler, M. F. (2006). Seasonal availability of abundant, energy-rich prey influences the abundance and diet of a marine predator, the steller sea lion *eumetopias jubatus*. *Marine Ecology. Progress Series (Halstenbek)*, 325, 281–293. Journal Article. <http://doi.org/10.3354/meps325281>
- Womble, J. N., Pendleton, G. W., Mathews, E. A., Blundell, G. M., Bool, N. M., & Gende, S. M. (2010). Harbor seal (*phoca vitulina richardii*) decline continues in the rapidly changing landscape of glacier bay national park, alaska 1992-2008. *Marine Mammal Science*, 26(3),

- 686–697. Journal Article. <http://doi.org/10.1111/j.1748-7692.2009.00360.x>
- Woodland, R. J., Magnan, P., Glémet, H., Rodríguez, M. A., & Cabana, G. (2012). Variability and directionality of temporal changes in ^{13}C and ^{15}N of aquatic invertebrate primary consumers. *Oecologia*, 169(1), 199–209. Journal Article. <http://doi.org/10.1007/s00442-011-2178-7>
- Wright, M., Sherriff, R. L., Miller, A. E., & Wilson, T. (2018). Stand basal area and temperature interact to influence growth in white spruce in southwest alaska. *Ecosphere (Washington, D.C.)*, 9(10), e02462-n/a. Journal Article. <http://doi.org/10.1002/ecs2.2462>
- Wu, J. P., Calvert, S. E., & Wong, C. S. (1999). Carbon and nitrogen isotope ratios in sedimenting particulate organic matter at an upwelling site off vancouver island. *Estuarine, Coastal and Shelf Science*, 48(2), 193–203. Journal Article. <http://doi.org/10.1006/ecss.1998.0409>
- Wu, J., Calvert, S. E., & Wong, C. S. (1997). Nitrogen isotope variations in the subarctic northeast pacific: Relationships to nitrate utilization and trophic structure. *Deep-Sea Research. Part I, Oceanographic Research Papers*, 44(2), 287–314. Journal Article. [http://doi.org/10.1016/S0967-0637\(96\)00099-4](http://doi.org/10.1016/S0967-0637(96)00099-4)
- Yarie, J. (2008). Effects of moisture limitation on tree growth in upland and floodplain forest ecosystems in interior alaska. *Forest Ecology and Management*, 256(5), 1055–1063. Journal Article. <http://doi.org/10.1016/j.foreco.2008.06.022>
- Zanden, M. J. V., & Joseph, B. R. (1999). Primary consumer ^{13}C and ^{15}N and the trophic position of aquatic consumers. *Ecology (Durham)*, 80(4), 1395–1404. Journal Article.
- Zanden, M. J. V., & Rasmussen, J. B. (2001). Variation in ^{15}N and ^{13}C trophic fractionation: Implications for aquatic food web studies. *Limnology and Oceanography*, 46(8),

- 2061–2066. Journal Article. <http://doi.org/10.4319/lo.2001.46.8.2061>
- Zhao, L., Castellini, M. A., Mau, T. L., & Trumble, S. J. (2004). Trophic interactions of antarctic seals as determined by stable isotope signatures. *Polar Biology*, 27(6), 368–373. Journal Article. <http://doi.org/10.1007/s00300-004-0598-0>
- (2009). Generic. http://doi.org/10.1007/978-90-481-3354-3_14
- (2015). Generic. <http://doi.org/10.1017/CBO9781139924856.003>